

THE ROLE OF PLAKOPHILIN3 IN REGULATING CELL ADHESION, CELL MIGRATION AND EPITHELIAL MESENCHYMAL TRANSITION (EMT)

By
MANSA GURJAR
LIFE09200904008

**TATA MEMORIAL CENTRE
MUMBAI**

*A thesis submitted to the
Board of Studies in Life Sciences
In partial fulfilment of requirements
for the Degree of*

**DOCTOR OF PHILOSOPHY
of
HOMI BHABHA NATIONAL INSTITUTE**



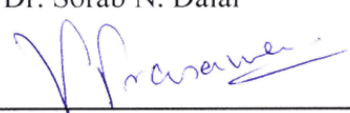
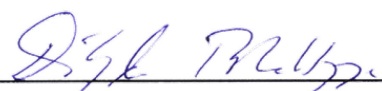
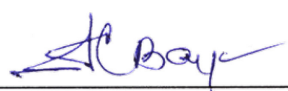


December, 2015

Homi Bhabha National Institute

Recommendations of the Viva Voce Committee

As members of the Viva Voce Committee, we certify that we have read the dissertation prepared by Mansa Gurjar entitled “**The role of plakophilin3 in regulating cell adhesion, cell migration and epithelial mesenchymal transition (EMT)**” and recommend that it may be accepted as fulfilling the thesis requirement for the award of Degree of Doctor of Philosophy.

 Chairperson – Dr. Milind Vaidya	16/12/2015 Date:
 Convener – Dr. Sorab N. Dalal	16/12/2015 Date:
 Member – Dr. Prasanna Venkatraman	16/12/2015 Date:
 Member – Dr. Dibyendu Bhattacharyya	16/12/2015 Date:
 External Examiner – Dr. Akhil C. Banerjee	16/12/2015 Date:

Final approval and acceptance of this thesis is contingent upon the candidate's submission of the final copies of the thesis to HBNI.

I hereby certify that I have read this thesis prepared under my direction and recommend that it may be accepted as fulfilling the thesis requirement.

Date: 16/12/2015

Place: NAVI MUMBAI



Dr. Sorab N. Dalal
Guide

STATEMENT BY AUTHOR

This dissertation has been submitted in partial fulfilment of requirements for an advanced degree at Homi Bhabha National Institute (HBNI) and is deposited in the Library to be made available to borrowers under rules of the HBNI.

Brief quotations from this dissertation are allowable without special permission, provided that accurate acknowledgement of source is made. Requests for permission for extended quotation from or reproduction of this manuscript in whole or in part may be granted by the Competent Authority of HBNI when in his or her judgment the proposed use of the material is in the interests of scholarship. In all other instances, however, permission must be obtained from the author.



Mansa Gurjar

DECLARATION

I, hereby declare that the investigation presented in the thesis has been carried out by me. The work is original and has not been submitted earlier as a whole or in part for a degree / diploma at this or any other Institution / University.

A handwritten signature in blue ink, appearing to read 'G. J. an' or similar, with a long horizontal stroke extending to the right.

Mansa Gurjar

List of Publications arising from the thesis

PUBLICATIONS IN REFEREED JOURNAL:

a. Published

M. Gurjar, K. Raychaudhuri, S. N. Dalal, Loss of the desmosomal plaque protein plakophilin 3 does not induce the epithelial mesenchymal transition. *J Biosci Tech* **6**, 647 (Jan 2015).

b. Other Publications:

1. E. Telles, M. Gurjar, K. Ganti, D. Gupta, S. N. Dalal, Filamin A stimulates cdc25C function and promotes entry into mitosis. *Cell Cycle* **10**, 776 (Mar 1, 2011).
2. L. Sehgal *et al.*, 14-3-3 γ -mediated transport of plakoglobin to the cell border is required for the initiation of desmosome assembly in vitro and in vivo. *Journal of Cell Science* **127**, 2174 (May 15, 2014).
3. K. Raychaudhuri, M. Gurjar, S. N. Dalal, Plakophilin3 and Plakoglobin recycling are differentially regulated during the disassembly of desmosomes. *J Biosci Tech* **6**, 634 (Jan 2015).

CONFERENCES:

1. **Second Global Cancer Genomics Consortium Symposium 2012** held at ACTREC, Kharghar, Navi Mumbai, from November 19, 2012 to November 20, 2012. Presented poster titled, “*The role of plakophilin3 in regulating cell migration*”. M. Gurjar, and S. N. Dalal.
2. **Gordon Research Seminar on Cell Contact & Adhesion 2013** held at Renaissance Tuscany Il Ciocco Resort in Lucca (Barga) Italy, from June 1, 2013 to June 2, 2013. Presented poster titled, “*Plakophilin3 expression results in an increase in the level of desmosomal components and the formation of calcium*”.

independent desmosomes”. M. Gurjar, K. Raychaudhuri, S. Mahadik, A. Atak, L. Sehgal, M. S. Karkhanis, P. Gosavi and S. N. Dalal.

3. **Gordon Research Conference on Cell Contact & Adhesion 2013** held at Renaissance Tuscany Il Ciocco Resort in Lucca (Barga) Italy, from June 2, 2013 to June 7, 2013. Presented poster titled, “*Plakophilin3 expression results in an increase in the level of desmosomal components and the formation of calcium independent desmosomes*”. M. Gurjar, K. Raychaudhuri, S. Mahadik, A. Atak, L. Sehgal, M. S. Karkhanis, P. Gosavi and S. N. Dalal.
4. **FEBS EMBO 2014 Conference** held at the Palais des Congrès – 2, Place de la Porte Maillot, Paris, France from August 30, 2014 to September, 4 2014. Presented poster titled, “*Plakophilin3 expression results in an increase in the level of desmosomal components and the formation of calcium independent desmosomes*” . M. Gurjar, K. Raychaudhuri, S. Mahadik, A. Atak, L. Sehgal, M. S. Karkhanis, P. Gosavi and S. N. Dalal.

WORKSHOP:

1. **Fourth Bangalore Microscopy Course 2012** held at National Centre for Biological Sciences (NCBS), Bangalore, from September 23, 2012 to September 30, 2012.

ACKNOWLEDGEMENTS

I began my journey in scientific research as a trainee in ACTREC and I am very thankful to Sorab and Dr. Zingde for providing me the opportunity to first work here as an undergraduate trainee. Sorab as my PhD mentor and Dr. Zingde as my doctoral committee ex-chairperson continued to guide me during these past years as a PhD student. Working with Sorab has been a wonderful experience and I am happy to have had his guidance, support and encouragement to work towards my PhD thesis. I am also thankful to all the present and past members of my doctoral committee – Dr. Surekha Zingde, Dr. Rajiv Kalraiya, Dr. Milind Vaidya, Dr. Dibyendu Bhattacharyya and Dr. Prasanna Venkatraman for their support and guidance.

The support of all my lab mates has been instrumental in helping me work towards my thesis. The first lessons in scientific thinking as well as planning and performing experiments came from Elphine and I am very grateful for having her both as a teacher and a friend when I first joined the lab. Dipika, who joined the lab with me, is still my best friend and a great sounding board for talking science and more. Kumar has not only made significant contributions towards my work but also been a pillar of strength in this journey. I would also like to thank trainees that have contributed towards my work – Jervis, Snehal, Apurva, Trupti, Shraddha and Kruthi. I would like to thank all other present and past lab members for their help and support – Amol, Samrat, Prajakta, Amitabha, Lalit, Rashmi, Srikanta, Khrievono, Mugdha, Sonali, Arunabha, Akash, Sarika, Nileema, Pawar, Arun and Vishal.

I am thankful to Dr. Sanjeev Galande and Rahul Jangid from IISER, Pune and Dr. Sanjay Gupta and Divya Reddy for their help in collaborative work. I am also thankful to Dr. Shubha Tole, Dr. Alpha Yap, Dr. Reinhard Windoffer and Dr. Rudolf E.

Leube for providing reagents. I would like to thank Dr. Sudipta Maiti and Dr. Vidita Vaidya for use of their confocal microscope facilities. I would like to thank Dr. Krishanu Ray and Lalit Borde from TIFR for helping with some part of the electron microscopy imaging.

ACTREC has provided an environment that is conducive to research and I would like to thank the Director, Deputy Director and the administration for their efforts in providing a good infrastructure. I would like to thank everyone at the ACTREC microscopy facilities – Tanuja, Jayraj, Mansi and especially Vaishali who contributed significantly in planning some of the experiments. I would also like to thank the ACTREC electron microscopy, genomics, flow cytometry and common instruments room facilities. I would like to thank CSIR, ACTREC, DBT, HBNI and Nature publishing group for financial support. The student community at ACTREC has always been very helpful and it has been a wonderful experience to be a part of it.

Last but not the least; I would like to thank my family and friends for being with me every step of the way.

Mansa Gurjar

TABLE OF CONTENTS

SYNOPSIS OF PH.D. THESIS	21
ABBREVIATIONS.....	35
LIST OF FIGURES	43
LIST OF TABLES.....	45
CHAPTER 1. INTRODUCTION.....	49
1.1. Cell-Cell adhesion	50
1.1. Tight Junctions	51
1.1.1. Components of tight junctions.....	52
1.1.2. Functions of tight junctions	54
1.1.3. Diseases of tight junctions	55
1.2. Adherens Junctions	56
1.2.1. Components of adherens junctions.....	56
1.2.2. Functions of adherens junctions	58
1.2.3. Diseases of adherens junctions	60
1.3. Gap Junctions	60
1.3.1. Components of gap junctions	61
1.3.2. Functions of gap junctions.....	61
1.3.3. Diseases of gap junctions	64
1.4. Desmosomes.....	65
1.4.1. Components of desmosomes	67
1.4.2. Desmosomes are highly insoluble structures.....	70
1.4.3. Functions of desmosomes – “hyperadhesion”	73
1.4.4. Diseases of desmosomes	74
1.4.5. Desmosomal protein functions in cell signalling	76
1.4.6. Desmosomes in cancer	78
1.5. Desmosomal Cadherins	82
1.5.1. Structure of desmosome – desmosomal cadherins	83
1.5.2. Mouse models of desmogleins	84
1.5.3. Mouse models of desmocollins	87
1.6. Desmosomal Plaque Proteins.....	89

1.6.1. Structure of desmosome – the desmosomal plaque.....	91
1.6.2. Mouse models of plakoglobin	92
1.6.3. Mouse models of plakophilins.....	93
1.6.4. Mouse models of desmoplakin	94
1.7. Desmosome assembly	94
1.8. Plakophilin 3	101
1.9. Desmocollin 2	104
1.10. CDX transcription factors.....	107
1.11. C/EBP transcription factors.....	109
1.12. Cell migration	111
1.13. Actin cytoskeleton in cell migration	113
1.14. Actin reorganization regulation by Rho GTPases	117
1.15. Actin reorganization regulating pathways	120
1.16. Epithelial mesenchymal transition	122
1.17. Epithelial markers.....	123
1.18. Mesenchymal markers.....	124
1.19. EMT regulating transcription factors.....	125
CHAPTER 2. AIMS AND OBJECTIVES	131
CHAPTER 3. MATERIALS AND METHODS	135
3.1. Cell lines	135
3.1. Plasmids and constructs	135
3.2. DSC2 shRNA cloning.....	136
3.2.1. shRNA design.....	136
3.2.2. Annealing and phosphorylation of oligos.....	137
3.2.3. Cloning into pLKO.hygro vector.....	138
3.3. Transfection	138
3.4. Lentivirus Production and transduction.....	139
3.5. Calcium switch assays.....	139
3.6. Electron Microscopy	140
3.7. Immunofluorescence and confocal microscopy.....	140
3.8. Hanging drop assays	142
3.9. Western blotting	142

3.9.1. SDS PAGE:	142
3.9.2. Immunoblotting:	144
3.10. Immunoprecipitation	147
3.11. In-vitro GST pulldown	148
3.11.1. Preparation of GST proteins	148
3.11.2. In-vitro GST pulldown	149
3.12. Active Rho-GTPases assay	150
3.12.1. Preparation of GST proteins	150
3.12.2. Active Rho-GTPases pulldown	151
3.13. Luciferase reporter assays	152
3.14. Triton-X soluble and insoluble fractionation	152
3.15. Reverse transcriptase PCR and quantitative real time PCR	153
3.16. mRNA stability assays	154
3.17. Nuclear and cytoplasmic fractionation	155
3.18. Protein stability assays	155
3.19. Fluorescence recovery after photo bleaching (FRAP) for filamentous actin	155
3.20. Cell-extracellular matrix adhesion assays	156
3.21. Immunohistochemistry	156
3.22. Reagents	157
3.22.1. 2x BBS for calcium phosphate transfection	157
3.22.2. PBS(phosphate-buffered saline)	157
3.22.3. Laemmli's buffer	157
3.22.4. 30% acrylamide/0.8% bisacrylamide	157
3.22.5. 10x Running buffer (SDS-PAGE)	158
3.22.6. Transfer Buffer:	158
3.22.7. TBST	158
CHAPTER 4. RESULTS	161
4.1. Role of PKP3, adherens junctions and actin cytoskeleton in initiation of desmosome formation and regulation of desmosome size and assembly. ..	161
4.1.1. DsRed tagged PKP3 localizes to the cell border independent of calcium concentration	162
4.1.2. PKP3 overexpression increases cell-cell adhesion	165

4.1.3. PKP3 overexpression increases desmosome size	169
4.1.4. PKP3 overexpression increases cell membrane/ border localization of other desmosomal proteins	171
4.1.5. PKP3 overexpression increases total protein levels of other desmosomal proteins and mRNA levels of DSC2.....	181
4.1.6. PKP3 overexpression does not stabilize DSC2 mRNA.....	185
4.1.7. PKP3 overexpression leads to an increase in nuclear localization of C/EBP α and PKP3 interacts with C/EBP α	188
4.1.8. Increased DSC2 expression in DsRed PKP3 over expressing cells is not necessary and sufficient for all the phenotypes observed on PKP3 overexpression	195
4.1.9. How does DsRed PKP3 overexpression lead to an increase in the protein levels of other desmosomal proteins.....	199
4.2. Identification of changes in actin filament dynamics and modifications induced by PKP3 loss and their relevance to cell adhesion, migration and metastasis.	203
4.2.1. Does PKP3 knockdown have an effect on actin filament formation?	203
4.2.2. PKP3 knockdown increases Myosin IIA protein levels	205
4.2.3. PKP3 knockdown does not have an effect on the activity of small Rho GTPases	207
4.2.4. PKP3 interacts with actin regulating proteins like PAK1, RhoA and filamin A	209
4.3. Role of PKP3 in regulating cell adhesion, cell migration and EMT. ..	216
4.3.1. PKP3 loss does not lead to EMT in vitro and in vivo	216
CHAPTER 5. DISCUSSION	223
5.1. Role of PKP3, adherens junctions and actin cytoskeleton in initiation of desmosome formation and regulation of desmosome size and assembly...	223
5.2. Identification of changes in actin filament dynamics and modifications induced by PKP3 loss and their relevance to cell adhesion, migration and metastasis.	229
5.3. Role of PKP3 in regulating cell adhesion, cell migration and EMT. ..	233
CHAPTER 6. REFERENCES	237
REPRINTS OF PUBLISHED PAPERS FROM THESIS	274

SYNOPSIS



Homi Bhabha National Institute

Ph. D. PROGRAMME

SYNOPSIS OF PH.D. THESIS

- 1. Name of the Student: Mansa Gurjar.**
- 2. Name of the Constituent Institution: Tata Memorial Centre, ACTREC**
- 3. Enrolment No.: LIFE09200904008.**
- 4. Title of the Thesis: The role of plakophilin3 in regulating cell adhesion, cell migration and Epithelial Mesenchymal Transition (EMT).**
- 5. Board of Studies: Life Sciences**

INTRODUCTION:

Desmosomes are calcium dependent adherens like junctions found in all epithelial tissues and in cardiac muscles, that mediate cell-cell adhesion (1). Desmosomes are composed of the desmosomal cadherins - desmocollins and desmogleins, which are transmembrane proteins that form a zipper like structure on the extracellular face of the cell membrane through calcium dependent homophillic and heterophillic interactions resulting in cell-cell adhesion (1). The desmosomal plaque proteins are present on the intracellular face of the desmosome and include the armadillo family proteins, plakoglobin and the plakophilins, and the plakin family member desmoplakin. Desmoplakin interacts with the intermediate filament cytoskeleton creating an intercellular network that provides mechanical strength and rigidity to the tissue (1).

Plakophilins are desmosomal plaque proteins which belong to the p120^{ctn} subfamily of armadillo repeat containing proteins. Plakophilin 3 (PKP3) is the most ubiquitously expressed member of the plakophilin family of desmosomal plaque proteins. A complex between PKP3, plakoglobin and E-cadherin is present at the cell membrane in the absence of calcium and loss of any of these proteins prevents desmosome formation upon addition of calcium to the medium (2-4). Our lab has previously reported that loss of PKP3 results in increased tumour formation and metastasis *in vivo*. This is characterised by a decrease in desmosome size and cell-cell adhesion and an increase in cell migration and anchorage independent growth (5). The mechanisms by which PKP3 loss results in these phenotypes needs further investigation and whether PKP3 overexpression can lead to inverse phenotypes.

Loss of PKP3 leads to increased cell migration (5). During cell migration, epithelial cells undergo a major morphological change to lead to formation of structures like filopodia and lamellipodia. These morphological changes are driven by rearrangements of the actin cytoskeleton of the cell and the energy for cell motility is also derived from the ATP hydrolysis within the actin filaments. Thus the actin cytoskeleton has a major role to play in cell migration (6). Therefore, PKP3 loss might lead to changes in the regulation of actin reorganization and turnover.

ZEB1, an oncogenic transcription factor that promotes epithelial–mesenchymal transition (EMT) leading to a decrease in PKP3 expression at the invasive front of the tumour leading to increased invasiveness and migration of the tumours (7). Consistent with this observation, loss of PKP3 results in increased tumour formation and metastasis in vivo (5). Accumulating evidence suggests a critical role for EMT in cancer progression and metastasis. Further, the activation of EMT results in the dissolution of desmosomes and adherens junctions, permitting mesenchymal cell migration (8). This leads to the hypothesis that PKP3 loss plays a role in induction of EMT.

AIMS AND OBJECTIVES:

1. Role of PKP3, adherens junctions and actin cytoskeleton in initiation of desmosome formation and regulation of desmosome size and assembly.
2. Identification of changes in actin filament dynamics and modifications induced by PKP3 loss and their relevance to cell adhesion, migration and metastasis.
3. Role of PKP3 in regulating cell adhesion, cell migration and EMT.

RESULTS AND DISCUSSION:

1. Role of PKP3, adherens junctions and actin cytoskeleton in initiation of desmosome formation and regulation of desmosome size and assembly.

DsRed PKP3 was overexpressed in HCT116 cells to determine its effect on desmosome formation. Desmosomes are calcium dependent cell-cell adhesion junctions and the localization of desmosomal proteins to the cell border is dependent on calcium (1, 2). Hanging drop assays to measure cell-cell adhesion demonstrated that PKP3 overexpression lead to an increase in cell-cell adhesion in normal calcium as well as low calcium conditions. Similar results were obtained in dispase assays. Electron micrographs show that there is a significant increase in the size of desmosomes on overexpression of DsRed PKP3 in normal calcium as well as low calcium conditions. These results show that the calcium dependency of desmosomes is reduced on overexpression of DsRed PKP3.

Desmosomal proteins like desmocollin 2, desmoglein 2 and desmoplakin do not localize to the cell membrane/ border when cells are grown in low calcium conditions. Plakoglobin and PKP3 also have minimal cell border localization in low calcium conditions. Only on restoring normal calcium levels can these desmosomal proteins localize to the cell membrane/ border and lead to desmosome formation (2). Calcium switch assays demonstrated that overexpressed DsRed PKP3 was retained at the cell border even in low calcium medium and after switch to normal calcium medium there was no significant difference in cell border intensity of DsRed PKP3. Similarly, calcium switch assays followed by immunofluorescence staining showed that the overexpression of DsRed PKP3 leads to an increase in cell border/ membrane localization of desmoplakin, desmoglein2, desmocollin 2/3, plakoglobin and E- cadherin in low calcium medium as well as normal calcium medium. Thus DsRed PKP3 overexpression reduces

the calcium dependency of localization of other desmosomal proteins to the cell border/membrane.

The increased cell border/ membrane localization of desmosomal proteins on DsRed PKP3 overexpression could be attributed to increase in total protein levels in these cells. Western blot showed that the overexpression of DsRed PKP3 leads to an increase in expression of desmosomal proteins like desmoplakin, desmoglein2, desmocollin 2/3, plakoglobin, as well as adherens junction cadherins like E- cadherin and P- cadherin. Reverse transcriptase PCR and quantitative real time PCR for cell-cell adhesion proteins like desmoplakin, desmoglein2, desmocollin 2, plakoglobin, E- cadherin, P- cadherin, β catenin and ZO-I showed that there was a significant increase only in desmocollin 2 (DSC2) mRNA. PKP3 is known to localize to the nucleus and bind to ETV1 transcription factor and this association has been implicated in having a role in neural crest formation (11). Similarly, PKP3 is shown to be a part of RNA stress granules and known to bind to RNA binding proteins like FXR1, G3BP, and PABPC1, and it has been shown to affect mRNA stability of plakophilin 2 and desmoplakin (12, 13).

A knockdown of PKP3 in these cells resulted in a reversal of the increase in cell-cell adhesion, which was accompanied by a decrease in the levels of the different adhesion proteins suggesting that PKP3 over-expression was necessary and sufficient for the increase in cell-cell adhesion. In contrast, inhibiting the expression of DSC2 did not lead to a decrease in the levels of the desmosomal proteins but did lead to a decrease in cell-cell adhesion and defects in localization of the desmosomal proteins to the cell border suggesting that DSC2 expression is essential for desmosome formation.

The C/EBP family of transcription regulating proteins might have a role to play in regulating DSC2 transcription (9). DsRed PKP3 overexpression does not change the

levels of C/EBP α . However, DsRed PKP3 overexpression lead to an increase in nuclear localization of C/EBP α and immunoprecipitation experiments also showed that PKP3 interacts with C/EBP α . These results suggest that PKP3 might stimulate DSC2 expression by regulating the localization of C/EBP α .

2. Identification of changes in actin filament dynamics and modifications induced by PKP3 loss and their relevance to cell adhesion, migration and metastasis.

The increase in cell migration on PKP3 loss could be ascribed to changes in cell morphology brought about by reorganization of the actin cytoskeleton (5, 6). To determine if there was a change in filamentous actin content of the cells on PKP3 loss, FITC-tagged phalloidin staining of the migrating cells at the leading edge of a wounded monolayer in HCT116 based PKP3 knockdown cells was performed to specifically stain filamentous actin. An increase in filamentous actin upon PKP3 loss was observed although Western blots show that the total actin levels in these cells are unaffected. Similarly, FRAP experiments performed on the actin filaments of migrating cells also show that PKP3 knockdown slows the turnover of actin in the filamentous form. This suggests that although actin filament formation is increased due to PKP3 knockdown, due to the shift in the dynamic equilibrium of actin from monomeric form to filamentous form, the rate of reaction to the filamentous form is reduced. These results also suggest that PKP3 knockdown has a stabilizing effect on filamentous actin possibly by affecting dissociation of filamentous actin.

Western blots performed to determine changes in actin reorganization regulating proteins show that PKP3 knockdown decreases the levels of myosin IIA but does not change the expression of Rac 1/2/3, cdc42, RhoA, filamin A, FAK, phospho-FAK, β 1-integrin, α 5-

integrin, afadin 6, N-WASP, profilin, cofilin, phospho-cofilin S3, ERM, phospho-ERM, Mypt1, phospho-Mypt1 S507, Diap1, gelsolin, myosin IIB and myosin IIC. However, real time PCR shows that there is no significant difference in Myosin IIA mRNA levels upon PKP3 loss. Myosin IIA is a motor protein associated with actin filaments in non-muscle cells that has functions in regulating cell contractility. Previous reports suggest that myosin IIA is a tumour suppressor (10) and that myosin IIA knockdown can increase cell motility (11). PKP3 loss decreases myosin IIA protein but has no effect on myosin IIA mRNA. Immunoprecipitation experiments performed to determine if PKP3 loss leads to changes in actin cytoskeleton by interacting with actin reorganization regulating proteins show that PKP3 interacts with PAK1, filamin A and RhoA. GST pulldowns further show that PKP3 interacts with the CRIB domain of PAK1.

3. Role of PKP3 in regulating cell adhesion, cell migration and EMT.

The established regulators of EMT are the transcription factors Snail, Slug, Twist 1 and Zeb 1. Snail, Slug, Twist 1 and Zeb 1 are all known to directly or indirectly repress E-cadherin expression and induce vimentin expression while Slug and Zeb1 are also known to promote dissolution of desmosomes (reviewed in (12)). PKP3 knockdown does not lead to any change in the expression of EMT regulating transcription factors with Snail being the only tested EMT regulating transcription factor that is expressed with no significant difference between the HCT116 derived vector control and the PKP3 knockdown cells. Repression of E-cadherin expression, an adherens cell-cell junction cadherin or change in E-cadherin localization from cell membrane to cytoplasm and induction of vimentin expression, a type III intermediate filament protein, are classical markers of EMT (reviewed in (12)). Previous results from our lab have demonstrated that

vimentin is not expressed in the vector control or the PKP3 knockdown cells (13). We have also observed that PKP3 knockdown does not change E-cadherin localization to the membrane (2). Thus PKP3 knockdown does not lead to change in any of the tested molecular markers of EMT in vitro. An increase in cell migration accompanied by a decrease in cell-ECM adhesion is an important functional change observed in EMT. As our previous results showed that PKP3 knockdown leads to an increase in cell migration (5), we hence investigated whether PKP3 loss also leads to a decrease in cell-ECM adhesion. Pkp3 knockdown does not result in the acquisition of the EMT phenotype of decrease in cell-ECM substrate adhesion. Although PKP3 knockdown did not show expression of EMT markers in vitro, the increased primary tumour growth and lung metastasis observed in immunocompromised mice lead to the question whether an EMT is observed when these cells grow as tumours in immunocompromised mice. Expression of mesenchymal markers like vimentin and MMP9 in the tumour as well as the lung metastasis, in both the vector control as well as the PKP3 knockdown samples of tumours grown in immunocompromised mice show that EMT does indeed take place in vivo, but it is not induced or enhanced by PKP3 knockdown. Thus PKP3 knockdown does not induce or enhance EMT in vivo.

CONCLUSIONS

The overexpression on DsRed tagged PKP3 leads to increase in desmosome size and cell-cell adhesion. This is mediated by an increase in the expression of other desmosomal proteins like desmoplakin, desmoglein2, desmocollin 2/3, plakoglobin, as well as adherens junction cadherin like E-cadherin and an increase in their localization to the cell membrane/ border. Further, DSC2 mRNA is increased upon DsRed PKP3 overexpression

indicating a role for PKP3 in the mRNA stability or transcription of DSC2. The increase in cell migration on PKP3 loss could be mediated by the decrease in myosin IIA motor protein. It might also be attributed to the interaction of PKP3 with actin reorganization regulating proteins like PAK1, RhoA and filamin A. PKP3 loss does not lead to increase in metastasis through induction of the EMT.

FUTURE DIRECTIONS:

The mechanism by which DsRed tagged PKP3 overexpression leads to increase in other desmosomal proteins like desmoplakin, desmoglein2, desmocollin 2/3, plakoglobin, as well as adherens junction cadherin like E- cadherin could be elucidated. Whether the increase in DSC2 mRNA on DsRed PKP3 overexpression is due to increase in mRNA stability or increase in transcription and the role of PKP3 in this process could to be investigated. Further investigation could determine the mechanism by which PKP3 decreases myosin IIA protein levels. The functional significance of the interaction of PKP3 with actin reorganization regulating proteins like PAK1, RhoA and filamin A could be determined. PKP3 loss does not lead to induction of the EMT, however, it does lead to an increase in tumour formation and metastasis and the alternative mechanisms behind this phenomenon could be delineated.

REFERENCES:

1. B. V. Desai, R. M. Harmon, K. J. Green, Desmosomes at a glance. *J Cell Sci* **122**, 4401 (Dec 15, 2009).
2. P. Gosavi *et al.*, E-cadherin and plakoglobin recruit plakophilin3 to the cell border to initiate desmosome assembly. *Cell Mol Life Sci* **68**, 1439 (Apr, 2011).
3. C. Michels, T. Buchta, W. Bloch, T. Krieg, C. M. Niessen, Classical cadherins regulate desmosome formation. *J Invest Dermatol* **129**, 2072 (Aug, 2009).
4. T. Yin *et al.*, Mechanisms of plakoglobin-dependent adhesion: desmosome-specific functions in assembly and regulation by epidermal growth factor receptor. *The Journal of biological chemistry* **280**, 40355 (Dec 2, 2005).
5. S. T. Kundu *et al.*, Plakophilin3 downregulation leads to a decrease in cell adhesion and promotes metastasis. *International journal of cancer* **123**, 2303 (Nov 15, 2008).
6. T. D. Pollard, L. Blanchoin, R. D. Mullins, Actin dynamics. *Journal of cell science* **114**, 3 (Jan, 2001).
7. K. Aigner *et al.*, The transcription factor ZEB1 (deltaEF1) represses Plakophilin 3 during human cancer progression. *FEBS Lett* **581**, 1617 (Apr 17, 2007).
8. J. P. Thiery, Epithelial-mesenchymal transitions in tumour progression. *Nat Rev Cancer* **2**, 442 (Jun, 2002).
9. C. Smith *et al.*, Regulation of desmocollin gene expression in the epidermis: CCAAT/enhancer-binding proteins modulate early and late events in keratinocyte differentiation. *Biochem J* **380**, 757 (Jun 15, 2004).
10. D. Schramek *et al.*, Direct in vivo RNAi screen unveils myosin IIa as a tumor suppressor of squamous cell carcinomas. *Science* **343**, 309 (Jan 17, 2014).

-
11. M. H. Jorrich, W. Shih, S. Yamada, Myosin IIA deficient cells migrate efficiently despite reduced traction forces at cell periphery. *Biol Open* **2**, 368 (Apr 15, 2013).
 12. M. Zeisberg, E. G. Neilson, Biomarkers for epithelial-mesenchymal transitions. *J Clin Invest* **119**, 1429 (Jun, 2009).
 13. N. Khapare *et al.*, Plakophilin3 loss leads to an increase in PRL3 levels promoting K8 dephosphorylation, which is required for transformation and metastasis. *PLoS One* **7**, e38561 (2012).

PUBLICATIONS IN REFEREED JOURNAL:

a. Published

M. Gurjar, K. Raychaudhuri, S. N. Dalal, Loss of the desmosomal plaque protein plakophilin 3 does not induce the epithelial mesenchymal transition. *J Biosci Tech* **6**, 647 (Jan 2015).

b. Other Publications:

1. E. Telles, M. Gurjar, K. Ganti, D. Gupta, S. N. Dalal, Filamin A stimulates cdc25C function and promotes entry into mitosis. *Cell Cycle* **10**, 776 (Mar 1, 2011).
2. L. Sehgal *et al.*, 14-3-3 γ -mediated transport of plakoglobin to the cell border is required for the initiation of desmosome assembly in vitro and in vivo. *Journal of Cell Science* **127**, 2174 (May 15, 2014).
3. K. Raychaudhuri, M. Gurjar, S. N. Dalal, Plakophilin3 and Plakoglobin recycling are differentially regulated during the disassembly of desmosomes. *J Biosci Tech* **6**, 634 (Jan 2015).

CONFERENCES:


1. **Second Global Cancer Genomics Consortium Symposium 2012** held at ACTREC, Kharghar, Navi Mumbai, from November 19, 2012 to November 20, 2012. Presented poster titled, “*The role of plakophilin3 in regulating cell migration*”. M. Gurjar, and S. N. Dalal.
2. **Gordon Research Seminar on Cell Contact & Adhesion 2013** held at Renaissance Tuscany Il Ciocco Resort in Lucca (Barga) Italy, from June 1, 2013 to June 2, 2013. Presented poster titled, “*Plakophilin3 expression results in an increase in the level of desmosomal components and the formation of calcium independent desmosomes*”. M. Gurjar, K. Raychaudhuri, S. Mahadik, A. Atak, L. Sehgal, M. S. Karkhanis, P. Gosavi and S. N. Dalal.
3. **Gordon Research Conference on Cell Contact & Adhesion 2013** held at Renaissance Tuscany Il Ciocco Resort in Lucca (Barga) Italy, from June 2, 2013 to June 7, 2013. Presented poster titled, “*Plakophilin3 expression results in an increase in the level of desmosomal components and the formation of calcium independent desmosomes*”. M. Gurjar, K. Raychaudhuri, S. Mahadik, A. Atak, L. Sehgal, M. S. Karkhanis, P. Gosavi and S. N. Dalal.
4. **FEBS EMBO 2014 Conference** held at the Palais des Congrès – 2, Place de la Porte Maillot, Paris, France from August 30, 2014 to September, 4 2014. Presented poster titled, “*Plakophilin3 expression results in an increase in the level of desmosomal components and the formation of calcium independent desmosomes*” . M. Gurjar, K. Raychaudhuri, S. Mahadik, A. Atak, L. Sehgal, M. S. Karkhanis, P. Gosavi and S. N. Dalal.

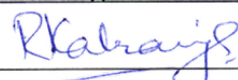

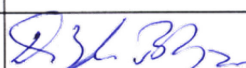
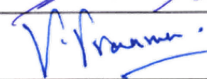
WORKSHOP:

1. **Fourth Bangalore Microscopy Course 2012** held at National Centre for Biological Sciences (NCBS), Bangalore, from September 23, 2012 to September 30, 2012.

Signature of Student:

Date:


 24-3-15
Doctoral Committee:

Sr. No.	Name	Designation	Signature	Date
1	Dr. Rajiv Kalraiya	Chairman		24/3/15
2	Dr. Sorab N. Dalal	Guide & Convener		24/3/15
3	Dr. Dibyendu Bhattacharyya	Member		25/3/15
4	Dr. Prasanna Venkatraman	Member		27/3/15

Forwarded through:


Dr. S.V. Chiplunkar,
Director,
ACTREC-TMC.

Dr. S. V. Chiplunkar
 Director
 Advanced Centre for Treatment, Research &
 Education in Cancer (ACTREC)
 Tata Memorial Centre
 Kharghar, Navi Mumbai 410210.



Dr. K. S. Sharma,
Director Academics,
TMC.

PROF. K. S. SHARMA
 DIRECTOR (ACADEMICS)
 TATA MEMORIAL CENTRE,
 PAREL, MUMBAI

ABBREVIATIONS

1. 14-3-3 = The name 14-3-3 refers to the particular elution and migration pattern of these proteins on DEAE-cellulose chromatography and starch-gel electrophoresis. The 14-3-3 proteins eluted in the 14th fraction of bovine brain homogenate and were found on positions 3.3 of subsequent electrophoresis by Moore and Perez (1967)
2. aa = amino acid
3. ADP = Adenosine diphosphate
4. AF6 = ALL-1 fused gene from chromosome 6, also called as afadin
5. AKT = The "Ak" in Akt was a temporary classification name for a mouse bred and maintained by Jacob Furth that developed spontaneous thymic lymphomas. The "t" stands for 'thymoma'; the letter was added when a transforming retrovirus was isolated from the Ak strain, which was termed "Akt-8". When the oncogene encoded in this virus was discovered, it was termed v-Akt. Thus, the later identified human analogues were named accordingly. Also called PKB or protein kinase B.
6. aPKC = atypical protein kinase C
7. ATP = Adenosine triphosphate
8. Bcl-2 = B-cell CLL (Chronic Lymphocytic Leukaemia) / lymphoma 2
9. C/EBP = CCAAT/ enhancer-binding protein
10. cAMP = Adenosine 3'5' cyclic monophosphate

11. CAR = Coxsackie adenovirus receptor
12. Cdc42 = cell division cycle 42
13. CDH1 = cadherin 1, E-cadherin
14. CDRE = canonical CDX response element
15. CDX = caudal type homeobox
16. CDX2-AS = CDX2 alternatively spliced
17. c-Myc = myelocytomatosis viral oncogene, cellular homologue
18. Cox-2 = cyclooxygenase-2
19. CpG = A C (cytosine) base followed immediately by a G (guanine) base (a CpG).
20. CRC = colorectal carcinoma
21. C-TAK1 = Cdc25C-associated kinase 1
22. Cx = connexin
23. DFNB49 = nonsyndromic deafness, autosomal recessive (dominant is termed as A, recessive is termed as B) type 49
24. Dlg = disc large protein
25. DM = dense midline
26. Dp, DP = desmoplakin
27. Dsc/ DSC = desmocollin
28. Dsg/ DSG = desmoglein

-
29. EC = extracellular cadherin repeats
 30. EDA = ectodysplasin-A
 31. EDAR = ectodysplasin-A receptor
 32. EDTA = Ethylene diamine tetraacetic acid
 33. EGA = estimated gestational age
 34. EGF = epidermal growth factor
 35. EGFR = epidermal growth factor receptor
 36. EGTA = Ethylene glycol tetraacetic acid
 37. EMT = Epithelial mesenchymal transition
 38. EPLIN = epithelial protein lost in neoplasm; also known as Lima-1
 39. ERK = extracellular signal-regulated kinases
 40. ESAM = endothelial cell-selective adhesion molecule
 41. FAK = focal adhesion kinase
 42. FGF = Fibroblast growth factor
 43. FXR1 = fragile-X-related protein
 44. G3BP = ras-GAP-SH3-binding protein
 45. GJ = gap junction
 46. GUK = guanylate kinase

- 47. IAP = intestinal alkaline phosphatase
- 48. IDP = inner dense plaque
- 49. IF = intermediate filament
- 50. IP3 = Inositol trisphosphate
- 51. JACOP = junction-associated coiled-coil protein
- 52. JAM4 = Junctional adhesion molecule 4
- 53. JAM-A = Junctional adhesion molecule A
- 54. KU70/80 complex = Ku is a nuclear protein originally identified by Mimori et al. (1981) as an autoantigen that was recognized by the sera of a Japanese patient with scleroderma polymyositis overlap syndrome. The name Ku was derived from the first two letters of the family name of this patient. Autoantibodies against Ku are also found in patients with other autoimmune diseases, e.g., systemic lupus erythematosus and scleroderma. The human Ku protein is a complex composed of two protein subunits of about 70 and 80 kDa
- 55. LEF = lymphoid enhancer factor
- 56. Lgl = Lethal giant larvae
- 57. Lis1 = Lissencephaly-1
- 58. LOH = loss of heterozygosity
- 59. MAGI = membrane-associated guanylate kinase inverted
- 60. MAGUK = membrane-associated guanylate kinase

-
61. MAPK = Mitogen-Activated Protein Kinase
 62. MDCK = Marine Darby Canine Kidney epithelial cells
 63. MEK = Mitogen/Extracellular signal-regulated kinase. Also known as MAPKK or Mitogen-activated protein kinase kinase
 64. miR = microRNA
 65. MMP = matrix metalloproteinase
 66. MS4A12 = membrane-spanning 4-domains, subfamily A, member 12
 67. MUPP1 = multi-PDZ domain protein-1
 68. NaOH = sodium hydroxide
 69. Nde1 = nuclear distribution E (NudE) family neurodevelopment protein 1
 70. NF- κ B = nuclear factor kappa-light-chain-enhancer of activated B cells
 71. NM-IF = nuclear matrix – intermediate filament
 72. Nrf-2 = nuclear factor erythroid 2–related factor 2
 73. NSCLC = non-small cell lung cancers
 74. ODP = outer dense plaque
 75. p27Kip1 = cyclin-dependent kinase inhibitor 1B (p27, Kip1)
 76. PABPC1 = Poly (A) binding protein
 77. PAGE = polyacrylamide gel electrophoresis
 78. Par3 = Partitioning protein 3
-

- 79. Par6 = Partitioning protein 6
- 80. PATJ = Pals1-associated tight junction protein
- 81. PCR = polymerase chain reaction
- 82. PDZ = PDZ is an acronym combining the first letters of three proteins — post synaptic density protein (PSD95), Drosophila disc large tumour suppressor (Dlg1), and zonula occludens-1 protein (zo-1) — which were first discovered to share the domain. Also called DHR (Dlg homologous region) or GLGF (relatively well conserved tetra peptide in these domains)
- 83. PERP = p53 apoptosis effector related to PMP-22\
- 84. PF = Pemphigus foliaceus
- 85. Pg/ PG = plakoglobin
- 86. PGE2 = prostaglandin E2
- 87. PI3K = phosphoinositide-3-kinase
- 88. PKC = protein kinase C
- 89. Pkp/ PKP = plakophilin
- 90. PLEKHA7 = pleckstrin homology domain containing, family A member 7
- 91. PM = plasma membrane
- 92. PPAR γ = peroxisome proliferator-activated receptor gamma
- 93. PrP(c) = prion protein Common or Cellular
- 94. Ptk7 = protein tyrosine kinase 7

-
95. PV = Pemphigus vulgaris
 96. RA = Retinoic acid
 97. Rap1 = Ras-proximate-1 or Ras-related protein 1 GTPase
 98. RPC155 = RNA polymerase III 155kDA polypeptide, also known as POLR3A
 99. RT-PCR = reverse transcriptase PCR
 100. SCC = squamous cell carcinoma
 101. Scrib = scribble
 102. SDS = sodium dodecyl sulphate
 103. Sec = secretory pathway
 104. SERCA2 = Sarcoendoplasmic reticulum Ca^{+2} -ATPase isoform 2
 105. SH3 = Src (Sarcoma) Homology 3 Domain
 106. siRNA = small interfering RNA
 107. SLC5A8 = Solute carrier family 5, member 8
 108. Src = Sarcoma family kinases
 109. STAT3 = Signal transducer and activator of transcription 3
 110. TCF = T-cell specific, HMG-box transcription factor
 111. TER = transepithelial resistance
 112. TPA = 12-O-tetradecanoyl-phorbol-13-acetate

- 113. UPF1 = Up-frameshift suppressor 1 homolog
- 114. Wnt = identified as 'wingless' in *Drosophila* and 'int1' in mice - the int/ Wingless family was renamed the Wnt family and int1 became Wnt1
- 115. ZEB = Zinc finger E-box-binding homeobox
- 116. ZO = zonula occludens
- 117. ZONAB = ZO-1-associated nucleic acid binding protein

LIST OF FIGURES

Figure 1.1. Tissue organization in an organ: Lumen of the gut.....	49
Figure 1.2. Electron micrograph of a tight junction.....	51
Figure 1.3. Schematic of tight junctions	53
Figure 1.4. Electron micrograph of an adherens junction between two murine intestinal epithelial cells	57
Figure 1.5. Schematic of the cadherin-catenin complex of adherens junctions.....	58
Figure 1.6. Electron micrograph of a gap junction	62
Figure 1.7. Schematic of gap junctions.....	63
Figure 1.8. Schematic of desmosomes superimposed on an electron micrograph of a desmosome.....	66
Figure 1.9. Schematic of different isoforms of plakophilins, desmogleins and desmocollins being expressed during various stages of keratinocyte differentiation in the epidermis.....	68
Figure 1.10. Schematic of domains of different desmosomal proteins.....	69
Figure 1.11. Desmosomes are highly insoluble structures, part of the NM-IF pool.....	71
Figure 1.12. Desmosomal adhesion downregulation as a part of multistep process of tumour development	78
Figure 1.13. Loss of desmosomes can lead to cancer progression through multiple pathways	80
Figure 1.14. Arrangement of desmosomal cadherins genes on a section of 18q12.1 human chromosome.....	82
Figure 1.15. Electron micrographs depicting desmosome formation	95
Figure 1.16. DSC2 promoter.....	105
Figure 1.17. C/EBP family proteins.....	110
Figure 1.18. A migrating cell.....	112
Figure 1.19. Types of actomyosin stress fibres.....	114
Figure 1.20. Rho GTPase cycling	119
Figure 1.21. All roads lead to actin polymerization.....	120
Figure 1.22. Actin dynamics	121
Figure 1.23. EMT transcription factors.....	127
Figure 4.1. DsRed PKP3 co-localizes with GFP-DSC2a and YFP-E-cadherin	163
Figure 4.2. DsRed PKP3 overexpression leads to calcium independent localization of DsRed PKP3 to the cell border	164
Figure 4.3. PKP3 overexpression increases de novo cell-cell adhesion	166
Figure 4.4. PKP3 overexpression increases retention of cell-cell adhesion	167
Figure 4.5. PKP3 overexpression is necessary and sufficient to increase cell-cell adhesion.....	168
Figure 4.6. PKP3 overexpression increases desmosome size.....	169
Figure 4.7. PKP3 overexpression increases desmosome size in a calcium switch assay ..	171
Figure 4.8. PKP3 overexpression increases cell membrane localization of desmocollin 2/3.....	173
Figure 4.9. PKP3 overexpression increases cell membrane localization of desmoglein 2	174
Figure 4.10. PKP3 overexpression increases cell border localization of desmoplakin	175
Figure 4.11. PKP3 overexpression increases cell border localization of plakoglobin.....	176
Figure 4.12. PKP3 overexpression increases cell membrane localization of E-cadherin..	177
Figure 4.13. PKP3 overexpression increases cell border localization of p120 catenin	178
Figure 4.14. PKP3 overexpression is necessary and sufficient for increase in cell border localization of desmoplakin	179

Figure 4.15. PKP3 overexpression is necessary and sufficient for increase in cell membrane localization of desmoglein 2	180
Figure 4.16. DsRed PKP3 overexpression leads to an increase in other desmosomal proteins.....	182
Figure 4.17. DsRed PKP3 overexpression leads to an increase in DSC2 mRNA.....	183
Figure 4.18. DsRed PKP3 overexpression is necessary and sufficient increase in	185
Figure 4.19. PKP3 overexpression does not stabilize DSC2 mRNA	186
Figure 4.20. DsRed PKP3 overexpression does not change expression of transcription factors known to regulate DSC2 expression.....	189
Figure 4.21. DsRed PKP3 overexpression leads to an increase in nuclear localization of the transcription factor C/EBP α and, PKP3 interacts with C/EBP α	191
Figure 4.22. DsRed PKP3 overexpression does not change localization of the transcription factors C/EBP β and C/EBP δ	192
Figure 4.23. Effect of C/EBP α , β and δ knockdown on DSC2 expression up on DsRed PKP3 overexpression.....	193
Figure 4.24. Increase in cell-cell adhesion on PKP3 overexpression is dependent on increase in DSC2 transcription	194
Figure 4.25. Increase in cell border localization of desmoplakin on PKP3 overexpression is dependent on increase in DSC2 transcription	196
Figure 4.26. Increase in cell border localization of desmoglein 2 on PKP3 overexpression is dependent on increase in DSC2 transcription	197
Figure 4.27. Increase in expression of other desmosomal proteins on PKP3 overexpression is NOT dependent on increase in DSC2 transcription.....	198
Figure 4.28. Desmosomal protein stability is not affected by proteasomal and lysosomal inhibitors	201
Figure 4.29. Desmosomal protein stability is beyond the detection limit of cycloheximide chase assays	201
Figure 4.30. PKP3 overexpression leads to a decrease in the Triton soluble fraction and an increase in the Triton insoluble fraction of other desmosomal proteins.....	202
Figure 4.31. PKP3 knockdown shifts the equilibrium between G-actin and F-actin to F-actin.....	205
Figure 4.32. PKP3 knockdown slows F-actin turnover in dorsal stress fibres	207
Figure 4.33. PKP3 knockdown slows F-actin turnover in ventral stress fibres.....	209
Figure 4.34. PKP3 knockdown reduces Myosin IIA protein levels, but does not affect Myosin IIA mRNA	210
Figure 4.35. PKP3 knockdown does not have an effect on the activity of small Rho GTPases	211
Figure 4.36. PKP3 knockdown does not have an effect on the activity of small Rho GTPases, except in the context of de novo cell-cell adhesion junction formation.....	212
Figure 4.37. PKP3 interacts with the actin regulating protein like PAK1	214
Figure 4.38. PKP3 interacts with actin regulating proteins like RhoA and filamin A	216
Figure 4.39. Plakophilin 3 knockdown does not lead to EMT in vitro.....	219
Figure 4.40. Plakophilin 3 knockdown does induce EMT in vivo	220
Figure 5.1. Model showing how PKP3 overexpression can lead to increase in cell-cell adhesion.	228
Figure 5.2. Model showing how PKP3 loss could lead to increased cell migration.....	233

LIST OF TABLES

Table 3.1. List of primers used for cloning.....	137
Table 3.2. List of antibodies used for immunofluorescence.....	142
Table 3.3. Table for making resolving gel for SDS-PAGE	143
Table 3.4. Table for making stacking gel for SDS-PAGE.....	143
Table 3.5. List of antibodies used for Western blotting.....	147
Table 3.6. List of primers used for RT-PCR.....	154

INTRODUCTION

1. INTRODUCTION

A simple hierarchy of the constitution of an organism is as such – organisms are made of organs, organs are made of tissues, tissues are made of cells, cells made of organelles and organelles are made of biomolecules. Cell-cell adhesion is the property of cells to “stick” to each other and forms the basis of tissue architecture. Different types of tissues like epithelial tissues, connective tissues, muscles, etc. have varying requirements of cell adhesion owing to the differences in their tissue architecture (Figure 1.1).

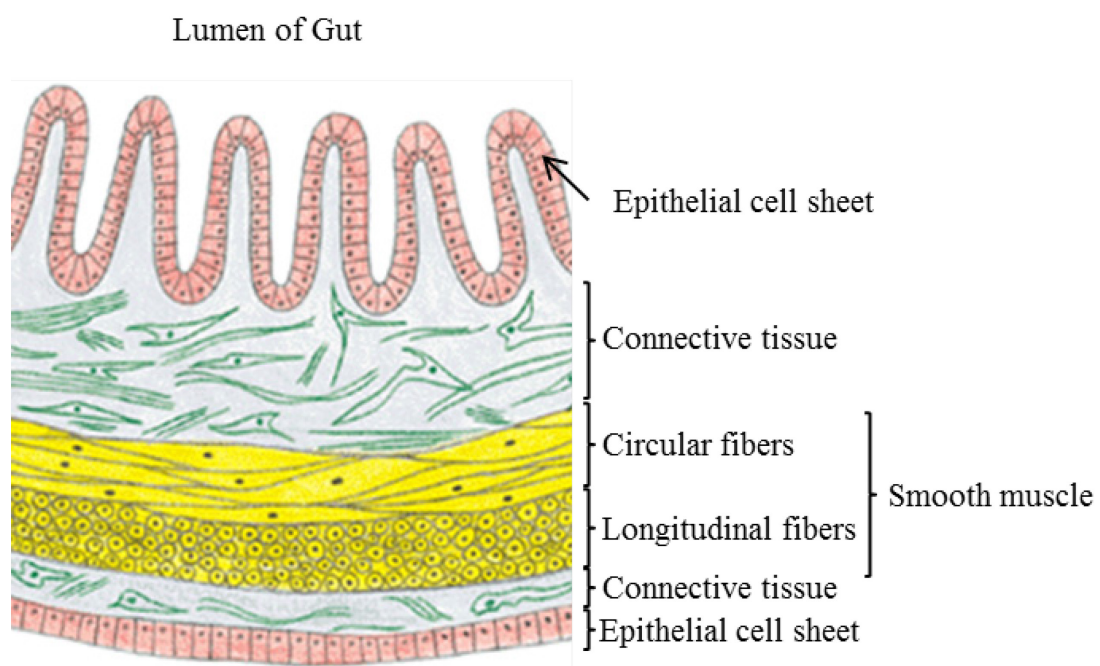


Figure 1.1. Tissue organization in an organ: Lumen of the gut – As a representative of the tissue organization in an organ, the lumen of the gut shows the placement of the different types of tissues and the distinctive architecture of tissue organization for each types of tissue (Adapted from [8]).

1.1. Cell-Cell adhesion

The topic of this thesis focuses on the cell-cell adhesion junctions formed in epithelial tissues, and as such the use of this term in the thesis will always refer to epithelial cell-cell adhesions. Cell-cell adhesion junctions in other tissues have many similarities to epithelial cell-cell junctions as well as many distinguishing characteristics which are beyond the scope of discussion of the current topic. Epithelial tissues have a defined packed structure and are formed on a thin basal lamina of extracellular matrix followed by a layer of connective tissue that is mostly composed of extracellular matrix (Figure 1.1). The different types of epithelial cell-cell junctions are:

1. Tight junctions
2. Adherens junctions
3. Desmosomes
4. Gap junctions

Cell-cell adhesion junctions help maintain epithelial cell structure and cell polarity and importantly lay the foundation for tissue formation and integrity. Even during cell division, cell-cell junctions are maintained [21]. Cell-cell adhesion junctions provide mechanical strength to tissues, form tissue barriers, and drive selective affinity towards cells of the same tissue [8, 22]. Cell-cell adhesion junctions are dynamic structures that are reorganized and recycled during tissue formation, tissue morphogenesis and tissue repair. Deregulation of this process of assembly and disassembly of cell-cell junctions' leads to diseases which disrupt the functions of epithelial tissues and is also part of the process of transformation of epithelial cells into carcinomas having invasive

and metastatic properties. Both of these phenomena will be discussed in greater detail later in this chapter.

1.1. Tight Junctions

Tight junctions are calcium dependent cell-cell adhesion junctions present at the apical end of the lateral membrane between two epithelial cells in a tissue that forms a barrier. Tight junctions are localized at the region with the apposing cell membranes such that this region appears to be “pinched” when observed under an electron microscope with a marked exclusion of an intercellular gap (Figure 1.2). Recent studies have defined the barrier created by the tight junctions as permselectivity – selective permeability based

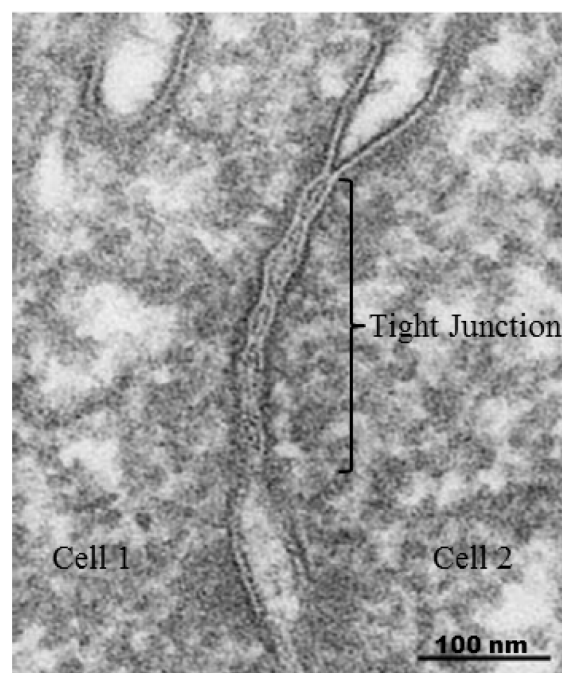


Figure 1.2. Electron micrograph of a tight junction – The plasma membranes of the apposing cells give a “pinched” appearance (Adapted from [14])

on size, electrical resistance, and ionic charge that is stringently regulated by the molecular components of the tight junctions (reviewed in [23]). In freeze fracture EM images, the “pinched” part of the tight junctions corresponds to continuous rows of 10-nm

transmembrane particles presumed to contain an oligomerized array of claudins (Figure 1.2) (reviewed in [23]). Tight junctions are found in epithelial tissues, endothelial tissues and in myelin sheaths and as such are responsible for formation of skin barrier, blood-brain barrier, blood-testis barrier and the intestinal gut epithelium barrier (reviewed in [14]).

1.1.1. Components of tight junctions

Tight junction components can be divided into transmembrane proteins and plaque proteins. Transmembrane proteins include – claudins, occludin and tricellulin, immunoglobulin superfamily membrane proteins with two extracellular Ig-like domains – JAM-A, JAM4, coxsackie adenovirus receptor (CAR), and endothelial cell-selective adhesion molecule (ESAM). Cytoplasmic plaque proteins include – the membrane-associated guanylate kinase (MAGUK) family having PDZ domains like ZO-1, ZO-2 and ZO-3, PDZ domain containing MAGUK-like family proteins like MAGI-1, MAGI-3, MUPP1 and PATJ, coiled-coil domains containing proteins like cingulin and JACOP/paracingulin, and the cytoskeleton attachments – actin cytoskeleton attachment by ZO proteins and cingulin (Figure 1.3). Signalling proteins such as aPKC-Par3-Par6 complex localize to the cytoplasmic side of the tight junctions and regulate mature tight junction formation and epithelial polarity (reviewed in [14]).

Occludin and claudins have 4 transmembrane domains with two extracellular loops but absolutely no sequence similarities. There are over 20 isoforms of claudins identified in human and mice with molecular weights ranging from 21 to 28 kDa that show tissue specific expression. The claudins and they are known to engage in homotypic as well as very specific heterotypic interactions within the same cell as well as between apposing cells. Claudins are palmitoylated at CxxC motifs in two membrane proximal

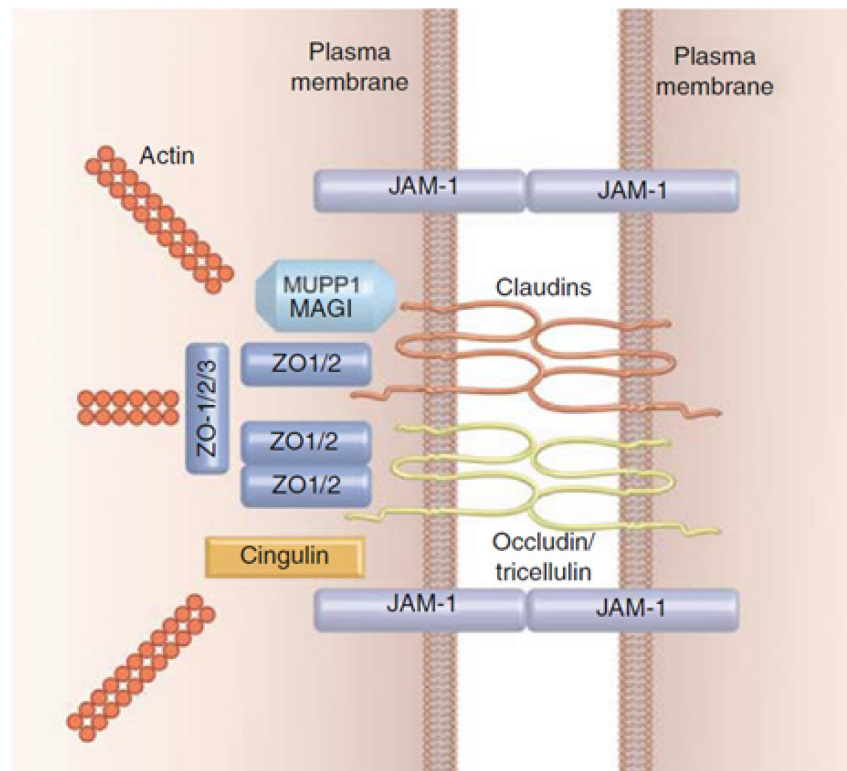


Figure 1.3. Schematic of tight junctions – *The MAGUK family ZO proteins and cingulin anchor the actin cytoskeleton to the tight junctions (Reproduced from [12]).*

regions and phosphorylated at serine or threonine residues in the cytoplasmic carboxyl terminal. Occludin is an approximately 65 kDa protein that is highly phosphorylated at multiple serine and threonine residues. Both claudins and occludin, at their carboxyl terminals, interact with the MAGUK family proteins. Tricellulin also has four transmembrane domains and is predominantly present in tight junctions at tricellular edges. Tricellulin binds the MAGUK family protein ZO-1 at the cytoplasmic carboxyl terminal and has been shown to be responsible for recessive, nonsyndromic deafness DFNB49 (reviewed in [14]).

The MAGUK family proteins ZO-1, ZO-2 and ZO-3 are capable of interacting with all the transmembrane tight junction proteins and function as scaffolds in the cytoplasmic plaque of tight junctions that connect the tight junctions to the actin

cytoskeleton as well as recruit other structural and signalling proteins to the tight junction (Figure 1.3). ZO-1 and ZO-2 are indispensable for tight junction formation. The SH3-GUK module of ZO-1 is known to interact with adherens junction proteins like α -catenin and afadin and this interaction has been implicated to be important for the recruitment of ZO-1 to the membrane proximal region. The MAGUK family proteins are also important in the maturation of adherens junctions from spot like junctions to belt like junctions with linear actin cables. ZO-1 and ZO-2 are also required for Rac 1 RhoGTPase activation and myosin II recruitment during adherens junction maturation. These along with other observations support the hypothesis that ZO-1 and ZO-2 are involved in sequential steps in the assembly of adherens junctions and tight junctions as well as their physical segregation in the membrane (reviewed in [14]).

1.1.2. Functions of tight junctions

The paracellular barrier formed by the tight junctions is proposed to have two physiologic components: a system of charge-selective small pores, 4 Å in radius, and a second system created by larger discontinuities in the barrier, lacking charge or size specificity. The first system is influenced by claudin expression patterns and the second non-pore pathway is controlled by pro-inflammatory cytokines, cytoskeletal dynamics, myosin light chain activity and any factor affecting cell homeostasis (reviewed in [23]). Tissues having different claudin expression patterns show varying degrees of permselectivity. Classically, the “tight” ness or “leaky” ness of a tight junction is represented by electrical conductance across the epithelial tissue in the terms of transepithelial resistance (TER). TER of the proximal tubule in dogs is as low as 7 $\Omega \cdot \text{cm}^2$ while that of a rabbit’s urinary bladder is as high as 300,000 $\Omega \cdot \text{cm}^2$. High TER corresponds to “tight” tight junctions, which can maintain high electrochemical gradients

by active trans-cellular transport, whereas low TER corresponds to “leaky” tight junctions, which have high permeability and allow para-cellular transport. It should be noted that even when the TER is low, para-cellular transport is charge selective and generally shows a preference for Na^+ ions over Cl^- ions with the ratio differing from 10 to 0.1 [23]. The TER is dependent on the claudin expression pattern of a particular tight junction (reviewed in [23]). Thus, apart from electrical resistance, the permselectivity of tight junctions also leads to an ionic charge selective barrier. Similarly, the pore size determines a size discrimination based paracellular transport. Finally, the magnitude of the solute permeability is also determined by the cell geometry and the claudin composition of the tight junctions (reviewed in [23]). The complex nature of the tight junctions and the wide array of proteins expressed by them lead to a many diverse functional characteristics like regulation of cell polarity, signalling, transcription, cell cycle and vesicle trafficking (reviewed in [23]).

1.1.3. Diseases of tight junctions

There are seven known human diseases caused by mutations in tight junction proteins. The best studied of these diseases is Hypomagnesaemia hypercalciuria with nephrocalcinosis caused by mutations in the claudin-16 or claudin-19 gene that leads to defective renal Mg^{+2} reabsorption (reviewed in [23, 24]). The expression of tight junction proteins is also affected in different types of carcinomas. Low expression of ZO proteins is linked with poor prognosis while overexpression of ZONAB, a transcription factor that is regulated by ZO proteins, is upregulated in hepatocellular carcinomas (reviewed in [23, 24]). Tight junction proteins localization to the membrane as well as expression is lost during epithelial mesenchymal transition (EMT) and these proteins are often used as biomarkers of epithelial phenotype (reviewed in [25]). Claudin-1 has been shown to

promote transformation and metastasis in colon cancers (reviewed in [24]). Likewise, claudins, CAR, JAM-A and other tight junction proteins are also known to be targeted by pathogens to gain entry within the host cells (reviewed in [24]).

1.2. Adherens Junctions

Adherens junctions are calcium dependent cell-cell junctions that form the “adhesion belt” or “zonula adherens” just below the tight junctions in the apical region of epithelial cells characterised by 10 – 20 nm space between the apposing plasma membranes (Figure 1.4).

1.2.1. Components of adherens junctions

The calcium binding trans-membrane components of adherens junctions are termed as classical cadherins, namely – E-cadherin, P-cadherin and N-cadherin, the cytoplasmic proteins that bind the cadherins are termed as catenins, namely – p120 catenin, β -catenin and plakoglobin (also known as γ -catenin). α -catenin binds to β -catenin and anchors the actin cytoskeleton of the cell through EPLIN to the adherens junctions (reviewed in [26]). The homophillic interactions of cadherins from neighbouring cells in the presence of calcium initiates cell-cell contact and is also responsible for sorting of different cell types during tissue formation (reviewed in [26]). The catenins have a variety of binding partners and these interactions affect the strength and stability of cell-cell contacts as well as perform cell signalling functions and aide in mechanosensing (reviewed in [26, 27]) (Figure 1.5). Microtubule plus ends have been shown to be targeted to adherens junctions in a CLIP-170 dependent manner, while dynein has been shown to interact with β -catenin and proposed to tether microtubules to adherens junctions. Recent

Adherens Junction

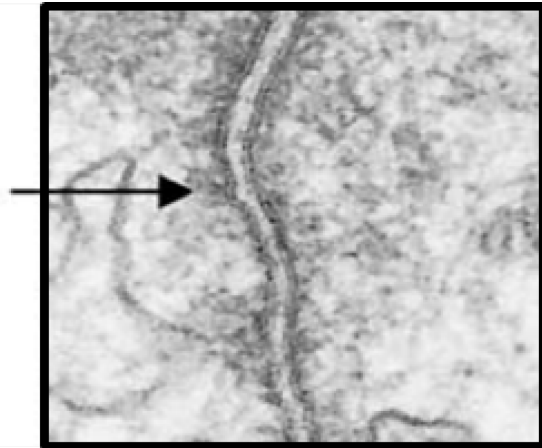


Figure 1.4. Electron micrograph of an adherens junction between two murine intestinal epithelial cells (*Adapted from [2]*).

studies have also shown microtubule minus ends to interact with adherens junctions via p120 catenin and the PLEKHA7–Nezha complex. Cadherins have also been shown to interact with polarity determining proteins like Par3 and Par6 of the aPKC-Par3-Par6 complex located at the apical edge of the epithelial cells as well as the Scrib-Dlg-Lgl complex localized at the lateral membrane (reviewed in [26]).

Adherens junctions also have calcium independent adhesions formed by nectin-afadin complexes. Nectins are immunoglobulin like transmembrane proteins with four isoforms that associate with AF6/ afadin at the cytoplasmic carboxyl- terminal PDZ domain of the nectins. Afadin is an actin binding protein that binds to α -catenin and might link the nectin-afadin complex to the cadherin-catenin complex and anchor actin filaments to adherens junctions. Nectins are also shown to have stronger heterophillic interactions rather than homophillic interactions and promote adhesion between heterotypic cell-cell contacts like neuronal synapse formation by recruiting cadherins (reviewed in [26]).

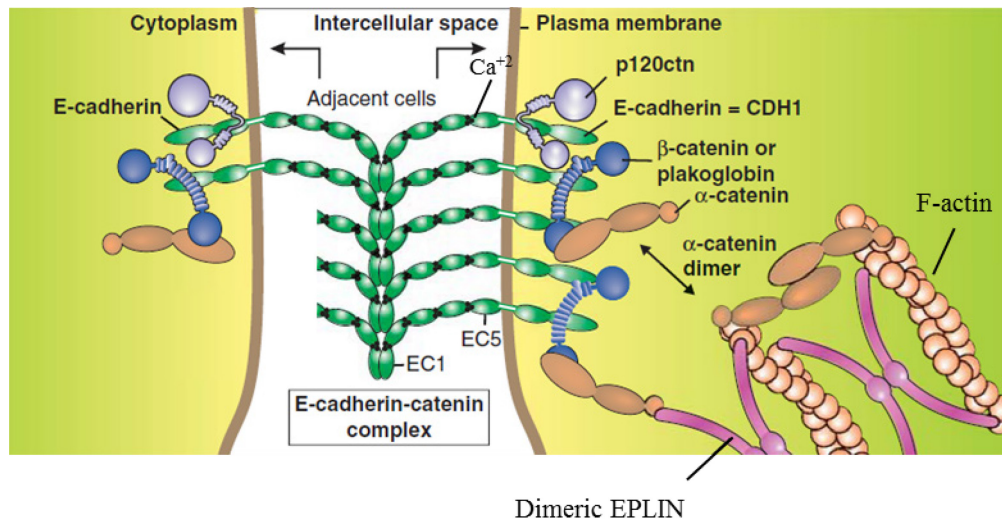


Figure 1.5. Schematic of the cadherin-catenin complex of adherens junctions – *E-cadherin has 5 extracellular cadherin repeats (EC) with calcium binding pockets in between two EC domains. E-cadherins of neighbouring cells interact in homophilic manner to give rise to the adhesion between the two cells. The membrane proximal cytoplasmic domain of E-cadherin interacts with p120 catenin whereas the carboxyl terminal tail of E-cadherin interacts with β-catenin or plakoglobin which in turn interact with monomeric α-catenin. Dimeric α-catenin can cross-link filamentous actin (F-actin) which is anchored to the cadherin-catenin complex by dimeric EPLIN and α-catenin (Adapted from [18]).*

1.2.2. Functions of adherens junctions

The major function of adherens junctions is to maintain adhesion between cells and the disruption of adherens junctions leads to a disruption of tissue architecture. Adherens junctions are the first cell-cell adhesion junctions formed between the apposing plasma membranes of two cells and they are required for the assembly of tight junctions as well as desmosomes ([28] and reviewed in [29]). The binding of Ca²⁺ ions in the extracellular domains of the cadherins causes a conformational change that enables the

formation of homophillic cadherin interactions between the neighbouring cells and, the use of Ca^{+2} chelators like EDTA and EGTA causes dissociation of adherens junctions (reviewed in [26]).

Adherens junctions in tissues might appear as stable structures but they are highly dynamic in nature. Cadherins are synthesized and transferred from the Golgi to the adherens junctions via an exocyst dependent mechanism and recycled through endosomes (reviewed in [26]). The localization of the cadherin-exocyst complex to the apical surface is regulated by PALS1, a component of tight junctions (reviewed in [26]). Several pathways regulate the localization and stability of cadherins at the cell membrane, thus governing junction formation. The interaction of p120 with afadin strengthens the p120-cadherin bond in a Rap1 dependent manner and p120 catenin masks a dileucine motif on the juxtamembrane region of the cytoplasmic domain of cadherins that is responsible for endocytosis and thus stabilizes the cadherins at the cell membrane (reviewed in [26]). The Cdc42-Par6-aPKC pathway stabilizes the adherens junctions via control of the Arp2/3 dependent pathway (reviewed in [26]).

The formation of adherens junctions is regulated by transcriptional and post-translational control of cadherin expression. E-cadherin expression is repressed by zinc finger family transcription factors that induce EMT like Snail, Slug, Twist, Zeb1 and Zeb2 of which bind to the E-box in the E-cadherin promoter (reviewed in [26]). E-cadherin expression is positively regulated by microRNAs like miR-200 that target and repress EMT transcription factors and miR-373 that recognizes a site in the promoter of E-cadherin gene ([30] and reviewed in [26]). Changes in the adherens junction length and actomyosin contractility is the driving force for many morphogenetic changes ranging from gastrulation to cell intercalation (reviewed in [29]).

1.2.3. Diseases of adherens junctions

During cancer progression, epithelial tumours lose E-cadherin expression and acquire N-cadherin expression, a phenomenon known as cadherin switching and this serves as a biomarker for tumorigenesis as well as EMT (reviewed in [18]). N-cadherin positive epithelial tumour cells are able to interact with N-cadherin positive tissues like the stroma and the endothelium thereby promoting angiogenesis as well as invasion and survival in secondary organs (reviewed in [18]). E-cadherin functions as a tumour suppressor by sequestering β -catenin at the adherens junction thus preventing β -catenin from entering the nucleus and activating transcription in complex with the TCF/ LEF transcription factors upon the induction of Wnt signalling ([31, 32] and reviewed in [18, 33]). Abnormal phosphorylation of tyrosine residues in the cytoplasmic domain of E-cadherin leads to the recruitment of the E3 ubiquitin ligase Hakai and leads to internalization and proteasomal degradation of E-cadherin (reviewed in [18]). Loss or mislocalization of p120 catenin is also implicated in many cancer types (reviewed in [18]). Matrix metalloproteases like MMP3, MMP7, MMP9 and MMP14 as well as the serine protease kallikrein 6 have been shown to cleave the EC domains of E-cadherin, known as ectodomain shedding, and the soluble fragments of the EC domains have been shown to act as psuedoligands that block normal E-cadherin interactions and promote invasion (reviewed in [18]).

1.3. Gap Junctions

Gap junctions are cell-cell junctions found in all cells in solid tissues that form intercellular channels permitting cell-cell transfer of ions and small molecules serving a diverse array of functions. The formation of gap junctions brings the apposing plasma membranes very close to each other leaving a small “gap” of 2-4 nm, after which the

junctions are named and sterically excluding all other integral membrane proteins (Figure 1.6).

1.3.1. Components of gap junctions

Gap junctions are formed by head-to-head docking of hexameric assemblies called connexons or hemichannels on apposing plasma membranes. Connexons are formed of integral membrane proteins called connexins that have cytoplasmic amino-terminus, four transmembrane domains, two extracellular loops, one cytoplasmic loop and a cytoplasmic carboxyl-terminus (reviewed in [17, 34]).

Connexins are found in all tissues except differentiated skeletal muscle, with many tissues expressing more than one type of connexin giving rise to heteromeric connexons as well as heterotypic hemichannels (reviewed in [17, 34]). There are 21 different types of connexins in humans and they are named based on their predicted molecular weight (Cx43 is ~43kDa). Connexins are divided into five sub-groups based on their sequence similarity and the length of their cytoplasmic loop into α , β , γ ,

δ and ϵ . Connexins are then abbreviated with “GJ” for gap junction and then numbered according to the order of their discovery (Cx43 is GJ $\alpha 1$). Connexons have a six-fold symmetrical structure with a pore in the centre that narrows from 40 Å to 15 Å at the boundary of the extracellular gap caused by the tilting of the transmembrane domain (reviewed in [17, 34]) (Figure 1.7).

1.3.2. Functions of gap junctions

The term “gating” is often used to describe changes in opening and closing of gap junction channels. Voltage gating is considered as a fast process that leads to

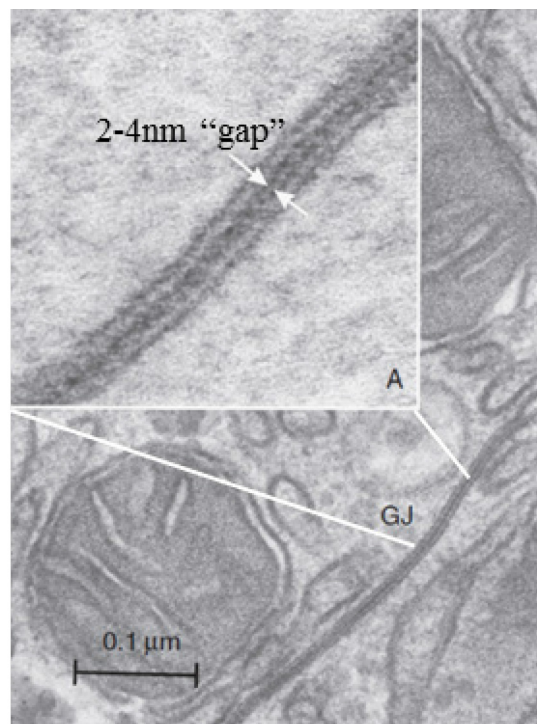


Figure 1.6. Electron micrograph of a gap junction – the inlay shows a higher magnification highlighting the small 2-4 nm “gap” between the apposing cell membranes that is a characteristic feature of gap junctions. GJ = Gap junction (Adapted from [17]).

incomplete closing of connexons and has been shown to have physiological role in Purkinje fibres expressing Cx45 in the heart that are responsible for conducting action potentials from the conduction system to the myocardium expressing Cx43 (reviewed in [17, 34]). Chemical gating through pH and/ or Ca^{+2} is considered as a slow process that leads to complete closing of connexons and has been proposed to have independent as well as interdependent functions with a regulatory role for the calcium binding protein, calmodulin suggested in this mechanism.

Electrical changes in trans junctional voltage as well as chemical changes in the cellular environment like pH and Ca^{+2} gradients cause structural changes in gap junctions and affect the size of the pores. These structural changes are due to changes in the conformation of the carboxyl-terminus of connexins that enables its interaction with the

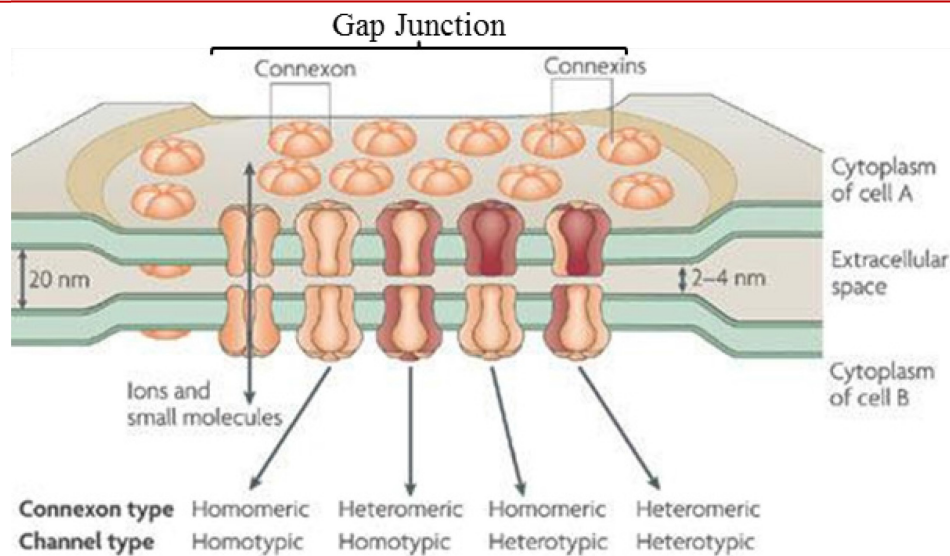


Figure 1.7. Schematic of gap junctions – *Molecular model of Gap Junctions as discussed in the text. (Adapted from [1]).*

cytoplasmic loop that physically blocks the pore (reviewed in [17, 34]). Molecules that are less than 1kDa in size can enter the pore of a gap junction, which means that all ions should pass through the pore. However, gap junctions show charge selectivity, with the unitary conductance being determined by the connexin isotypes present in the individual junctions. The ability of gap junctions to share ions between neighbouring cells is crucial for the function of electrically excitable cells like neurons, myocytes, and cardiomyocytes. The permeability properties of a connexon are also determined by the reversible post-translational modifications of the connexins as well as their protein-protein interactions. Interaction of connexins with ZO-1 has been shown to be important for membrane localization of connexins. Gap junctions are permeable to a variety of biological molecules like second messengers and metabolites, such as ATP, ADP, Ca^{+2} , cAMP, IP3, glutamate, glutathione, and siRNA, but the physical basis of the selectivity for these molecules in different types of gap junctions is unclear (reviewed in [17, 34]).

1.3.3. Diseases of gap junctions

Myoendothelial gap junctions made of Cx37, Cx40, Cx43 and Cx45 regulate vasoconstriction through IP3-mediated release of Ca^{+2} from intracellular stores also causing a Ca^{+2} release in endothelial cells. The β cells of the pancreas are coupled by Cx36 gap junctions that have functions for sensing glucose levels and insulin secretion. Pathological conditions like hypertension, diabetes and atherosclerosis are associated with changes in connexin expression and regulation (reviewed in [34]). In the gastrointestinal tract, the interstitial cells of Cajal are electrically coupled to each other and to the outer muscular layer through gap junctions. Hirschsprung's disease arises due to reduced expression of Cx43 in the interstitial cells of Cajal or muscles of the gut and results in disturbances of colon motility (reviewed in [34]). Connexons can also form half junctions or free hemichannels that play a role in exchange of ions and small molecules between the cell and its extracellular environment. Hemichannel dysfunction has also been shown to play a role in pathogenesis of diverse conditions ranging from atherosclerosis to inflammation and bacterial infections. Connexins also have complex functions in regulating cell growth, migration and gene regulation in a gap junction formation dependent as well as independent manner. The gap junction dependent functions could be by the transfer of growth and gene regulatory factors like Ca^{+2} , cAMP, IP3 or siRNA while the gap junction independent functions could be by the interaction of connexins with proteins like ZO-1, β -catenin, caveolin, drebin and various kinases and phosphatases. Cx43 is the most widely studied tumour suppressor and other connexins like Cx26, Cx30 and Cx32 have been shown to have similar functions. The growth suppression function of these connexins is independent of their coupling function because it is observed in the absence of cell-cell contacts, in the presence of gap junction inhibitors, in cells expressing connexins incapable of junction formation and in cells

expressing only the carboxyl-terminus fragment of connexins (reviewed in [34]). As such, decrease of gap junction intercellular communication and alteration of connexins expression is frequently observed in many tumours (reviewed in [35]).

During EMT, the cadherin switch from E-cadherin to N-cadherin prevents the formation of gap junctions and induces the endocytosis of Cx43 via a non-clathrin dependent pathway (reviewed in [35]). In keratinocytes, growth of cells on laminin-5 induces $\alpha 3 \beta 1$ focal adhesions that increases localization of Cx43 to the plasma membrane and increases gap junction formation (reviewed in [35]). Cx43 is also shown to increase MMP2 and MMP9 expression in multiple tumour types while Cx26 seems to have the opposite effect of decreasing MMP9 expression and increasing E-cadherin expression (reviewed in [35]). In prostate cancer cells Cx26 interacts with FAK and leads to increased migration and invasion while in breast cancer cells Cx26 plays a contradictory role by decreasing cell migration and invasion (reviewed in [35]). In human renal carcinoma cells, Cx32 acts a tumour suppressor by reducing the expression of the members of the serine protease family of urokinase-type plasminogen activator thereby inhibiting invasion (reviewed in [35]). Thus gap junction function as well as connexin expression plays a major role in cancer progression.

1.4. Desmosomes

Desmosomes are cell-cell adhesion junctions found in all epithelial tissues and cardiac muscles that provide mechanical strength and integrity to the tissues. Desmosomes are calcium dependent junctions with desmosomal cadherins having calcium binding pockets in their extracellular domains. However, desmosomes are capable of maturing to a calcium independent state called as “hyperadhesion”. Desmosomes form a characteristic electron dense structure when viewed by an electron

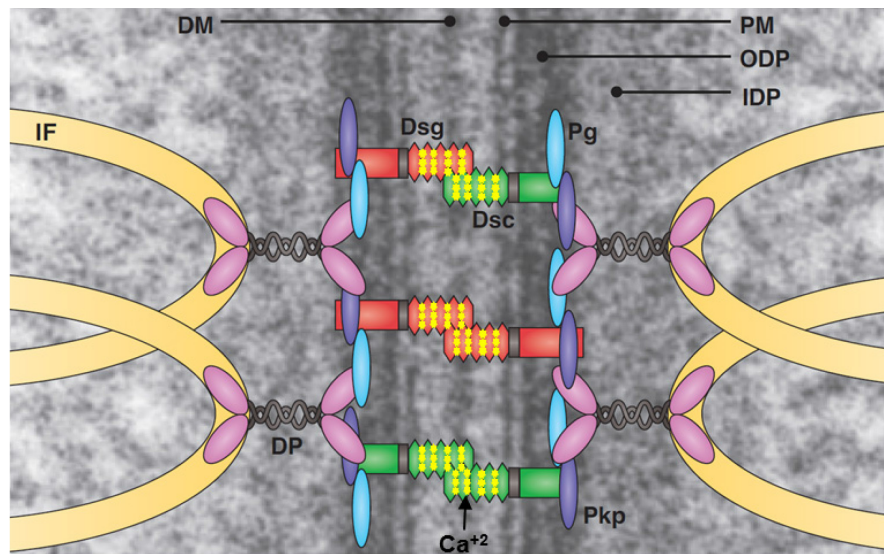


Figure 1.8. Schematic of desmosomes superimposed on an electron micrograph of a desmosome – Mature hyperadhesive desmosomes have the appearance of a dense midline (DM) between the apposing plasma membranes (PM) which is considered to be the point of interaction of the desmosomal cadherins. Desmosomal cadherins, desmogleins (Dsg) and desmocollins (Dsc) can interact in a homotypic or heterotypic manner when calcium ions (Ca^{+2}) bind to their extracellular domains. On the intracellular side of the desmosomal cadherins, the electron micrograph shows the outer dense plaque (ODP) that also contains the armadillo family proteins plakoglobin (Pg) and plakophilins (Pkp) and the amino-terminus of the plakin family protein desmoplakin (DP). Desmoplakin (DP) anchors the intermediate filaments (IF) cytoskeleton of the cell which leads to the appearance of the inner dense plaque (IDP) on the electron micrograph (adapted from [5])

microscope distinguished by the anchoring of intermediate filaments to the desmosomal junction and additionally the hyperadhesive desmosomes having a dense midline (DM) between the apposing plasma membranes (reviewed in [5, 36-46]) (Figure 1.8).

1.4.1. Components of desmosomes

The desmosome has two types of desmosomal cadherins, desmocollins and desmogleins, both having a single transmembrane domain, five extracellular domains and cytoplasmic carboxyl-terminus. The extracellular domains of the desmosomal cadherins have calcium binding sites and the conformational change brought about by calcium binding is required for the homophillic or heterophillic interactions between the desmosomal cadherins that results in adhesion. When desmosomes mature to become hyperadhesive, the interface of the interaction between the desmosomal cadherins gives the appearance of a dense midline on an electron micrograph. The hyperadhesive state is proposed to be a result of calcium ions being sterically trapped leading to calcium independence.

The outer dense plaque observed in the electron micrograph of a desmosome is a result of the cytoplasmic carboxyl-terminus tails of desmosomal cadherins interacting with the desmosomal plaque proteins of the armadillo family, plakoglobin (PG) and plakophilins (PKP). The armadillo family proteins in turn interact with the amino-terminus of the plakin family member desmoplakin (DP). The inner dense plaque observed in the electron micrograph is a result of desmoplakin carboxyl-terminal anchoring the intermediate filament cytoskeleton (reviewed in [5, 36-46]) (Figure 1.8).

Different isoforms of desmocollins, desmogleins and plakophilins are expressed in different tissue types as well as at different stages of differentiation. Plakophilin 3 (PKP3) is the only plakophilin isoform that is expressed in all epithelial cells with the exception of hepatocytes. Desmosomes also contain or localize additional proteins for specialized functions in a cell-type specific manner. These additional components include proteins that are required for junction assembly and integrity like the p63 effector PERP,

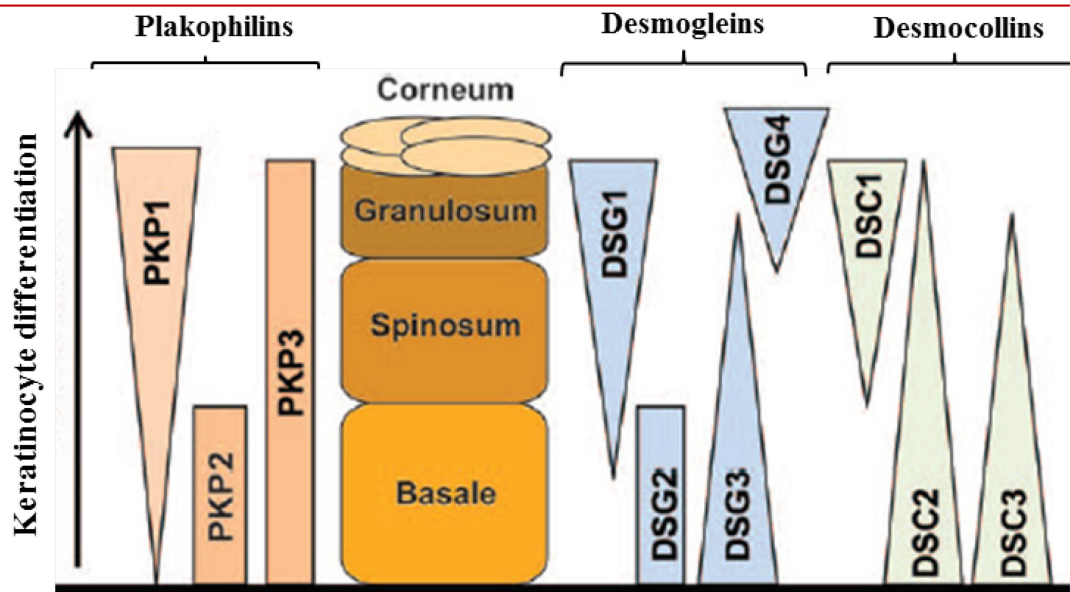


Figure 1.9. Schematic of different isoforms of plakophilins, desmogleins and desmocollins being expressed during various stages of keratinocyte differentiation in the epidermis. (Adapted from [13])

pinin and the prion protein PrP(c); proteins that contribute to the cornified envelope and corneodesmosomes like envoplakin, periplakin and corneodesmosin; and proteins involved in cytoskeletal remodelling, differentiation and signalling like the periplakin-binding protein kazrin and the ErbB2-binding protein Erbin (reviewed in [5, 36-46]) (Figure 1.9).

The desmogleins and desmocollins have E-cadherin like extracellular domains with calcium binding sites and are considered to be structurally close to the classical cadherins of the adherens junctions. Desmogleins (DSG) have longer cytoplasmic carboxyl-terminal tails as compared with desmocollins; both have membrane proximal catenin binding regions. Desmocollins (DSC) have two splice variants, ‘a’ and ‘b’ with varying lengths of the cytoplasmic tail. The armadillo proteins are named after the *Drosophila* protein armadillo, the human homologue of armadillo being β -catenin of the adherens junctions. The desmosomal armadillo protein PG (also known as γ -catenin) is

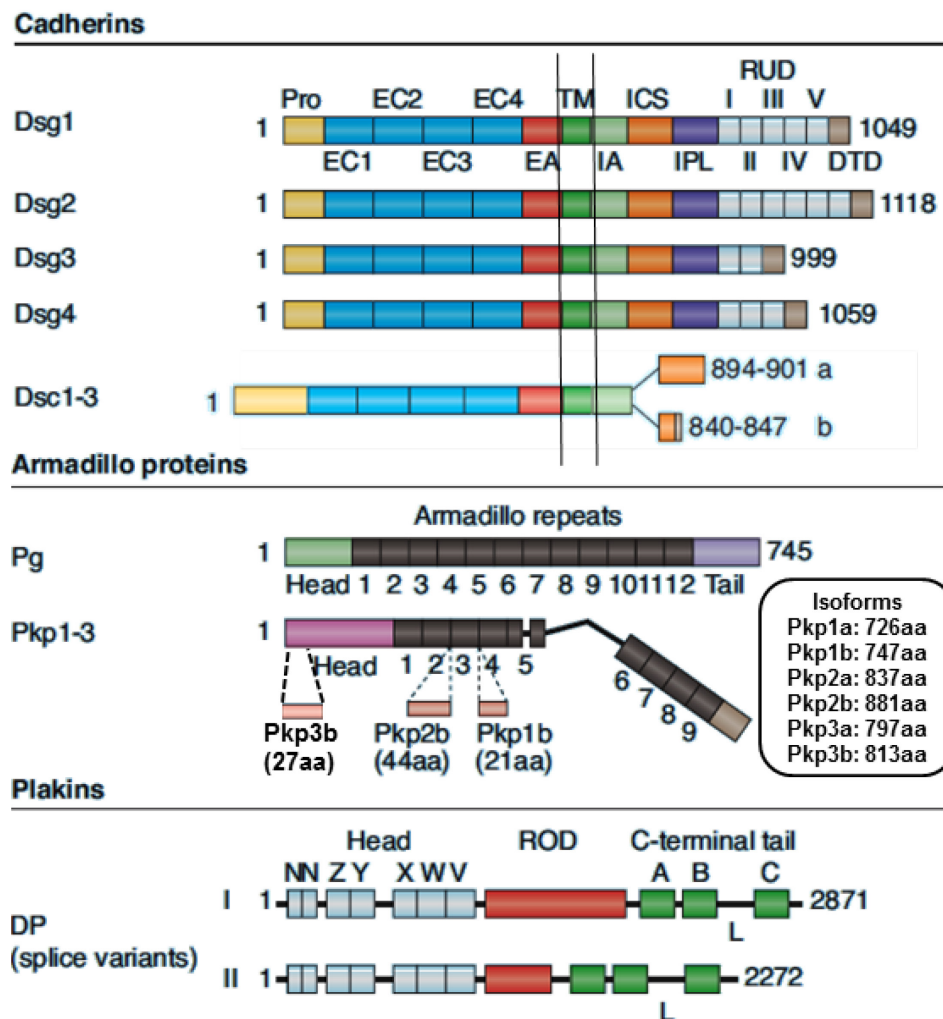


Figure 1.10. Schematic of domains of different desmosomal proteins – *Dsg*, desmoglein; *Pro*, propeptide; *EC*, extracellular repeat domain; *EA*, extracellular anchor domain; *TM*, transmembrane domain; *IA*, intracellular anchor; *ICS*, intracellular catenin-binding region; *IPL*, intracellular proline-rich linker; *RUD*, repeat unit domain; *DTD*, desmoglein terminal domain; *Dsc*, desmocollin; *Pg*, plakoglobin; *Pkp*, plakophilin; *DP*, desmoplakin; *NN*, *Z*, *Y*, *X*, *W*, *V*, series of predicted alpha-helical bundles; *A*, *B*, *C*, intermediate-filament-binding domain homology units; *L*, linker (adapted from [5, 6]).

homologous to β -catenin and is found in both adherens junctions as well as desmosomes and is indispensable for desmosome formation. The armadillo proteins PKPs are homologous to the adherens junction armadillo protein p120 catenin and considered to be

a part of p120 catenin family. A unique feature of the PKPs is a proline containing linker between arm repeats five and six that leads to a kink in the structure of plakophilins. Plakophilins also have two splice variants, 'a' and 'b'. The plakin family member desmoplakin (DP) is required for anchoring intermediate filaments to the desmosome and is indispensable for desmosome formation. There are two desmoplakin splice variants 'I' and 'II'. Both have identical amino-terminal head domains. The head domain contains a series of predicted α -helical bundles called as NN, Z, Y, X, W and V. The rod domain is required for the dimerization of desmoplakin that is essential for its function. The carboxyl-terminus tail of desmoplakin anchors the intermediate filaments and contains three intermediate filament binding domain homology units A, B and C along with a linker between B and C (reviewed in [5, 36-46]) (Figure 1.10).

1.4.2. Desmosomes are highly insoluble structures

The earliest experiments done to study desmosomal components demonstrated that desmosomes were highly insoluble structures that required 2% SDS along with a reducing agent 1% β -mercaptoethanol or 8M urea or prolonged exposure to 0.1M NaOH for the desmosomal proteins to appear in the soluble fraction [47-49]. Extracts prepared in an acidic citric acid – sodium citrate buffer at pH2.6 had to be dialysed for hours against SDS-containing buffer to dissolve desmosomes [49]. A protocol developed for the serial extraction of cellular components showed that the nuclear matrix – intermediate filament (NM-IF) pool that contained desmosomes was the least soluble of all protein fractions and constituted about 5% of the total protein [20]. Serial extraction of the non-ionic detergent soluble proteins and ammonium sulphate treatment performed on MDCK cells left behind a hollow looking NM-IF structure (Figure 1.11) [20]. The non-ionic detergent insolubility of desmosomes is an indicator of the strong adhesive forces present in the

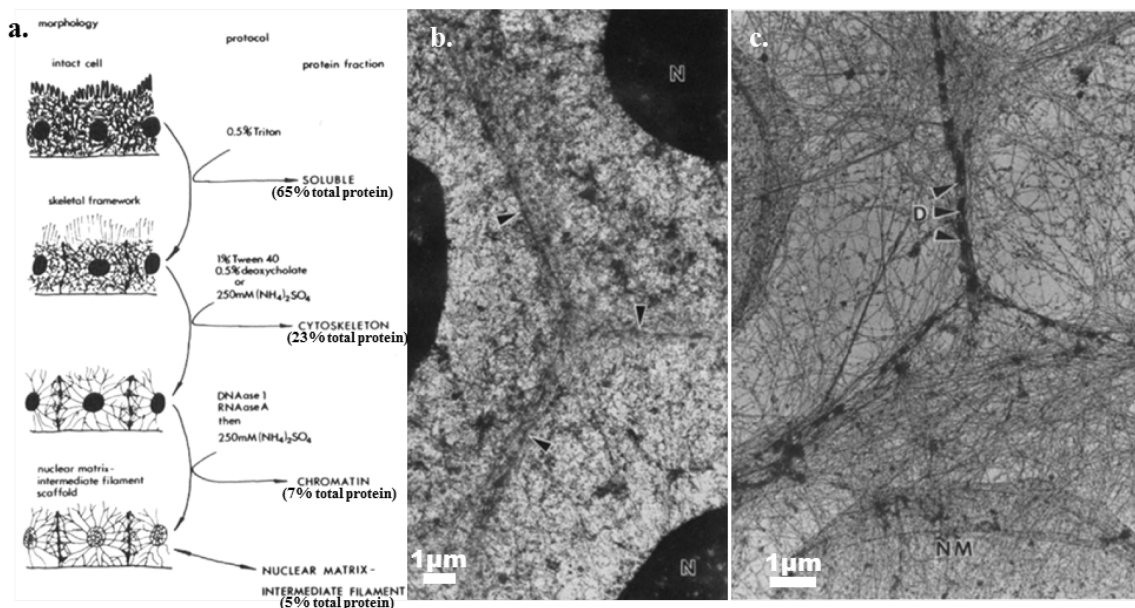


Figure 1.11. Desmosomes are highly insoluble structures, part of the NM-IF pool – *a.* schematic of the protocol followed for serial extraction of cellular components, *b.* electron micrograph of MDCK cells after soluble protein (0.5% Triton) extraction, desmosomes are marked with black arrows, *c.* electron micrograph of MDCK cells after extraction of soluble proteins, cytoskeleton and chromatin – only NM-IF left forming hollow structures of nuclear matrix (NM) and intermediate filaments connected by desmosomes (D and marked with black arrows) (adapted from [20]).

desmosomes but it makes them very difficult to study biochemically because dissolving them disrupts the interactions between the different components of the desmosome. Many biochemical assays done with non-ionic detergent soluble proteins should be interpreted with caution when concerning desmosomal components as they would not give information about the desmosomal components that are part of an intact desmosome – they would give information about events upstream of desmosome assembly or downstream of desmosome disassembly (reviewed in [43]).

Desmosomal components are non-ionic detergent soluble when cultured in low calcium medium ($<0.1\text{M Ca}^{+2}$) and prone to degradation. Thus the non-ionic detergent insolubility of the desmosomal components also contributes to their longer half-life increasing it 7-fold to 12-fold [50]. The half-life of DP in non-ionic detergent soluble pool is about 8 hours in MDCK cells, whereas the half-life of DP in non-ionic detergent insoluble pool is >72 hours [51]. Pulse chase experiments show that desmosomal components become non-ionic detergent insoluble shortly after they are synthesized but before they are transported to the cell surface and, if cells are cultured in low calcium medium, desmosomal components remain in the soluble fraction and get degraded [52, 53]. Desmosomal proteins from stable desmosomes are recycled by internalisation into desmosome-associated vacuoles that fuse with lysosomes resulting in protein degradation [54]. Recent studies show that half desmosome internalisation is dependent on PKC and transport by a kinesin dependent mechanism as well as on actin cytoskeleton. The internalised half desmosomes have co-localized desmosomal proteins that do not recycle back to the membrane when desmosome assembly is triggered and instead localize to the centrosomes. Also, the fate of the half desmosomes is degradation by both proteasomal and lysosomal systems [55]. Triton insolubility has thus been established as a known trait of stable desmosomal proteins and is used widely to determine the stability of these proteins (reviewed in [56]).

A recent report suggests that desmosomal components are palmitoylated and the palmitoylation of PKPs is essential for their partitioning into the Triton insoluble fraction as well as desmosome formation [57]. The same report also suggested that palmitoylation of PKPs is essential for incorporation of PKPs in caveolin-1 containing lipid rafts which have been shown to contain DSG2 [57, 58]. Thus the Triton insoluble nature of desmosomal components is a precursor to desmosome formation, is essential for

desmosomal protein stability and it might be dependent on the palmitoylation of these proteins.

1.4.3. Functions of desmosomes – “hyperadhesion”

Desmosomes assemble in the mouse embryo as early as E3.5 at the appearance of the blastocoel cavity and establishment of epithelial polarity (reviewed in [59]) and hyperadhesion of desmosomes is observed from E4.5 [60]. Epidermal commitment in mouse embryos happens at E9.5, while hyperadhesion of epidermal desmosomes is observed by E14 [60]. The human epidermis forms from a single layer of embryonic surface ectoderm. The ectoderm proliferates in the fourth week of estimated gestational age (EGA) and produces two layers of cells – the inner layer of cells is the basal layer while the outer layer is called the periderm, and proliferation takes place in both cell layers. In humans, desmosomes are observed from five weeks EGA between the basal and periderm cells. While it is possible that desmosomes appear at earlier stages in development, samples from these stages are unavailable. The formation of desmosomes is thus a very early event preceding maturation of basement membrane zone (reviewed in [44]).

Hyperadhesion is a property of desmosomes that distinguishes it from other intercellular junctions and it is the normal state in which desmosomes are found in tissues *in vivo*. The hyperadhesive desmosomes of the epidermis resist disruption by EGTA, which chelates extracellular Ca^{+2} , and are characterised by the presence of a DM. The normal range of calcium concentration in human serum is 2.12 – 2.62 mM, and remedial treatment is given if it falls below about 1.9 mM, hence it is highly unlikely that calcium levels are the physiological mode of cell-cell junction regulation (reviewed in [61]). Wounding the epidermis causes the desmosomes near the wound edge to become calcium

dependent, they lose the appearance of DM and the intercellular space is narrowed by 10 nm. The transition to Ca^{+2} dependence is accompanied by the re-localization of protein kinase C α (PKC α) to the desmosomal plaque and an inside-out signalling mechanism has been proposed to be responsible for the change in adhesiveness [62, 63].

PKP2 has been advocated as to provide the scaffolding for a PKP2-DP-PKC α complex during de novo desmosome assembly [64]. Sarcoendoplasmic reticulum Ca^{+2} -ATPase isoform 2 (SERCA2), a major regulator of intracellular Ca^{+2} homeostasis in the skin, has been shown to regulate desmosome assembly via activation of PKC α [65]. However, PKC α null mice show normal epidermal development and show no obvious defects in desmosome formation or maturation [60] other than a delayed wound re-epithelialization, which is characterised by a failure of desmosomes to convert to a calcium dependent state [66]. Likewise, the use of conventional PKC inhibitor in wild type mice is shown to convert E12 epidermis desmosomes from calcium dependent state to hyperadhesive state [60]. This mechanism is proposed to be conserved in humans as acute wounds shows PKC α localizing to desmosomes at the wound edge and desmosomes being calcium dependent, whereas chronic wounds show cytoplasmic PKC α and desmosomes remaining hyperadhesive [66].

1.4.4. Diseases of desmosomes

Desmosomes form strong adhesive cell-cell junctions and are essential for the tissues like epidermis and cardiac muscles that experience mechanical stress as desmosomes enhance their force-resisting mechanical properties. Desmosomes are also found in more specialized junctions of the meninges and the lymphatic endothelial cells. Desmosome function is required for the development and differentiation of these tissues and desmosomal components are frequently mutated in inherited diseases having a

cardio-cutaneous phenotype (reviewed in [5, 36-46]). Recessive DSG1 mutations lead to striate palmoplantar keratoderma (SPPK) or palmoplantar keratoderma (PPK) with hypotrichosis and hyper-IgE. Dominant and recessive mutations in DSG2 lead to arrhythmogenic right ventricular cardiomyopathy (ARVC) alone and recessive mutations in DSG2 also lead to dilated cardiomyopathy. No inherited mutations that cause disease have been reported for DSG3, however recessive mutations in DSG4 lead to hypotrichosis or Monilethrix-like hypotrichosis. No inherited mutations have been reported for DSC1. Recessive mutations in DSC2 lead to ARVC alone or ARVC with PPK and woolly hair. Recessive mutations in DSC3 lead to hypotrichosis with skin vesicles. Dominant mutations in PG lead to ARVC alone, recessive mutations in PG lead to focal and diffuse PPK with woolly hair or ARVC with PPK and total alopecia or lethal acantholytic epidermolysis bullosa or PPK with woolly hair and ARVC also called as Naxos disease. Recessive mutations in PKP1 lead to ectodermal dysplasia/ skin fragility syndrome with ARVC. Dominant as well as recessive mutations in PKP2 lead to ARVC alone. No inherited mutations have been reported for PKP3. Dominant mutations in DP lead to ARVC alone, SPPK alone or PPK with woolly hair and ARVC, recessive mutations in DP lead to SPPK with woolly hair and ARVC, skin fragility and woolly hair, lethal acantholytic epidermolysis bullosa or Naxos-like disease affecting only DPI or dilated cardiomyopathy with woolly hair and keratoderma. Nonsense mutations in corneodesmosin lead to hypotrichosis simplex of the scalp (reviewed in [5, 67]). Autoantibodies targeting DSG3 can cause blistering of the epidermis called as Pemphigus foliaceus (PF) while autoantibodies targeting DSG1 can cause blistering of the epidermis and oral mucosa called as Pemphigus vulgaris (PV) (reviewed in [5]). Exfoliative toxin A, a serine protease produced by *Staphylococcus aureus*, causes blisters in bullous impetigo and its more generalized form, staphylococcal scalded-skin syndrome by

cleaving extracellular domain of DSG1 [68]. Thus diseases related to dysregulation of desmosomes show a cardio-cutaneous phenotype.

1.4.5. Desmosomal protein functions in cell signalling

Desmosomal proteins have been shown to have a wide array of functions in cell signalling (reviewed in [45, 69]). Both DSG1 and DSG2 are caspase 3 targets and promote apoptosis [70, 71]. Bcr has been identified as the RhoA GEF that regulates activation of RhoA/ MAL signalling and regulates the expression of differentiation markers such as DSG1 in keratinocytes [72]. DSG1 has been shown to promote keratinocyte differentiation in an adhesion-independent manner through suppression of EGFR-ERK1/2 signalling [73]. Keratinocytes of transgenic mice expressing DSG2 from the involucrin promoter are resistant to apoptosis and show enhanced survival which is dependent on EGFR activation and NF- κ B activity. These keratinocytes showed activation of PI3K /AKT, MEK-MAPK and STAT3 pathways, all of which promote cell survival in response to apoptotic stimuli [74]. EGFR inhibition leads to accumulation of DSG2 at the plasma membrane, which is accompanied by the inhibition of ADAM proteases and MMP-dependent shedding of the DSG2 ectodomain and increased tyrosine phosphorylation of the DSG2 cytoplasmic domain [75, 76].

PG has been reported to both promote apoptosis by decreasing the levels of Bcl-X(L) [77] and suppress apoptosis by increasing the levels of Bcl-2 [78]. Suppression of c-Myc promotes cell cycle exit and is an important event in keratinocyte terminal differentiation [79]. PG activates the c-Myc promoter by binding to Tcf-4 and could contribute to tumour progression [80] but some reports suggest that the PG-Tcf/Lef-1 complex might suppress c-Myc transcription [79, 81] (Figure 1.13).

PKP1 has been shown to localize to the nucleus and bind to ssDNA and the loss of PKP1 leads to increased survival upon DNA damage [82]. PKP1 binds to eIF4A1 and upregulates global translation rates and promotes increase in cell size as well as proliferation [83] (Figure 1.13). PKP2 is essential for induction calcium dependent junction formation by targeting active RhoA to the intercellular interfaces of cell-cell adhesion and formation of cortical actin [84]. PKP2 deficient cells show slower cell migration accompanied by slower focal adhesion dynamics [85]. PKP2 has been shown to localize to the nucleus [86] by phosphorylation on S82 mediated by C-TAK1 that generates a 14-3-3 proteins binding site [87]. PKP2 has been shown to be a part of RNA polymerase III holoenzyme and to specifically bind to RPC155 [88] (Figure 1.13). PKP2 knockdown has been also shown to lead to a global increase in phosphorylation of PKC substrates which could be a contributing factor to the pathological effects of PKP2 loss [64]. PKP3 is known to localize to the nucleus and bind to ETV1 transcription factor and this association has been implicated in having a role in neural crest formation [89]. Similarly, PKP1 and PKP3 are shown to be a part of RNA stress granules and known to bind to RNA binding proteins like FXR1, G3BP, and PABPC1, and it has been shown to affect the stability of the PKP2 and DP mRNAs [90, 91] (Figure 1.13).

In differentiated cells of the epidermis, DP plays a crucial role in rearrangement of microtubules by recruitment of ninein from the centrosome to the desmosomes and accumulation of cortical microtubules that are anchored to cell-cell junctions instead of centrosome (centrosome still maintains the ability to nucleate microtubules) [92]. Likewise, other centrosomal components like Lis1 and Ndel1 have been shown to be recruited to desmosomes by DPI in differentiated epidermal cells and the loss of these proteins leads to defects in microtubule reorganisation as well as desmosome turnover

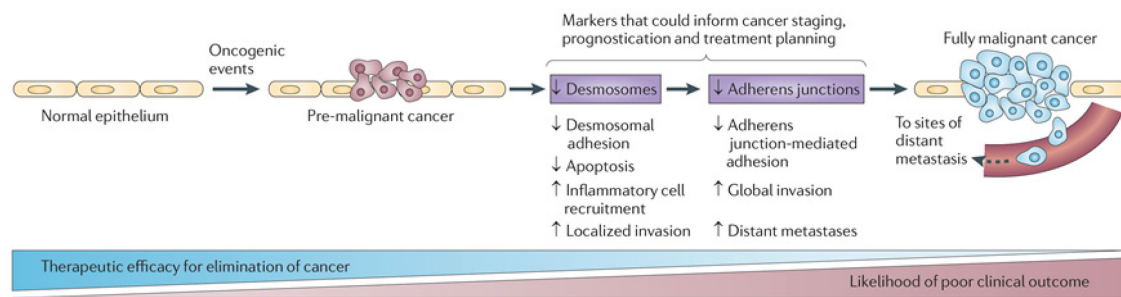


Figure 1.12. Desmosomal adhesion downregulation as a part of multistep process of tumour development – *Oncogenic events like mutations in tumour suppressor genes or proto-oncogenes could drive de novo tumour formation in epithelial tissues. Desmosome loss probably occurs before loss of adherens junction and lays the seeds for invasion and further with adherens junction loss the tumour progresses to metastasis. These attributes of tumour progression can be used as prognostic indicators for treatment of patients (reproduced from [15]).*

[93]. Thus desmosomal proteins have numerous functions in different cell signalling pathways apart from functional as structural molecules of the desmosome.

1.4.6. Desmosomes in cancer

The loss of desmosomal components would result in loss of cell-cell adhesion and would favour tumour progression and metastasis – this line of thought has been supported by many reports that have reported loss of desmosomal components, sometimes in addition to a general loss of the epithelial phenotype in various carcinomas. However, as some desmosomal proteins regulate cellular signalling pathways, an increase in the expression of some desmosomal proteins is associated with tumour progression (reviewed in [15, 38, 46, 69, 94-96]) (Figure 1.12).

Introduction of desmosomal components in non-adhesive fibroblasts L929 generates cell-cell adhesion and reduces their invasive potential [97]. The EMT

transcription factor Slug induces loss of desmosomal adhesion associated with loss of DSG and DP from cell-cell contacts [98, 99]. Similarly, loss of DP correlated with loss of differentiation, increase in invasion and presence of lymph node metastases in oral squamous cell carcinoma (SCC) [100]. In contrast, the presence of desmosomes in metastatic colorectal carcinomas (CRC) is associated with tumour cell survival [101].

PG expression introduced in SCC9 cells which lack desmosomes, and are PG and E-cadherin deficient, induces desmosome formation [102]. However, expression of PG in SCC9 cells also leads to increased total and nuclear β -catenin levels that leads to increase in Bcl-2 expression and inhibition of apoptosis [78] (Figure 1.13). LOH mutations in PG are found in breast and ovarian tumours [103] as well as in prostate cancers where it is also associated with increased Bcl-2 expression [104]. In non-small cell lung cancers (NSCLC), β -catenin was found to be upregulated while PG was found to be downregulated and in NSCLC cells rescued by expressing PG, decreased cell growth as well as decreased anchorage independent growth was observed [105]. Histone deacetylase inhibitors TSA and NaB increased PG expression in human bladder carcinoma cell lines thereby reducing the tumour load in a xenograft mouse model [106].

In SCC of the oropharynx, presence of PKP4 was inversely correlated with tumour growth while presence of PKP1 and PKP3 was inversely correlated with metastasis [107]. Knockdown of PKP3 in CRC cells promotes cell migration, anchorage independent growth accompanied by increase in tumour formation and metastasis in a mouse xenograft model [108]. The EMT transcription factor, Zeb2, represses expression of desmosomal proteins like PKP2 and DP [109] while Zeb1 represses PKP3 transcription by binding to conserved E-box elements in the PKP3 promoter [110]. Upregulation of Zeb1 along with downregulation of PKP3 is observed at the tumour-host interface in invasive cancers [110]. However in NSCLC, upregulation of PKP3 promotes tumour

growth and migration and is associated with poor survival, disease stage and metastasis [111]. Also, in gastrointestinal cancer patients, higher levels of PKP3 mRNA in blood correlated with cancer progression and metastasis [112]. In breast cancers, although PKP1 and PKP2 expression remains unchanged, PKP3 expression is increased and correlated with metastasis [113].

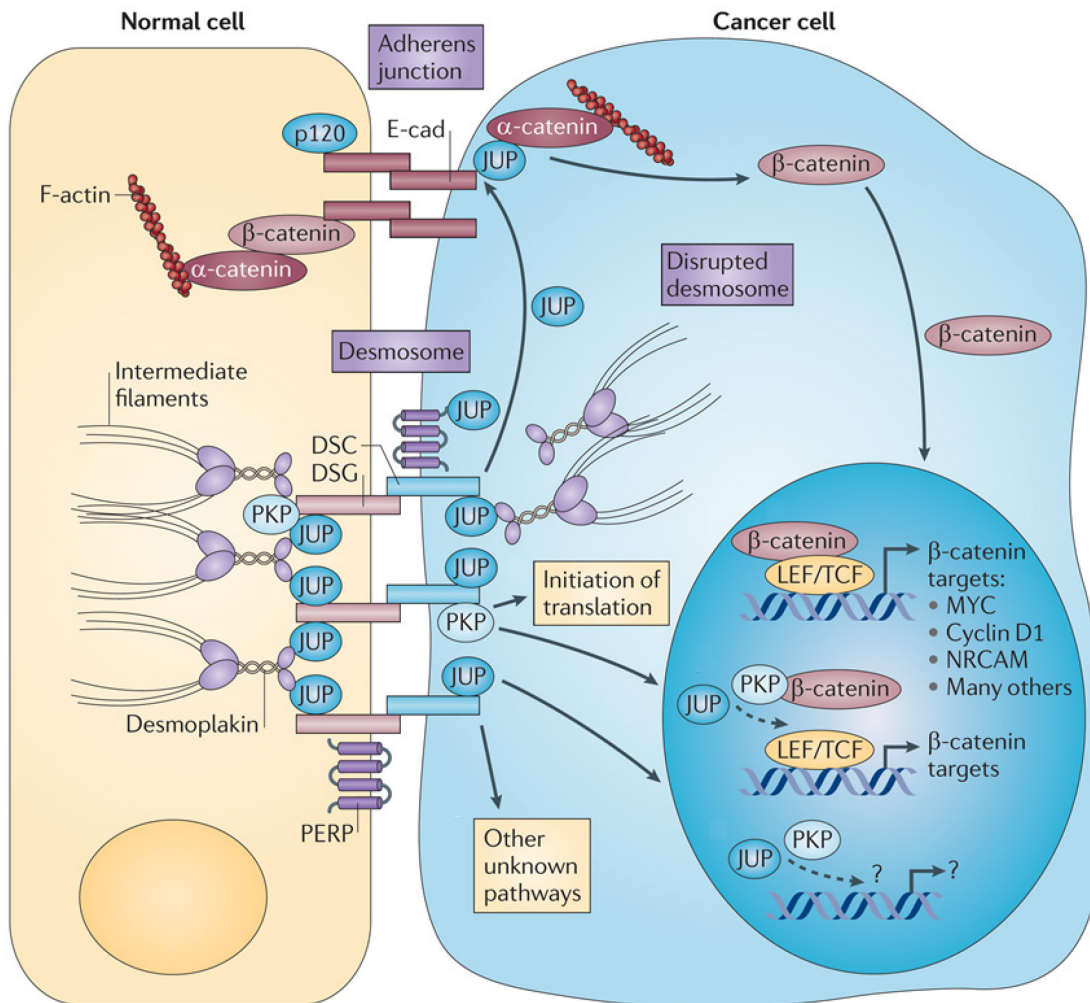


Figure 1.13. Loss of desmosomes can lead to cancer progression through multiple pathways – Stable adherens junctions and desmosomes maintain cell-cell adhesion and keep their cytoplasmic components localized to the cell-cell junctions. Loss of adhesion leads to change in localization of the cytoplasmic components away from the cell-cell adhesion junctions and promotes their functions in other cellular compartments that could help the cell gain oncogenic characteristics (Adapted from [15]).

Switching of DSC expression from DSC2 to either DSC1 or DSC3 has been reported in CRC and is associated with development of CRC [114]. Other reports suggest that in CRC, reduced expression of DSC1, DSC2 as well as DSC3 is linked to higher tumour grade, whereas reduced DSC2 and CDX2 expression is linked to poor survival [115]. In oesophageal SCC, miR-25 mediated downregulation of DSC2 enhances invasion and metastasis [116]. Likewise, in CRC, p53 mediated methylation of the DSC3 promoter leads to a reduction in DSC3 expression [117] and loss of DSC2 leads to activation of Akt/ β -catenin pathway and promotes tumour growth in colorectal cancer cells [118] (Figure 1.13). Silencing of DSC3 expression by methylation of its promoter is also observed in invasive and metastatic breast cancers [119].

EGFR inhibitors used for treatment of head and neck cancers induce desmosome formation by promoting cell membrane localization of desmosomal components accompanied by partitioning of desmosomal components in the Triton insoluble fraction, reduction of DSG2 and PG phosphorylation and reduction in MMP dependent proteolysis of DSGs and DSCs in oral SCC cells [75]. Antibody induced internalisation of DSG2 leads to cleavage of DSG2 and induction of apoptosis mediated by the carboxyl-terminal fragment of DSG2 in intestinal epithelial cells [71]. In diffuse type gastric carcinomas, reduced DSG2 expression was observed [120]. However, in SCC of the skin, increased DSG2 expression correlated with poor prognosis and risk of metastasis [121]. In oral SCC, DSG1 expression is reduced at the invasive front of poorly differentiated and highly invasive tumours [122]. Induction of apoptosis leads to the caspase-3 dependent cleavage of DSG1 into distinct 17kDa and 140 kDa products [70] whereas DSG2 is cleaved to give a 70 kDa product [123] (Figure 1.13). DSG3 is overexpressed in head and neck cancers and correlated with increased migration, invasion in vitro as well as with increased tumour growth in a xenograft mouse model [124].

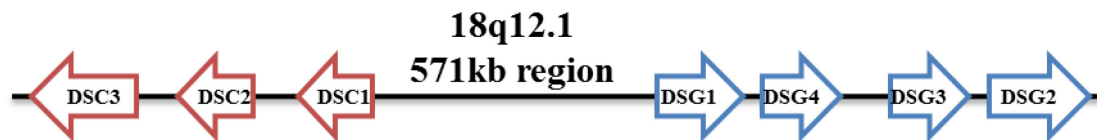


Figure 1.14. Arrangement of desmosomal cadherins genes on a section of 18q12.1 human chromosome.

1.5. Desmosomal Cadherins

Desmosomal cadherins are encoded by individual genes clustered in the 18q12.1 region of the human chromosome. The four DSG genes are in the head-to-tail orientation while the three DSC genes are in the head-to-tail orientation in the opposite directions (Figure 1.14). Desmosomal cadherins have tissue specific expression, DSG2 and DSC2 are ubiquitously expressed in all tissues that form desmosomes, whereas DSG1 and DSC1 are expressed in the highly differentiated layers of stratified epithelia and DSG3 and DSC3 are expressed in the undifferentiated basal layers of stratified epithelia. The tissue distribution of DSG4 is unique – it is found in salivary gland, testis, and prostate, as well as the highly differentiated cells of the epidermis (reviewed in [61, 125]) (Figure 1.9). The desmogleins and desmocollins within a species show 51-55% sequence identity, and the specific isoforms between mammalian species show 73-83% sequence identity (reviewed in [61, 125]).

The extracellular domains of DSGs and DSCs are composed of four extracellular cadherin repeats (EC1-4) having about 110 aa each and a membrane proximal domain called as extracellular anchor (EA) domain which are highly similar to the EC domains of classical cadherins. Furthermore, the inter-domain regions possess low-affinity calcium-binding sites, which are occupied at physiological extracellular calcium concentrations of >1 mM and are functional because they maintain the molecules in an extended, adhesion-

competent configuration. This feature of the desmosomal cadherins makes them calcium dependent like the adherens junctions. The major difference between the DSGs and DSCs is in their cytoplasmic domains. Both have a membrane proximal intracellular anchor (IA) domain and an intracellular cadherin segment (ICS) similar to classical cadherins providing a binding site for ARM family proteins. The 'b' variants of DSCs have lost this domain and are not capable of forming a functional desmosomal plaque so their function remains unresolved. DSGs have some additional domains, an extended intracellular domain containing a proline-rich linker (IPL) region followed by a repeated unit domain (RUD) of 29 aa repeats and a glycine-rich C-terminal DSG-terminal domain (DTD) (reviewed in [61, 125]) (Figure 1.10).

1.5.1. Structure of desmosome – desmosomal cadherins

The formation of the adhesive bond between the extracellular domains of the desmosomal cadherins on apposing plasma membranes is very similar to the binding between classical cadherins. This trans-interaction by the classical cadherins involves strand swapping by the EC1 domains where the side chains have conserved tryptophan residues that are inserted into the hydrophobic pockets of apposed molecules. The tryptophan residue and the side pockets are conserved in desmosomal cadherins and is likely the mechanism by which they interact ([126] and reviewed in [61]). This strand swapping mechanism seems to favour homophillic interactions among classical cadherins, but desmosomal cadherins are known to take part in both homophillic and heterophillic interactions ([127-129] and reviewed in [61]). It seems that all desmosomes in vivo contain at least one DSG and one DSC, and their ratio seems to be critical for cell-cell adhesion ([130] and reviewed in [61]). Additionally, different isoforms of the desmosomal cadherins co-expressed in tissues are present within the same desmosome

and some studies have also reported a preference for heterophilic interactions between the desmosomal cadherins ([131] and reviewed in [61]). However, recently it has been demonstrated that even though desmosomes contain both cadherin types, the trans interactions between the apposing cells for an individual cadherin are homophilic in nature ([126, 132] and reviewed in [61]). Lanthanum infiltration and electron tomography of vitreous sections have shown that the desmosomal cadherin EC domains are arranged in the “x-y” plane in a quadratic array with a repeat of $\sim 70 \text{ \AA}$, which is very similar to that found in the C-cadherin crystal structure. The inter-membrane distance is $\sim 35 \text{ nm}$, also very close to the 38.5 nm determined from the C-cadherin crystal structure (reviewed in [61]). This demonstrates that desmosomes have an extremely regular structure.

1.5.2. Mouse models of desmogleins

Heterozygous or homozygous DSG2 null mice die at or shortly after embryo implantation i.e. between E5.5 and E6.5. The DSG2 null mutation leads to disruption of DP localization without affecting the adherens junction proteins like E-cadherin and β -catenin and disrupts the formation of the inner cell mass and the embryonic stem population arising from the inner cell mass. DSG2 was observed in DP negative junctions in wild type embryonic stem cells and thus it was proposed that DSG2 has desmosome independent functions that are necessary for early embryo development and survival [133].

DSG3 null mice were normal at birth but by day 8-10 weighed less than wild type mice and by day 18 were grossly runted as well as showed hair loss on weaning. This was attributed to formation of oral lesions similar to PV patients, including suprabasilar acantholysis and "tombstoning" of basal cells [134]. Bald skin of DSG3 null

mice showed cystic telogen hair follicles without hair shafts accompanied by acantholysis between the cells surrounding the telogen club and the basal layer of the outer root sheath epithelium [135]. In a skin carcinogenesis model in DSG3 null mice, no difference was observed in the DSG3 null mice as compared to the wild type mice and DSG3 did not show a tumour suppressor function [136].

P-cadherin and DSG3 double null mice die before weaning, although P-cadherin null mice have no apparent defect in epithelial cell adhesion, while DSG3 null mice show PV phenotype. The majority of the double mutant animals die around 1 week after birth, possibly due to malnutrition. Thus loss of P-cadherin leads to a more severe DSG3 mutant phenotype in the double knockout mice. This was the first *in vivo* evidence of possible synergism between classical and desmosomal cadherins [137].

DSG3 is normally expressed in the basal layers of the epidermis. Expression of DSG3 specifically to the differentiated suprabasal epidermis by introducing it as a transgene in mice under the involucrin promoter resulted in the phenotype of gross scaling of the stratum corneum and excessive transepidermal water loss leading to death shortly after birth with severe dehydration. The structure of the stratum corneum was altered proving an important role for differential expression of DSG isoforms for differentiation and barrier function of the epidermis [138]. In a similar study, K1 promoter was used to express DSG3 to the suprabasal layer of the epidermis and flaky skin, epidermal blistering and hair loss was observed resembling dermatitis and ichthyosis. Desmosomes were normal in structure, but the epidermis was hyperproliferative and showed abnormal differentiation, the sharp contrast with the results obtained by involucrin promoter driven expression of DSG3 were proposed to be due to the earlier expression of K1 compared to involucrin during keratinocyte differentiation [139]. Transgenic mice expressing an N-terminal deletion mutant of DSG3

downstream of the epidermal specific K14 promoter showed perturbed cell-cell adhesion including swelling of paws, flakiness on the back, and blackening of tail tip. Aberrant cytoplasmic localization of desmosomal components along with smaller and fewer desmosomes was observed and a very peculiar hair coat phenotype of wet spiked hair due to continuous grooming was observed. This was accompanied by skin thickening with an increase in spinous and stratum corneum layers, changes in salivary gland composition, alterations in integrin expression and hyperproliferation [140]. Thus DSG isoforms have a role to play in differentiation of stratified epithelia and a mutation in DSGs can lead to a cascade of changes that compromise cell-cell adhesion.

To test the hypothesis whether one DSG isoform could substitute for another DSG isoform, DSG1 was expressed under K14 promoter specific for epidermis, salivary and mammary epithelia expression in DSG3 null mice. DSG3 null with DSG1 epidermis transgene expressing mice showed delayed and decreased hair loss with DSG1 expression in the telogen club. The DSG1 transgene expression efficiency was poor in oral mucosa which lead to DSG3 null phenotypes of the oral lesions being unchanged along with similar low weights [141]. Thus this study provides a genetic basis for DSG isoform compensation hypothesis.

As a mouse model of PV, splenocytes from DSG null mice immunized with DSG3 protein were adoptively transferred into Rag-2 null immunodeficient mice expressing DSG3. Anti-Dsg3 IgG was stably produced in the recipient mice for more than 6 months without further boosting. The PV phenotypes were reproduced in these mice with disruption of cell-cell adhesion, erosions of their oral mucous and telogen hair loss [142]. To develop a syngeneic mouse model for PV the DSG3 null mice were rescued with DSG1 expression driven by K5 promoter for expression of DSG1 in the basal layers of stratified squamous mucosa. These mice developed fewer oral lesions, had better

weight gain and better survival compared to DSG3 null mice. These mice were immunized with recombinant DSG3 and their splenocytes were adoptively transferred to Rag-2 null immunodeficient mice expressing DSG3 resulting in a syngeneic model PV mouse model which showed characteristics of PV including stable anti-DSG3 antibody production and suprabasilar acantholysis [143]. Such mice models for PV would help in determining the immunological mechanisms underlying this autoimmune disease.

1.5.3. Mouse models of desmocollins

DSC1 null mice exhibit flaky skin and a striking punctate epidermal barrier defect soon after birth. Fragile epidermis and granular layer acantholysis leading to localized lesions compromises skin barrier function is observed. Neutrophils accumulate in the lesions and further degrade the tissue, leading to flaking of lesional epidermis, but rapid wound healing prevents the formation of overt lesions. The epidermis is also hyperproliferative and overexpresses keratins 6 and 16, indicating abnormal differentiation. From week six, DSC1 null mice develop ulcerating lesions resembling chronic dermatitis. This dermatitis is accompanied by localized hair loss associated with formation of utriculi and dermal cysts, denoting hair follicle degeneration. Thus, DSC1 is essential for cell-cell adhesion, barrier maintenance and epidermis differentiation [144].

Expression of a truncated DSC1 that lacks both the DSC1a and DSC1b carboxyl-terminal domains by exon 17 deletion was performed to determine the functions of the cytoplasmic domains of DSC1. The truncated DSC1 was incapable of binding to desmosomal plaque proteins but integrated into desmosomes and did not show skin phenotypes exhibited by DSC1 null mice. Thus the DSC1 extracellular domain is essential for structural integrity of the skin but not its carboxyl-terminus [145].

DSC2 null mice do not show any obvious phenotypes and develop normally. The cardiomyocytes exhibit distinct and ultrastructural well organized desmosomes but the mutant hearts display a decreased stress resistance [146].

DSC3 null mice are embryonic lethal at E2 prior to implantation as well as prior to appearance of the first mature desmosomes or compaction that takes place at the eight cell stage with the early blastocyst cells starting to show disintegration. Thus DSC3 is proposed to be essential for cell-cell adhesion in early cleavage-stage embryos independently of classical desmosomes [147]. Epidermis specific DSC3 null mice controlled by the K14 promoter showed that loss of DSC3 leads to epidermal blistering and telogen hair phenotypes that are comparable to PV features [148]. Thus this study showed for the first time that it is possible that a subset of PV afflicted individuals could have autoantibodies targeting DSC3, which was proved in a subsequent report [149].

DSC1 is normally expressed in differentiated epidermis, in the stratum granulosum. Misdirecting the expression of DSC1 to the basal layers of the epidermis using K14 promoter in mice did not produce any phenotypes different from wild type mice. This suggested that differentiation specific expression of desmocollin isoforms were markers but not regulators of keratinocyte differentiation [150]. DSC3 is expressed in the basal layer of the epidermis. The expression of either DSC3a or DSC3b was misdirected to the suprabasal layers of the epidermis using K1 promoter. Both the DSC3 isoforms showed a phenotype of ventral alopecia and altered keratinocyte differentiation in adulthood. The hair follicular changes observed were similar to transgenic mice with altered β -catenin stability and increased β -catenin stability and transcriptional activity were observed in the DSC3 expressing mice prior to the phenotypic change [151]. Thus for the first time, DSC3b isoform was shown to have functions similar to the DSC3a isoform.

1.6. Desmosomal Plaque Proteins

The major families of the desmosomal plaque proteins are the armadillo family and the plakin family. Armadillo family of proteins is named after the first such protein discovered in *Drosophila* called armadillo having characteristic repeats of ~40 aa called ARM domain. The X-ray crystallography structure of β -catenin shows that a typical ARM repeat consists of three α helices which form a right handed superhelix. This superhelix structure forms a long positively charged groove that is a binding site for many ligands including cadherins. PG like its homologues β -catenin and armadillo has an amino-terminal domain, a central ARM repeat domain that is a series of twelve imperfect 42 aa repeats and a carboxyl-terminal domain (Figure 1.10). PG has the unique property of being localized in both adherens junctions and desmosomes. The first 4 ARM repeats and the carboxyl-terminus domain of PG are required for binding to DSG while the complete ARM domain is required and essential for binding to DSC. The E-cadherin binding site in PG is similar to its homologue β -catenin, within the central part of the ARM repeat and the binding of E-cadherin and PG is not affected by the mutations in desmosomal cadherin sites in PG (reviewed in [125]). PG also binds to DP in the amino-terminus region of DP [152].

PKPs show dual localization at the desmosomes and in the nucleus and are highly homologous to p120 catenin, an ARM protein that binds to the membrane proximal region of E-cadherin cytoplasmic domain. PKPs are also expressed in cells lacking desmosomes like fibroblasts and lymphocytes where they are almost exclusively nuclear and suggest a constitutive nuclear function for them in such cell types. The PKP4 isoform is not exclusive to desmosomal cell-cell contacts; it is also found to interact with classical cadherins of the adherens junctions and found to be an accessory molecule to

desmosomes. PKPs have an amino-terminus head domain, central ARM domain having ten ARM repeats and a carboxyl-terminus domain. A proline contain linker region between ARM repeats five and six gives rise to a kink in the structure of PKPs. PKP1, PKP2 and PKP3 are have two isoforms 'a' and 'b', with the 'b' isoform being longer and most studies done on PKPs have not differentiated between these isoforms for their separate functions (Figure 1.10). The amino-terminus domain of PKPs is sufficient to direct its localization to the desmosomal plaque and mediates its interaction with other desmosomal proteins like DSGs, DSCs, PG and DP. IF binding to the amino-terminus of PKPs has also been reported but it is observed only in vitro and not in vivo at the desmosomal plaque, where DP alone seems to be responsible for IF anchoring. However interaction between IFs and PKPs cannot be ruled out to have a physiological context. Overexpression of the PKP1 ARM domain is capable of inducing changes in actin filament dynamics by formation of filopodial protrusions. PKP1 has also been reported to bind seven Zn^{+2} ions in vitro that promotes oligomerization of PKP1, although the in vivo function of this binding is unknown (reviewed in [125]).

The plakin proteins are a family of large cytoskeleton linker proteins (200-700 kDa) that are central components in the anchoring of the cytoskeleton to cell-cell junctions and have multiple functions in cross-talk between cytoskeleton networks by cross-linking them to each other. They are characterised by a head plakin domain, a coiled-coil rod domain and a plakin repeat domain that binds cytoskeleton. Out of seven members of the plakin family, four are known to be associated with the desmosome – DP, plectin, envoplakin and periplakin. DP is the most prominent plakin family member present in the desmosomes that is indispensable for IF anchoring to the desmosomes and desmosome function. Alternative splicing gives rise to two isoforms DPI and DPII that differ in the length of their α -helical coiled-coil rod domain that mediates the dimerization

of DP. The amino-terminal head domain of DP has the plakin domain that contains a series of α -helical bundles called NN, Z, Y, X, W and V that mediates junctional localization via interaction with the armadillo family proteins. The carboxyl-terminus plakin repeat domains called 'A', 'B' and 'C' along with a specialized highly conserved linker domain 'L' is involved in binding to IFs. Each repeat is composed of 4.5 copies of a 38aa motif that forms a globular structure with a unique fold containing a conserved basic groove that might represent an IF binding site. Plectin is a 500 kDa IF binding protein that primarily localizes to hemidesmosomes and focal adhesions of keratinocytes as well as in the Z-discs of myocytes and intercalated discs of cardiomyocytes. Plectin in desmosomes has been found to be associated with DP and IFs but is not essential for desmosome function and appears to play a dispensable auxiliary role. Envoplakin is a 210 kDa protein found in terminally differentiated keratinocytes where it localizes along IF filaments and partially co-localizes with DP. It is non-essential for desmosome function. Periplakin is a 195 kDa protein that is found in terminally differentiated keratinocytes where it heterodimerizes with envoplakin and forms a network radiating from the desmosomes. Although periplakin lacks the plakin repeat domains, it can bind to IFs through the linker domain in the carboxyl-terminus. Thus plectin, envoplakin and periplakin might strengthen the IF to desmosome anchoring but are not indispensable for desmosome function (reviewed in [36, 41, 125]).

1.6.1. Structure of desmosome – the desmosomal plaque

The desmosomal plaques have a layered structure divided into an outer dense plaque (ODP) that is up to 20 nm from the plasma membrane and is the region of multiple desmosomal proteins interacting with each other, and an inner dense plaque (IDP) that is up to 50 nm from the plasma membrane and attaches the IF to the desmosome.

Immunogold labelling has shown that PKP lies very close to the plasma membrane as is the carboxyl-terminus of DSC 'b' isoforms while PG, the N-terminus of DP, the carboxyl-terminus of DSC 'a' isoforms and the entire cytoplasmic domain of DSGs are further from the plasma membrane but lie within the ODP region such that the RUD domains of DSGs are at the inner face of the ODP while the DTD is internal to the ODP (Figure 1.10). The carboxyl –terminus of DP lies within the IDP about 40 nm away from the plasma membrane such that the shorter isoform DPII is stretched out while the longer isoform DPI is coiled or folded. Electron tomography of the ODP showed a 2D interconnected quasiperiodic lattice with a spatial organisation similar to the extracellular side (reviewed in [61]) (Figure 1.8).

1.6.2. Mouse models of plakoglobin

PG null embryos showed severe heart defects, with desmosomes greatly reduced having ultrastructural abnormalities and died at E10.5. Some of the embryos that survived died at birth due to cardiac dysfunction, and with skin blistering and subcorneal acantholysis [153]. Another study confirmed that PG loss lead to embryonic lethality due to heart defects but surprisingly found typical desmosomes in other embryonic epithelia such as the intestinal epithelium and the epidermis [154]. In embryonic skin from PG null mice, β -catenin is localized to desmosomes and is associated with desmoglein. Although this substitution does not completely compensate for PG loss, it could explain the relatively late embryonic lethality and the lack of defects in the organization of the epidermis [155]. Amino-terminal deleted PG and wild type PG when expressed in mice under K14 promoter showed that the proliferative potential of the epidermal cells was reduced along with a decrease in the length of the growth phase of the hair follicle cycle,

shortening hairs by 30%. This effect suggests that PG participates in the transduction of growth-suppressive signals to normal epithelial cells [156].

1.6.3. Mouse models of plakophilins

There are currently no mouse models for PKP1 null mutations, but keratinocytes cultured from PKP1 deficient human subjects having ectodermal dysplasia/ skin fragility syndrome when rescued with retroviral expression of PKP1 showed increased protein levels of desmosomal proteins but not increased transcripts of desmosomal proteins accompanied by decrease in cell migration, increase in calcium independent desmosomes, increase in desmosome size and number [157]. PKP2 null mice are embryonic lethal at E10.5 – E11 exhibiting lethal heart defects characterised by loss of DP localization to the cell border in cardiomyocytes but embryonic epithelia show normal junctions [158]. PKP2 heterozygous null mice show decreased amplitude and a shift in gating and kinetics of sodium current ion channels in the heart supporting a role for cross-talk between desmosomes and sodium channel complex as well as suggest sodium channel dysfunction to be the underlying cause of the lethal heart defects observed in PKP2 null mice [159]. PKP3 null mice showed reduced number of desmosomes and adherens junctions in the basal layer of the epidermis were prone to dermatitis and showed hair follicle abnormalities. The basal layer of the epidermis of PKP3 null mice was thicker and keratinocytes were three times more proliferative but also more apoptotic and the overall differentiation of the epidermis was unaffected. The basal layer of the epidermis of PKP3 null mice showed loss of at least half of the lateral desmosomes but the apical desmosomes were preserved [160].

1.6.4. Mouse models of desmoplakin

DP null embryos showed not just loss of anchorage of IF to desmosomes but a collapse of the IF network as well as defects in desmosomal assembly and/or stabilization and proved to be embryonic lethal at E6.5 [161]. Rescue of extra-embryonic tissues by aggregation of tetraploid wild type and diploid mutant morulae, lead to longer survival, but death was observed shortly after gastrulation with defects in heart muscle, neuroepithelium and skin epithelium, all of which possess desmosomes, as well as the microvasculature, which does not. Vascular tissue has specialized junctions composed of DP, PG and VE-cadherin. The timing of lethality is similar to that of the VE-cadherin null embryo, suggesting that cause of death may be a defect in vasculature, not reported for PG null embryos [162]. DP when knocked out in mice under K14 promoter that is specific for epidermis, salivary and mammary epithelia specific showed that although the number of epidermal desmosomes in DP null skin is similar to wild type, they lack IF attachments which compromises their function causing intercellular separation and loss of integrity of the epidermis. DP null keratinocytes have fewer desmosomes *in vitro* and are unable to undergo actin reorganization and membrane sealing during epithelial sheet formation along with having reduced adherens junctions [163].

1.7. Desmosome assembly

Cell aggregation assays show that close apposition of plasma membranes happens immediately after cells come into contact with one another and desmosome formation seems to start at 15 minutes, while a complete desmosome can be seen at 90 minutes post aggregation [19] (Figure 1.15). As desmosomes are calcium dependent junctions, calcium switch assays, where cells are cultured in low calcium (<0.1mM)

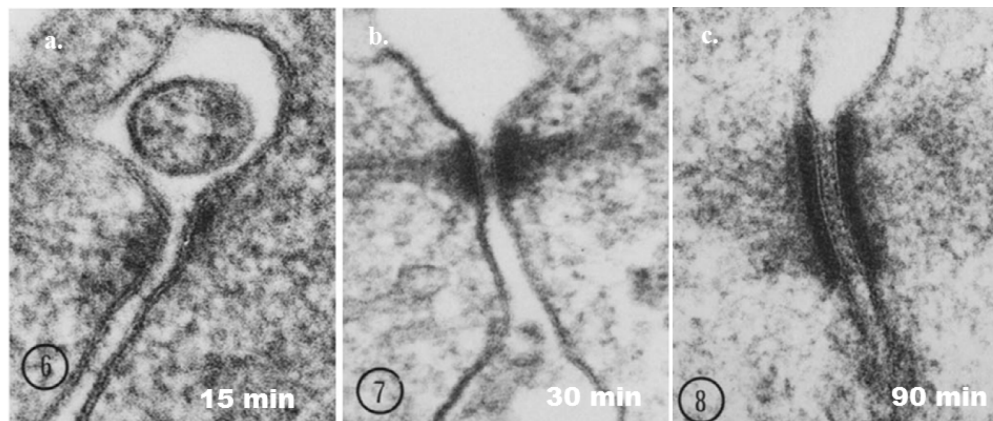


Figure 1.15. Electron micrographs depicting desmosome formation – *Desmosome formation between differentially labelled (latex and gold) C4I human cervical squamous cell carcinoma cells visualized a. 15 min post aggregation showing formation electron dense region near plasma membrane of apposing membranes that are not aligned to each other (x 190,000), b. 30 min post aggregation showing formation of junction with two distinct plaques on apposing plasma membranes in perfect alignment with each other and poorly differentiated filamentous material oriented at right angles to the plane of the plaques (x 160,000), and c. 90 min post aggregation showing desmosome formation with the intercellular space well organised as well as IF oriented obliquely to the plane of the plaques (x 160,000) (adapted from [19]).*

medium and switched to media with normal calcium (1.8 – 2 mM) medium, are performed to study desmosome formation (reviewed in [164]). Early experiments have revealed that the biosynthesis of desmosomal proteins and their transport to the membrane takes place at the same rate in low calcium medium as well as normal calcium medium. However, the half-life and turnover of these proteins is drastically different in these two conditions; in low calcium conditions, the half-life is decreased by a factor of seven to twelve times probably owing to the fact that they are more Triton soluble in low calcium conditions and half-desmosomes form but get internalized and possibly degraded [50, 165, 166]. DP is partitioned from Triton soluble pool to Triton insoluble pool upon

induction of cell-cell contact within 4 hours after synthesis and the ratio of the Triton insoluble pool to the Triton soluble pool increases by three-fold in MDCK cells [51]. The desmosomal cadherins DSC3 and DSG3 interact with each other at 60 minutes post switch from low calcium to high calcium while DSC3 and PG interact just 10 minutes post switch from low calcium to high calcium in Triton soluble complexes in human squamous cell carcinoma keratinocytes [167]. The palmitoylation of PKPs has been shown to be necessary for their partitioning into the Triton insoluble fraction as well as incorporation into desmosomes [57]. Thus extracellular calcium as well as palmitoylation is an important determinant of Triton insolubility and stability of desmosomal proteins.

Desmosome formation is dependent on the adherens junctions; in the absence of classical cadherins like E-cadherin and P-cadherin, desmosomal components do not localize to the cell membrane/ border [168, 169]. E-cadherin and PKP3 complex is formed even in low calcium conditions and is essential for desmosome formation [169]. Desmosomes do not form in cells lacking α -catenin. Introduction of full length α -catenin as well as middle domain or carboxyl-terminal domain of α -catenin rescues the phenotype and leads to desmosome formation [170]. Similarly, the assembly of desmosomal components can be induced by PKP1 but the desmosomal junction formation requires the presence of a classical cadherin [171]. Thus adherens junction formation is a precedent for desmosome formation.

PG being the only protein common to both adherens junctions as well as desmosomes plays a very important role in desmosome formation. The amino-terminal domain of PG is important for its incorporation into desmosomes while the carboxyl-terminal domain of PG is important for internalisation and/ or disassembly of desmosomes [172]. PG null keratinocytes show impaired cell membrane/ border localization of desmosomal components but not adherens junction components [173].

Desmosome like structures in PG null keratinocytes have β -catenin substituting for PG with impaired recruitment of PKP1 and DP [174]. Another study confirms that in PG knockdown cells, other desmosomal proteins cannot localize to the cell membrane/ border [169]. 14-3-3 γ has been shown to bind to PG in a PKC μ dependent manner and is required for kinesin-1 dependent transport of PG to the cell border [175]. Thus PG is indispensable for desmosome formation.

DP incorporation into de novo desmosomes seems to be divided into three phases starting with DP being transported to the cell border within 3 minutes to nascent junctions, followed by a separate pool of DP interacting with PKP2 in cytoplasmic particles within 15 minutes and finally actin filaments and RhoA activity mediated incorporation of DP and PKP2 containing cytoplasmic particles into desmosomal junctions [176]. It has also been suggested that in migrating cells of an epithelial sheet, the continuous assembly and disassembly of desmosomes is dependent on actin cytoskeleton [177].

The amino-terminus head domain of PKP1 binds to the carboxyl-terminal domain of DSG and particularly 1-34aa binds to DP while the carboxyl terminal of PKP1 686-726 aa are required for its localization to the cell border [178, 179]. PKP3 knockdown leads to impairment of desmosome formation and decreased cell-cell adhesion [108]. 14-3-3 γ binds to PKP3 and DP and could play a role in transport of these proteins to the desmosome [175]. Results from our laboratory suggest that PKP3 forms a complex with kinesin-1 (unpublished data). A recent report suggests that PKP3 mediates desmosome assembly through Rap1 GTPase mediated adherens junction maturation as well as phase three of DP accumulation at de novo desmosomes [180]. PKP2 also seems to act as a scaffold for the formation of DP-PKP2-PKC α complex that leads to the phosphorylation of DP and is essential for desmosome assembly [64]. PKC α localization

to the plasma membrane and desmosome formation are dependent on SERCA2 calcium ATPase [65]. Thus PKPs have been shown to play different roles in desmosome formation and PKC α could be a mediator of calcium dependent signalling for desmosome formation.

The two types of desmosomal cadherins DSCs and DSGs seem to play very different roles in desmosome formation. DSG2 is transported to the plasma membrane by the kinesin-1 motor protein while DSC2 is transported to the plasma membrane by kinesin-2 motor protein; knockdown of both kinesin-1, as well as kinesin-2 impairs desmosome formation without affecting adherens junctions in SCC9 and A431 cells [181]. In contrast, another report suggests that kinesin-1 motor protein forms a complex with E-cadherin, β -catenin and p120 catenin of the adherens junctions but not with occludin, JAM-A or DSG2 while kinesin-2 motor protein does not form a complex with any of these epithelial junctional proteins in T84 metastatic colon carcinoma cells and the disassembly of adherens junctions and tight junctions is dependent on microtubules [182]. The reasons such contrasting reports could be that the latter study was based purely on biochemical assays that could have failed to detect direct interactions between kinesin and their desmosomal cadherin cargos and might have pulled down large complexes with different functional relevance. Also, the two studies were carried out in different cell systems that might have different mechanisms for desmosome junction assembly.

A recent report suggests that DSC2 forms calcium dependent homophillic bonds during de novo desmosome formation while DSG2 takes part in formation of mature calcium independent desmosomes by forming heterophillic bonds with DSC2 [183]. Another report where an extracellular crosslinking agent was used suggests that desmosomal cadherins only form homophillic trans interactions [126]. The nature of

desmosomal cadherins interaction as to being homophillic or heterophillic is debatable and so is its significance with respect to desmosome assembly and maturation.

The cytoplasmic tails of DSC 'a' isoforms fused to connexin 32 transmembrane region are capable of recruiting desmosomal plaque proteins like DP and PG to the cell border. However, the cytoplasmic tail of DSGs fused to connexin 32 transmembrane region acts as a dominant negative that not only fails to recruit desmosomal proteins to the chimera but also leads to disruption of all endogenous desmosomes [184]. PG binds to 735-776 aa in the cytoplasmic tail of DSG1 which is a highly conserved region in the cadherin family and responsible for this dominant negative effect [185]. Similarly the ICS (779-866 aa) domain of DSG3 is required for binding to PG and its incorporation into desmosomes [186]. While DSG2 and DSC2 can get incorporated into desmosomes in most cell types, the isoform specificity of other desmosomal cadherins is pivotal for desmosome formation [187]. A recent report suggest that the cytoplasmic juxtamembrane region of DSC2 is essential for binding to PKP2 as well as PKP3 and this interaction is indispensable for desmosome formation [188]. Thus the cytoplasmic domains of desmosomal cadherins play a crucial role in regulating desmosome assembly mediated by their distinct interactions with the desmosomal plaque proteins.

Desmosomal components have been shown to be present in small endocytic vesicles as well as complex multivesicular bodies during desmosome assembly [189]. While Sec6 and Sec8 containing exocysts are required for adherens junctions formation, at a later stage, Sec3 containing adherens exocysts are recruited to the plasma membrane and are required for formation of desmosomes [190]. It could be speculated that desmosomal proteins form complexes within the cytoplasm that get transported to the cell membrane through such vesicles.

Desmosomes have also been shown to be associated with cholesterol containing membrane rafts. DSG2 has been shown to be associated with membrane rafts in cells forming desmosomes and, DSC2 was shown to be part of caveolin-1, flotillin and particularly osteolysin containing membrane rafts [191, 192]. Depletion of cholesterol affected this association as well weakened cell-cell adhesion [191, 192]. DSG2 has been shown to be associated with caveolin-1 and that disruption of lipid rafts results in accumulation of DSG2 accompanied by shift of DSG2 to non-raft fractions [58]. PG ARM repeats 6-8 interact with flotillin 1 and flotillin 2 and this interaction is required for association of both E-cadherin and PG with membrane rafts [193]. Palmitoylation of PKP2 and PKP3 is necessary for its incorporation into caveolin-1 containing lipid rafts [57]. Thus multiple reports suggest the association of desmosomal molecules with lipid raft micro domains of the cell membrane to be essential for desmosome formation, with one report alluding palmitoylation of desmosomal proteins to be required for such association.

Desmosomes are stable structures that are not lost even during major cell morphological changes that happen during cell division but at the same time, desmosomes are also flexible and dynamic structures with the desmosomal protein turnover being observed even in stable desmosomes at the plasma membrane of the cell [194]. EGFR inhibition leads to an increase in desmosome formation and a reduction in calcium dependence of desmosome formation accompanied by an increase in stability of desmosomal proteins [75]. Concurrently, EGFR activation results in tyrosine (643,724 and/ or 729) phosphorylation of PG accompanied by loss of DP from cell border and decreased cell-cell adhesion [173]. 14-3-3 σ interacts with cytoplasmic PKP3 mediated by serine 285 phosphorylation on PKP3 and regulates the exchange of cytoplasmic PKP3 with the desmosomal PKP3 by favouring incorporation of PKP3 into desmosomes but is

not associated with the desmosome [195]. Thus desmosome dynamics could potentially be controlled by different pathways through post-translational modifications on desmosomal proteins.

1.8. Plakophilin 3

PKPs are part of the p120 catenin subfamily of armadillo proteins. The p120 family of proteins can also be divided into two sub groups – the first group containing p120, ARVCF, δ -catenin (also called NPRAP) and PKP4 (also called p0071) having 65-81.5 % homology amongst its members, and the second group containing PKP1, PKP2 and PKP having 51 – 60.9 % homology amongst its members. These two groups share 50% homology between them and are thus evolutionarily comparatively distantly related. The genes of the p120 family are dispersed throughout the genome and the PKP3 gene is located on the 11p15 chromosome. Hence the gene expression is probably not coordinately regulated as it is for the desmosomal cadherins (reviewed in [196-198]). PKP3 was identified in 1999 by two independent groups and is expressed in desmosomes of all epithelia except hepatocytes [199, 200]. PKP3 is predominantly localised to desmosomes, however it has also been observed to localize to the cytoplasm, and other evidence suggests that it might localize to the nucleus like other ARM domain proteins [199]. Deletion of the amino-terminus head domain of PKP3 leads to its localization primarily in the nucleus with diffuse cytoplasmic localization. Deletion of the ARM domain and carboxyl-terminus domain leads to formation of aggregates in the cytoplasm along with diffuse cytoplasmic localization and reduced cell border localization [201]. All PKPs have two splice variants (Figure 1.10). The splice variants of PKP3, PKP3a and PKP3b, differ from each other at the amino-terminus by the splicing of the newly identified exon 1b probably driven by an alternative promoter which has a binding site for the C/EBP

family of transcription factors. PKP3a is broadly expressed among epithelial cells while PKP3b is expressed only in stratified epithelia [6]. PKP3 expression is repressed by the binding of the EMT transcription factor Zeb1 and Snail to the E-box sites in the PKP3 promoter [110]. The canonical PKP3 sequence is of the PKP3a isoform. Yeast two-hybrid assays show that PKP3 interacts with all major desmosomal components like DSG1-3, DSC1-3, PG, DP and keratin 18 [201]. Similarly immunoprecipitation experiments show that PKP3 binds to Dsg1-3, Dsc3a and -b, DP, and PG [201].

PKP3 localizes to RNA stress granules and binds to RNA binding proteins like Poly (A) binding protein (PABPC1), fragile-X-related protein (FXR1), and ras-GAP-SH3-binding protein (G3BP) and found in the same fractions of density gradient separated proteins as translation initiation complex protein eIF-4E and the ribosomal protein S6 [91]. Interaction of PKP3 with G3BP, PABPC1, and UPF1 (plays a role in non-sense mediated mRNA decay) but not with FXR1 was dependent on RNA binding, and PKP3 as well as FXR1 could stabilize DP and PKP2 mRNA levels and increase their protein expression [90]. PKP3 has been shown to be essential for neural crest development in *Xenopus laevis* embryos and localizes in the cell-cell contacts, cytoplasm as well as nucleus in the naïve ectoderm cells [202]. In *Xenopus laevis*, PKP3 interacts with the ETV1 transcription factor in the nucleus and positively modulates its transcription activity [89]. 14-3-3 σ interacts with PKP3 in a serine 285 phosphorylation dependent manner in the cytoplasm and limits its exchange with the desmosomes [195]. This association is probably regulated in protein kinase A dependent phosphorylation and protein phosphatase 2A dependent dephosphorylation of the serine 285 residue of PKP3 [203]. PKP3 has also been shown to form a complex with the Rap1 GTPase and stabilise adherens junctions as well as facilitate desmosome assembly by accumulating DP containing junction precursors [180].

Palmitoylation of PKP3 at C569 is necessary for its partitioning into Triton insoluble protein fractions as well as incorporation into desmosomes [57]. PKP3 is essential for desmosome formation and a complex of PKP3– E-cadherin along with PG is present at the membrane even in low calcium conditions is required to initiate desmosome formation [169]. During de novo desmosome assembly, PKP3 and DSC2 containing vesicles/ aggregates are seen to be transported to the cell membrane and PKP3 returning back to the cytoplasm [204]. Interestingly, both PG and PKP3 are dependent for anterograde transport from cytoplasm to the desmosome on microtubules but for retrograde transport only PKP3 is dependent on microtubules [205]. 14-3-3 γ enables PG transport to the desmosome mediated by kinesin-1 and is also shown to bind to PKP3 [175]. Results from our laboratory show that PKP3 also binds to kinesin-1 (unpublished data). There are reports of other uncharacterised protein-protein interactions of PKP3 in the literature. PKP3 interacts with a dynamin-related protein known to be found in endoplasmic reticulum (ER) tubules and secretory vesicles, dynamin 1-like [111], estrogen receptor β in the nucleus [206] and focal adhesion protein ZF21 that promotes dephosphorylation Tyr397 of FAK [207]. PKP3 can also get tyrosine phosphorylated by the tyrosine kinase CSF-1R [208].

PKP3 null mice show reduced desmosomes and adherens junctions in the basal layer of the epidermis, were prone to dermatitis, had hair follicle abnormalities and increased thickness of epidermis accompanied by excess suprabasal layers but no changes in the levels of epidermal differentiation markers [160]. Interestingly, apical desmosomes and sealing between suprabasal layers of the epidermis was largely normal, but at least half of the lateral desmosomes of the basal layer of PKP3 null epidermis were lost. PKP3 null skin showed increase in the levels of DPI, but not DP11, and β -catenin levels in all layers of the epidermis. The degree of upregulation of other adherens junction and

desmosome proteins varied between different PKP3 null mice. Some PKP3 null mice had increased levels of PKP1 while others showed increased levels of PKP2 [160]. The increase in the levels of other PKP isoforms in PKP3 null mice show the existence compensation mechanisms for loss of PKP3 as well as show that there is a certain degree of functional redundancy between the various PKP isoforms. In PKP3 null mice with upregulation of PKP1, the levels of the adherens junction proteins like E-cadherin, β -catenin and α -catenin were increased as well [160]. The increase in adherens junction components on upregulation of PKP1 in PKP3 null mice is surprising and could indicate either compensation for cell-cell adhesion loss from loss of one type of cell-cell adhesion junction being compensated by another type of cell-cell adhesion junction, or the increase in PKP1 levels having an independent effect of increasing adherens junction proteins.

Loss of PKP3 leads to increased tumour formation and metastasis in vivo. This is characterised by a decrease in desmosome size and cell-cell adhesion and an increase in cell migration and anchorage independent growth [108]. PKP3 loss is observed in metastatic oropharyngeal tumours [107] and in the invasive front of colon carcinomas [110]. However, PKP3 expression is increased in non-small cell lung carcinomas (NSCLC) [111], breast cancers [113] and increased PKP3 mRNA was found in the blood of gastrointestinal cancer patients [112, 209]. Thus PKP3 functions in tumour progression could be context dependent and should be elucidated further to understand the underlying mechanisms.

1.9. Desmocollin 2

The desmosomal cadherins, DSCs and DSGs show 30% aa identity to each other as well as to classical cadherins of the adherens junction that have greater similarity in their extracellular domains. Desmocollins have two alternatively spliced isoforms 'a' and

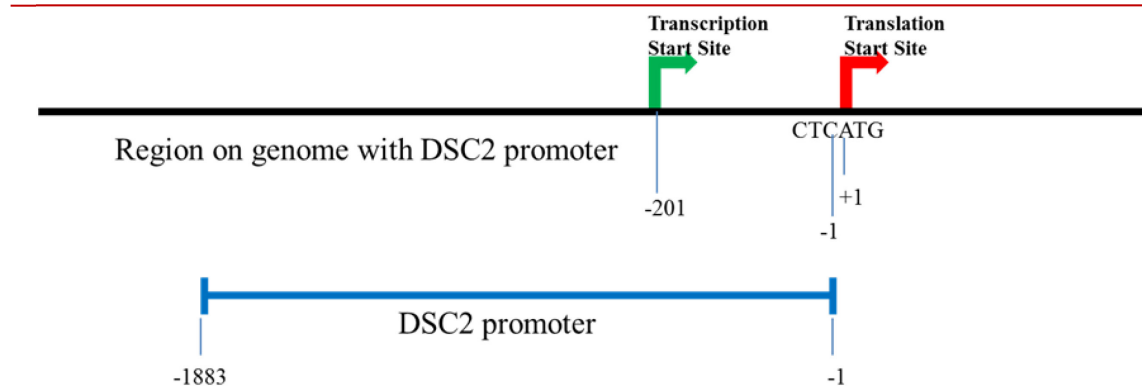


Figure 1.16. DSC2 promoter – The DSC2 promoter has been recognised as a region 1883 bp upstream of the translation start site of DSC2. The transcription start site is 201 bp upstream of the translation start site.

‘b’. The shorter ‘b’ isoform lacks does not seem to contain the sites necessary for binding to desmosomal plaque proteins and its function remains unresolved. Human desmosomal cadherin genes are arranged in a tandem on chromosome 18q12.1 and the DSC genes contain 17 exons, with the exon 16 being the alternatively spliced mini exon. DSC2 is the most ubiquitously expressed DSC isoform and the only DSC isoform present in simple epithelia (reviewed in [61]).

DSC2 mRNA transcription is seen during mouse embryonic development in two stages – from unfertilized egg up to the early 8-cell stage showing presence of maternal genome transcription, then from 16-cell morula stage or 32-cell early blastocyst stage onwards showing embryonic genome transcription [210]. However the maternal DSC2 isn’t translated as DSC2 protein synthesis starts from blastocyst stage where it regulates the assembly of early nascent desmosomes that form in the trophectoderm [211]. In the early mouse embryo, presence of contact-free cell surface seems to activate transcription of DSC2 as isolation and culture of inner cell masses induces an increase in the amount of DSC2 mRNA and proteins levels [210].

The human DSC2 promoter has been identified as a region 1.9 kb upstream of the translation start site having a CpG island, and binding sites for numerous transcription factors including AP-1, AP-2 and SP1 while a fragment of 525 bp upstream of translation start site showed increased activity only in epithelial cells [212] (Figure 1.16). The presence of CpG islands indicates a possible role for DNA methylation in DSC2 regulation. The DSC2 promoter has no obvious CCAAT or TATA boxes and has a transcription initiation site 201 bp upstream of translation start site [212] (Figure 1.16). The CCAAT/enhancer-binding protein (C/EBP) family has been implicated in regulating DSC transcription. DSC3 expression is activated by C/EBP β while DSC1 expression is activated by C/EBP α , while both DSC3 and DSC1 expression was activated by C/EBP δ . The authors of this report studied only DSC 1 and 3 isoforms and, C/EBP α , β and δ isoforms. They also observed all these 3 C/EBP isoforms are capable of binding to DSC promoter but not capable of activating it [213]. CDX1 and CDX2 are intestine-specific homeodomain transcription factors that have been associated with formation of tight junctions, adherens junctions as well as desmosomes [214]. The DSC2 promoter contains two CDX consensus binding sites and both CDX1 and CDX2 can bind to the DSC2 promoter. CDX binding also seems to relieve the effect of a potent repressor of DSC2 promoter [215]. Interestingly CDX1 and C/EBP α have been shown to interact to lead to transcriptional activation of another intestinal differentiation related gene PPAR γ [216]. PG mediated Lef-1 signalling along with ectodysplasin-A (EDA)/ ectodysplasin-A receptor (EDAR)/NF- κ B signaling cascade has been shown to activate DSC2 expression and lead to a DSC switch from DSC3 isoform to DSC2 isoform in placode keratinocytes [217]. Nrf-2 induced miR-29a and miR29b have been shown to target DSC2 mRNA and impair hyperadhesion of desmosomes in keratinocytes [218]. Loss of DSC2 promotes cell proliferation and tumorigenesis through activation of Akt/ β -catenin signalling pathway in

CRC [118]. Also in CRC, loss of DSC expression is correlated with higher tumour grade [115].

1.10. CDX transcription factors

Claudal is a homeobox gene originally identified in *Drosophila* and shown to be important for anterior-posterior patterning with high gradient of expression in the gut, gonads and genital disc ([219] and reviewed in [220]). There are three mammalian homologues of claudal – CDX1, CDX2/3 (CDX3 in the hamster and CDX2 in mice and humans) and CDX4; only two are expressed in the intestine – CDX1 and CDX2 (reviewed in [221]). CDX proteins generally function as transcriptional activators with few reports of CDX proteins acting as transcriptional repressors. A canonical CDX response element (CDRE) has been identified as ‘TTTATG’ which is recognised by all CDX members (reviewed in [220]). CDX1 null mice show homeotic transformations of the axial skeleton but no overt intestinal phenotype while CDX2 mice are lethal at E3.5 due to implantation failure and CDX2 heterozygous mice exhibit an intestinal phenotype of lesions in the pericaecal region and proximal colon (reviewed in [220]). Misdirecting the expression of CDX1 or CDX2 in the stomach or oesophagus has resulted in the conversion of the epithelium to small intestinal epithelium (reviewed in [220]). Similarly, Barrett's metaplasia which leads to oesophageal epithelium switching to intestinal epithelium results from ectopic expression of CDX2 in the oesophageal epithelium (reviewed in [222]). Loss of CDX2 in the colon leads to a shift to a cecum-like epithelial morphology and gain of cecum-associated genes which was more discernible with subsequent loss of CDX1 [220]. CDX2 is required for differentiation of the small intestinal epithelium, and both CDX1 and CDX2 contribute to homeostasis of the colon [220]. Thus CDX transcription factors play an important role in intestinal differentiation.

CDX1 and CDX2 have common functions as well as context-dependent transcriptional specificity in the intestinal epithelium (reviewed in [220]). CDX2 loss is observed with 30% of CRC and correlated with high tumour grade and poor prognosis (reviewed in [220]). Likewise, CDX2 overexpression in CRC cells decreases proliferation, invasion and cell migration (reviewed in [220]). Thus CDX2 seems to function as a tumour suppressor (reviewed in [220]). On the other hand, CDX2 over expression due to gene amplification in CRC was implicated as an oncogene that promotes cell proliferation and migration but a heterogeneous CDX2 expression is generally observed with CDX2 expression being lost at the invasive front of the tumours (reviewed in [223]). CDX expression is governed by a number of signalling pathways, including canonical Wnt, FGF and RA, as well as via autoregulation and cross-regulation (reviewed in [221]). Some of the targets of CDX transcriptional regulation are intestinal alkaline phosphatase (IAP), calcium channel MS4A12, Solute carrier family 5, member 8 (SLC5A8), polarity gene Ptk7, sucrase-isomaltase, glucagon, intestinal phospholipase A/ lysophospholipase, carbonic anhydrase, and lactase (reviewed in [221, 224]). CDX1 and CDX2 bind to DSC2 promoter and activate the expression of DSC2 probably by relieving the activity of a transcriptional repressor [215]. CDX2 also has roles in cell signalling not related to its transcriptional activity. CDX2 can increase cell proliferation by blocking proteasomal degradation of cyclin-dependent kinase inhibitor p27Kip1. CDX2 can bind to β -catenin and inhibit β -catenin's interaction with Tcf-4 and inhibit β -catenin driven transcription. CDX2 binds to the p65 subunit of NF- κ B and inhibits NF- κ B binding to the Cox-2 promoter leading to decreased Cox-2 production and increased PGE2 that stimulates proliferation and invasion in CRC. CDX2 interacts with KU70/80 complex specifically in CRC cells but not in leukaemia cells and inhibits DSB DNA repair. An alternatively spliced variant of CDX2 called CDX2-AS lacks DNA binding domain and does not have

any functions in transcription but rather has functions in processing of pre-mRNAs by RNA splicing of gut specific genes (reviewed in [225]).

1.11. C/EBP transcription factors

CCAAT/enhancer-binding protein (C/EBP) family transcription factors contain basic-leucine zipper (bZIP) class of DNA-binding (DBD) and dimerization domain (reviewed in [226]). For bZIP factors, the DBD can be designated as a composite DBD/NLS as it also serves as the primary nuclear localization signal (NLS). The bZIP domain is highly conserved in the bZIP superfamily and almost invariant in C/EBP family which makes them amenable to homotypic as well as heterotypic dimer formation as well as supports the argument for minimal selectivity among the homotypic-dimers for DNA target sites (reviewed in [4]). The C/EBP family has six identified isoforms – α , β , γ , δ , ϵ and ζ (C/EBP ζ also called CHOP, GADD153, and DDIT3) (Figure 1.17). C/EBP α , β and δ are coded by intronless genes. C/EBP γ and ζ do not have functional amino-terminus homology with other C/EBP family members (reviewed in [4]). C/EBP α has three translationally regulated isoforms – extended (~48 kDa), full-length (42 kDa) and truncated (30 kDa). C/EBP β also has three translationally regulated isoforms LAP* (38 kDa), LAP (35 kDa) and LIP (20 kDa). C/EBP ϵ has four alternatively spliced isoforms (32 kDa, 30 kDa, 27kDa and 14kDa). The smallest isoforms of each of these C/EBP family members lack the transactivation domain (TAD) and can function as dominant negatives (reviewed in [226]). An optimal symmetrical C/EBP consensus binding sequence has been identified as ‘RTTGCGYAAY’ (where R is A or G, and Y is C or T). However many variations are tolerated and most sites contain a conserved half-site along with a more divergent sequence that contains at least 2 bp of the consensus. C/EBP ζ / C/EBP heterodimers can bind to a different consensus DNA sequence identified

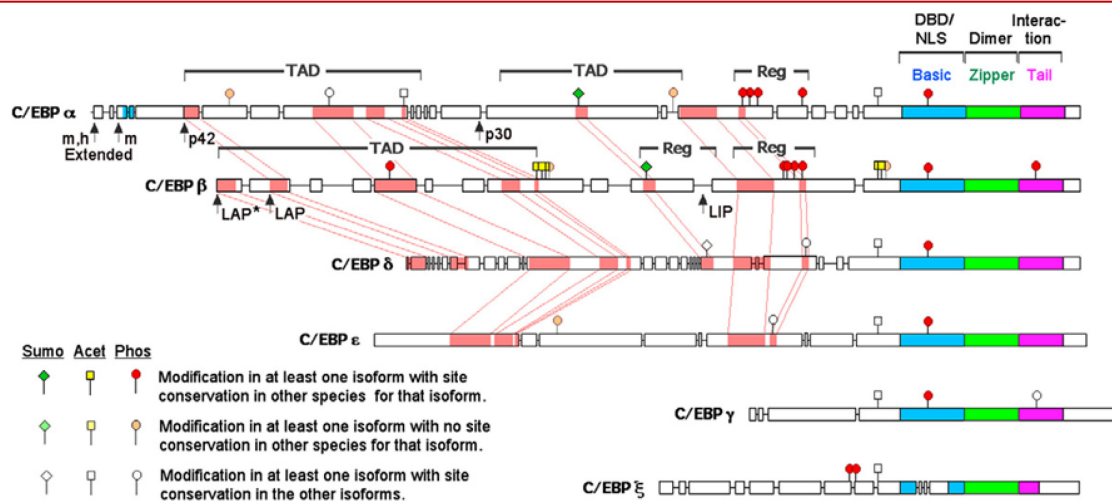


Figure 1.17. C/EBP family proteins – C/EBP is a six gene family with inter-species intra-isoform homology (open boxes) as well as intra-species inter-isoform homology (pink shaded boxes with inter connecting lines). bZIP regions homology is not displayed in this figure except for the modifications associated with the basic DBD of C/EBPζ. PTMs are shown as per the key indicated. Arrows indicate the various isoforms generated by alternative translation start codons (reproduced from [4]).

as ‘PuPuPuTGCAAT[A/C]CCC’(where Pu is a purine) (reviewed in [226]). C/EBP proteins also form dimers with other bZIP domain transcription factors, especially with members of the CREB/ATF family and these heterodimers can have different transactivating potential and/ or DNA binding specificity or affinity compared with the corresponding homodimers (reviewed in [4]). C/EBPs are also regulated by different post-translational modifications (PTMs) like phosphorylation, sumoylation and acetylation (reviewed in [4]) (Figure 17). C/EBPα acts as a repressor of E2F dependent transcription for targets like Myc and Dhfr; sumoylation of C/EBPα can inhibit its interaction with the SWI/SNF chromatin remodelling complex without altering its DNA binding ability and act as an inhibitor of its repressor activity (reviewed in [227]). DSCs expression is differentially regulated by C/EBPs. C/EBPα, C/EBPβ and C/EBPδ are all able to bind to DSC1 and DSC3 promoters, but only C/EBPα and C/EBPδ activate DSC1

expression while only C/EBP β and C/EBP δ activate DSC3 expression [213]. CDX1 transcription factor has been shown to interact with C/EBP α by mammalian two hybrid, GST pulldown and co-IP, and this interaction has been shown to be important for expression of PPAR γ that acts as a transcriptional regulator in intestinal differentiation [216]. Microarray data from our laboratory for PKP3 knockdown clones shows a decrease in C/EBP α in PKP3 knockdown cells [228].

1.12. Cell migration

Cell migration is a cellular process simply defined by the movement of a cell from one place to another. In multicellular animals, cells not only move through extracellular matrix but also on top of each other, between each other, and even through each other to reach their site of action (reviewed in [229]). In the physiological context cell migration is essential for a wide range of biological processes including embryogenesis, immune defence, angiogenesis, and wound healing. From the pathological point of view, cell migration is the driving force in disease conditions like tumour metastases, rheumatoid arthritis and atherosclerosis (reviewed in [230]). Cell migration has been widely studied in different contexts and different mechanisms and molecular pathways have been identified to contribute to this process. Cells can migrate either individually or as part of a collective in a sheet where intercellular interactions are maintained and coordinated movement of cells leads to the entire sheet moving forward (reviewed in [231]). Regardless of the context there are obvious morphological differences between a stationary cell and a migrating cell and a few basic steps are found to be common for most migrating cells. A migrating cell first establishes its direction of movement and forms a protrusion that defines its leading edge called as a lamellipodia. The formation of the lamellipodia leads to formation of new contacts with its substratum

followed by contraction of the cell body to generate a forward moving force. The contraction of the cell body forward leads to dissolution of existing contacts at the rear end of the cell (reviewed in [10]) (Figure 1.18). This multistep process has been in recent times been termed as “mesenchymal” migration (does not only relate to mesenchymal cells – can even be observed in amoeba-like *Dictyostellium*) to separate it from fast and gliding like migration called “amoeboid” migration. “Amoeboid” migration is the primary mode of migration for highly motile cells like neutrophils, dendritic cells and lymphocytes characterised by the formation of relatively weak contacts with the substratum and membrane blebbing rather lamellipodia formation (reviewed in [231]).

Mesenchymal cells are elongated, with integrin-dependent attachments called focal adhesions to the substratum, having actin meshwork forming a lamellipodia and actin stress fibres traversing through the cells, slow moving and having filopodial and lamellipodial membrane protrusions. Amoeboid cells are rounded, with weak sometimes integrin independent attachments to the substratum, having contractile actin cortex, fast

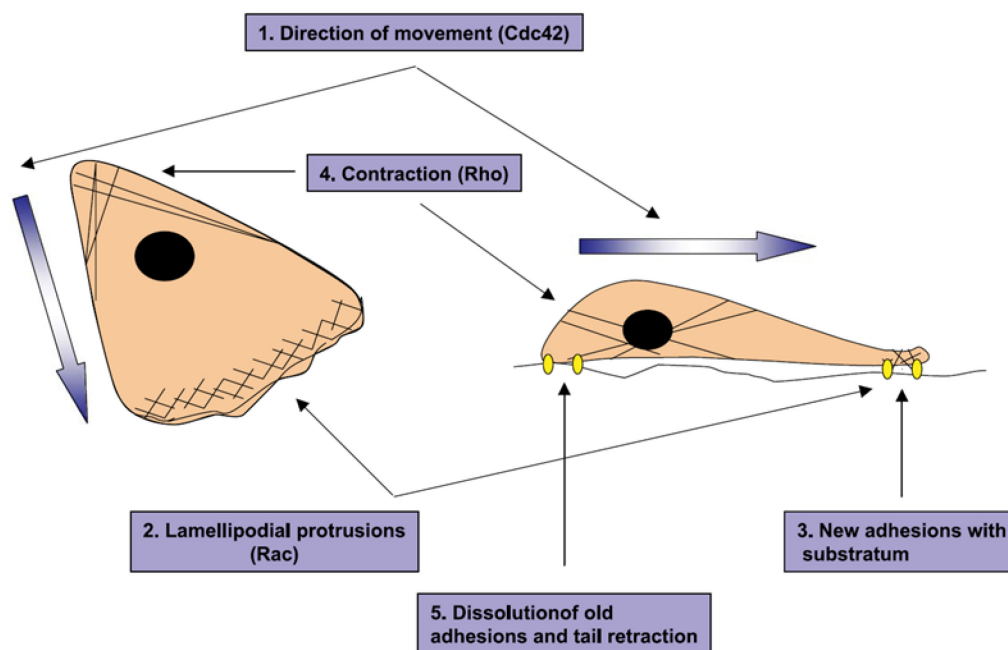


Figure 1.18. A migrating cell – A migrating cell performs a series of co-ordinated steps to move forward as described in the text (reproduced from [10]).

moving and having invasive blebbing (reviewed in [232]). In immune system functions as well as in pathological conditions like tumour metastasis, highly migratory and invasive cells can form specialized integrin-dependent structures called podosomes and invadopodia. As opposed to focal adhesions, podosomes and invadopodia are not associated with large actin filament bundles but are primary sites of rapid actin polymerization with a ring like actin structure that have the capacity for matrix degradation (reviewed in [231]). In collective migrating cells, there are two distinct types of interactions that regulate the movement of the sheet – the first is the interaction with the substratum which is similar to “mesenchymal” migration described for a single cell, the other is the interaction of cells with each other which is not only a mechanical coupling but also a biochemical coupling of signalling molecules. (reviewed in [233]). Recent reports show that apart from cell-substratum junctions being recycled, in collective migration, cell-cell junctions also follow a pattern of retrograde flow and recycling ([234] and reviewed in [235]).

1.13. Actin cytoskeleton in cell migration

Actin based protrusive and contractile forces are important in many processes like migration, morphogenesis, cytokinesis, endocytosis and phagocytosis. The regulation of actin reorganization is hence controlled by many different complex mechanisms. Abnormalities in actin dynamics are associated with pathological conditions like cancer, neurological disorders and myofibrillar myopathies. The most important role played by actin in all these contexts is that of force generation. Filamentous actin generates force concurrently by two distinct mechanisms – first by filamentous actin polymerization that pushes against cellular membranes, and second, by forming filaments with non-muscle myosin II that forms contractile structures in cells and depends on ATP-driven movement

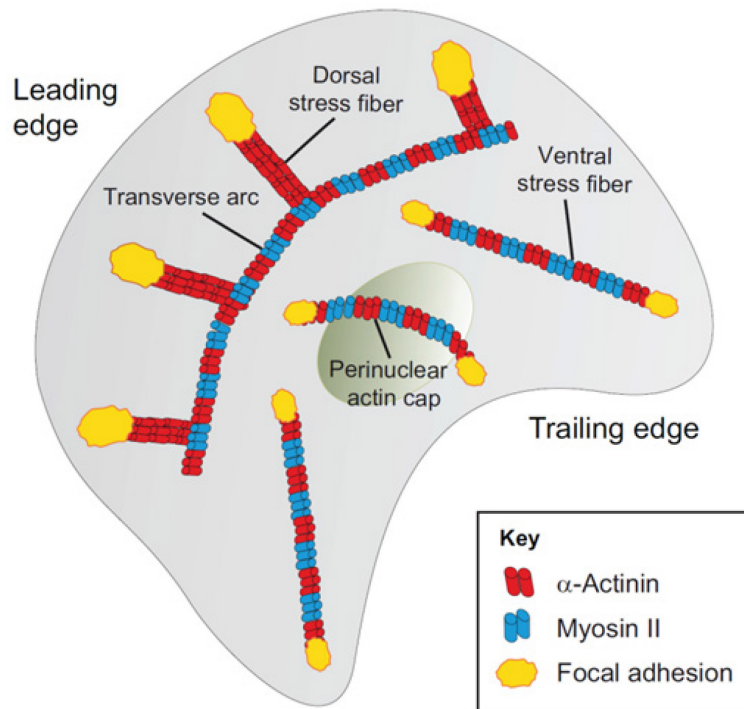


Figure 1.19. Types of actomyosin stress fibres – *Schematic representation of actomyosin stress fibres in a motile cell as described in the text (reproduced from [11]).*

of myosin II motors. Contractile bi-polar bundles of actomyosin cross-linked by α -actinin are termed as stress fibres. Stationary cells have stable thick stress fibres while motile cells have fewer, thinner and more dynamic stress fibres. Stress fibres are often linked to focal adhesions which are cell-extracellular matrix (ECM) junctions that anchor the actin cytoskeleton. Depending on their morphology and the manner of association with focal adhesions, stress fibres are divided into four categories – transverse arcs, dorsal stress fibres, ventral stress fibres and the perinuclear actin cap ([236, 237] and reviewed in [11, 238]) (Figure 1.19). Transverse actin arcs are curved actomyosin filament bundles having typical contractile actomyosin periodic bundles with α -actinin-myosin pattern that do not directly attach to focal adhesions but relay force through dorsal stress fibres that emanate from them ([236, 239] and reviewed in [11, 238]). Dorsal stress fibres emanate from

transverse actin arcs and at their distal ends they are attached to focal adhesions. Dorsal stress fibres lack myosin and do not typically contract but they can act as a platform for assembly of other types of stress fibres as well as connect them to focal adhesions ([239] [240] and reviewed in [11, 241]). Ventral stress fibres are contractile actomyosin bundles that are connected to focal adhesions at both ends and represent the major contractile machinery in interphase cells. Ventral stress fibres are mostly located at the posterior part of a polarized cell and occasional contractile cycles promote rear constriction and help cell movement ([242] and reviewed in [11, 243]). The perinuclear actin cap consists of actomyosin stress fibres positioned above the nucleus that are also connected to focal adhesions at both ends and helps regulate the shape of interphase cells. The perinuclear actin cap functions as a mechanotransducer to relay force to the nucleus and a subset of these stress fibres also attaches to the nuclear membrane and regulates the movement of the nucleus ([237, 244, 245] and reviewed in [11]) (Figure 1.19).

Different types of cell protrusions can exist at the leading edge, sometimes in conjunction with each other – filopodia, lamellipodia, membrane blebs, podosomes and invadopodia. Filopodia are thin exploratory extensions from the plasma membrane containing parallel bundles of actin filaments and are especially important for guidance of neuronal growth cones and angiogenic blood vessels. A model of filopodia assembly states that filopodia emerge from lamellipodial F-actin (filamentous actin) network nucleated by Arp2/3 complex with the help of actin bundling proteins like fascin and the anti-capping protein VASP in an N-WASP dependent manner. Filopodia can also be formed through an alternative mechanism that uses the actin nucleating and bundling proteins called formins like mDia proteins (reviewed in [229]).

Lamellipodia are fanlike protrusions, which look like a thin sheet, found in migrating cells made out of a meshwork of actin filaments that can extend to long

distances through ECM in vivo, pulling cells through the tissues. The lamellipodium contains the dorsal actin stress fibres while the lamella just behind the lamellipodium contains the transverse actin arc (reviewed in [11, 229]). The WASP-Arp2/3 cascade as well as formins and Spire family proteins have been shown to contribute to actin polymerization in the lamellipodium (reviewed in [229]).

Blebbing drives the plasma membrane forward by reversible detachment of the membrane from the cortical actin cytoskeleton, allowing cytoplasmic flow to push the membrane outwards rapidly due to hydrostatic pressure in the cell interior and is often observed in cells that are moving on a soft substratum. Alternatively, myosin II induced actomyosin contraction increases the hydrostatic pressure locally or globally thereby leading to focal rupture of the actin cortex from the membrane and inducing membrane blebbing. Reformation or reattachment of the actin cortex retracts the bleb. Multiple formins have been implicated in actin polymerization at membrane blebs, stabilization of the actin cortex requiring ERM (Exrin, Radixin and Moesin) proteins to attach the actin cortex to the plasma membrane. Although lamellipodia and membrane blebs are drastically different structures with the first favouring “mesenchymal” mode of migration and the later favouring “amoeboidal” mode of migration, it is possible to find these structures in conjunction in the same cell. However, an increase in blebbing leads to a decrease in lamellipodia and vice versa reflecting the antagonizing nature of the actin mechanical processes involved where one involves loss of actin interaction with the plasma membrane while the other requires close interaction of the actin filaments with the plasma membrane (reviewed in [229]).

Invadopodia and podosomes are actin-rich ECM degrading ring structures generally found on the ventral surface of migrating/ invading cells. Most of the actin machinery involved in formation of filopodia and lamellipodia is also required for

forming podosomes and invadopodia, with the key difference being that in addition to the actin polymerization machinery, the adaptor protein Tks5 and microtubules for delivery of vesicles containing proteases like MMPs are essential. Whether podosomes and invadopodia are different structures or invadopodia are just podosomes formation being deregulated and hijacked by malignant cells is debatable. While the defining distinction is that podosomes are found in normal cells, particularly immune system cells and invadopodia are found in malignant invasive cancer cells, there are some characteristics that have been reported to be different in these two types of structures. The first such distinction is that podosomes have been reported to only last for a few minutes, while invadopodia have been shown to last for hours. Also, classically, podosomes puncta have been identified at the leading edge of a cell migrating in 2D while invadopodia have been identified under the nucleus (reviewed in [229, 246]). The energy to propel the cell forward is thus always drawn from filamentous actin structures. Actin polymerization by itself is an exothermic process that can supply the energy required to propel a cell forward (reviewed in [247]).

1.14. Actin reorganization regulation by Rho GTPases

The Rho GTPases can be considered to be the master regulators of actin cytoskeleton with additional functions in cell polarity, gene expression, microtubule dynamics and vesicular trafficking. In the context of cell migration, Rho GTPases are responsible to initiate a signalling cascade that takes extracellular cues from cell surface receptors to ultimately regulate actin polymerization (reviewed in [10]) (Figure 1.21). Rho GTPases are a family of ubiquitously expressed proteins with about 20 members identified in mammals. They act as a molecular switch to control the activity of their downstream effectors by cycling between a GDP-bound inactive form and a GTP-bound

active form. The best studied Rho GTPases are RhoA, Rac1 and Cdc42. The classical functions of these Rho GTPases in actin polymerization have been defined as follows – RhoA regulates assembly of contractile actomyosin stress fibres while cdc42 regulates actin polymerization that forms filopodial protrusions and Rac1 regulates actin polymerization that drives lamellipodial protrusions. Additionally all three Rho GTPases promote focal adhesion formation and thus together regulate cell migration (Figure 1.18). The activity of the Rho GTPases is tightly regulated by three groups of proteins – guanine nucleotide exchange factors (GEFs), GTPase activating proteins (GAPs) and guanine nucleotide dissociation inhibitors (GDIs) (Figure 1.20). GEFs promote the exchange of GDP for GTP to activate the GTPase, GAPs enhance the intrinsic GTPase activity to inactivate the GTPase while GDIs inhibit this cycle by sequestering and solubilizing the GDP-bound form. Extracellular signals interact with these three groups of proteins, predominantly the GEFs and regulate Rho GTPases. The active Rho GTPases bind to their effectors and activate signalling cascades that ultimately affect actin polymerization (reviewed in [10]) (Figure 1.21).

PI3K can be activated by receptor tyrosine kinases or G protein coupled receptors. The PI3K lipid product PIP₃ binds to pleckstrin homology (PH) domain containing GEFs like Tiam-1 and Dbl family proteins, translocating them to the membrane at the leading edge of a migrating cell and promote Rho GTPase activity to drive actin polymerization. A possible positive feedback loop might exist as Rac1 also directly binds to PI3K and stimulates production of PIP₃. Thus the activity of Rho GTPases is primarily induced by their localization to the plasma membrane and Rho GDIs are effective in inhibiting them by sequestering them to the cytoplasm. Apart from the PI3K pathway activating conventional GEFs, focal adhesions can also activate Rho GTPases through DOCK180/ELMO1 complex or PIX GEFs that can be a similar signal

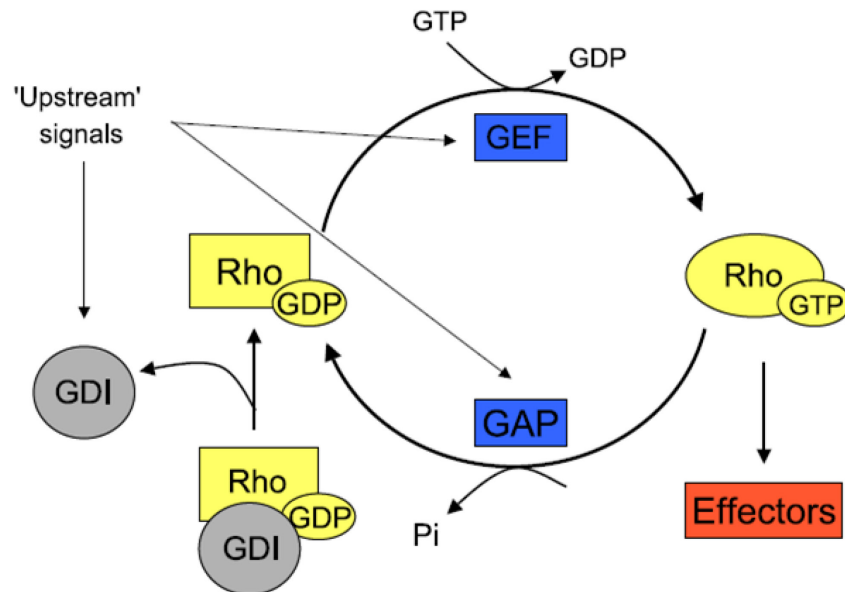


Figure 1.20. Rho GTPase cycling – *Rho GTPases are regulated by upstream signals that affect the activity of guanine nucleotide exchange factors (GEFs), GTPase activating proteins (GAPs) and guanine nucleotide dissociation inhibitors (GDIs). Only the GTP bound active form of Rho GTPases is capable of binding to its downstream effectors (reproduced from [10]).*

transducer that activates Rac1 (reviewed in [10, 248]). Rac1 as well as Cdc42 can activate the p65-p21-activated kinase (p65PAK or PAK1) that activates LIM kinase (LIMK) which in turn phosphorylates the actin severing protein cofilin on serine 3 inhibiting cofilin's severing activity and promoting actin polymerization. PAK1 also regulates focal adhesion turnover with the help of PIX and GIT1. LIMK-cofilin cascade is also activated by RhoA via p160ROCK kinase (ROCK). ROCK can also phosphorylate myosin light chain phosphatase (MLC phosphatase) and inhibit its phosphatase activity promoting the phosphorylation of myosin light chain (MLC) which in turn promotes myosin motor cross linking to actin filaments producing the actomyosin contractile filaments that generate force. Another downstream target of RhoA is the formin mDia which can nucleate actin filament formation as well as bundle actin filaments. The WASP/SCAR/WAVE family

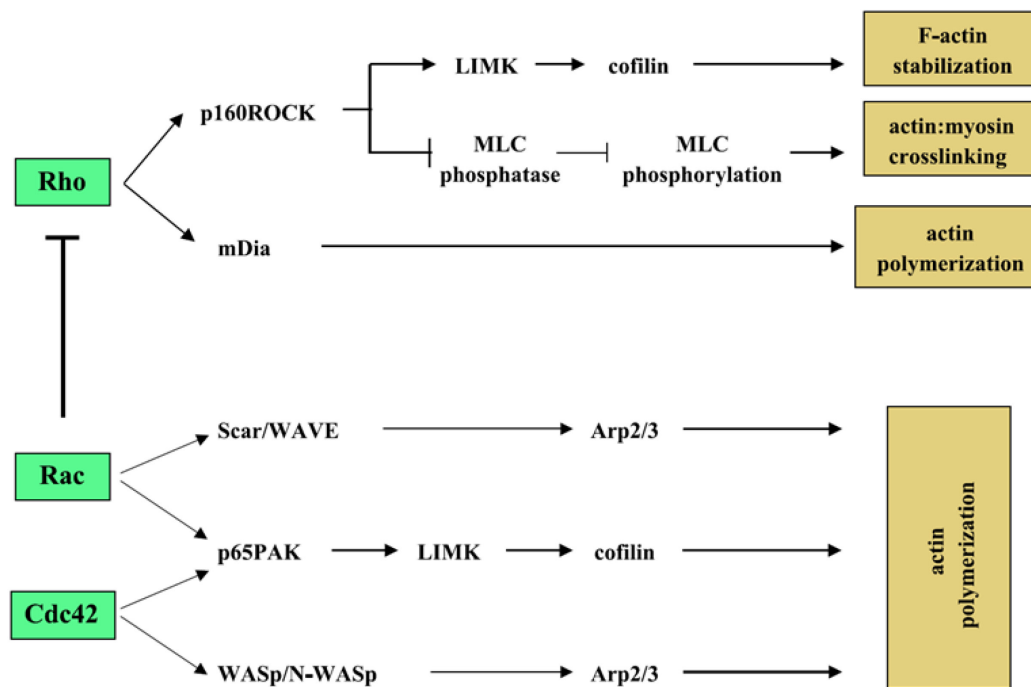


Figure 1.21. All roads lead to actin polymerization – The final effect of all Rho GTPase pathways is actin polymerization as described in the text (reproduced from [10]).

proteins can also be directly or indirectly activated by Rac1 and cdc42 which stimulates the Arp2/3 complex that initiates actin nucleation and de novo actin filament formation (reviewed in [10, 248]) (Figure 1.21).

1.15. Actin reorganization regulating pathways

Actin reorganization is controlled by various signals that are transduced by the Rho GTPases to the actin filament assembly and disassembly cycle. The regulation of this cycle is spatio-temporally controlled to give rise to various F-actin based structures. A simplified model of actin dynamics has been proposed by Pollard et al. (Figure 1.22). The actin monomer binding protein profilin (black), with the help of thymosin β 4 (not shown) maintains a pool of monomeric ATP-bound actin subunits (light blue). Extracellular stimuli can signal through receptor tyrosine kinases or G-coupled proteins or cell

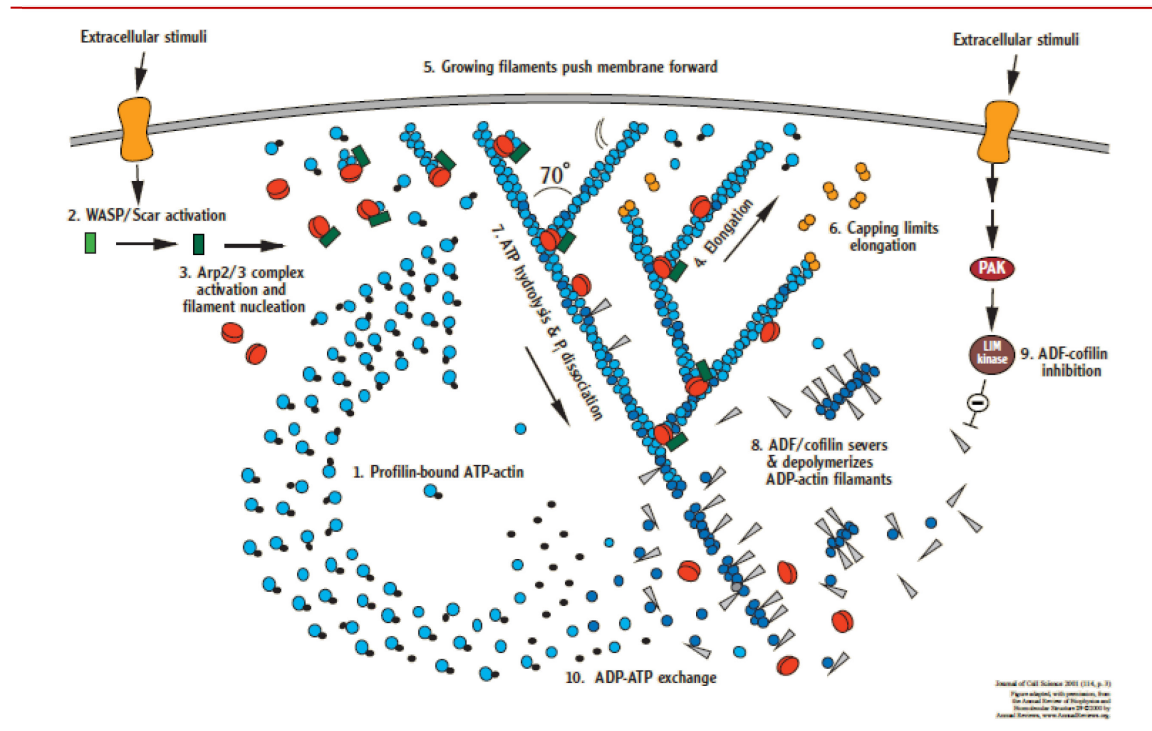


Figure 1.22. Actin dynamics – Schematic of actin polymerization and depolymerisation cycle in a migrating cell (reproduced from [16]).

adhesion complexes to Rho GTPases which in turn activate the WASP/Scar/WAVE family proteins (green) by freeing them from auto inhibition. Active WASP/Scar/WAVE proteins act as a scaffold for actin-ATP monomers and Arp2/3 complex (red) that contains seven subunits. Arp2/3 complex acts as a nucleator of de novo actin filament formation – nucleation of actin filaments is required because the initial steps of dimer and trimer formation of actin filaments are energetically unfavourable processes, while the elongation of the polymer at the barbed end from the trimer onwards is an energetically favourable process that takes place spontaneously by addition of profilin-actin complexes. Arp2/3 can also initiate the formation of the new filament as a branch on an old filament. The new filament elongates for a second or two until it is capped by capping protein (yellow). The incorporation of actin-ATP into the filament promotes a slow hydrolysis of the ATP to ADP that can take about six minutes unless catalysed by actin severing proteins like ADF/cofilin (grey). The ATP hydrolysis that leads to the filamentous actin

being ADP bound (dark blue) also destabilizes the filament and simultaneously dissociates Arp2/3 from that branch as well as recruits ADF/cofilin severing proteins. The ADF/cofilin severs the actin-ADP containing F-actin and then dissociates from actin-ADP. Profilin is the nucleotide exchange factor for actin and exchanges the ADP for ATP. Thus profilin again tightly binds to actin-ATP monomers replenishing the actin monomer pool ready for the next F-actin assembly cycle. The Rho GTPases also activate PAK which stimulates LIMK that phosphorylates and inhibits cofilin to decrease the rate of F-actin disassembly (reviewed in [16, 247, 249]).

Formins are a large family of 15 proteins that are Rho GTPase effectors regulated by Rho GTPases binding to the GTPase binding domain in formins and relieving their auto inhibition. Formins can nucleate as well as bundle actin filaments. Apart from formins and Arp2/3, other actin nucleating factors include Spire, Cobl, VopL, TARP and Lmod. Formins are characterised by the presence of a formin homology 2 domain (FH2) while other nucleators are characterised by the presence of a WASP homology domain 2 (WH2). Formins can also promote elongation of the filaments while the WH2 based nucleators recruit proteins of the Ena/VASP family to promote actin filament elongation. Cortactin plays a crucial role in Arp2/3 based branching of actin filaments by stabilizing the branch junctions (reviewed in [249, 250]). Cofilin family and gelsolin family proteins take part in severing of actin filaments (reviewed in [251]).

1.16. Epithelial mesenchymal transition

The Epithelial Mesenchymal Transition (EMT) is a developmental process by which epithelial cells get reprogrammed to a mesenchymal phenotype during gastrulation and neural crest formation as mesenchymal cells are free to migrate through the body cavity and allow for morphological plasticity. After migrating

to the suitable site, mesenchymal cells coalesce and repolarize to undergo a reverse transition – mesenchymal to epithelial transition (MET) to participate in novel cell-cell interactions forming new types of tissues and organs. EMT leads to the dissolution of cell-cell adhesion junctions like desmosomes and an increase in cell migration and invasion, which in pathological conditions like cancer is hijacked by the tumorigenic cells to lead to the acquisition of metastatic properties. The loss of desmosomal cell-cell adhesion is considered to be one of the hallmarks for EMT (reviewed in [252-254]).

1.17. Epithelial markers

Epithelia are organized as continuous simple single layered or stratified multi-layered sheets of cuboidal or columnar cells. Epithelial cells are highly polarized with an apico-basal axis and connected to each other by cell-cell junctions that not only serve to maintain mechanical integrity of the tissue but also establish the apico-basal polarity as described earlier. The cell-cell junctions thus restrain the epithelial cells from undergoing autonomous changes in shape, polarity or motility. Proteins of different cell-cell adhesion junctions hence serve as epithelial markers (reviewed in [252-254]). Tight junction proteins localization to the membrane as well as expression is lost during EMT and these proteins are often used as biomarkers of epithelial phenotype (reviewed in [25]). The adherens junction classical cadherin – E-cadherin is a classical epithelial marker. During cancer progression, epithelial tumours lose E-cadherin expression and often switch to N-cadherin expression, a phenomenon known as cadherin switching, and this serves as a biomarker for tumorigenesis as well as EMT (reviewed in [18]). N-cadherin positive epithelial tumour cells are able to interact with N-cadherin positive tissues like stroma and endothelium thereby giving access to vasculature as well as enabling penetration and survival in secondary organs (reviewed in [18]). During EMT, the cadherin switch from

E-cadherin to N-cadherin prevents the formation of gap junctions and induces the endocytosis of Cx43 via a non-clathrin dependent pathway (reviewed in [35]). E-cadherin expression on the other hand is promoted by microRNAs like miR-200 that targets and represses EMT transcription factors, and miR-373 that recognizes a site in the promoter of E-cadherin gene (reviewed in [26]). The EMT transcription factor Slug induces loss of desmosomal adhesion associated with loss of DSG and DP from cell-cell contacts [98, 99]. Similarly, the EMT transcription factor, Zeb2, represses expression of desmosomal proteins like PKP2 and DP [109] while Zeb1 represses PKP3 transcription by binding to conserved E-box elements in the PKP3 promoter [110]. Upregulation of Zeb1 along with downregulation of PKP3 is observed at the tumour-host interface in invasive cancers [110].

1.18. Mesenchymal markers

Mesenchymal cells have a spindle shaped structure and a less-defined morphology which can be amoeboid or polarized in the anterior-posterior orientation (front-rear polarity of a migrating cell) and they exhibit an invasive migratory phenotype. As they move, they interact with their microenvironment by weak transient adhesions either as single cells or groups of cells. Epithelial cells are on their microenvironment and cell-cell signalling at the cell-cell junctions for survival, growth and cell division. During EMT, major changes in gene expression are hence required to protect the mesenchymal cells from apoptosis following EMT which is brought about by EMT regulating transcription factors. These changes include expression of new adhesion proteins like N-cadherin as well as signalling molecules like CXCR4-R which protect and guide the mesenchymal cells to their targets. Mesenchymal cells also undergo an IF switch from expression of keratins to vimentin and to promote their migration, they tend to produce

their own ECM components like fibronectin, laminin and vitronectin. Invasion across basement membranes requires the expression of proteases like MMPs which serve as markers of mesenchymal phenotype. Mesenchymal cells also show changes in major cell signalling pathways like TGF- β , Wnt, EGF and FGF promote cell survival (reviewed in [252-254]). Overexpression or mutations that promote the nuclear function of β -catenin as the inducer of the canonical Wnt pathway by binding TCF/ LEF transcription factors is also considered to be a mesenchymal marker (reviewed in [18]).

1.19. EMT regulating transcription factors

The established “master” regulators of EMT are the transcription factors Snail, Slug, Twist 1, Twist 2, Zeb 1 and Zeb2. Snail, Slug, Twist 1 and Zeb 1 are all known to directly or indirectly repress E-cadherin expression and induce vimentin expression while Slug and Zeb1 are also known to promote dissolution of desmosomes (reviewed in [255-257]). These zinc finger family transcription factors repress the expression of E-cadherin by binding to the E-box in its promoter region (reviewed in [26]). PKP3 expression is repressed by the binding of the EMT transcription factor Zeb1 and Snail to the E-box sites in the PKP3 promoter [110]. Also, Zeb1, an oncogenic transcription factor that promotes epithelial–mesenchymal transition (EMT), decreases PKP3 expression at the tumour host interface, thus promoting increased invasiveness and migration of the tumours [258]. Different PTMs regulate the activity, subcellular localization and stability of EMT transcription factors. Glycogen synthase kinase-3 β (GSK3 β) phosphorylates Snail at two motifs; phosphorylation of the first motif leads to the nuclear export of Snail, and phosphorylation of the second motif leads to the ubiquitin (Ub)-mediated degradation of Snail. Snail phosphorylation by protein kinase D1 (PKD1) also leads to nuclear export of Snail. On the other hand, phosphorylation of Snail by PAK1 or large tumour

suppressor 2 (LATS2), or dephosphorylation of Snail by small C-terminal domain phosphatase1 (SCP1) promotes the nuclear retention of SNAIL1 and enhances its activity. Slug (also called SNAIL2) is degraded as a result of its p53-mediated recruitment to the p53–MDM2 complex. Twist 1 is phosphorylated by the MAPKs p38, JNK and ERK, which protects it from degradation as well as promotes its nuclear import and functions. Zeb 2 is sumoylated (Sumo) by Polycomb repressive complex 2 (PRC2) and subsequently exported from the nucleus, which inhibits its activity as a transcription factor (reviewed in [3]) (Figure 1.23).

Cell-cell adhesion thus plays an important role in maintaining epithelial tissues integrity. The loss of cell-cell adhesion junctions like desmosomes is an essential step in tumour progression to metastasis and thus understanding the regulation of desmosome mediated adhesion is necessary to study its role in metastasis. Our laboratory has previously reported that loss of PKP3 results in increased tumour formation and metastasis in vivo. This is characterised by a decrease in desmosome size and cell-cell adhesion and an increase in cell migration and anchorage independent growth [108]. PKP3 has also been shown to play an important role in desmosome formation and the E-cadherin-PG-PKP3 complex has been shown to be required at the membrane for initiation of desmosome assembly [169]. To further understand the role of PKP3 in cancer progression with respect to desmosome assembly, cell migration and EMT, the present study was initiated with the specific aims and objectives given below.

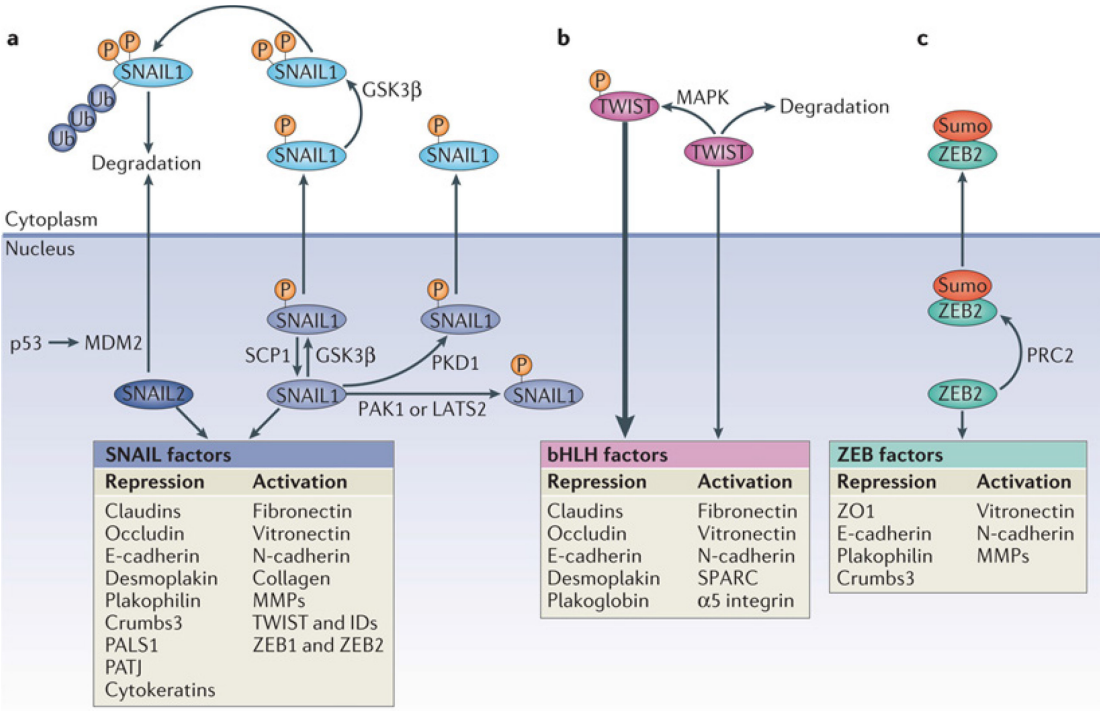


Figure 1.23. EMT transcription factors – EMT is driven by three families of transcription factors – Snail (Snail and Slug), basic helix-loop-helix (bHLH) (Twist 1 and Twist 2) and zinc-finger E-box-binding (Zeb 1 and Zeb2). Some of the mechanisms that control these transcription factors as well as their downstream effects, as described in the text, are presented in this schematic (reproduced from [3]).

AIMS AND OBJECTIVES

2. AIMS AND OBJECTIVES

1. Role of PKP3, adherens junctions and actin cytoskeleton in initiation of desmosome formation and regulation of desmosome size and assembly.
2. Identification of changes in actin filament dynamics and modifications induced by PKP3 loss and their relevance to cell adhesion, migration and metastasis.
3. Role of PKP3 in regulating cell adhesion, cell migration and EMT.

MATERIALS AND METHODS

3. MATERIALS AND METHODS

3.1. Cell lines

The HCT-116 based PKP3 knockdown clones used in this study were previously described [108]. HCT-116 based cells, HEK293 and HEK293FT were cultured in Dulbecco's modified Eagles medium (DMEM) (GIBCO) supplemented with 10% Fetal bovine Serum (GIBCO), 100 U of penicillin (Nicholas Piramal), 100 µg/mL of streptomycin (Nicholas Piramal) and 2 µg/mL of amphotericin B (HiMedia). The selection antibiotic for PKP3 knockdown was 5 µg/mL of blasticidin (Invitrogen), for DsRed PKP3 and GFP-Actin expression was 0.5 µg/mL of puromycin (Sigma), for DSC2 knockdown was 2 µg/mL of hygromycin (Invitrogen), for HEK293FT cells was 500 µg/mL of G418 (Sigma).

3.1. Plasmids and constructs

GFP-DSC2a plasmid was a kind gift from Dr. Reinhard Windoffer and Dr. Rudolf E. Leube. YFP-Ecad plasmid was a kind gift from Dr. Alpha Yap. pLKO.hydro, GST-CRIB and GST-RBD were purchased from Addgene. pEGFP-Actin from Clontech plasmid was cloned into the lentiviral vector pEF.55 digested with AgeI and XbaI [259]. DsRED PKP3.7R excised from DsRed PKP3.7R pcDNA3 [169] plasmid using NheI was cloned into pEF.55 lentiviral vector [259] digested with XbaI. PKP3 shRNA plasmids have been described earlier [108]. DSC2 promoter 1883 b.p upstream of the translation start site was amplified as a 5'NheI and 3'XhoI sequence from HCT116 genomic DNA and cloned into pGL3 vector digested with the same enzymes. The Renilla luciferase pRL-TK plasmid was a kind gift from Dr. Shubha Tole. The C/EBP α , C/EBP β and C/EBP δ shRNA EGFP-f plasmids have been described earlier [260].

3.2. DSC2 shRNA cloning

3.2.1. shRNA design

The ~20 b.p. shRNA target sequences were adapted from previously published DSC2 siRNA sequences [181, 261]. The complementary A and B oligonucleotides were designed to form a secondary structure with XhoI site ‘ctcgag’ (can also use PstI site ‘ctgcag’ to help screening for positive clones) in the loop as follows to give 5’AgeI and 3’EcoRI overhangs upon annealing:

Oligo A: 5’ ccgg(target sequence)ctcgag(reverse complement of target sequence)ttttg 3’

Oligo B: 5’ aattcaaaaa(target sequence)ctcgag(reverse complement of target sequence) 3’

Sr. No.	Name	Sequence
1	DSC2 shRNA 1 oligo A	5’-ccggAAGCTCCTGGAGATGACAAAG ctcgagCTTTGTCATCTCCAGGAGCTTttttg-3’
2	DSC2 shRNA 1 oligo B	5’-aattcaaaaaAAGCTCCTGGAGATGACAAAG ctcgagCTTTGTCATCTCCAGGAGCTT-3’
3	DSC2 shRNA 2 oligo A	5’-ccggAAGAGTGCTTTACAGCTGCAA ctcgagTTGCAGCTGTAAAGCACTCTTttttg-3’
4	DSC2 shRNA 2 oligo B	5’-aattcaaaaaAAGAGTGCTTTACAGCTGCAA ctcgagTTGCAGCTGTAAAGCACTCTT-3’
5	DSC2 shRNA 3 oligo A	5’-ccggAAGCAATTAATGATACAGCAG ctcgagCTGCTGTATCATTAATTGCTTttttg-3’
6	DSC2 shRNA 3 oligo B	5’-aattcaaaaaAAGCAATTAATGATACAGCAG ctcgagCTGCTGTATCATTAATTGCTT-3’
7	C/EBP α shRNA 1 oligo A	5’-ccggGCTGGAGCTGACCAGTGACAA ctcgagTTGTCACTGGTCAGCTCCAGCttttg-3’
8	C/EBP α shRNA 1 oligo B	5’-aattcaaaaaGCTGGAGCTGACCAGTGACAA ctcgagTTGTCACTGGTCAGCTCCAGC-3’
9	C/EBP α shRNA 2 oligo A	5’-ccggACGCGCCAGCAGCGCCGCCT ctcgagAGGCGGCGCTGCTGGGCGCGTttttg-3’
10	C/EBP α shRNA 2 oligo B	5’-aattcaaaaaACGCGCCAGCAGCGCCGCCT ctcgagAGGCGGCGCTGCTGGGCGCGT-3’

Sr. No.	Name	Sequence
11	C/EBP β shRNA 1 oligo A	5'-ccggATCCATGGAAGTGGCCAAC ctgcagGTTGGCCACTTCCATGGATtttttg-3'
12	C/EBP β shRNA 1 oligo B	5'-aattcaaaaaATCCATGGAAGTGGCCAAC ctgcagGTTGGCCACTTCCATGGAT-3'
13	C/EBP β shRNA 2 oligo A	5'-ccggCCAGGCCACCAGGCGTTGCAT ctgcagATGCAACGCCTGGTGGCCTGGtttttg-3'
14	C/EBP β shRNA 2 oligo B	5'-aattcaaaaaCCAGGCCACCAGGCGTTGCAT ctgcagATGCAACGCCTGGTGGCCTGG-3'
15	C/EBP δ shRNA 1 oligo A	5'-ccggTGCCTCCAAGCGAGGCTGTCA ctgcagTGACAGCCTCGCTTGGACGCAtttttg-3'
16	C/EBP δ shRNA 1 oligo B	5'-aattcaaaaaTGCGTCCAAGCGAGGCTGTCA ctgcagTGACAGCCTCGCTTGGACGCA-3'
17	C/EBP δ shRNA 2 oligo A	5'-ccggACAGCCTGGACTTACCACCAC ctgcagGTGGTGGTAAGTCCAGGCTGTtttttg-3'
18	C/EBP δ shRNA 2 oligo B	5'-aattcaaaaaACAGCCTGGACTTACCACCAC ctgcagGTGGTGGTAAGTCCAGGCTGT-3'
19	CDX2 shRNA 1 oligo A	5'-ccggCCGCAGAGCAAAGGAGAGGAA ctgcagTTCCTCTCCTTTGCTCTGCGGtttttg-3'
20	CDX2 shRNA 1 oligo B	5'-aattcaaaaaCCGCAGAGCAAAGGAGAGGAA ctgcagTTCCTCTCCTTTGCTCTGCGG-3'
21	CDX2 shRNA 2 oligo A	5'-ccggAGACAAATATCGAGTGTGTA ctgcagTACACACTCGATATTTGTCTtttttg-3'
22	CDX2 shRNA 2 oligo B	5'-aattcaaaaaAGACAAATATCGAGTGTGTA ctgcagTACACACTCGATATTTGTCT-3'
23	DSC2 promoter NheI 5'	5'-gcgcGCTAGCaattctagtcaattgctct-3'
24	DSC2 promoter XhoI 3'	5'-gcgcCTCGAGggagagggctcggggcaggt-3'

Table 3.1. List of primers used for cloning.

3.2.2. Annealing and phosphorylation of oligos

The following reaction was set up to anneal oligos A and B to form the shRNA with the 5' AgeI and 3' EcoRI overhangs:

Oligo A	9 μ L
Oligo B	9 μ L
Polynucleotide kinase buffer (NEB)	2 μ L
Total	20 μ L

PCR program for annealing:

1. 94°C for 4minutes
2. 70°C for 10minutes

The reaction was then allowed to slowly cool overnight in a water bath brought to 70°C and switched off. Phosphorylation of the annealed shRNA oligonucleotides was performed as per the following reaction:

Annealed oligos	2µl
10X T4 DNA Ligase	1µl
T4 PNK	1µl
Sterile MilliQ	6µl
Total	10µl

3.2.3. Cloning into pLKO.hygro vector

The pLKO.hygro vector was digested with AgeI and EcoRI and ligated with 0.2 µL of the phosphorylated annealed shRNA oligonucleotides.

3.3. Transfection

Transfection was performed either by calcium phosphate method or by using commercial transfection reagents like Lipofectamine LTX (Invitrogen), Fugene ExtremegeneHP (Roche) or PEI (Polysciences) as per the manufacturer's instructions.' For calcium phosphate transfection, cells were seeded to 50-70% confluence, 1 day before starting. Medium was changed immediately before transfection. DNA amount and total volume of transfection mix are as follows:

Plate Size	Amount of DNA (µg)	Sterile MilliQ (µL)	Sterile 0.5M CaCl ₂ (µL)	2x BBS (µL)	Total Volume (µL)
P35	5	45	50	100	200
P60	10	90	100	200	400
P100	25	225	250	500	1000

Mix was incubated at RT for 20 min and added dropwise on plate. The precipitate of the transfection mix was washed twice with PBS 16-20 hours post transfection and fresh media was added. Cells were harvested 48-72 hours post transfection.

3.4. Lentivirus Production and transduction

Lentiviruses were prepared in HEK293FT cell lines. Briefly, HEK293FT cells grown in P60 were transfected with 4 µg of lentiviral plasmids, 4 µg of psPAX2 plasmid and 2 µg of pMD2.G plasmid by calcium phosphate method as described earlier. The virus production was evident from the syncytia formation observed 24-48 hours post transfection. The virus containing tissue culture supernatant was collected 48-72 hours post transfection, filtered through 0.45 µm syringe filter (MDI), supplemented with 8 µg/mL polybrene and directly added on the target cells (P35 plate grown to 50% confluency) to be transduced. The cells were incubated with the viral supernatant for 24 hours for transduction followed by addition of fresh media. Cells were harvested 48 hours post transduction or sub cultured to P100 plate and subjected to selection antibiotic to generate stable cell lines. The DsRed PKP3 pEF.55 lentiviruses were used for generation of HCT116 based DsRed PKP3 expressing cells and GFP-Actin pEF.55 lentiviruses were used for generation of HCT116 based GFP-Actin expressing cells. After selection in puromycin, the puromycin resistant missed population of cells was used for experiments. DSC2 shRNA cloned in pLKO.hygro lentiviral vector was used to generate cells with DSC2 knockdown, clones were selected using hygromycin.

3.5. Calcium switch assays

Cells were seeded in DMEM (GIBCO) supplemented with 10% Fetal bovine Serum (GIBCO), 100 U of penicillin (Nicholas Piramal), 100 µg/mL of streptomycin (Nicholas Piramal) and 2 µg/mL of amphotericin B (HiMedia) (normal calcium medium). At ~80% confluency, 2x PBS washes were given and then DMEM without calcium (GIBCO) supplemented with 10% Fetal bovine Serum (GIBCO) (low calcium medium) was added to the cells. The cells were incubated in this low calcium medium for 20 hours

and cells for –Ca condition were harvested at this stage. For +Ca condition, after incubation for 20 hours in low calcium medium, cells were switched to normal calcium medium and harvested after 1 hour of incubation.

3.6. Electron Microscopy

Cells were cultured as a monolayer in P60 and fixed with 3% glutaraldehyde in 0.1M sodium cacodylate-HCL, pH 7.4 for 2 hours at 40⁰C followed by 1% osmium tetroxide for 1hr at 40⁰C (both from Ted Pella, Inc, USA). After dehydration, cells were embedded in Epon-812 resin (Ted Pella, Inc, USA) and polymerized at 60⁰C for 48 hours. Semi-thin (1 µm thick) sections were cut on ultra-microtome (Leica UC7, Germany), stained with toluidine blue and observed under light microscope to confirm the area of interest. Ultra-thin sections (70nm) were cut from the selected areas and mounted on formvar coated copper grids. Sections were contrasted with uranyl acetate and lead citrate and viewed under Jeol 1400 plus Transmission Electron Microscope at 120 KV. Some grids were observed under a Carl Zeiss LIBRA120 EFTEM transmission electron microscope, at an accelerating voltage of 120KV. Desmosome size was measured using integrated iTEM software (Olympus soft imaging solutions, GmbH, Germany).

3.7. Immunofluorescence and confocal microscopy

Cells were grown on coverslips and fixed and stained for immunofluorescence. Briefly, cells were washed twice in PBS, fixed in 4% paraformaldehyde (in PBS) for 20 minutes at RT or chilled methanol for 10 minutes at -20°C, washed twice with PBS, followed by permeabilization in 0.3% Triton-X (in PBS) for 10 minutes at RT and washed once with PBS and once with 0.1% NP40 (in PBS). Primary antibody solution was made in 3% BSA in 0.1% NP40 (in PBS) and 50 uL was spotted on labelled

parafilm. Coverslips were placed with cells side down on the antibody spot and incubated in humidified chamber at 4°C for 16-20 hours. The coverslips were inverted and 6 washes were given with 0.1%NP40 (in PBS) and 1x PBS alternately. Secondary antibody solution was prepared in 3% BSA in 0.1% NP40 (in PBS) and 50 uL was spotted on labelled parafilm. Coverslips were placed with cells side down on the antibody spot and incubated in humidified chamber at RT for 1 hour. The coverslips were inverted and 6 washes were given with 0.1%NP40 (in PBS) and 1x PBS alternately. DAPI (2.5 µg/mL in PBS) 50 uL was spotted on labelled parafilm. Coverslips were placed with cells side down on the DAPI spot and incubated in humidified chamber at RT for 5-10 minutes. The coverslips were inverted and 3 washes were given PBS. The coverslips were then mounted on 15-20 µL of Vectashield (Vector Labs) on a clean labelled grease free slide and sealed with thin layer of nail polish on the boundaries of the coverslips. FITC-tagged phalloidin (1:50 dilution in PBS) (Sigma) was used to specifically stain filamentous actin. For imaging migrating cells, a yellow tip was used to make a wound in the monolayer as described earlier [108] and cells were harvested after 24 hours. Images were taken with a 63x oil immersion objective on either on LSM510 Meta Zeiss, LSM710 Zeiss or LSM780 Zeiss confocal microscope. Mean fluorescence intensities at the cell border of >30 cells were quantitated using ImageJ software. The graph was plotted and significance was determined using the Student's t-test in GraphPad Prism software.

Sr. No.	Antibody name	Species	Company	Dilution	Fixation method
1	PKP3	Mouse	Invitrogen	1:100	Methanol
2	DSC2/3	Mouse	Invitrogen	1:30	Paraformaldehyde
3	DSG2	Mouse	Invitrogen	1:30	Paraformaldehyde
4	DP	Mouse	Abexome	1:100	Methanol
5	E-cadherin	Mouse	BD	1:100	Methanol
6	PG	Mouse	Abcam	1:25	Methanol
7	p120 catenin	Mouse	Gift from Dr. Alpha Yap	1:25	Methanol
8	C/EBP α	Rabbit	Santacruz	1:50	Paraformaldehyde

Sr. No.	Antibody name	Species	Company	Dilution	Fixation method
9	C/EBP β	Rabbit	Santacruz	1:50	Methanol
10	C/EBP δ	Rabbit	Santacruz	1:50	Methanol
11	All secondary antibodies	Goat	Invitrogen	1:100	-

Table 3.2. List of antibodies used for immunofluorescence.

3.8. Hanging drop assays

2×10^4 cells cultured in normal calcium or low calcium medium and were resuspended in 35 μ L of normal calcium or low calcium medium for 16 hours on the lid of a 35mm dish. The cells were fixed and then images of aggregates were captured on Axiovert 200 M Inverted Zeiss microscope with 5x or 10x objective. The number and area of aggregates in 20 fields was measured using Axiovision or ImageJ software. The numbers of aggregates of different sizes from 3 independent experiments was determined for normal calcium and for low calcium.

3.9. Western blotting

Cell lysates were prepared in Lamelli's buffer and separated on an SDS-PAGE gel and immunoblotted with antibodies for different proteins as follows:

3.9.1. SDS PAGE:

3.9.1.1. Sample Preparation:

Harvest cells by decanting medium, then wash with PBS and add Laemmli's Buffer without bromophenol blue and without β -mercaptoethanol (100 μ L for p35, 500 μ L for p60 and 1000 μ L for p100). Scratch the plate in circular motion using a tip, so that the sticky solution gathers up and all the cells get collected. With a pipette put the solution in labelled eppendorf. Place in boiling hot water bath for 10min. If not using

immediately, store at -20°C. When ready to use thaw at RT and perform protein estimation. Use the required amount of lysate and then add 3x Laemmli's Buffer with bromophenol blue and with β -mercaptoethanol. Place in boiling hot water bath for 10min.

3.9.1.2. Polyacrylamide gel preparation:

Clean plates, cast and spacer. Arrange the apparatus and check for leakage by adding MilliQ. Resolving gel was made as required; 50mL for maxi, 25mL for midi and 5mL for mini gel.

10mL	6%	7.50%	10%	12%	15%
MilliQ (mL)	5.30 mL	4.80 mL	4.00 mL	3.30 mL	2.30 mL
1.5M Tris pH8.8 (mL)	2.50 mL	2.50 mL	2.50 mL	2.50 mL	2.50 mL
10% SDS (mL)	0.10 mL	0.10 mL	0.10 mL	0.10 mL	0.10 mL
30% Acrylamide mix (mL)	2.00 mL	2.50 mL	3.30 mL	4.00 mL	5.00 mL
10% APS (mL)	0.10 mL	0.10 mL	0.10 mL	0.10 mL	0.10 mL
TEMED (μ L)	8.00 μ L	7.00 μ L	4.00 μ L	4.00 μ L	4.00 μ L

Table 3.3. Table for making resolving gel for SDS-PAGE.

Stacking gel to be made as required. 10mL for maxi gel, 5mL for midi gel and 2mL for mini gel.

6%	2.00 mL	3.00 mL	4.00 mL	5.00 mL	6.00 mL	8.00 mL	10.00 mL
MilliQ (mL)	1.40 mL	2.10 mL	2.70 mL	3.40 mL	4.10 mL	5.50 mL	6.50 mL
1M Tris pH6.8 (mL)	0.25 mL	0.38 mL	0.50 mL	0.63 mL	0.75 mL	1.00 mL	1.25 mL
10% SDS (μ L)	20.00 μ L	30.00 μ L	40.00 μ L	50.00 μ L	60.00 μ L	80.00 μ L	100.00 μ L
30% Acrylamide mix (mL)	0.33 mL	0.50 mL	0.67 mL	0.83 mL	1.00 mL	1.30 mL	1.70 mL
10% APS (μ L)	20.00 μ L	30.00 μ L	40.00 μ L	50.00 μ L	60.00 μ L	80.00 μ L	100.00 μ L
TEMED (μ L)	2.00 μ L	3.00 μ L	4.00 μ L	5.00 μ L	6.00 μ L	8.00 μ L	10.00 μ L

Table 3.4. Table for making stacking gel for SDS-PAGE.

3.9.1.3. Gel Run:

Make 1x running buffer. Fill chamber about $\frac{1}{4}^{\text{th}}$ with single use running buffer. Clamp the gel along with its holder in the apparatus. If running only one gel, put a dummy plate on the other side. Fill with tap water to check for leakage. Then put in freshly made running buffer. Place the arranged apparatus in the chamber. Load samples with syringe. Load marker. Run the gel at required voltage.

3.9.2. Immunoblotting:

3.9.2.1. Transfer:

Make 1x Transfer Buffer. Keep the transfer chamber, cassette, Whatmann paper and sponges ready. On a magnetic stirrer, place a tray. Put the transfer chamber in the tray. Place a small magnet in the transfer chamber. Fill about half the transfer chamber with transfer buffer, and place 16°C cooling coil in it. Switch on the magnetic stirrer and check that the magnet is rotating properly in the centre of the chamber. In a tray, pour some transfer buffer. Place the cassette white side facing down. Put layers of sponge and Whatmann paper and make sure they are all wet with transfer buffer. Use a roller to ensure there are no air bubbles. When dye runs out or as per the molecular weight of protein of interest, stop the gel run. Remove plate from the chamber. Gently separate the plate, taking care not to damage the gel. Depending upon the expected position of protein of interest, cut the gel. (Spacer of maxi gel could be used for this). The gel should be kept wet using transfer buffer after it is removed from the electrophoresis chamber, it will curl up if it dries. Measure the cut gel size and cut the nitrocellulose membrane so as to cover the entire cut gel. DO NOT TOUCH THE MEMBRANE WITH YOUR HANDS AT ANY POINT. The plastic protective sheets can help during cutting. Further in the procedure, forceps or gloves may be used. Place the membrane on the Whatmann paper in

the transfer assembly. Cut a corner to mark orientation. Arrange the gel on the membrane in the required orientation. Remove air bubbles using a roller. Place layers of Whatmann paper and sponge, again remove air bubbles. Check all layers are arranged properly. Keep your hand to maintain the arrangement. The following steps should be done quickly - Close the cassette, without disturbing the arrangement, tightly with its clamp, place the cassette in transfer chamber and add more transfer buffer in the transfer chamber to completely fill it. Close the lid, ensuring properly polarity. Set up the transfer for 3 hours at 55V for maxi gel and 1 hour at 100V for mini gel.

3.9.2.2. Immunostaining of blot:

Plastic boxes can be used to place the blots for washing steps and sealed plastic bags for incubation steps. Remove the blot in TBST. Using a glass plate and blade, the blot may be cut into sections at this point to stain for different proteins of interest. Temporary staining with Ponceau S staining solution may be done to help in visualising and cutting sections. Mark each section properly for identification. Block with 5% milk in TBST for 1 hour on rocker. Give 3x TBST washes. Incubate with primary antibody solution at 4°C overnight on rocker. Primary antibody solution is to be made in 1% BSA in TBST with 0.02% sodium azide. Collect primary antibody solution; it may be reused up to 3 times or more depending on the antibody. Give 3x TBST washes, 5 min each. Incubate with secondary antibody solution for 1hr. on rocker. Secondary antibody (HRP conjugated) solution to be made in 2.5% milk in TBST with 1% goat serum. Give 3x TBST washes, 10 min each.

3.9.2.3. Developing of blot:

From this point onwards, work in low light as developing solution is light sensitive. Mix Pierce SuperSignal Pico Developing solutions in 1:1 ratio. Place blot on

plastic sheet on a flat surface and spread the developing mix. Cover and keep for 10 min. Developing machine needs to be switched on 10 min in advance. After incubation is over cover with plastic sheet, place in developing cassette and take place X-Ray film (cut a corner to mark orientation) on the blot for different time durations in a cassette. Remove the X-Ray film after required exposure and develop in Optimax X-Ray Film Processor.

Sr. No.	Antibody name	Species	Company	Dilution	Difference from standard method if any
1	PKP3	Mouse	Invitrogen	1:2000	
2	DSC2/3	Mouse	Invitrogen	1:500	
3	DSG2	Mouse	Invitrogen	1:500	
4	DP	Mouse	Abexome	1:100	
5	E-cadherin	Mouse	BD	1:500	
6	PG	Mouse	Abcam	1:250	
7	p120 catenin	Mouse	Gift from Dr. Alpha Yap	1:1000	
8	α -E-catenin	Goat	Santacruz	1:500	
9	β -catenin	Rabbit	Abcam	1:250	
10	ZO-1	Rabbit	Invitrogen	1:100	
11	P-cadherin	Mouse	BD	1:250	
12	C/EBP α	Rabbit	Santacruz	1:250	5% BSA
13	Lamin A	Rabbit	Abcam	1:2000	
14	α -tubulin	Rabbit	Abcam	1:2000	
15	β -actin	Mouse	Sigma	1:5000	
16	p53	Mouse	Santacruz	1:500	
17	GFP	Mouse	Clontech	1:15000	
18	β 1-integrin	Mouse	BD	1:1000	
19	α 5-integrin	Rabbit	Santacruz	1:3000	
20	FAK	Rabbit	CST	1:1000	5% BSA
21	p-FAK	Rabbit	CST	1:250	5% BSA
22	N-WASP	Rabbit	CST	1:1000	5% BSA
23	RhoA	Mouse	Santacruz	1:200	
24	Rac 1/2/3	Rabbit	CST	1:1000	5% BSA
25	cdc42	Mouse	Santacruz	1:200	
26	Filamin A	Mouse	Chemicon	1:2000	
27	Gelsolin	Mouse	Sigma	1:1000	
28	Profilin	Rabbit	CST	1:1000	5% BSA
29	Cofilin	Rabbit	CST	1:1000	5% BSA
30	p-cofilin	Rabbit	CST	1:500	5% BSA
31	PAK1	Rabbit	CST	1:1000	5% BSA
32	ERM	Rabbit	CST	1:100	5% BSA
33	p-ERM	Rabbit	CST	1:100	5% BSA

Sr. No.	Antibody name	Species	Company	Dilution	Difference from standard method if any
34	Mypt1	Rabbit	CST	1:100	5% BSA
35	p-Mypt1 S507	Rabbit	CST	1:100	5% BSA
36	Diap 1	Rabbit	CST	1:100	5% BSA
37	Myosin IIA	Rabbit	CST	1:100	5% BSA
38	Myosin IIB	Rabbit	CST	1:100	5% BSA
39	Myosin IIC	Rabbit	CST	1:100	5% BSA
40	Secondary anti-mouse	Goat	Pierce	1:5000	
41	Secondary anti-rabbit	Goat	Pierce	1:5000	
42	Secondary anti-goat	Donkey	Santacruz	1:2000	

Table 3.5. List of antibodies used for Western blotting.

3.10. Immunoprecipitation

HCT116 cell lysates were prepared in EBC lysis buffer (50 mM Tris pH8.0, 120 mM NaCl, 0.5% NP-40) with protease inhibitors (Leupeptin 10 µg/mL, Aprotinin 20 µg/mL, phenylmethylsulfonyl fluoride 1mM, sodium fluoride 50 mM, sodium orthovanadate 1 mM). 5% of the extract was kept aside for whole cell lysate. For immunoprecipitation, lysates were incubated with target protein specific antibodies or an isotype control antibody and incubated at 4°C on rocker for 3 hours. The following amount of different antibodies were used – 10 µL of mouse anti-PKP3 (Invitrogen), 70 µL of mouse anti-HA 12CA5 supernatant, 20 µL of rabbit anti-C/EBPα (Santacruz), 20 µL of rabbit anti-HA (Santacruz), 10 µL of rabbit anti-PAK1 (Cell Signalling), 5 µL of mouse anti-myc 9E10 (Santacruz). The immune complexes were pulled down with 30 – 40 µL Protein G sepharose beads (Amersham) 50% slurry by incubation at 4°C on rocker for 1 hour followed by centrifugation at 4°C 1200 rpm and 3x washes with NET-N (20mM Tris pH 8.0, 100mM NaCl, 1mM EDTA, 0.5% NP-40). After the final wash, 50 µL of 3x Laemmli's buffer with bromophenol blue and β-mercaptoethanol was added and

samples were separated on an SDS-PAGE gel and immunoblotted with antibodies for required proteins.

3.11. In-vitro GST pulldown

3.11.1. Preparation of GST proteins

To generate bacterially purified GST tagged proteins, BL21, a protease negative strain of E.coli was transformed separately with plasmids expressing GST alone, GST PKP3, GST PKP3 Δ ARM and GST PKP3 Δ NH3 and inoculated in a 5mL LB broth with ampicillin in a 50mL conical tube. The culture was incubated for 16-18 hours at 37 °C with shaking (200rpm). This was used as a starter culture for 100mL LB broth with ampicillin in 2L flask and was incubated for 1 hour at 37 °C with shaking (200rpm). After 1 hour the flasks were kept in cold room (4°C) for 30 minutes and then protein production was induced with 44 μ L of 1M IPTG to achieve a final concentration of 0.4 mM. The flasks were then incubated in shaker incubator for 3 hours at 37 °C with shaking (200rpm). The culture was transferred to a 50 mL round bottom tube on ice. The cells were pelleted by centrifugation at 5000 rpm (SS-34 rotor, Sorvall) for 10 minutes at 4°C. The supernatant was discarded and the cell pellets were resuspended gently in 10 mL of 0.1% Triton X-100 in PBS. These uniform cell suspensions were sonicated (Branson) at 50 duty cycles for 10 seconds and placed on ice for 10 sec. This step was repeated 3 times. The suspension was centrifuged at 5000 rpm (SS-34 rotor, Sorvall) for 10 minutes at 4°C. The supernatant was carefully collected in a fresh 15 mL screw cap conical tube and 150 μ L of 50% slurry of glutathione sepharose beads (Amersham) was added to each tube and incubated on a rocker for 1 hour at 4°C. The beads were pelleted down by centrifuging at 3000 rpm (Rotor number 8, Rota 6R-V/Fm PlastoCrafts) for 1 minute at 4°C. The supernatants were discarded and beads were collected in a fresh 1.5 mL

eppendorf tube on ice. The conical tubes were rinsed with ice-cold NET-N (20mM Tris pH 8.0, 100mM NaCl, 1mM EDTA, 0.5% NP-40) to collect the additional beads present on the surface of the tubes followed by 3 washes with ice cold NET-N buffer. Finally the beads were resuspended in ice-cold NET N buffer in 1.5 mL eppendorf tubes final volume 1mL. These beads were stored at 4°C and were used up to 1-2 weeks period. To check the quality of proteins expressed and immobilized to the beads, 5µl of the slurry of glutathione sepharose beads were mixed with 10 µl of 1X Laemmli's buffer with β-mercaptoethanol and bromophenol blue and boiled for 10 minutes in a boiling water bath. The samples were loaded on a 10% SDS-PAGE gel. The gel was stained for 1 hour with Coomassie blue followed by destaining using destaining solution (methanol: acetic acid: water in the ratio 4:1:5).

3.11.2. In-vitro GST pulldown

Cells lysates prepared from 2x P100 plates in 1000 µL EBC lysis buffer (50 mM Tris pH8.0, 120 mM NaCl, 0.5% NP-40) with protease inhibitors (Leupeptin 10 µg/mL, Aprotinin 20 µg/mL, phenylmethylsulfonyl fluoride 1mM, sodium fluoride 50 mM, sodium orthovanadate 1 mM) on ice were incubated with either GST PKP3, GST PKP3 ΔARM, GST PKP3ΔNH3 or GST control for 5 hours at 4°C on rocker (The amount of GST control, GST PKP3, GST PKP3 ΔARM and GST PKP3ΔNH3 beads was equivalent as determined by SDS PAGE followed by Coomassie blue staining). Complexes bound to the GST proteins were pulled down by centrifugation at 3000 rpm 4°C, followed by 3x washes with NET-N (20mM Tris pH 8.0, 100mM NaCl, 1mM EDTA, 0.5% NP-40). 50µL of 3X Laemmli's buffer with β-mercaptoethanol and bromophenol blue was added to the pellet and boiled for 10 minutes in a boiling water bath, separated on an SDS-PAGE gel and immunoblotted with antibodies for Rho A and filamin A.

3.12. Active Rho-GTPases assay

3.12.1. Preparation of GST proteins

GST control, GST-RBD and GST-CRIB plasmids transformed in BL21(DE3) strain of *E. coli* were stored as glycerol stocks. Starter culture using glycerol stock was prepared in 100 mL LB broth with ampicillin in 1 L flask by incubation for 16-18 hours at 37 °C with shaking (200rpm). The starter culture was inoculated in 1L LB broth with ampicillin in 2L flask and incubated at 37 °C with shaking (200rpm) for 1 hour for GST control and GST-CRIB and 1.5 hours for GST-RBD. The flasks were kept at 4°C for 30 minutes. IPTG was added to induce protein production - 440µl of 1M IPTG to achieve a final concentration of 0.4 mM for GST, 550µl of 1M IPTG to achieve a final concentration of 0.5 mM for GST-RBD and 220µl of 1M IPTG to achieve a final concentration of 0.2 mM for GST-CRIB. This was followed by incubation for 16-18 hours at 24 °C with shaking (200rpm). The cultures were pelleted down in 250 mL bottle by centrifuging at 5000 rpm (Rotor number 4, Rota 6R-V/Fm PlastoCrafts) for 10 minute at 4°C. This pellet was stored at -80°C for 1 hour or until further processing. Pellet was resuspended in 25 mL chilled bacterial lysis buffer (50mM Tris pH 7.5, 1% Triton-X, 150 mM NaCl, 5 mM MgCl₂, 1 mM DTT) with protease inhibitors (Leupeptin 10 µg/mL, Aprotinin 20 µg/mL, phenylmethylsulfonyl fluoride 1mM, sodium fluoride 50 mM, sodium orthovanadate 1 mM), transferred to a 50 mL round bottom tube and incubated on ice for 5 minutes. These uniform cell suspensions were sonicated (Branson) at 50 duty cycles for 15 seconds and placed on ice for 1 minute. This step was repeated 6 times. The suspension was centrifuged (SS-34 rotor, Sorvall) at 15000 rpm for 30 minutes at 4°C. The supernatant was carefully collected in a fresh 15 mL screw cap conical tube and 1 mL of 50% slurry of glutathione sepharose beads (Amersham) was added to each tube

and incubated on a rocker for 30 minutes at 4°C. The beads were pelleted down by centrifuging at 2000 rpm (Rotor number 8, Rota 6R-V/Fm PlastoCrafts) for 1 minute at 4°C. This was followed by 3x washes with bacterial wash buffer (50mM Tris pH 7.5, 0.5% Triton-X, 150 mM NaCl, 5 mM MgCl₂, 1 mM DTT) with protease inhibitors (Leupeptin 10 µg/mL, Aprotinin 20 µg/mL, phenylmethylsulfonyl fluoride 1mM, sodium fluoride 50 mM, sodium orthovanadate 1 mM). After the final wash, beads were resuspended to a total volume of 3 mL in storage buffer (bacterial wash buffer with protease inhibitors + 10% glycerol). The uniformly suspended slurry was aliquoted in pre-chilled 1.5 mL eppendorf tubes and stored at -80°C. The GST-proteins were quantitated by using 5µl of the slurry of glutathione sepharose beads mixed with 10 µL of 1X Laemmli's buffer with β- mercaptoethanol and bromophenol blue and boiled for 10 minutes in a boiling water bath. The samples were loaded on a 10% SDS-PAGE gel. The gel was stained for 1 hour with Coomassie blue followed by destaining using destaining solution (methanol: acetic acid: water in the ratio 4:1:5). The same batch of beads should be used for independent replicates of an experiment to maintain consistency.

3.12.2. Active Rho-GTPases pulldown

Cells lysates prepared in modified RIPA buffer (50 mM Tris pH8.0, 1% NP-40, 125 mM NaCl, 10 mM MgCl₂, 0.25% sodium deoxycholate, 0.1% SDS) with protease inhibitors (Leupeptin 10 µg/mL, Aprotinin 20 µg/mL, phenylmethylsulfonyl fluoride 1mM, sodium fluoride 50 mM, sodium orthovanadate 1 mM) on ice were quantitated and 2-3 mg protein in 500 µL buffer was incubated with either GST-CRIB (15 µL) for active Rac and active cdc42 assays or GST-RBD (20 µL) for active Rho assays or GST control (6 µL) for 30 min at 4°C on rocker (The amount of GST control and GST-PAK or GST-RBD beads was equivalent as determined by SDS PAGE followed by Coomassie blue

staining). Complexes containing the active Rho-GTPases were pulled down by centrifugation at 3000 rpm 4°C, followed by 3x washes with NET-N (20mM Tris pH 8.0, 100mM NaCl, 1mM EDTA, 0.5% NP-40). 10µL of 3X Laemmli's buffer with β -mercaptoethanol and bromophenol blue was added to the pellet and boiled for 10 minutes in a boiling water bath, separated on an SDS-PAGE gel and immunoblotted with antibodies for respective Rho-GTPases, β -actin and PKP3.

3.13. Luciferase reporter assays

HCT116 based DsRed PKP3 and vector control cells were cultured as a confluent monolayer in 24-well plates. 0.5 µg of DSC2 promoter PGL3 firefly luciferase reporter plasmid was transfected along with 0.05µg of pRL-TK Renilla luciferase plasmid as an internal transfection control using Lipofectamine LTX as per the manufacturer's instructions. Cells were harvested 24 hours post transfection and luciferase assay was performed using Dual-Luciferase Reporter Assay kit (Promega) as per the manufacturer's instructions and readings for firefly luciferase (FL) and Renilla luciferase (RL) in 96-well opaque white plates (BD) taken on Berthold Mithras LB 940 Multimode Microplate Reader. Each experiment was performed in duplicates and three independent experiments were performed to get background corrected FL/RL fold change values of DsRed PKP3 cells relative to vector control cells. Graph was plotted using GraphPad Prism software.

3.14. Triton-X soluble and insoluble fractionation

The Triton-X soluble and insoluble fractionation was adapted from a method described earlier [262]. Cells were grown as a confluent monolayer in a P100 and washed with chilled PBS. 1 mL of chilled Triton buffer () and incubated on at 4°C on rocker for 10 minutes. The lysate formed was collected in a pre-chilled 1.5 mL eppendorf tube and

centrifuged at max speed 4°C 30 minutes. The supernatant is the Triton soluble fraction and is collected in a new pre-chilled 1.5 mL eppendorf tube. The pellet is given a wash with PBS and then resuspended in 1 mL of Laemmli's Buffer without bromophenol blue and without β -mercaptoethanol and placed in boiling hot water bath for 10min. The prepared samples are quantitated followed by Western blotting or stored at -80°C until further use.

3.15. Reverse transcriptase PCR and quantitative real time PCR

RNA was prepared using RNeasy Plus kit (Qiagen). 2 μ g of RNA was converted to cDNA using High-Capacity cDNA Reverse Transcription Kit (Applied Biosystems). For reverse transcriptase PCR Taq polymerase was used to amplify the targets using GAPDH as a control and separated on a 2% agarose gel and images were captured using a gel documentation system. Quantitative real time PCR was performed using SYBR® Green PCR Master Mix (Applied Biosystems) using GAPDH as a control. Fold change was determined by relative quantitation method by determining $2^{-\Delta\Delta C_t}$ values or quantitation was done by determining the $2^{-\Delta C_t}$ values. The graph was plotted and significance was determined using the Student's t-test in GraphPad Prism V5 software.

Sr. No.	Name	Sequence
1	DSC2 RT 5'	5'-GTTTTACTCAGCCCCGTCTTG-3'
2	DSC2 RT 3'	5'-GCCCATCTTCTTCTTGTCGT-3'
3	DSG2 RT 5'	5'-TACGCCCTGCTGCTTCTCC-3'
4	DSG2 RT 3'	5'-TCTCCCTCCCGAAGAGCCACG-3'
5	DP1 RT 5'	5'-ATTCCAAAAGCAGGCTTTAGA-3'
6	DP1 RT 3'	5'-AGGACTTTGATTTTCACCAGA-3'
7	DP2 RT 5'	5'-AAGGTTGAGGGTTCTACTGC-3'
8	DP2 RT 3'	5'-TTGTCTTGCTCCAGGACTT-3'
9	PG RT 5'	5'-CTACGGCAACCAGGAGAGC-3'
10	PG RT 3'	5'-GGGACACACGGATAGCACCT-3'

Sr. No.	Name	Sequence
11	E-cadherin RT 5'	5'-CGTCCTGGGCAGAGTGAATT-3'
12	E-cadherin RT 3'	5'-GGGTTATGAAACCGTAGAGGC-3'
13	P-cadherin RT 5'	5'-AGAAGACCCTGACAAGGAGAA-3'
14	P-cadherin RT 3'	5'-GAGGGCTTCCATTGTCCAT-3'
15	ZO-1 RT 5'	5'-CAAGAGCACAGCAATGGAGGA-3'
16	ZO-1 RT 5'	5'-TCCCCACTCTGAAAATGAGGA-3'
17	C/EBP α RT 5'	5'-GGTGGACAAGAACAGCAACGA-3'
18	C/EBP α RT 3'	5'-GTCATTGTCACTGGTCAGCTC-3'
19	C/EBP β RT 5'	5'-CAAGCACAGCGACGAGTACAA-3'
20	C/EBP β RT 3'	5'-AACAAGTTCCGCAGGGTGCT-3'
21	C/EBP δ RT 5'	5'-CGCGAGCGCAACAACAT-3'
22	C/EBP δ RT 3'	5'-GCTTCTCGTTCTCAGCCGAC-3'
23	C/EBP γ RT 5'	5'-TTTCGTAACCGTCGCTCCTC-3'
24	C/EBP γ RT 3'	5'-CCACGCTAAGCTGCCAAAAA-3'
25	C/EBP ϵ RT 5'	5'-CAGCCGAGGCAGCTACAATC-3'
26	C/EBP ϵ RT 3'	5'-TGCCTTCTTGCCCTTGTGTAA-3'
27	C/EBP ζ RT 5'	5'-GAGGAAGTGTTACGGCTCGG-3'
28	C/EBP ζ RT 3'	5'-TCTCATCCAAAGTAGCCAGCA-3'
29	CDX1 RT 5'	5'-CGCCCTACGAGTGGATGC-3'
30	CDX1 RT 3'	5'-CGGTACTTGTCCTTGGTCCG-3'
31	CDX2 RT 5'	5'-CGGCAGCCAAGTGAAAACCA-3'
32	CDX2 RT 3'	5'-CTCTCCTTTGCTCTGCGGTT-3'
33	GAPDH RT 5'	5'-TGCACCACCAACTGCTTAGC-3'
34	GAPDH RT 3'	5'-GGCATGGACTGTGGTCATGAG-3'
35	Myosin IIA RT 5'	5'-AAGGCATCTACCCGCCTGAA-3'
36	Myosin IIA RT 3'	5'-GCACGACAAACGGCAGGTC-3'
37	Slug RT 5'	5'-AGACCCCCATGCCATTGAAG-3'
38	Slug RT 3'	5'-GGCCAGCCCAGAAAAAGTTG-3'
39	Snail RT 5'	5'-TAGCGAGTG GTTCTTCTGCG-3'
40	Snail RT 3'	5'-AGGGCTGCTGGAAGGTAAAC-3'
41	Twist 1 RT 5'	5'-AGCTGAGCAAGATTCAGACCC-3'
42	Twist 1 RT 3'	5'-GCAGCTTGCCATCTTGGAGT-3'
43	Zeb 1 RT 5'	5'-AGGATGACCTGCCAACAGAC-3'
44	Zeb 1 RT 3'	5'-CTTCAGGCCCCAGGATTTCTT-3'
45	c-Myc RT 5'	5'-CAGCTGCTTAGACGCTGGATT-3'
46	c-Myc RT 3'	5'-GTAGAAATACGGCTGCACCGA-3'
47	PPIA RT 5'	5'-GGTCCTGGCATCTTGTCCAT-3'
48	PPIA RT 3'	5'-CAAACACCACATGCTTGCCA-3'

Table 3.6. List of primers used for RT-PCR.

3.16. mRNA stability assays

Cells grown as a monolayer were treated with Actinomycin D (Celon laboratories) used as 5 μ g/mL up to 18 hours or 10 μ g/mL up to 3 hours (Stock 0.5 mg/mL

in PBS). Cells were then harvested and quantitative real time PCR was performed in duplicates. The % mRNA remaining was calculated by considering the mRNA levels at 0 time point to be 100%. Graph was plotted using GraphPad Prism software.

3.17. Nuclear and cytoplasmic fractionation

Cells were harvested by trypsinization and nuclear and cytoplasmic fractions were isolated as per the manufacturer's instructions using the NE-PER kit from Promega. Western blotting was performed and α -tubulin and lamin A antibodies were used as controls for cytoplasmic and nuclear fractions respectively.

3.18. Protein stability assays

Cells grown as a monolayer were treated with Cycloheximide (Sigma) used as 500 μ g/mL (Stock 20 mg/mL in MilliQ) for different time points up to 18 hours or 200 μ g/mL (Stock 20 mg/mL in MilliQ) for different time points up to 72 hours. Similarly, MG132 (Sigma) was used as 5 μ M for 6 hours (Stock 5 mM in DMSO) or NH₄Cl (Sigma) used as 50 mM for 6 hours (Stock 5M in MilliQ). Cells were then harvested and Western blotting was performed.

3.19. Fluorescence recovery after photo bleaching (FRAP) for filamentous actin

FRAP experiments for filamentous GFP Actin were conducted as described earlier [263]. Briefly, GFP Actin expressing cells were culture in a glass bottom dish for at least 3 days to form a monolayer and a wound was made with a pipette tip and cells at the edges of the wound that were migrating were imaged after 12 hours. 3 pre-bleach images were captured and a rectangular area on an actin filament was selected for

bleaching with an Argon 488 laser at 100% power with 100 iterations. Images were captured at the rate of 8 images of 4 z-stacks each per minute on LSM510 Meta confocal microscope with 63x oil immersion objective for a total of 10 minutes post bleaching. Images were aligned and quantitation was performed using ImageJ software. The equation used to calculate corrected FRAP intensity was as previously described [264]:

$$\text{Normalised FRAP Intensity(\%)} = 100 \times \left(\frac{I_n - I_1}{I_{\text{pre}} - I_1} \right) / \left(\frac{I_{\text{Wn}}}{I_{\text{W1}}} \right)$$

I_{pre} and I_1 represent the intensities measured in the ROI from the prebleach and the first post-bleach frames, respectively. I_{Wn} and I_{W1} represent the whole cell intensity measured in frame 'n' and in the first post-bleach frame, respectively. The FRAP curve was generated using non-linear regression analysis in GraphPad Prism software.

3.20. Cell-extracellular matrix adhesion assays

The extracellular matrix (ECM) substrates – Matrigel (BD Biosciences), laminin 5 (Sigma), collagen IV (Sigma) and fibronectin (BD Biosciences) were coated at the concentration of 10 µg/mL in a 96-well plate and incubated overnight at 4°C. After a wash with PBS, the ECM substrates were incubated with 2% BSA for 2 hours at 37°C. 40,000 cells in 100 µL of DMEM with 0.1% BSA were seeded and incubated at 37°C with 5% CO₂ for 30-60 minutes. Non adherent cells were washed gently twice with PBS and the adherent cells were quantitated using MTT (Sigma).

3.21. Immunohistochemistry

The tissue blocks used for immunohistochemistry have been described earlier [108]. Five micron sections of paraffin-embedded formalin fixed tissues were prepared and immunohistochemistry was performed by standard methods [108]. Antigen retrieval

was performed by microwaving the tissue for 10 minutes in 3M sodium citrate buffer. Vimentin antibody was used at 1:50 dilution (Sigma M 0725) and staining was performed using M.O.M. staining kit (Vector Laboratories) according to manufacturer's instructions. MMP9 antibody was used at 1:100 dilution (Abcam ab38898) and staining was performed using ABC staining kit (Vector Laboratories) according to manufacturer's instructions. Images were captured using a 10x objective on a Zeiss Axiovert upright microscope.

3.22. Reagents

3.22.1. 2x BBS for calcium phosphate transfection

50mM BES, 280mM NaCl, 1.5mM Na₂HPO₄.

3.22.2. PBS(phosphate-buffered saline)

Total	1L
NaCl	8 g
KCl	0.2 g
KH ₂ PO ₄	0.2 g
Na ₂ HPO ₄ ·7H ₂ O	1.15 g
MilliQ	Make up volume to 1L

3.22.3. Laemmli's buffer

Total	100 mL
1M Tris pH 6.8	5 mL
Glycerol	10 mL
10% SDS	20 mL
Bromophenol blue	0.1 g
MilliQ	Make up volume to 95 mL

Before use add 5% β-mercaptoethanol.

3.22.4. 30% acrylamide/0.8% bisacrylamide

Mix 30.0 g acrylamide and 0.8 g N,N'-methylenebisacrylamide with H₂O in a total volume of 100 mL. Filter the solution through filter paper and store in the dark.

CAUTION: Acrylamide monomer is neurotoxic. A mask should be worn when weighing acrylamide powder. Gloves should be worn while handling the solution and the solution should not be pipetted by mouth.

3.22.5. 10x Running buffer (SDS-PAGE)

Total	1L
Tris-Base	30.31 g
Glycine	150 g
SDS	10 g
MilliQ	Make up volume to 1L

3.22.6. Transfer Buffer:

Total	4L
Tris base	12.1g
Glycine	57.6g
10% SDS	4mL
Methanol	800mL
MilliQ	Make up volume to 4L

First take about 2L MilliQ. Add all powders and dissolve well. Then add 10% SDS. Add methanol last. Can be reused twice.

3.22.7. TBST

Total	3L
2.5M NaCl	180mL
Tris pH 8.0	30mL
Tween-20 (use cut tip or 10mL pipette)	3mL
MilliQ	Make up volume to 3L

RESULTS

4. RESULTS

4.1. Role of PKP3, adherens junctions and actin cytoskeleton in initiation of desmosome formation and regulation of desmosome size and assembly.

Desmosomes are calcium dependent cell-cell adhesion junctions and the localization of desmosomal proteins to the cell border is dependent on calcium ([169] and reviewed in [5, 43, 46, 61]). Desmosomes being calcium dependent junctions, calcium switch assays, where cells are cultured in low calcium (<0.1mM) containing medium and then switched to normal calcium (1.8 – 2 mM) medium, are performed to study desmosome formation (reviewed in [164]). Desmosome formation is dependent on the adherens junctions; in the absence of classical cadherins like E-cadherin and P-cadherin, desmosomal components are unable to localize to the cell membrane/ border [168, 169]. A complex of E-cadherin-PG-PKP3 is formed even in low calcium conditions and is essential for desmosome formation [169]. 14-3-3 γ has been shown to bind to PG in a PKC μ dependent manner and is required for kinesin-1 dependent transport of PG to the cell border [175]. 14-3-3 γ also binds to PKP3 and DP and could play a similar role in transport of these proteins to the desmosome [175]. Results from our laboratory suggest that even PKP3 forms a complex with kinesin-1 (unpublished data). To further elucidate the role of PKP3 in desmosome assembly, we generated HCT116 based cells stably overexpressing DsRed fluorophore tagged PKP3.

4.1.1. DsRed tagged PKP3 localizes to the cell border independent of calcium concentration

HCT116 cells are difficult to transfect using standard transfection methods and previous attempts made in the laboratory to generate PKP3 overexpressing HCT116 cells had failed. DsRed PKP3 was cloned from pcDNA vector [169] into the lentiviral vector pEF.55 [259] and lentiviruses were produced in HEK293T cells as described in materials and methods. HCT116 cells were infected with DsRed PKP3 lentiviruses and selected with puromycin to generate a mixed population of DsRed PKP3 overexpressing HCT116 cells and cell border localization of DsRed PKP3 was observed when these cells were imaged on a confocal microscope (Figure 4.1 a). DsRed PKP3 expression was shown to co-localize with interacting partners like the desmosomal cadherin GFP-DSC2a (Figure 4.1 b) as well as with the adherens junction cadherin YFP-E-cadherin consistent with our previously reported results [169] (Figure 4.1 c). These results suggest that the DsRed PKP3 fusion shows localization similar to endogenous PKP3.

Desmosome assembly is generally studied in the context of a calcium switch assay as described earlier. In brief, cells are cultured in low calcium conditions for 20 hours to inhibit desmosome formation, then de novo desmosome assembly is studied by switching to normal calcium medium for up to one hour [169] (Figure 4.2 a). PKP3 localizes to the cell border in low calcium conditions even when desmosomes are not formed and is able to form a complex with E-cadherin and PG [169]. However, on switching to normal calcium medium the cell border localization of PKP3 increases [169]. However, in DsRed PKP3 cells, DsRed PKP3 is observed in high amounts at the cell border even in low calcium conditions and the cell border localization of DsRed

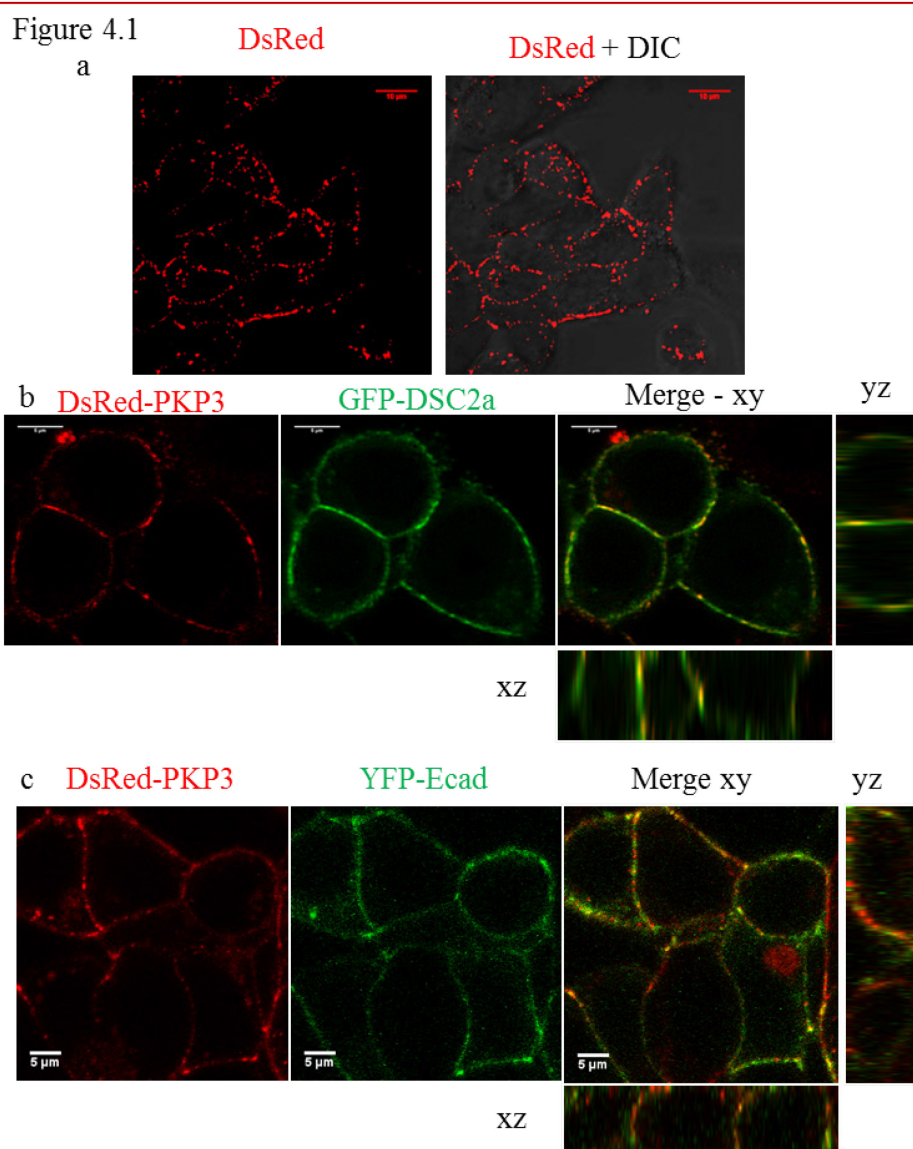


Figure 4.1. DsRed PKP3 co-localizes with GFP-DSC2a and YFP-E-cadherin –
DsRed PKP3 was stably expressed in HCT116 cells. a. DsRed PKP3 HCT116 cells imaged using a 63x oil immersion objective on a confocal microscope showing cell border localization as confirmed by the DIC merge image. b. DsRed PKP3 HCT116 cells were transfected with GFP-DSC2a and imaged using a 63x oil immersion objective on a confocal microscope showing co-localization in the merged image. c. DsRed PKP3 HCT116 cells were transfected with YFP-E-cadherin and imaged using a 63x oil immersion objective on a confocal microscope showing co-localization in the merged image. Scale bars included in all images.

Figure 4.2

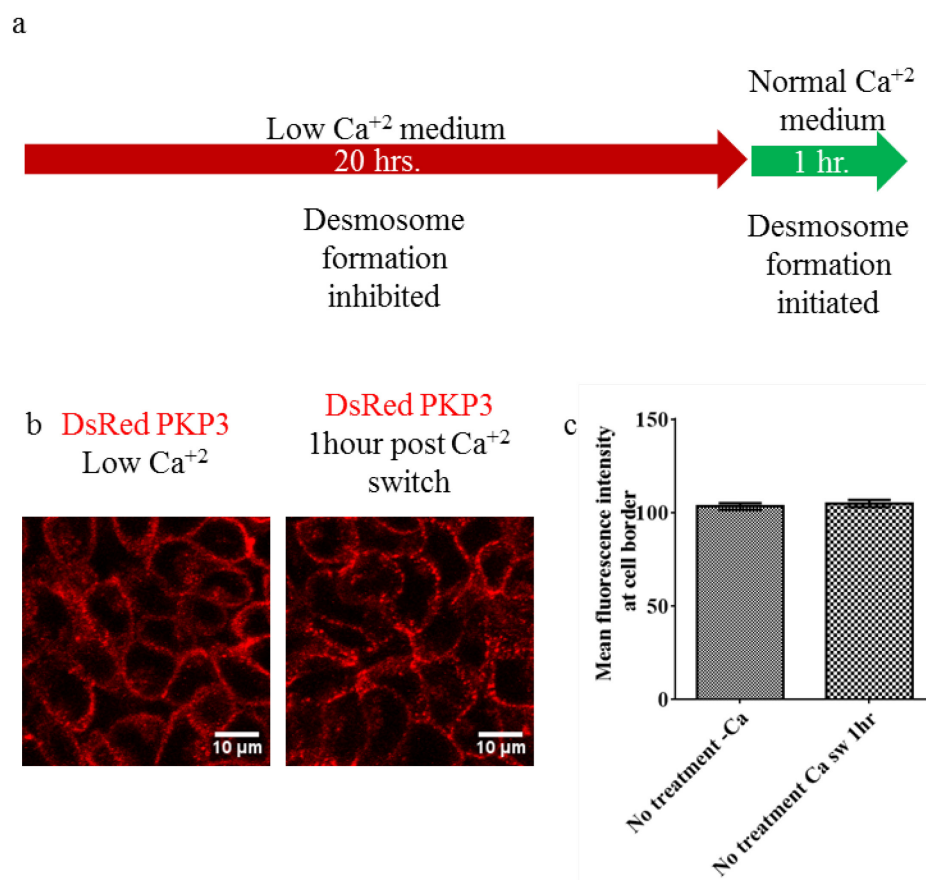


Figure 4.2. DsRed PKP3 overexpression leads to calcium independent localization of DsRed PKP3 to the cell border – DsRed PKP3 was stably expressed in HCT116 cells. a. Schematic of a calcium switch assay to study *de novo* desmosome assembly. b-c. DsRed PKP3 HCT116 cells cultured in low calcium medium imaged using a 63x oil immersion objective on a confocal microscope and then changed to normal calcium medium and imaged up to one hour showing cell border localization. b. The border intensity was quantitated using ImageJ software from 30 representative cells and c. the mean and standard error for three independent experiments was plotted using GraphPad Prism software. Statistical significance was determined using Student's *t*-test. Scale bars are included in all images.

PKP3 does not increase on switching the cells to normal calcium medium (Figure 4.2 b & c). This observation leads us to infer that the PKP3 overexpressing cells are not suitable for studying desmosome assembly as PKP3 transport to the cell border seems to have become calcium independent. This observation, however, leads to other intriguing questions. PKP3 is the most ubiquitously expressed PKP family member and is capable of interacting with all other desmosomal components as well as adherens junction cadherin E-cadherin [169, 201]. Is PKP3 overexpression sufficient to lead to calcium independent and/or hyperadhesive desmosomes? Does PKP3 overexpression alter the expression and/or localization of other desmosomal proteins?

4.1.2. PKP3 overexpression increases cell-cell adhesion

PKP3 overexpression leads to calcium independent localization of PKP3 to the cell border. PKP3 knockdown leads to loss of cell membrane/ border localization of desmosomal proteins and decreased cell-cell adhesion [108]. To determine the effect of PKP3 overexpression on cell-cell adhesion, two distinct cell-cell adhesion assays were performed. Hanging drop assays (see materials and methods) enable determination of the capability of cells to form aggregates from a single cell suspension and represent the ability to form de novo cell-cell adhesion junctions. On the other hand, disperse assays (see materials and methods) enable determination of the capability of cells to retain existing cell-cell adhesion junctions by subjecting the monolayer to mechanical stress. PKP3 overexpressing cells showed increased cell-cell adhesion in low calcium medium as well as normal calcium medium in both these assays (Figure 4.3 and Figure 4.4). Furthermore, PKP3 knockdown in DsRed PKP3 cells lead to a reversal of this phenotype showing decreased cell-cell adhesion (Figure 4.5). Thus, PKP3 overexpression is necessary and sufficient to increase de novo cell-cell adhesion as well as retain

Figure 4.3

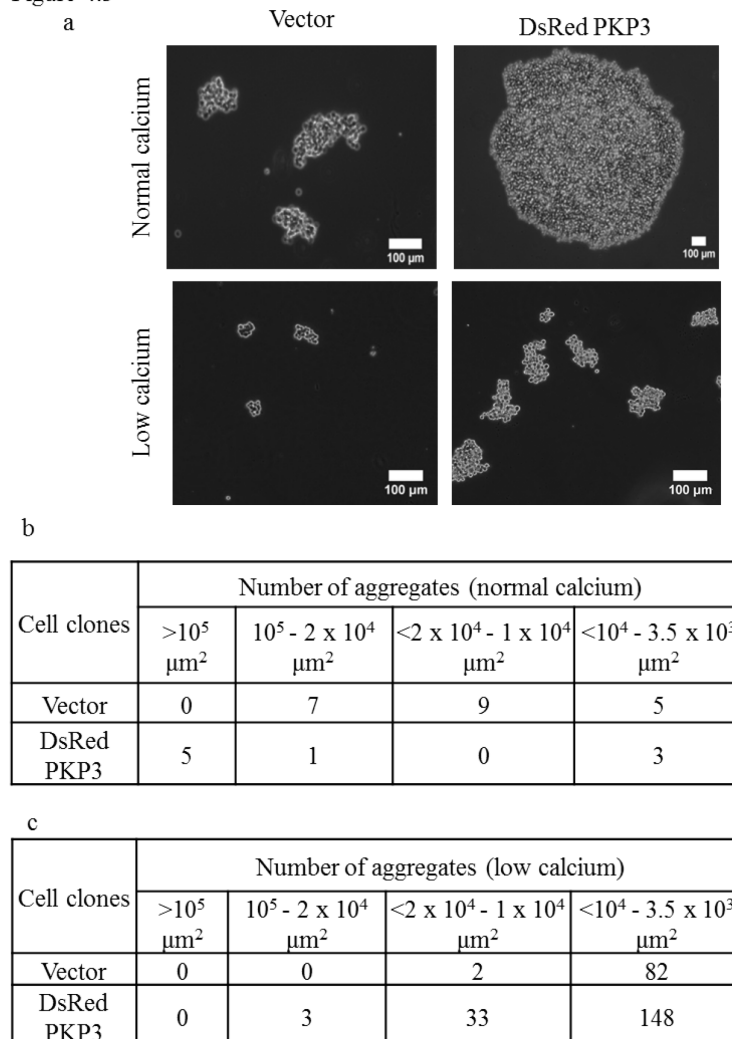


Figure 4.3. PKP3 overexpression increases de novo cell-cell adhesion –DsRed PKP3 cells and vector control cells, were either cultured in low calcium medium or normal calcium medium and hanging drop assays were performed as described in materials and methods, a. Representative images of cell aggregates imaged using 10x or 5x objective on Zeiss Axiovert microscope are shown. b. Table showing the number and size of aggregates measured using ImageJ software from five random fields for each triplicate and from three independent experiments for cells cultured in normal calcium medium and, c. for cells cultured in low calcium medium. Scale bars are included in all images.

Figure 4.4

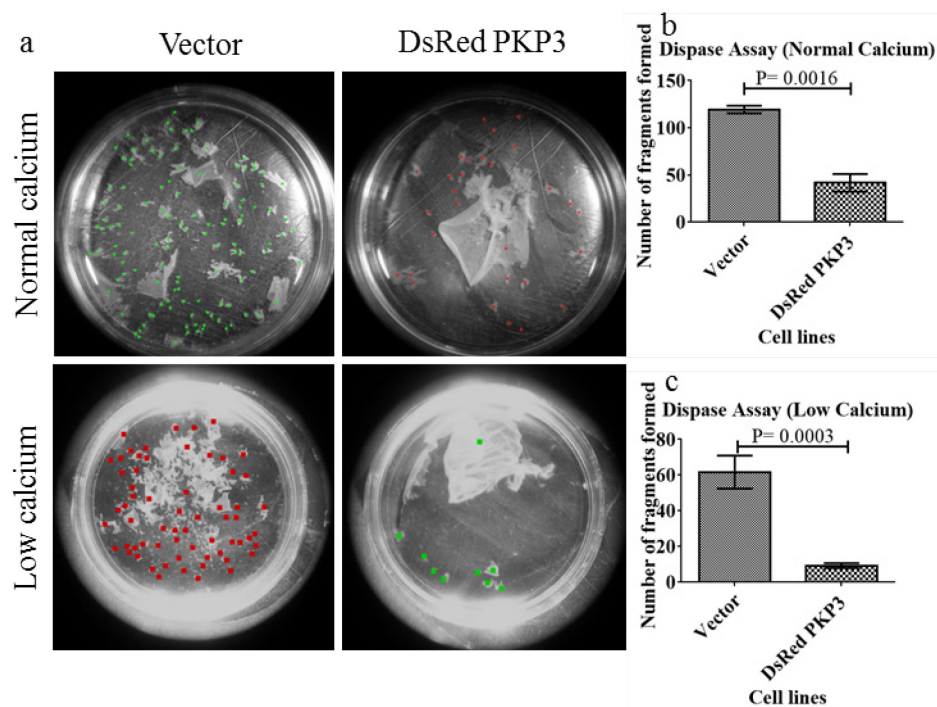


Figure 4.4. PKP3 overexpression increases retention of cell-cell adhesion –DsRed PKP3 cells and vector control cells were either cultured in low calcium medium or normal calcium medium and disperse assays were performed in triplicates and three independent experiments as described in the materials and methods. *a*. Representative images of monolayer fragments imaged using Olympus dissecting microscope. *b-c*. Fragments were counted using ImageJ software and graph was plotted using GraphPad Prism software, *b*. for normal calcium medium and, *c* for low calcium medium. Statistical significance was determined using Student's *t*-test. This data has been adapted from [9].

cell-cell adhesion when resisting mechanical stress, in low calcium medium as well as normal calcium medium. However, the cell-cell adhesion observed in DsRed PKP3 cells in low calcium medium is still lesser than in normal calcium medium showing a decrease in dependence on calcium but not a complete independence from calcium sensitive cell-cell adhesion junction formation.

Figure 4.5

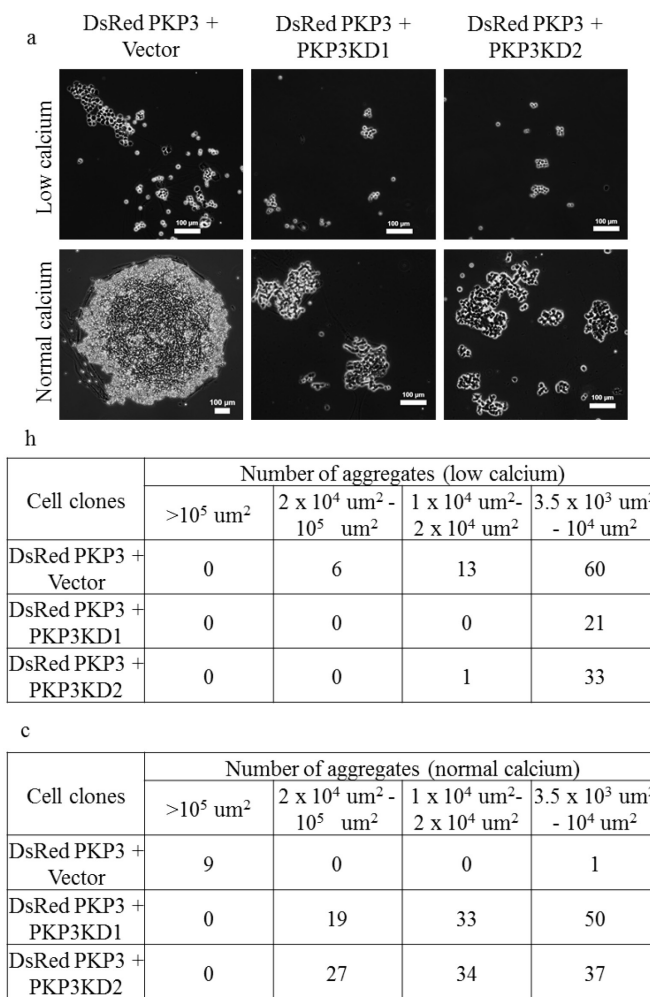


Figure 4.5. PKP3 overexpression is necessary and sufficient to increase cell-cell adhesion –DsRed PKP3 overexpressing vector control cells and DsRed PKP3 cells with PKP3 knockdown, were either cultured in low calcium medium or normal calcium medium and, hanging drop assays were performed as described in materials and methods, a. Representative images of cell aggregates imaged using 10x or 5x objective on Zeiss Axiovert microscope are shown. b. Table showing the number and size of aggregates measured using ImageJ software from five random fields for each triplicate and from three independent experiments for cells cultured in normal calcium medium and, c. for cells cultured in low calcium medium. Scale bars are included in all images.

Figure 4.6

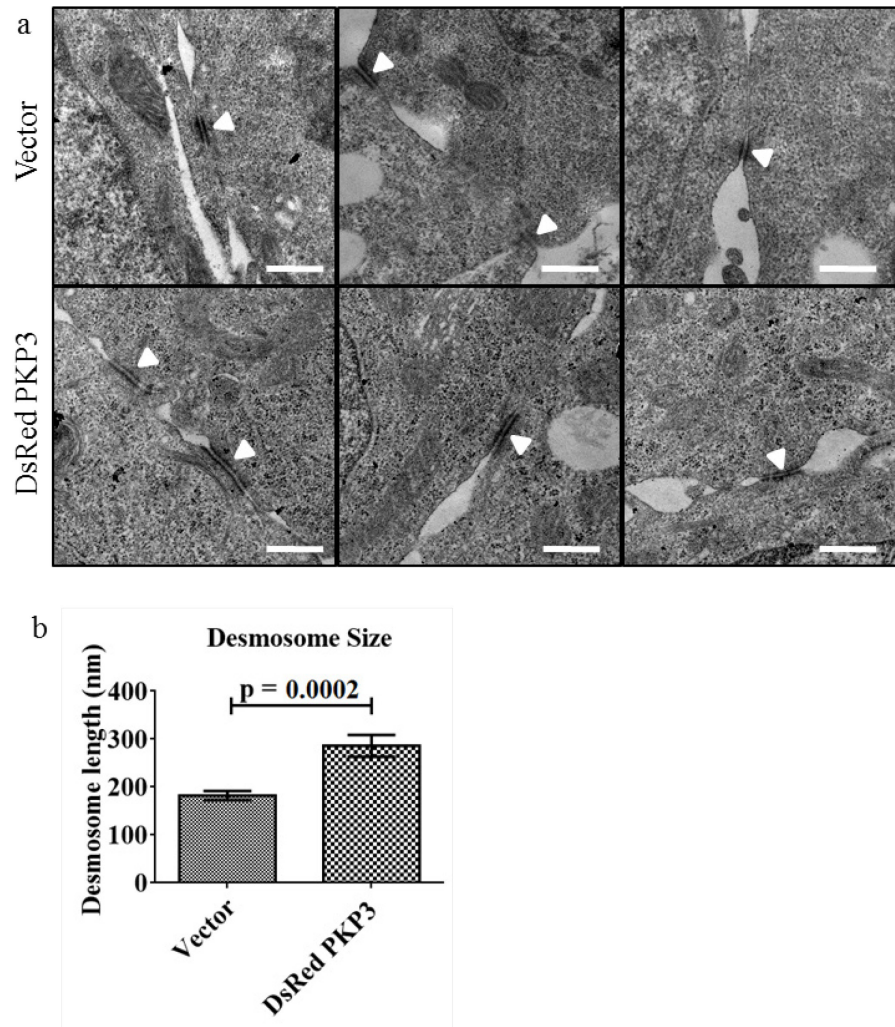


Figure 4.6. PKP3 overexpression increases desmosome size – *DsRed PKP3* cells and the vector control cells were cultured as a confluent monolayer and processed for imaging by an electron microscope. *a.* Representative images taken at 12,000x magnification (Scale bar = 500 nm) are shown. White arrow heads mark desmosomes. *b.* The size of >30 desmosomes were measured using iTEM software and graph showing mean and standard error was plotted using GraphPad software. Statistical significance was determined using Student's *t*-test. Scale bars of 500 nm are included in all images.

4.1.3. PKP3 overexpression increases desmosome size

PKP3 is an essential desmosomal plaque protein that is indispensable for desmosome assembly [108, 169]. Hence, increase in cell-cell adhesion on PKP3

Figure 4.7

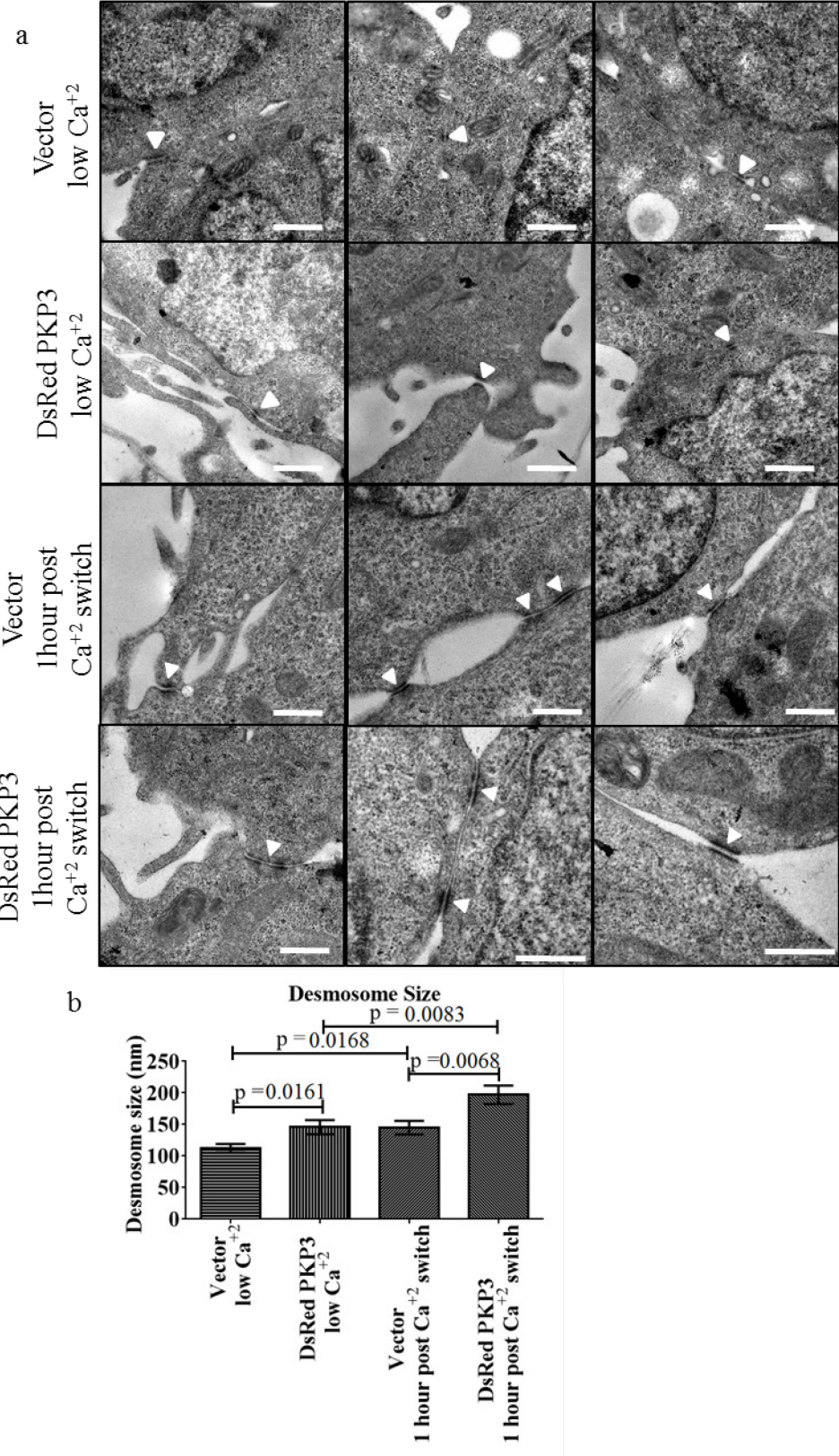


Figure 4.7. PKP3 overexpression increases desmosome size in a calcium switch assay – *DsRed PKP3 cells and the vector control cells were cultured in calcium switch assays, as a confluent monolayer and processed for imaging by an electron microscope. a. Representative images taken at 12,000x magnification (Scale bar = 500 nm) are shown. White arrow heads mark desmosomes. b. The size of >30 desmosomes were measured using iTEM software and graph showing mean and standard error was plotted using GraphPad software. Statistical significance was determined using Student's t-test. Scale bars of 500 nm are included in all images.*

overexpression could be due to increase in desmosome size and/ or number. Desmosome size in PKP3 overexpressing cells and vector control cells as determined by electron microscopy shows that PKP3 overexpression does indeed lead to an increase in desmosome size (Figure 4.6). The increase in desmosome size in DsRed PKP3 cells is also observed when cells are cultured in low calcium, as well as, when a calcium switch assays were performed and de novo desmosome formation is measured after one hour of switching to normal calcium medium (Figure 4.7). Thus PKP3 overexpression increases desmosome size and reduces dependence of desmosome assembly on calcium.

4.1.4. PKP3 overexpression increases cell membrane/ border localization of other desmosomal proteins

Desmosomal proteins like DSC2, DSG 2 and DP do not localize to the cell membrane/ border when cells are cultured in low calcium conditions. PG and PKP3 also have minimal cell border localization in low calcium conditions. Only on restoring normal calcium levels can these desmosomal proteins localize to the cell membrane/ border and lead to desmosome formation [169]. PKP3 knockdown leads to a decrease in cell membrane/ border localization of other desmosomal proteins [169]. The increase in

desmosome size on PKP3 overexpression could be due to increase in all desmosomal proteins at the cell membrane/ border. Likewise, PKP3 localization to the cell border became calcium independent on overexpression of PKP3; hence, it could possibly potentiate calcium independent localization of other desmosomal proteins too. Calcium switch assays followed by immunofluorescence staining demonstrated that PKP3 overexpression leads to an increase in cell border/ membrane localization of DSC2/3, DSG2, DP, PG and E-cadherin in low calcium medium as well as after one hour of switching to normal calcium medium (Figure 4.8, Figure 4.9, Figure 4.10, Figure 4.11 and Figure 4.12). Additionally, knockdown of PKP3 in the DsRed PKP3 cells leads to reversal of this phenotype with decreased cell membrane/ border localization of DSG2 and DP and staining for DSG2 and DP observed in the DsRed PKP3 with PKP3 KD cells only in cells where the knockdown efficiency is less (Figure 4.14 and Figure 4.15). Thus PKP3 overexpression increases cell membrane/ border localization of other desmosomal proteins and reduces the calcium dependency of localization of other desmosomal proteins to the cell border/ membrane. These results are in agreement with the increase in cell-cell adhesion established for the DsRed PKP3 cells. Interestingly, the adherens junction catenin, p120 catenin, does not show any difference in cell border localization in low calcium in DsRed PKP3 cells but shows decreased cell border localization upon switch to normal calcium in DsRed PKP3 cells (Figure 4.13). Since, p120 catenin and PKP3 are closely related proteins it can be conjectured that excess PKP3 triggers some negative feedback mechanism by which it reduces p120 catenin at the cell border.

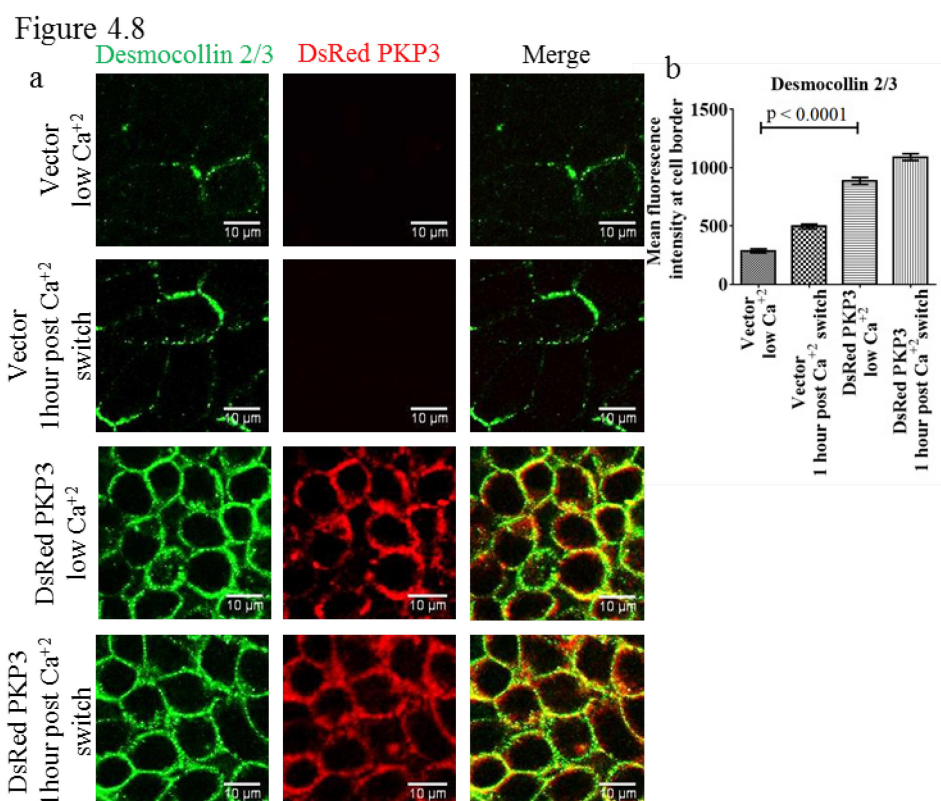


Figure 4.8. PKP3 overexpression increases cell membrane localization of desmocollin 2/3 – DsRed PKP3 cells and the vector control cells were cultured in low calcium medium for 20 hours. Calcium was replenished in the medium and images taken after one hour. Cells were fixed and stained for desmocollin 2/3 and images were captured on a confocal microscope with 63x oil immersion objective. *a.* Representative images for each condition are shown. *b.* Mean fluorescence intensities at the cell border of >90 cells were quantitated from 3 independent experiments using ImageJ and graph showing mean and standard error plotted using GraphPad Prism. Mean fluorescence intensity was compared using Student's *t*-test. Scale bars are included in all images.

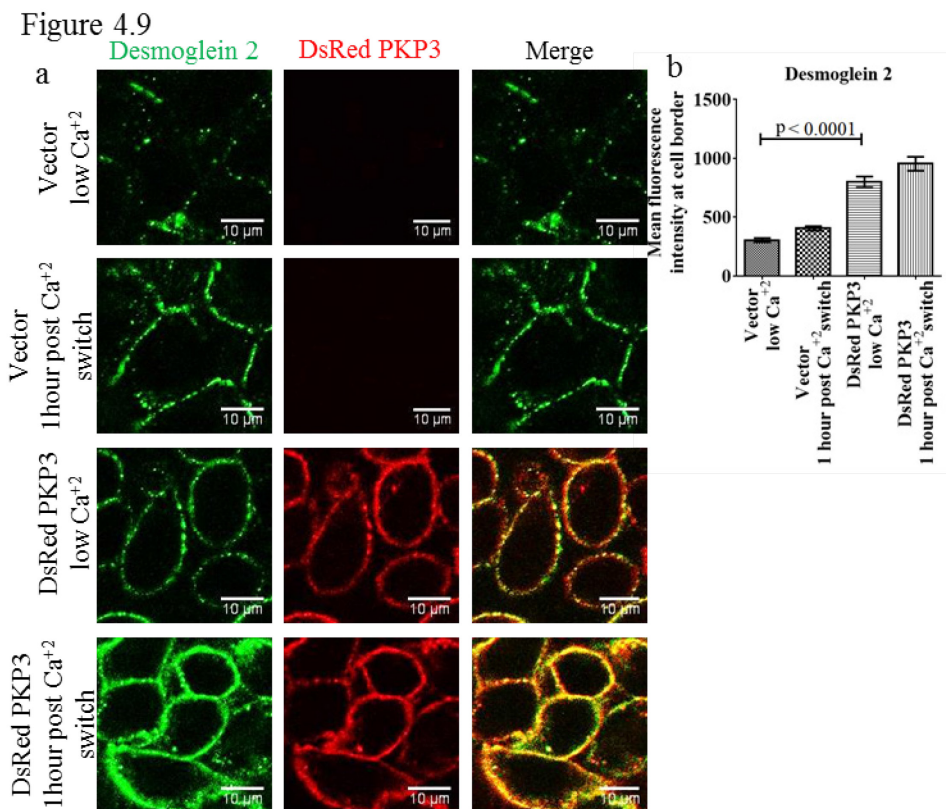


Figure 4.9. PKP3 overexpression increases cell membrane localization of desmoglein 2 – DsRed PKP3 cells and the vector control cells were cultured in low calcium medium for 20 hours. Calcium was replenished in the medium and images taken after one hour. Cells were fixed and stained for desmoglein 2 and images were captured on a confocal microscope with 63x oil immersion objective. *a.* Representative images for each condition are shown. *b.* Mean fluorescence intensities at the cell border of >90 cells were quantitated from 3 independent experiments using ImageJ and graph showing mean and standard error plotted using GraphPad Prism. Mean fluorescence intensity was compared using Student's *t*-test. Scale bars are included in all images.

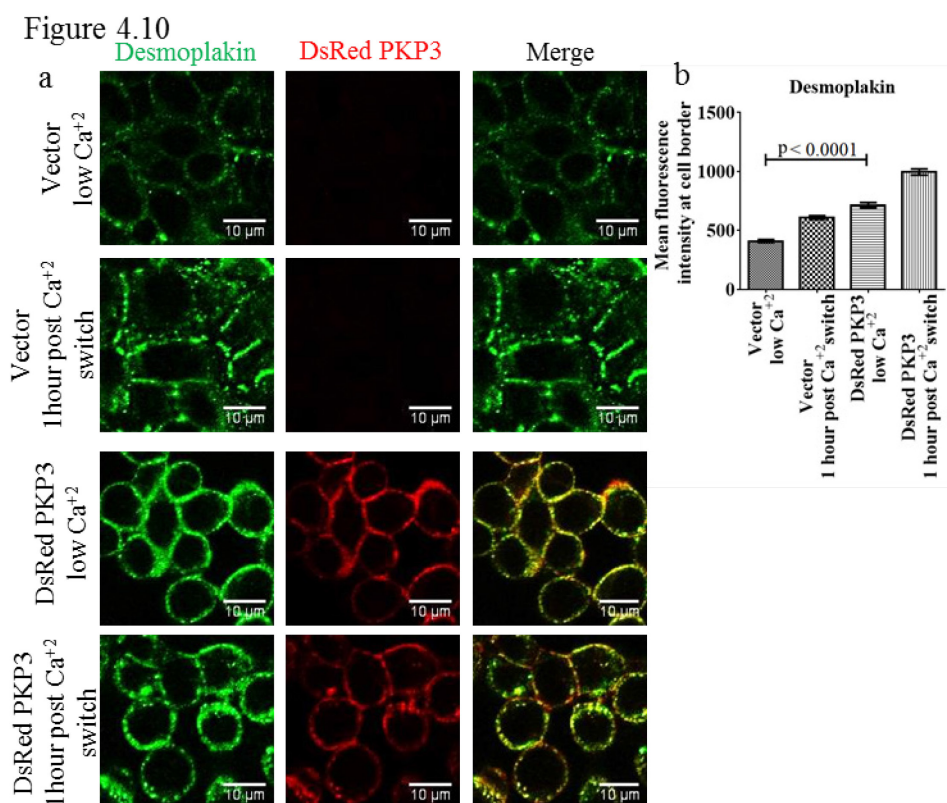


Figure 4.10. PKP3 overexpression increases cell border localization of desmoplakin – DsRed PKP3 cells and the vector control cells were cultured in low calcium medium for 20 hours. Calcium was replenished in the medium and images taken after one hour. Cells were fixed and stained for desmoplakin and images were captured on a confocal microscope with 63x oil immersion objective. *a.* Representative images for each condition are shown. *b.* Mean fluorescence intensities at the cell border of >90 cells were quantitated from 3 independent experiments using ImageJ and graph showing mean and standard error plotted using GraphPad Prism. Mean fluorescence intensity was compared using Student's *t*-test. Scale bars are included in all images.

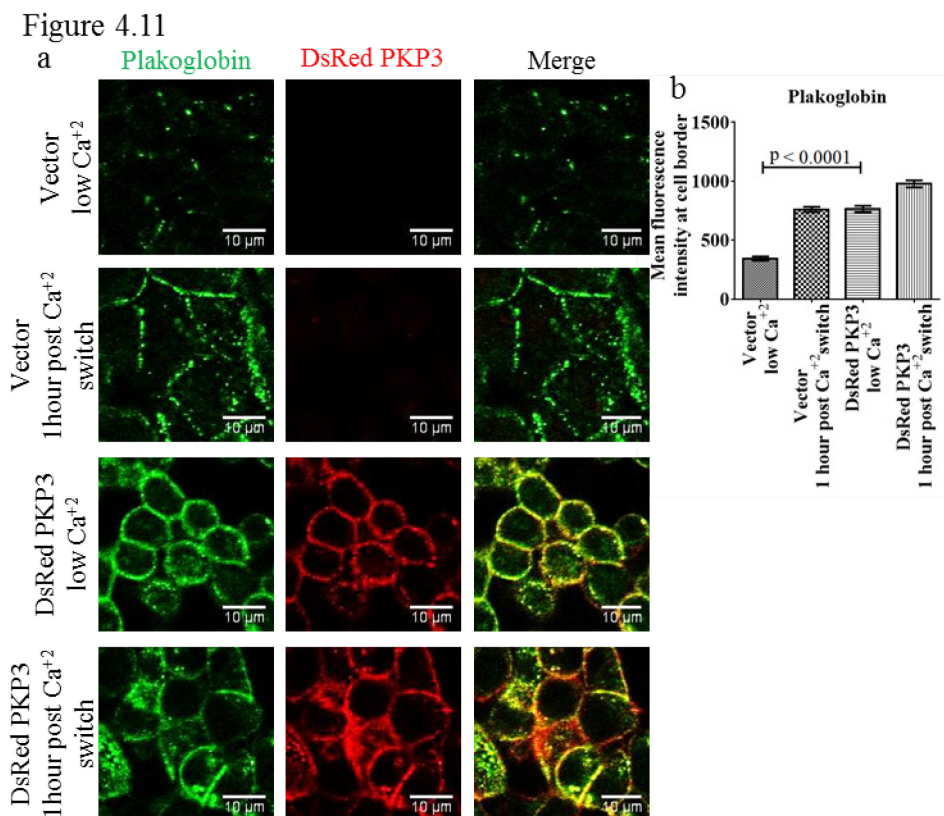


Figure 4.11. PKP3 overexpression increases cell border localization of plakoglobin – DsRed PKP3 cells and the vector control cells were cultured in low calcium medium for 20 hours. Calcium was replenished in the medium and images taken after one hour. Cells were fixed and stained for plakoglobin and images were captured on a confocal microscope with 63x oil immersion objective. a. Representative images for each condition are shown. b. Mean fluorescence intensities at the cell border of >90 cells were quantitated from 3 independent experiments using ImageJ and graph showing mean and standard error plotted using GraphPad Prism. Mean fluorescence intensity was compared using Student's *t*-test. Scale bars are included in all images.

Figure 4.12

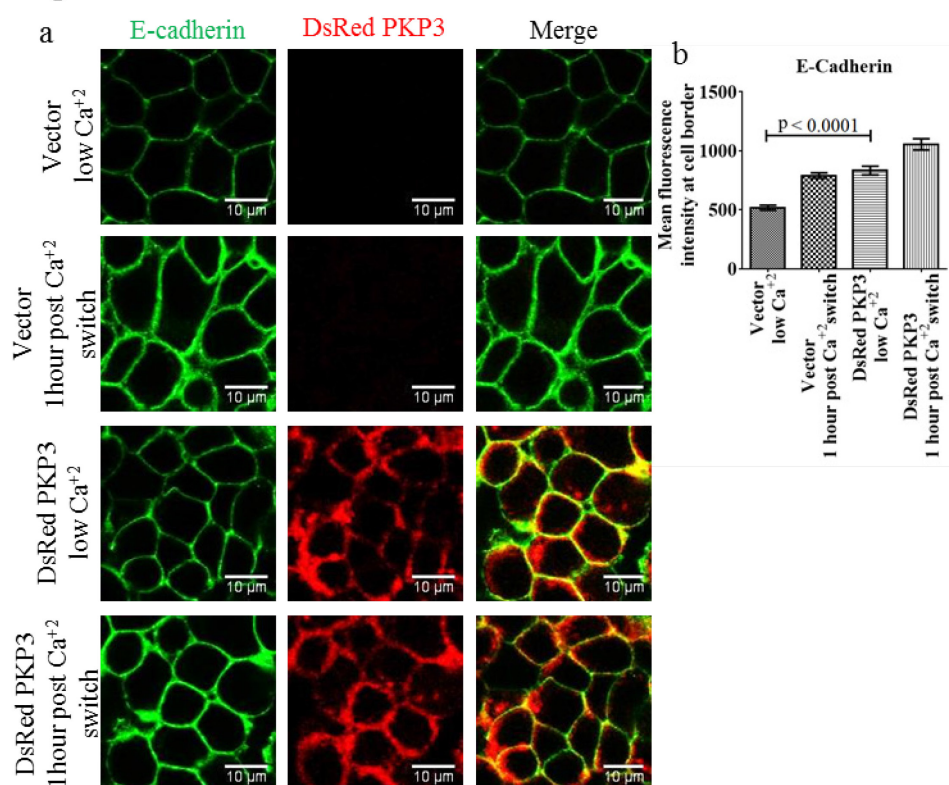


Figure 4.12. PKP3 overexpression increases cell membrane localization of E-cadherin – *DsRed PKP3* cells and the vector control cells were cultured in low calcium medium for 20 hours. Calcium was replenished in the medium and images taken after one hour. Cells were fixed and stained for E-cadherin and images were captured on a confocal microscope with 63x oil immersion objective. *a*. Representative images for each condition are shown. *b*. Mean fluorescence intensities at the cell border of >90 cells were quantitated from 3 independent experiments using ImageJ and graph showing mean and standard error plotted using GraphPad Prism. Mean fluorescence intensity was compared using Student's *t*-test. Scale bars are included in all images.

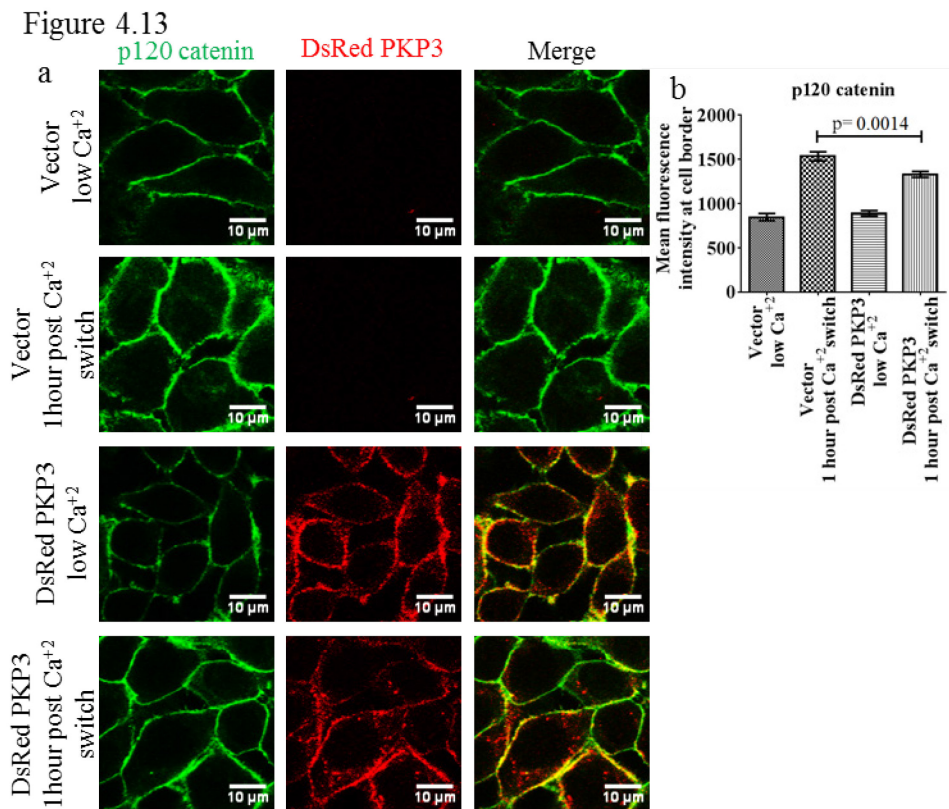


Figure 4.13. PKP3 overexpression increases cell border localization of p120 catenin – DsRed PKP3 cells and the vector control cells were cultured in low calcium medium for 20 hours. Calcium was replenished in the medium and images taken after one hour. Cells were fixed and stained for p120 catenin and images were captured on a confocal microscope with 63x oil immersion objective. a. Representative images for each condition are shown. b. Mean fluorescence intensities at the cell border of >90 cells were quantitated from 3 independent experiments using ImageJ and graph showing mean and standard error plotted using GraphPad Prism. Mean fluorescence intensity was compared using Student's *t*-test. Scale bars are included in all images.

Figure 4.14

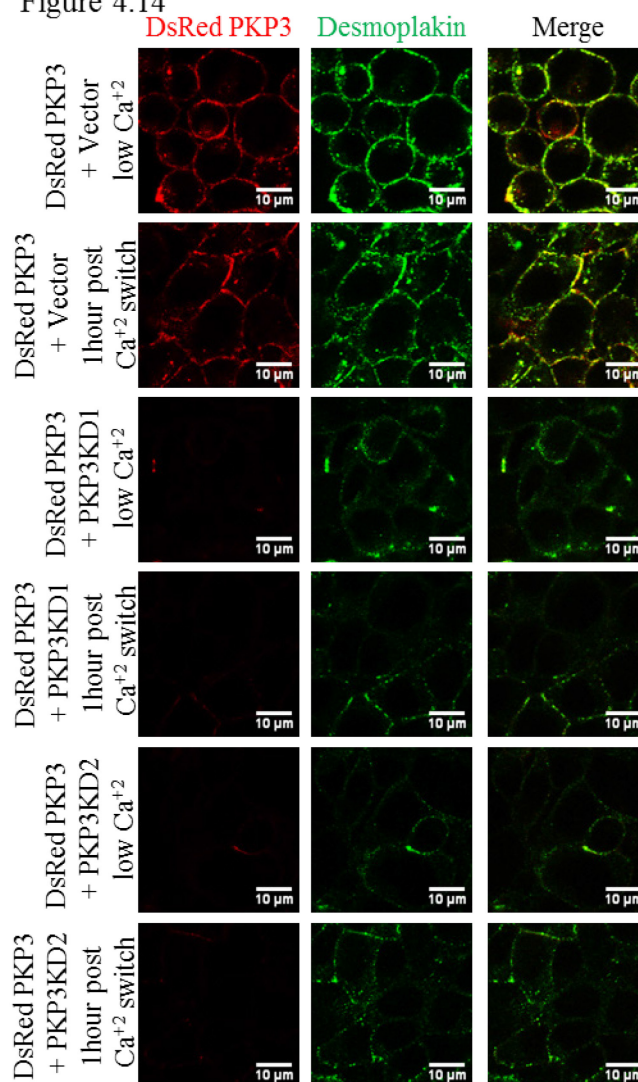


Figure 4.14. PKP3 overexpression is necessary and sufficient for increase in cell border localization of desmoplakin –DsRed PKP3 with PKP3 knockdown and the vector control cells were cultured in low calcium medium for 20 hours. Calcium was replenished in the medium and images taken after one hour. Cells were fixed and stained for desmoplakin and images were captured on a confocal microscope with 63x oil immersion objective. Representative images for each condition are shown. Scale bars are included in all images.

Figure 4.15

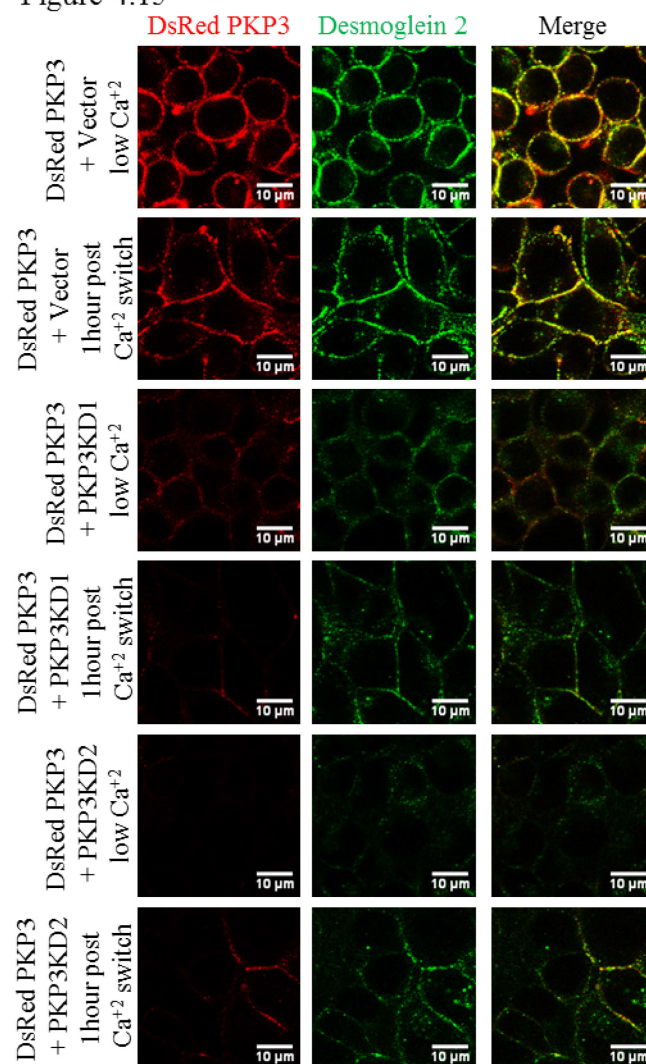


Figure 4.15. PKP3 overexpression is necessary and sufficient for increase in cell membrane localization of desmoglein 2 –DsRed PKP3 with PKP3 knockdown and the vector control cells were cultured in low calcium medium for 20 hours. Calcium was replenished in the medium and images taken after one hour. Cells were fixed and stained for desmoglein 2 and images were captured on a confocal microscope with 63x oil immersion objective. Representative images for each condition are shown. Scale bars are included in all images.

4.1.5. PKP3 overexpression increases total protein levels of other desmosomal proteins and mRNA levels of DSC2

The increase in cell membrane/ border localization of other desmosomal proteins seemed to be unusually high upon PKP3 overexpression. Although PKP3 knockdown does not lead to changes in proteins levels of other desmosomal proteins [108], we wanted to determine whether PKP3 overexpression can regulate total protein levels of other desmosomal proteins. Western blots showed that the overexpression of DsRed PKP3 leads to an increase in expression of desmosomal proteins like DP, DSG2, DSC 2/3, PG, as well as adherens junction cadherins like E- cadherin and P- cadherin. However the expression of adherens junction proteins β catenin and α -E-catenin or the tight junction protein ZO-I is not affected (Figure 4.16). Interestingly, in agreement with the immunofluorescence staining results, p120 catenin levels are decreased in DsRed PKP3 cells as compared to the vector control cells (Figure 4.16). We next wanted to determine if the increase in protein levels was due to increased mRNA levels. Reverse transcriptase PCR and quantitative real time PCR for cell-cell adhesion proteins like DP, DSG2, DSC 2, PG, E- cadherin, P- cadherin, β catenin and ZO-I showed that there was a significant increase only in DSC2 mRNA (Figure 4.17, c). Knockdown of PKP3 in the DsRed PKP3 cells leads to a decrease in desmosomal proteins like DP, DSG2, DSC 2 and PG (Figure 4.18 a). Likewise, knockdown of PKP3 in the DsRed PKP3 cells also decreases DSC2 mRNA levels (Figure 4.18 b). Thus PKP3 overexpression is necessary and sufficient for as increase in mRNA of DSC2 and increase in protein levels of other desmosomal proteins.

Figure 4.16

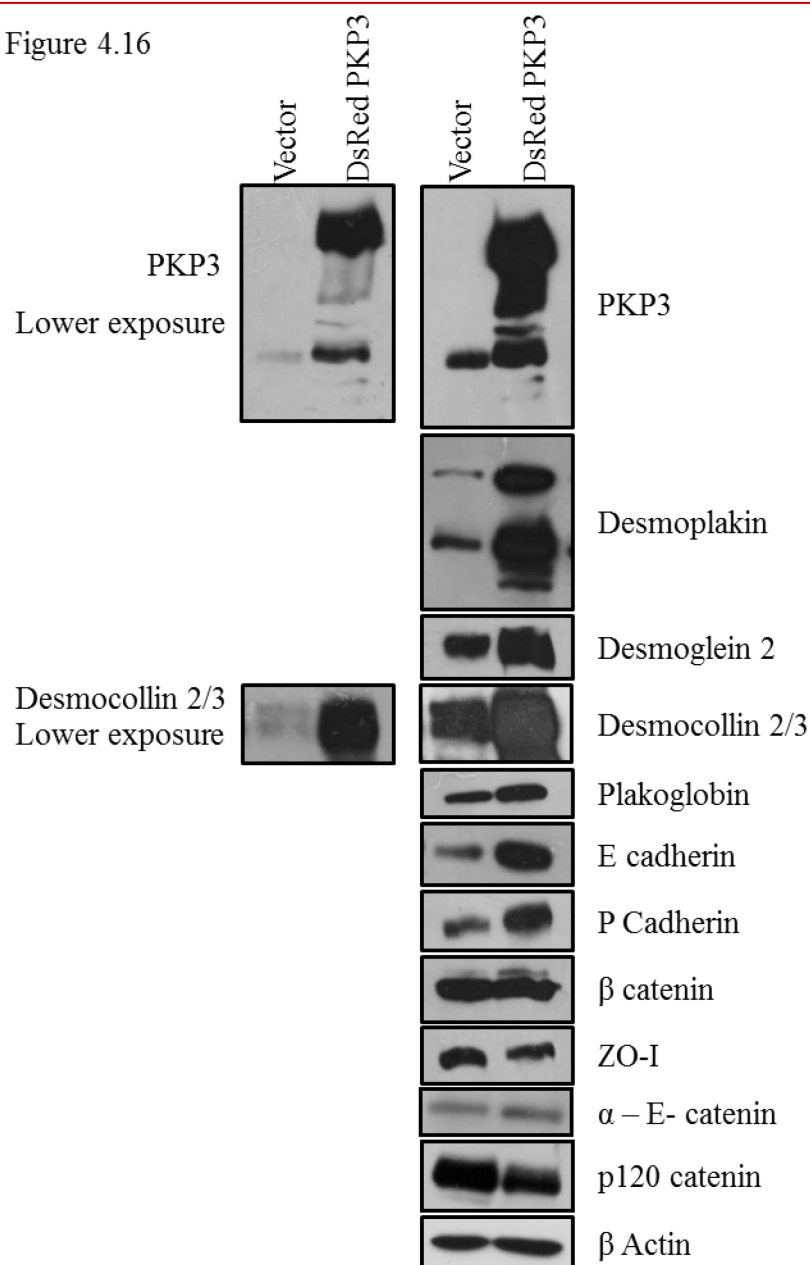


Figure 4.16. DsRed PKP3 overexpression leads to an increase in other desmosomal proteins – *DsRed PKP3 cells and the vector control cells were cultured as a monolayer. Cell lysates were separated on an SDS-PAGE gel and immunoblotted as shown with the indicated antibodies using β actin as a loading control.*

Figure 4.17

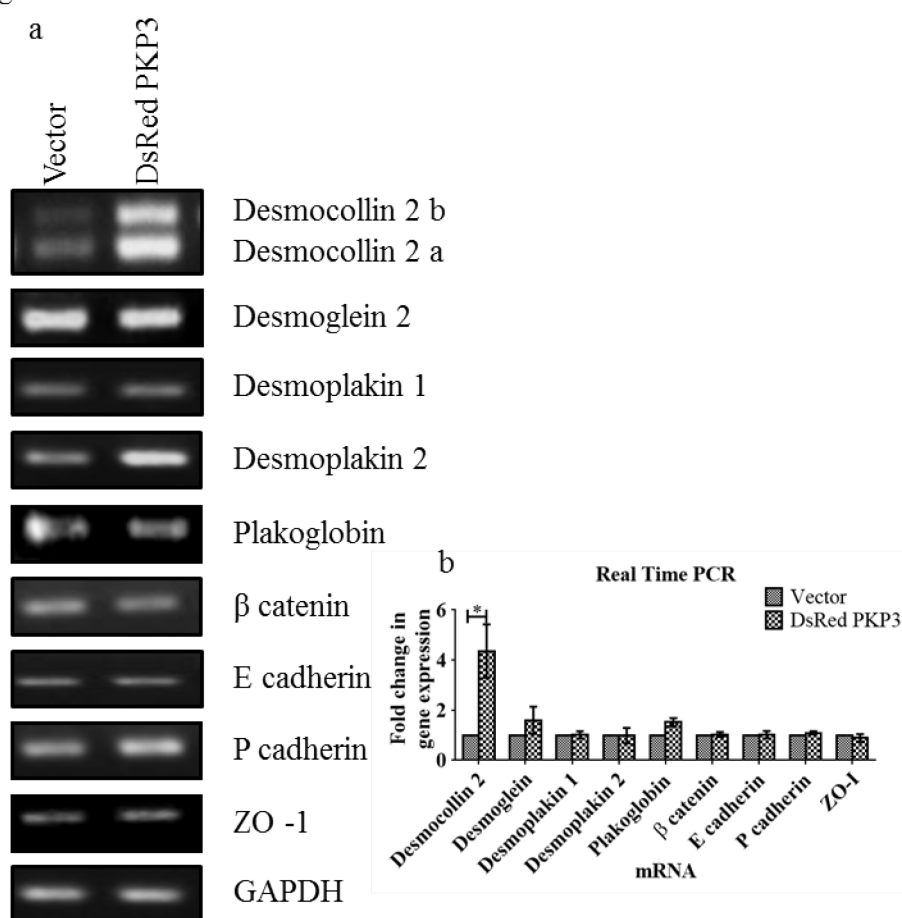
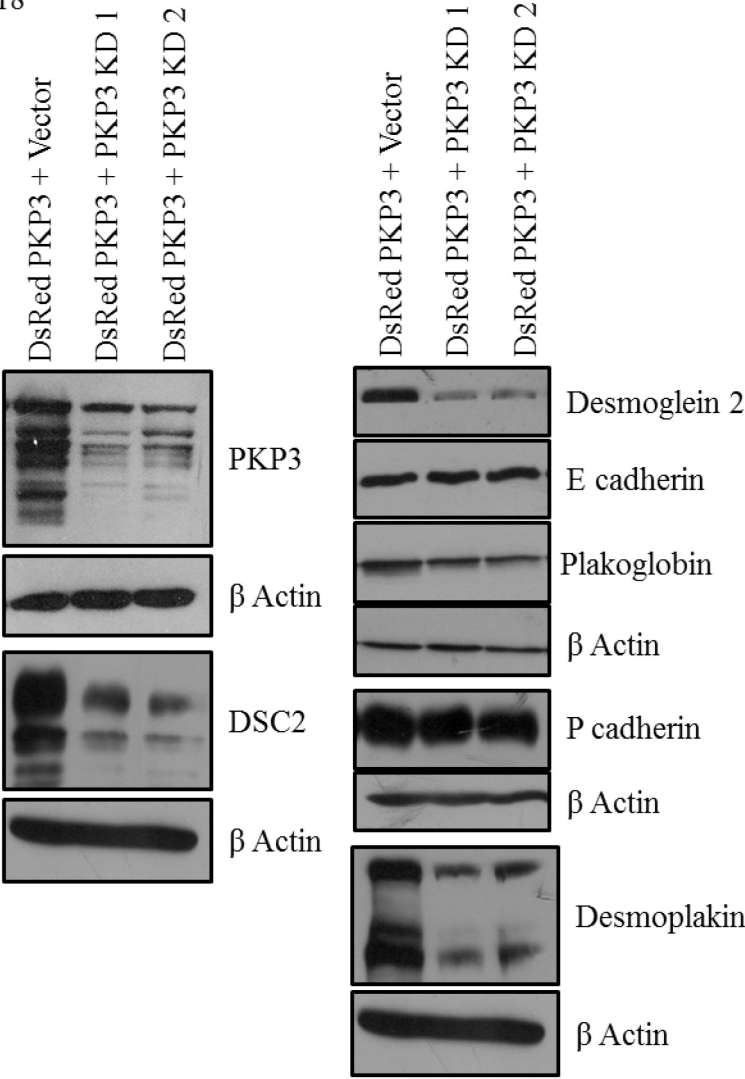


Figure 4.17. DsRed PKP3 overexpression leads to an increase in DSC2 mRNA

– DsRed PKP3 cells and the vector control cells were cultured as a monolayer. RNA was purified and a. RT-PCR was performed for the indicated mRNAs with GAPDH as a loading control, b. Real time PCR analysis was performed for the indicated mRNAs with GAPDH as a control. The values were normalized to 1 for the vector control cell line and error bars are plotted using GraphPad Prism software. The fold change in gene expression was compared using Student's *t*-test. * indicates $P < 0.05$.

Figure 4.18

a



b

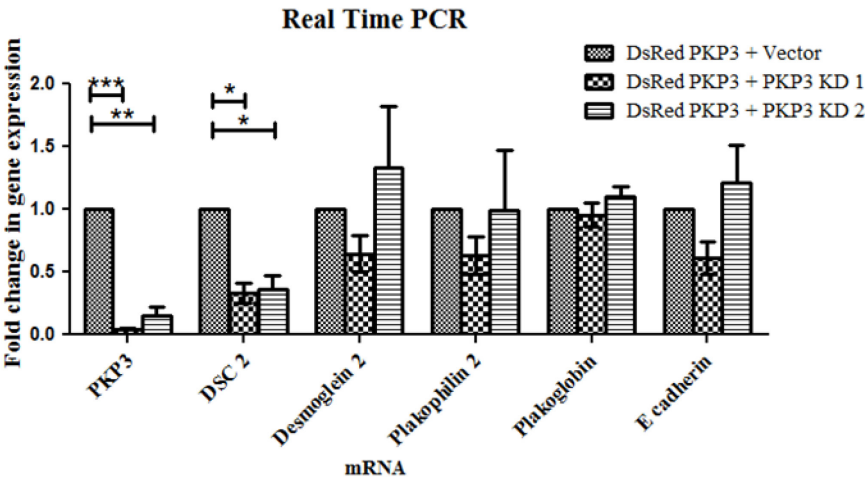


Figure 4.18. DsRed PKP3 overexpression is necessary and sufficient increase in other desmosomal proteins – DsRed PKP3 with PKP3 knockdown and the vector control cells were cultured as a monolayer. a. Cell lysates were separated on an SDS-PAGE gel and immunoblotted as shown with the indicated antibodies using β actin as a loading control. b. RNA was purified and Real time PCR analysis was performed for the indicated mRNAs with GAPDH as a control. The values were normalized to 1 for the vector control cell line and error bars are plotted using GraphPad Prism software. The fold change in gene expression was compared using Student's *t*-test. * indicates $P < 0.05$, ** indicates $P < 0.01$, *** indicates $P < 0.001$.

4.1.6. PKP3 overexpression does not stabilize DSC2 mRNA

PKP3 is known to localize to the nucleus and bind to ETV1 transcription factor and this association has been implicated in having a role in neural crest formation (11). Similarly, PKP3 is shown to be a part of RNA stress granules and known to bind to RNA binding proteins like FXR1, G3BP, and PABPC1, and it has been shown to affect mRNA stability of plakophilin 2 and desmoplakin (12, 13). It is hence likely that PKP3 increases DSC2 mRNA either by increasing DSC2 transcription in the nucleus or by binding to DSC2 mRNA and increasing DSC2 mRNA stability. DSC2 promoter has been identified as a region up to 1883 b.p. upstream of its translation start site and the transcription start site has been identified 201 b.p. upstream of the translation start site [212] (Figure 4.19 a). Dual luciferase assays performed for the DSC2 promoter showed that there was no change in DSC2 promoter activity on PKP3 overexpression (Figure 4.19 b). We also ensured that the amount of DSC2 promoter plasmid that we were transfecting – 0.5 μ g – to perform these assays was within the

Figure 4.19

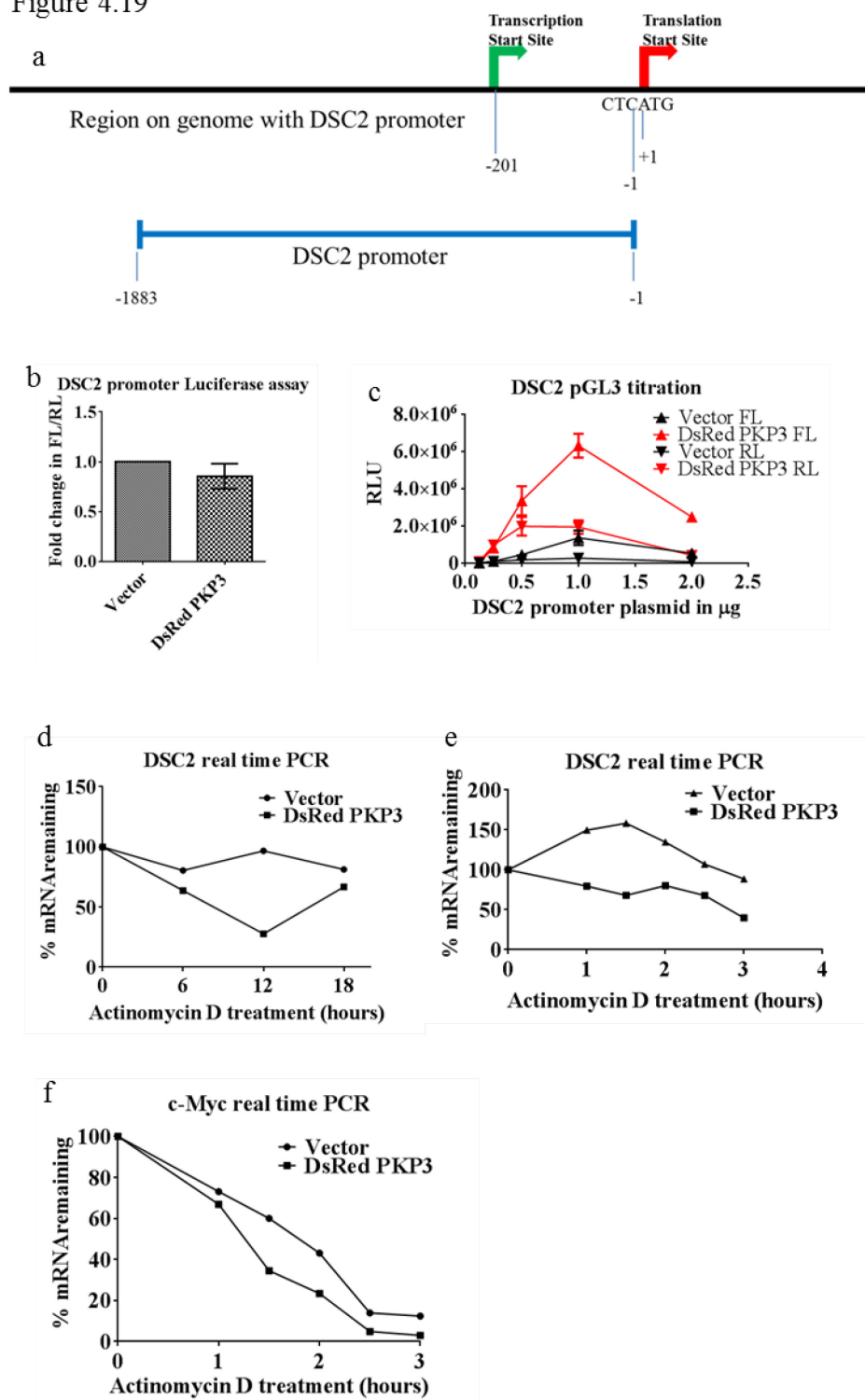


Figure 4.19. PKP3 overexpression does not stabilize DSC2 mRNA – *a.* Schematic of DSC2 promoter, *DsRed PKP3* cells and the vector control cells were cultured as a monolayer and *b,c.* Dual luciferase reporter assays was performed to determine the activity of the DSC2 promoter, *b.* fold change in firefly luciferase

normalized to Renilla luciferase was plotted showing mean and standard error using GraphPad Prism, c. Relative luciferase units values for both firefly luciferase and Renilla luciferase were plotted using GraphPad Prism for different amounts of DSC2 promoter firefly luciferase plasmid transfected, d-f. Cells were treated with 5 µg/mL actinomycin D or vehicle control and harvested at various time points and quantitative real time PCR was performed using GAPDH or PPIA as control d,e. Percentage change in DSC2 expression normalized to 1 for 0 time point, f. percentage change in c-Myc expression normalized to 1 for 0 time point, was plotted using GraphPad Prism.

linear range of this assay (Figure 4.19 c). Stability assays for mRNA using actinomycin D treatment performed showed that there was no increase in DSC2 mRNA stability on PKP3 overexpression (Figure 4.19 d,e). As a positive control, the mRNA stability assay was performed for the c-Myc mRNA, and the half-life observed is consistent with that reported previously for c-Myc mRNA (Figure 4.19 f). Interestingly, while there was no change in the degradation pattern for c-Myc mRNA between DsRed PKP3 and vector control cells, we could see that DSC2 mRNA was getting degraded faster in DsRed PKP3 cells as compared to the vector control cells (Figure 4.19 d,e) although at every time point there was more DSC2 mRNA in DsRed PKP3 cells as compared to the vector control for the respective time point (data not shown). Thus PKP3 overexpression increases DSC2 mRNA but probably decreases DSC2 mRNA stability due to the excessive DSC2 mRNA being degraded by the cell. Hence we propose that PKP3 overexpression increases DSC2 transcription and are testing this hypothesis by performing nuclear run-on assays.

4.1.7. PKP3 overexpression leads to an increase in nuclear localization of C/EBP α and PKP3 interacts with C/EBP α

Literature review showed that the transcription factor family of C/EBP proteins and CDX proteins and particularly the transcription factor C/EBP α were possible candidates for regulation of DSC 2 mRNA expression [115, 213, 215, 216]. RT-PCR assays showed that there was no significant change in mRNA levels of all the C/EBP and CDX family transcription factors tested (Figure 4.20). Microarray data from our laboratory for PKP3 knockdown clones shows a decrease in C/EBP α in PKP3 knockdown cells [228]. Western blots showed that there was no change in C/EBP α protein levels on PKP3 overexpression (Figure 4.21 a). However, immunofluorescence staining and nuclear-cytoplasmic fractionation for C/EBP α showed increased nuclear localization of C/EBP α and particularly the truncated isoform of C/EBP α on PKP3 overexpression (Figure 4.21 b,c,d). The truncated isoform of C/EBP α can act as an inhibitor for the function of the full length C/EBP α isoform as well as other members of the C/EBP family by forming heterodimers with them (reviewed in [4, 226]). Further, immunoprecipitation experiments showed that PKP3 forms a complex with all the C/EBP α isoforms (Figure 4.21 e). Thus, PKP3 could directly or indirectly have an effect on C/EBP α function and that could in turn affect DSC2 transcription. However, C/EBP α knockdown using shRNA did not seem to make any noticeable change in DSC2 expression (Figure 4.23 a). While C/EBP β seemed to show decreased nuclear localization on PKP3 overexpression, C/EBP δ did not show any change in localization on PKP3 overexpression (Figure 4.22). Knock down of C/EBP β as well as C/EBP δ also did not show any noticeable change in DSC2 expression (Figure 4.23 c,d). Thus, PKP3 could play a role in modulating C/EBP α function but whether this interaction is

responsible for the change in DSC2 transcription remains unclear and further experiments are required to draw conclusions.

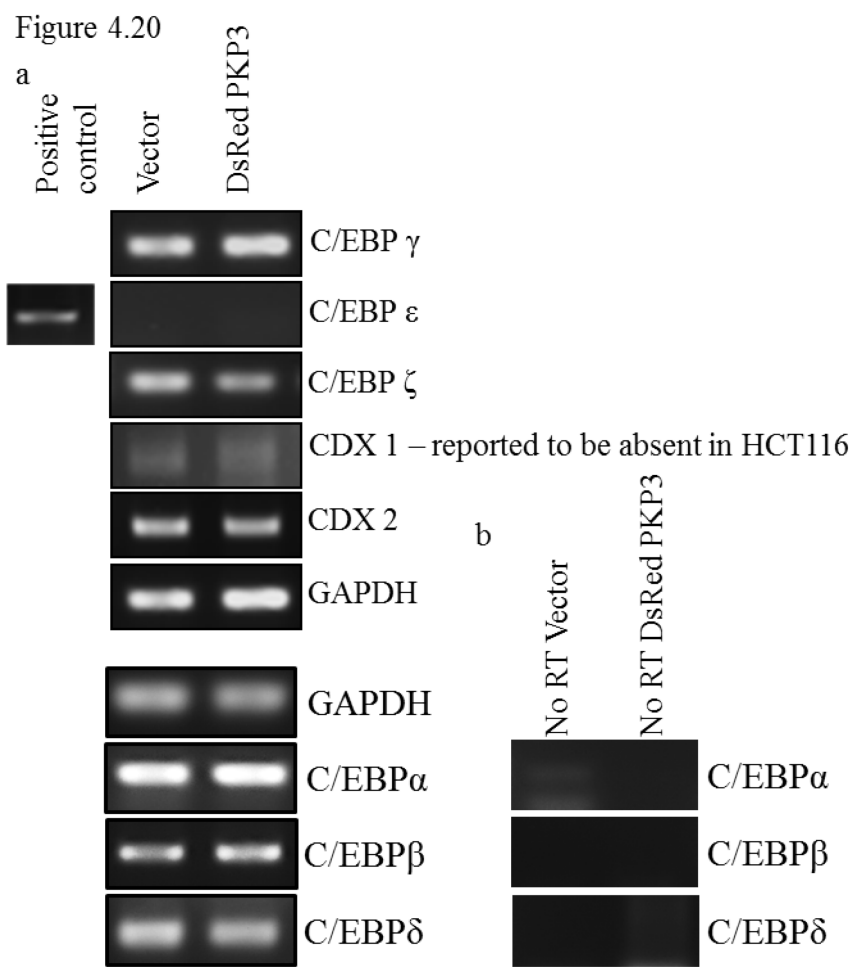


Figure 4.20. DsRed PKP3 overexpression does not change expression of transcription factors known to regulate DSC2 expression – *DsRed PKP3 cells and the vector control cells were cultured as a monolayer and, a,b. RNA was purified and RT-PCR was performed for the indicated mRNAs with GAPDH as a loading control as well as no RT controls for intronless genes and positive controls for genes that are not expressed.*

Figure 4.21

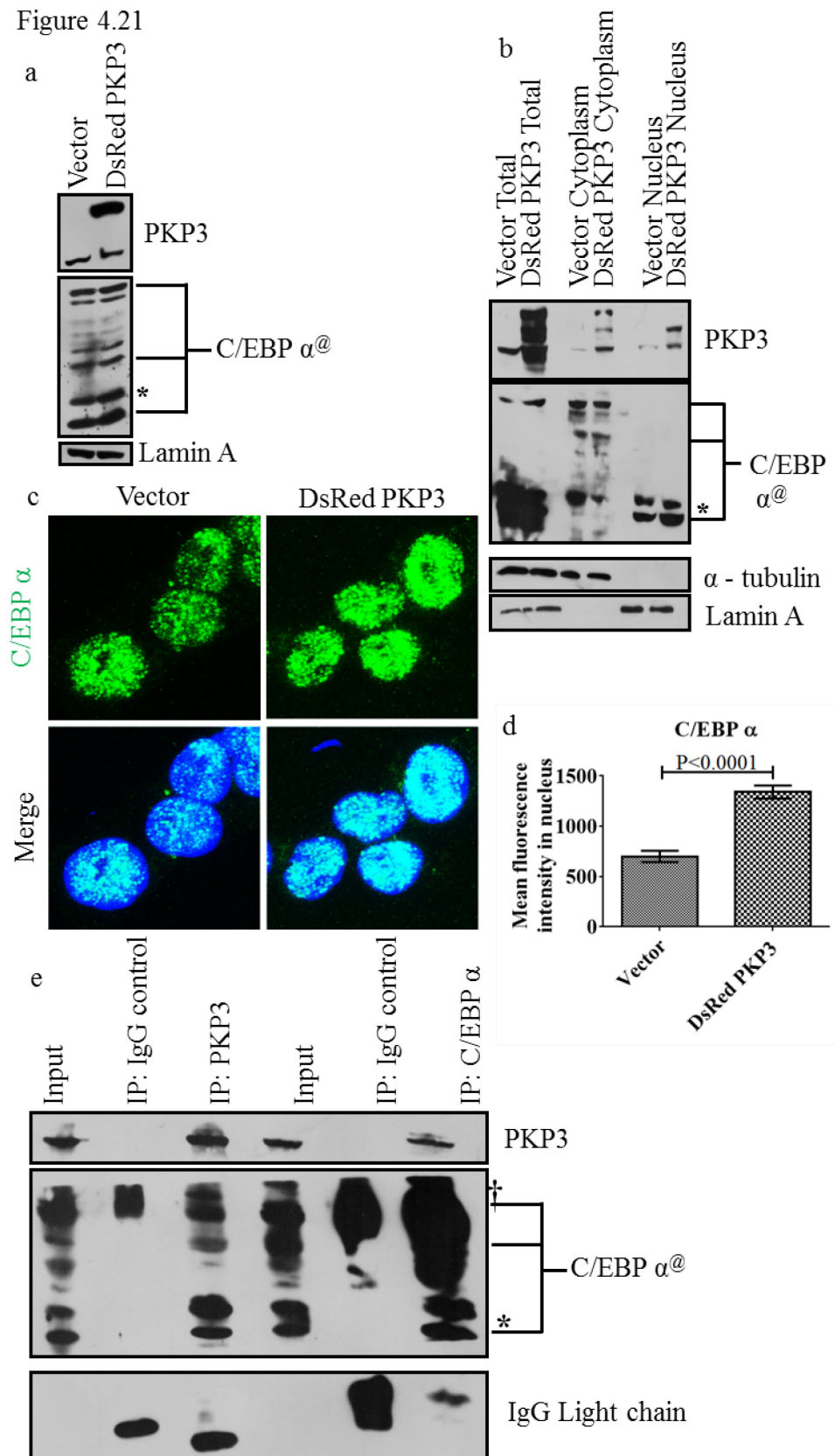


Figure 4.21. DsRed PKP3 overexpression leads to an increase in nuclear localization of the transcription factor C/EBP α and, PKP3 interacts with C/EBP α – DsRed PKP3 cells and the vector control cells were cultured as a monolayer and a. Protein lysates were separated on an SDS-PAGE gel and immunoblotted as shown with the indicated antibodies with lamin A as a loading control. b. Total cell extract as well as cytoplasmic and nuclear fractionated protein lysates were separated on an SDS-PAGE gel and immunoblotted as shown with the indicated antibodies, with Lamin A as a control for nuclear fractions and α tubulin as a loading control for cytoplasmic fractions. c,d. Cells were fixed and stained for C/EBP α with nuclei counterstained with DAPI and images were captured on a confocal microscope with 63x oil immersion objective. c. Representative images are shown. d. Mean fluorescence intensity in the nucleus for C/EBP α of >90 cells were quantitated from 3 independent experiments. Mean fluorescence intensity was compared using Student's t-test and graph showing mean and standard error was plotted using GraphPad Prism. e. EBC extracts of HCT116 wild type cells were incubated with the indicated antibodies for immunoprecipitation. The immune complexes were resolved on a SDS-PAGE gel and Western blotted with the indicated antibodies. @: C/EBP α has 3 isoforms – extended, full length and truncated, the expression of these isoforms is translationally regulated. *: This band is either non-specific or possibly a sumoylated form of truncated C/EBP α [20]. †: IgG Heavy chain. Scale bars are included in all images.

Figure 4.22

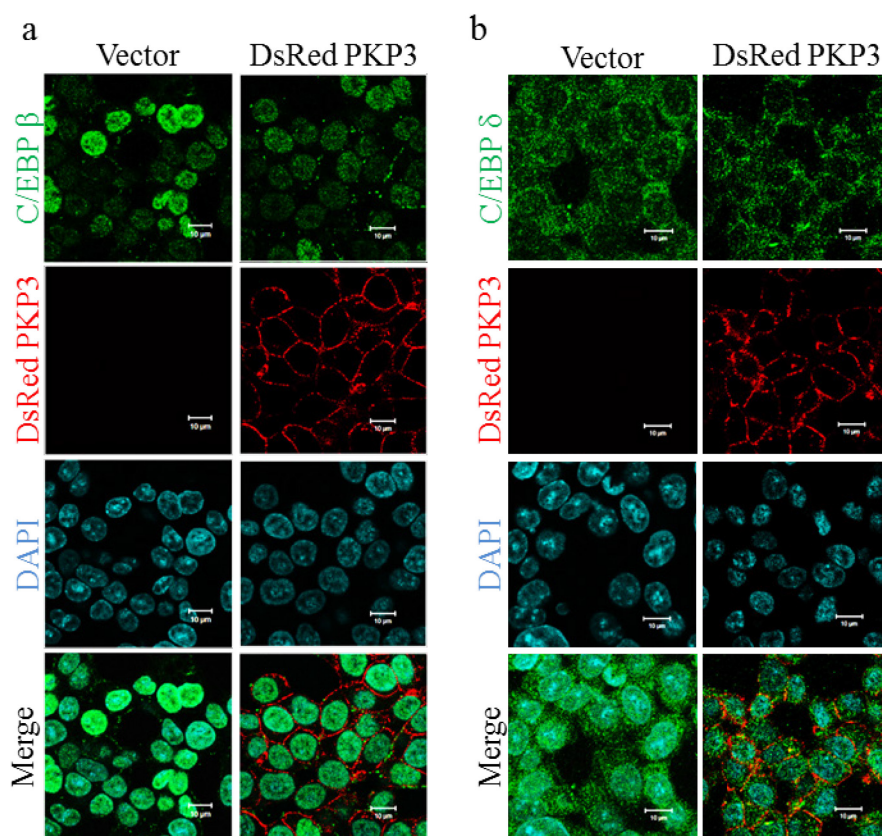


Figure 4.22. DsRed PKP3 overexpression does not change localization of the transcription factors C/EBP β and C/EBP δ – DsRed PKP3 cells and the vector control cells were cultured as a monolayer and, a,b. Cells were fixed and stained for the indicated antibodies with nuclei counterstained with DAPI and images were captured on a confocal microscope with 63x oil immersion objective. Representative images for are shown. Scale bars are included in all images.

Figure 4.23

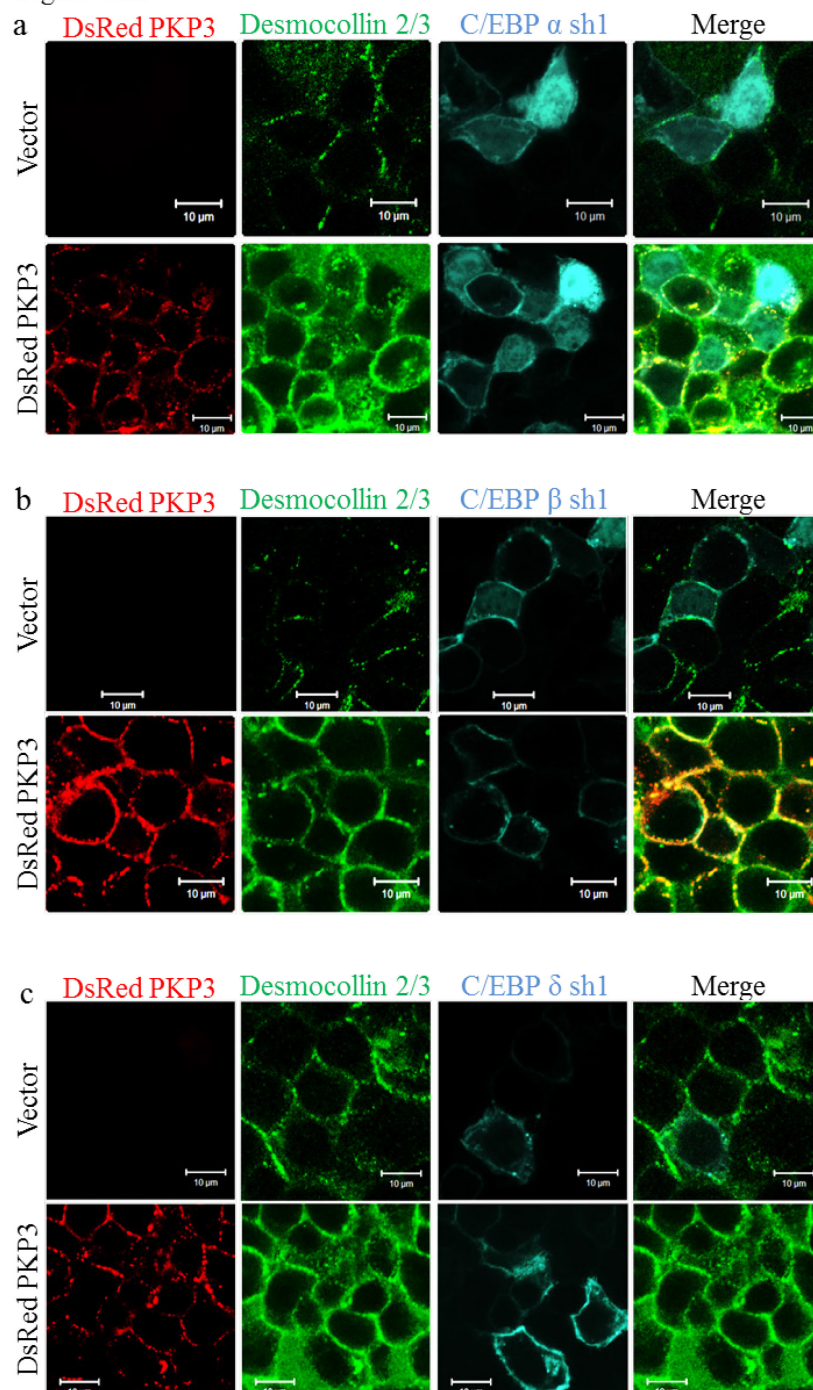
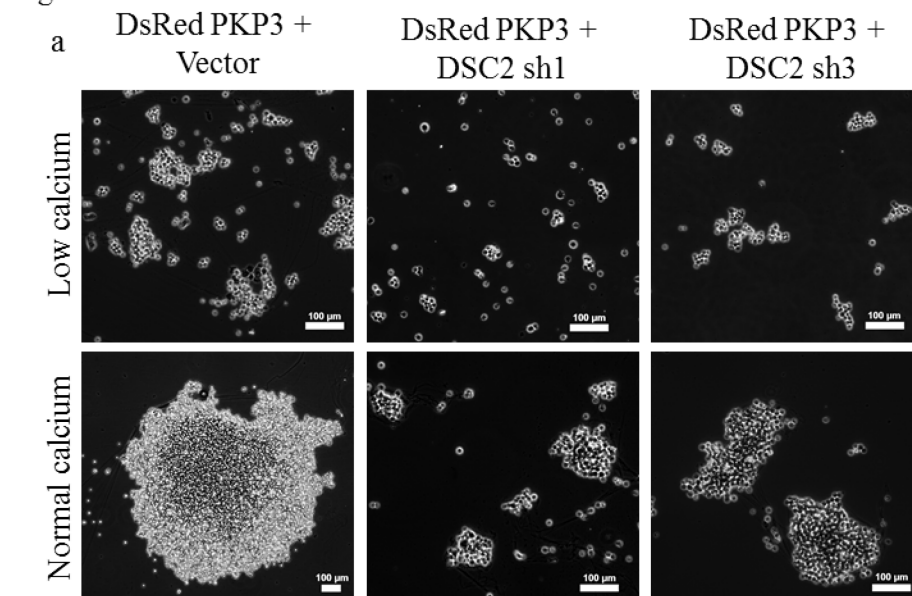


Figure 4.23. Effect of C/EBP α , β and δ knockdown on DSC2 expression up on DsRed PKP3 overexpression – DsRed PKP3 cells and the vector control cells were cultured as a monolayer and, a,b,c. EGFP-f expressing shRNA plasmids for the indicated C/EBP isoforms were transfected and the cells were stained with antibody for DSC2, representative images are shown. Scale bars are included in all

Figure 4.24



b

Cell clones	Number of aggregates (low calcium)			
	$>10^5 \text{ } \mu\text{m}^2$	$2 \times 10^4 \text{ } \mu\text{m}^2 - 10^5 \text{ } \mu\text{m}^2$	$1 \times 10^4 \text{ } \mu\text{m}^2 - 2 \times 10^4 \text{ } \mu\text{m}^2$	$3.5 \times 10^3 \text{ } \mu\text{m}^2 - 10^4 \text{ } \mu\text{m}^2$
DsRed PKP3 + Vector	0	21	25	70
DsRed PKP3 + DSC2 sh1	0	0	0	21
DsRed PKP3 + DSC2 sh3	0	0	1	14

c

Cell clones	Number of aggregates (normal calcium)			
	$>10^5 \text{ } \mu\text{m}^2$	$2 \times 10^4 \text{ } \mu\text{m}^2 - 10^5 \text{ } \mu\text{m}^2$	$1 \times 10^4 \text{ } \mu\text{m}^2 - 2 \times 10^4 \text{ } \mu\text{m}^2$	$3.5 \times 10^3 \text{ } \mu\text{m}^2 - 10^4 \text{ } \mu\text{m}^2$
DsRed PKP3 + Vector	18	12	6	6
DsRed PKP3 + DSC2 sh1	0	15	34	56
DsRed PKP3 + DSC2 sh3	1	34	15	12

Figure 4.24. Increase in cell-cell adhesion on PKP3 overexpression is dependent on increase in DSC2 transcription – *DsRed PKP3* overexpressing vector control cells and *DsRed PKP3* cells with *DSC2* knockdown were cultured as a monolayer and, a-c. Cells were either cultured in low calcium medium or normal calcium medium and hanging drop assays were performed as described in materials and methods. a.

Representative images of cell aggregates imaged using 10x or 5x objective on Zeiss Axiovert microscope are shown. b. Table showing the number and size of aggregates measured using ImageJ software from five random fields for each triplicate and from three independent experiments for cells cultured in low calcium medium and, c. for cells cultured in normal calcium medium. Scale bars are included in all images.

4.1.8. Increased DSC2 expression in DsRed PKP3 over expressing cells is not necessary and sufficient for all the phenotypes observed on PKP3 overexpression

Since DSC2 is a desmosomal cadherin, we hypothesized that the increase in DSC2 transcription on PKP3 overexpression could lead to more desmosome formation which could in turn stabilize other desmosomal proteins at the cell membrane in desmosome associated complexes and hence lead to an increase in the protein levels of other desmosomal proteins. Hanging drop assays showed that the increase in cell-cell adhesion in PKP3 overexpression was dependent on DSC2 (Figure 4.24). Immunofluorescence staining assays showed that the localization of DP and DSG2 was also dependent on DSC2 (Figure 4.25 and Figure 4.26). However, Western blots showed that the protein levels of other desmosomal proteins in DsRed PKP3 cells did not change on DSC2 knockdown (Figure 4.27). Thus, not all phenotypes observed on PKP3 overexpression are dependent on increase in DSC2 transcription.

Figure 4.25

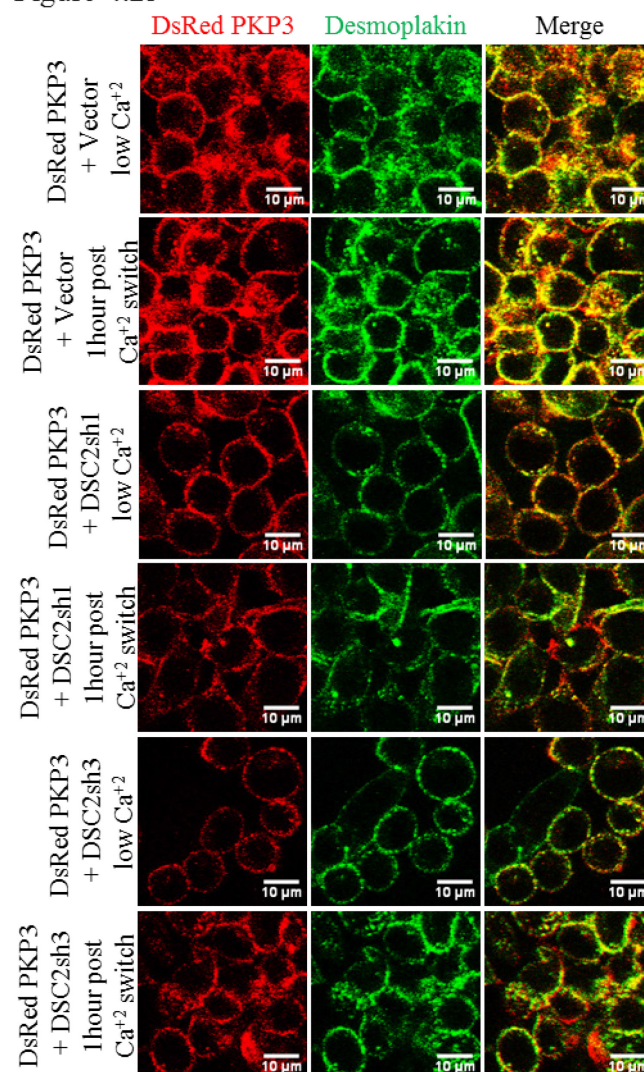


Figure 4.25. Increase in cell border localization of desmoplakin on PKP3 overexpression is dependent on increase in DSC2 transcription – *DsRed PKP3* overexpressing vector control cells and *DsRed PKP3* cells with *DSC2* knockdown were cultured as a monolayer and cells were cultured in low calcium medium for 20 hours. Calcium was replenished in the medium and images taken after one hour. Cells were fixed and stained for desmoplakin and images were captured on a confocal microscope with 63x oil immersion objective. Representative images for each condition are shown. Scale bars are included in all images.

Figure 4.26

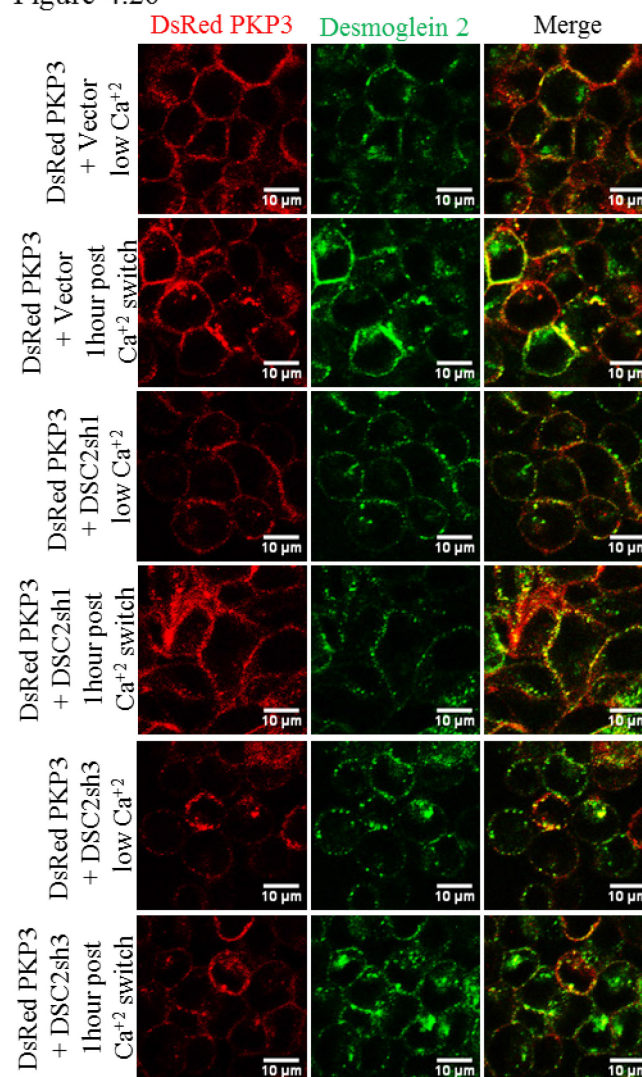


Figure 4.26. Increase in cell border localization of desmoglein 2 on PKP3 overexpression is dependent on increase in DSC2 transcription – *DsRed PKP3* overexpressing vector control cells and *DsRed PKP3* cells with *DSC2* knockdown were cultured as a monolayer and cells were cultured in low calcium medium for 20 hours. Calcium was replenished in the medium and images taken after one hour. Cells were fixed and stained for desmoglein 2 and images were captured on a confocal microscope with 63x oil immersion objective. Representative images for each condition are shown. Scale bars are included in all images.

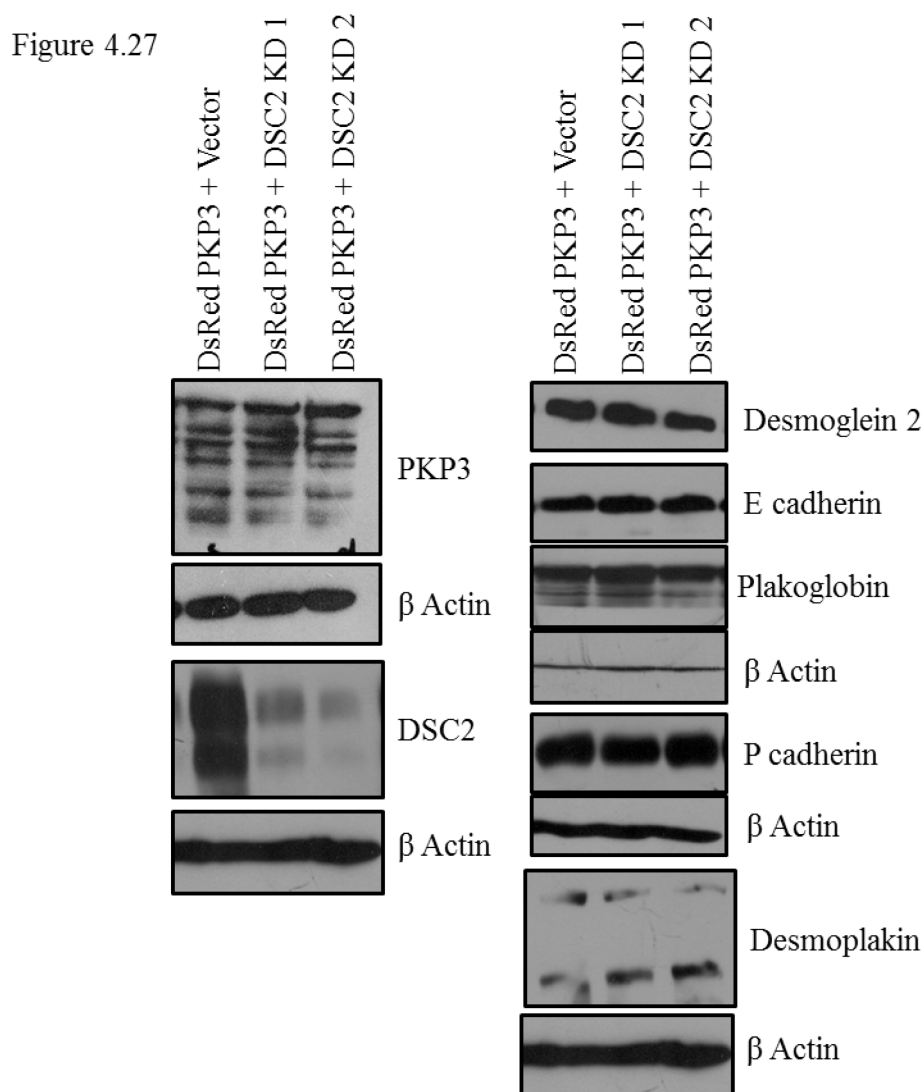


Figure 4.27. Increase in expression of other desmosomal proteins on PKP3 overexpression is NOT dependent on increase in DSC2 transcription – *DsRed PKP3* overexpressing vector control cells and *DsRed PKP3* cells with *DSC2* knockdown, were cultured as a monolayer and protein lysates were separated on an SDS-PAGE gel and immunoblotted as shown with the indicated antibodies with β actin as a loading control.

4.1.9. How does DsRed PKP3 overexpression lead to an increase in the protein levels of other desmosomal proteins

The increase in the protein levels of other desmosomal proteins on PKP3 overexpression was independent of the increase in DSC2 transcription. Cycloheximide treatment to block protein translation followed by Western blots at various time points were carried out to determine any changes in protein stability of other desmosomal proteins on PKP3 overexpression. Desmosomal proteins were found to be very stable and their half-life was beyond the detection limit of these assays (Figure 4.28). Since the cycloheximide assays proved to be inconclusive, we used proteasomal inhibitor MG132 and lysosomal inhibitor NH₄Cl to determine any change in protein stability of other desmosomal proteins on PKP3 overexpression. These assays were also inconclusive due to the long half-life of desmosomal proteins (Figure 4.29). The change in stability of desmosomal proteins is often determined by the ratio of Triton insoluble to soluble pool of the desmosomal proteins (reviewed in [43]). Desmosomes are not formed on loss of 14-3-3 γ , but the desmosomal proteins are still found almost entirely in the Triton-X insoluble fraction [175]. Also, a recent report shows that PKP1 overexpression in keratinocytes leads to formation of calcium independent desmosomes and Triton-X soluble pools of DP and DSG3 decrease while Triton-X insoluble pools of DP and DSG3 increase [262]. Triton-X fractionation assays followed by Western blot showed that there was an increase in the insoluble fraction of DSG2 and PG on PKP3 overexpression as well as a decrease in soluble fraction of DSG2 on PKP3 overexpression (Figure 4.30). Thus PKP3 overexpression preferentially partitions PG and DSG2 in the Triton-X insoluble fraction which accompanied by the increased cell membrane localization could lead to increased protein stability and thus increased total protein levels. This could also

be true of other desmosomal proteins that increase at protein level on PKP3 overexpression.

Figure 4.28

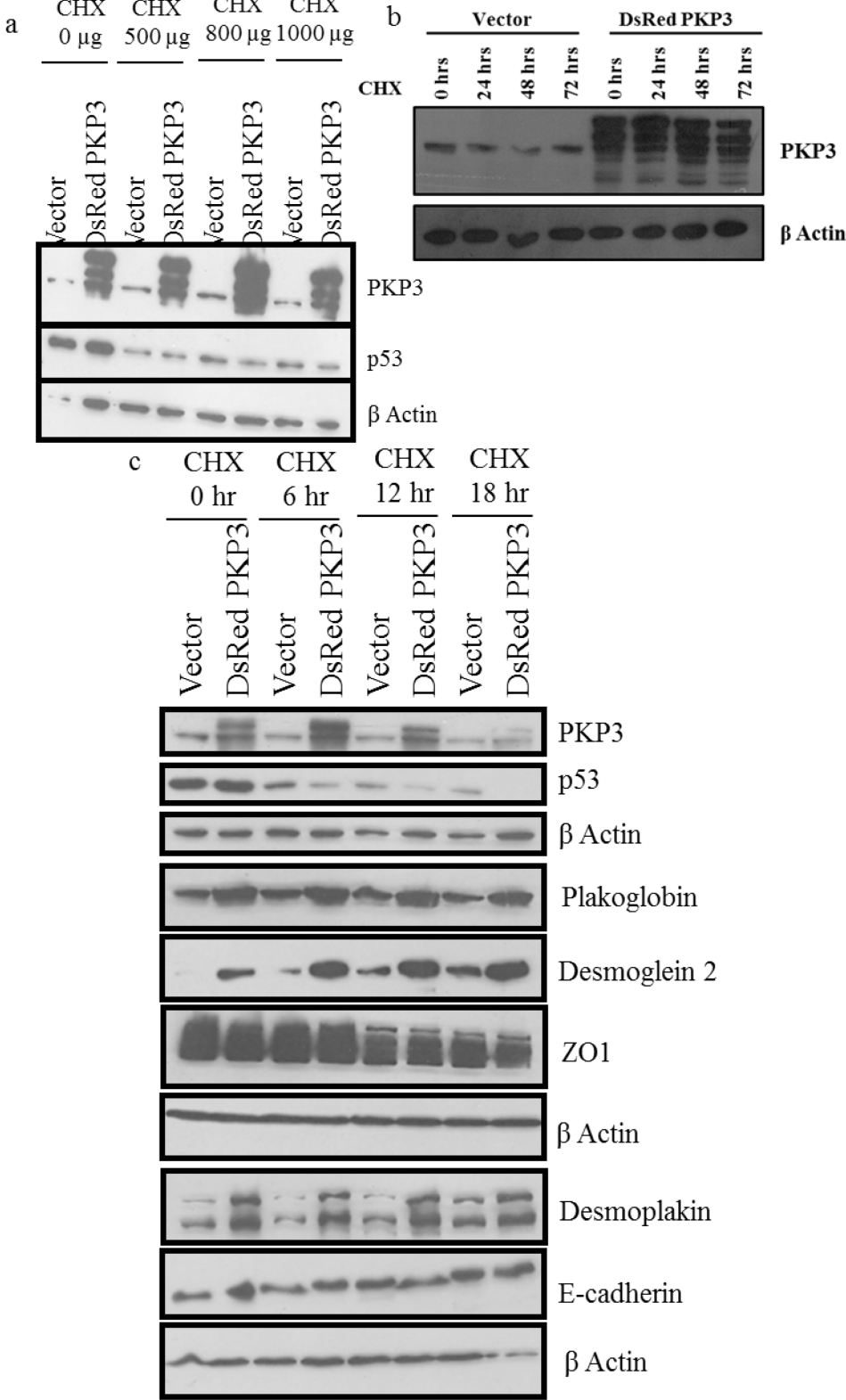


Figure 4.29. Desmosomal protein stability is beyond the detection limit of cycloheximide chase assays – *DsRed PKP3* cells and the vector control cells were cultured as a monolayer and, a,b,c. Cells were treated with cycloheximide (CHX) for a. 8 hours and, b,c. indicated time points. Protein lysates were separated on an SDS-PAGE gel and immunoblotted as shown with the indicated antibodies using β actin as a loading control.

Figure 4.29

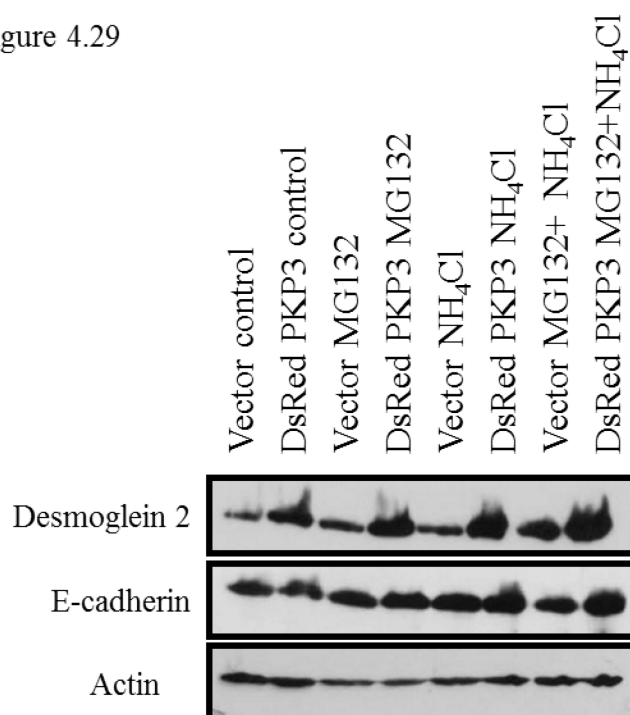


Figure 4.28. Desmosomal protein stability is not affected by proteasomal and lysosomal inhibitors – *DsRed PKP3* cells and the vector control cells were cultured as a monolayer and cells were treated with MG132 or NH₄Cl or both for 6 hours. Protein lysates were separated on an SDS-PAGE gel and immunoblotted as shown with the indicated antibodies using β actin as a loading control.

Figure 4.30

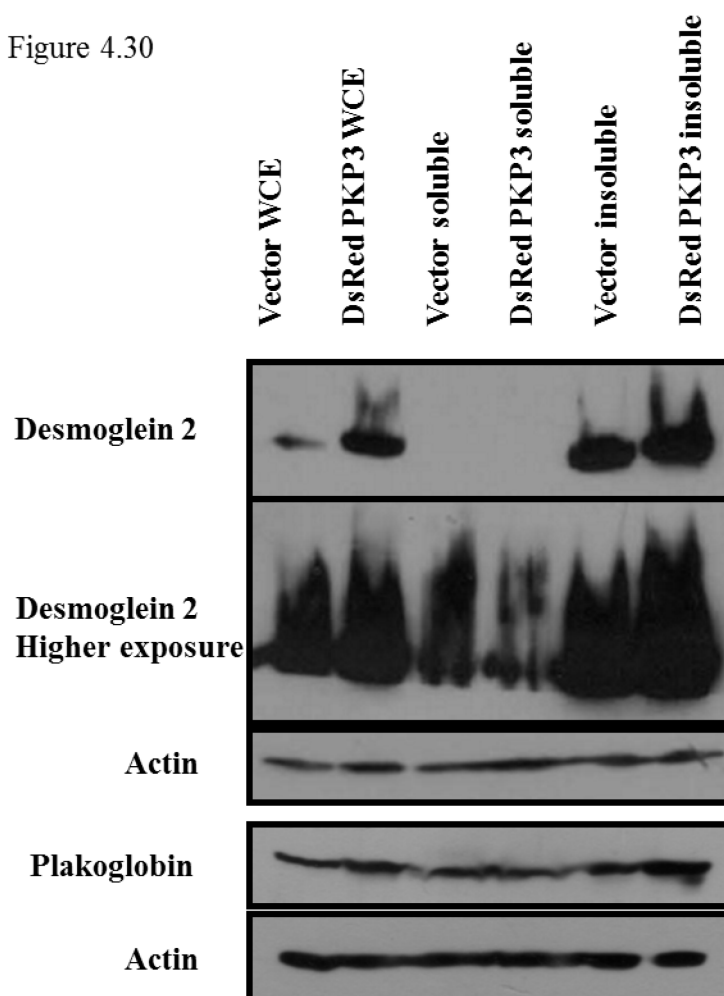


Figure 4.30. PKP3 overexpression leads to a decrease in the Triton soluble fraction and an increase in the Triton insoluble fraction of other desmosomal proteins – *DsRed PKP3 cells and the vector control cells were cultured as a monolayer and Triton soluble and insoluble fractionation was performed. Protein lysates were separated on an SDS-PAGE gel and immunoblotted as shown with the indicated antibodies using β actin as a loading control.*

4.2. Identification of changes in actin filament dynamics and modifications induced by PKP3 loss and their relevance to cell adhesion, migration and metastasis.

4.2.1. Does PKP3 knockdown have an effect on actin filament formation?

Results from our laboratory show that PKP3 knockdown leads to an increase in cell migration [108]. Cell migration is dependent on changes in cell morphology brought about by reorganization of the actin cytoskeleton (reviewed in [16, 241, 243, 265]). FITC-tagged phalloidin staining of the migrating cells at the leading edge of a wounded monolayer in HCT116 based PKP3 knockdown cells was performed to determine if there was a change in F- actin content of the cells on PKP3 loss. An increase in filamentous actin upon PKP3 loss was observed although Western blots show that the total actin levels in these cells are unaffected (Figure 4.31). Similarly, FRAP experiments performed on the actin filaments of migrating cells also show that PKP3 knockdown slows the turnover of actin in the filamentous form in dorsal stress fibres of migrating cells at the wound edge as well as ventral stress fibres of stationary cells in a monolayer (Figure 4.32 and Figure 4.33). This suggests that although actin filament formation is increased due to PKP3 knockdown, due to the shift in the dynamic equilibrium of actin from monomeric form to filamentous form, the rate of reaction to the filamentous form is reduced. These results also suggest that PKP3 knockdown has a stabilizing effect on filamentous actin possibly by affecting dissociation of filamentous actin.

Figure 4.31

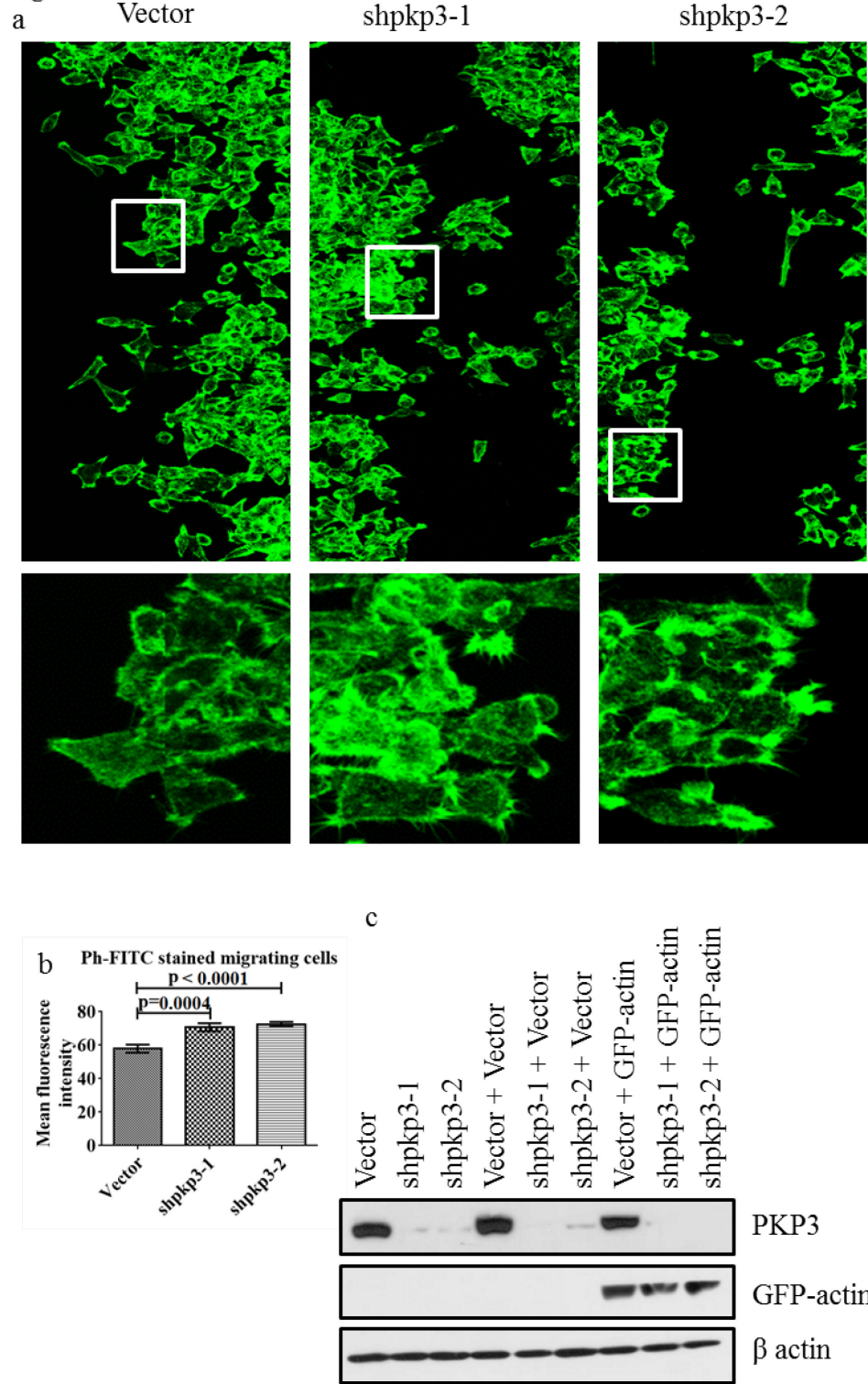


Figure 4.31. PKP3 knockdown shifts the equilibrium between G-actin and F-actin to F-actin – *a-b*, PKP3 knockdown and vector control cells were cultured as a monolayer and, *a,b*. A wound was made in the monolayer and after 20 hours, *a-b*. Cells were fixed and stained with FITC-tagged phalloidin for F-actin and images were captured on a confocal microscope with 63x oil immersion objective. *a*. Representative stitched images along the wound for each condition along with insets are shown. *b*. Mean fluorescence intensity of > 90 migrating cells along the wound were quantitated from 3 independent experiments. Mean fluorescence intensity was compared using Student's *t*-test and graph showing mean and standard error was plotted using GraphPad Prism. *c*. PKP3 knockdown and vector control cells stably transfected with EGFP-actin or vector plasmid, were cultured as a monolayer and protein lysates were separated on an SDS-PAGE gel and immunoblotted as shown with the indicated antibodies using β actin as a loading control. Scale bars are included in all images.

4.2.2. PKP3 knockdown increases Myosin IIA protein levels

The change in the actin dynamics on PKP3 knockdown could be due to a change in one of the many actin reorganization regulating proteins. Western blots performed to determine changes in actin reorganization regulating proteins show that PKP3 knockdown decreases the levels of myosin IIA but does not change the expression of Rac 1/2/3, cdc42, RhoA, filamin A, FAK, phospho-FAK, β 1-integrin, α 5- integrin, afadin 6, N-WASP, profilin, cofilin, phospho-cofilin S3, ERM, phospho-ERM, Mypt1, phospho-Mypt1 S507, Diap1, gelsolin, PAK1, myosin IIB and myosin IIC (Figure 4.34 a and [7]).

Figure 4.32

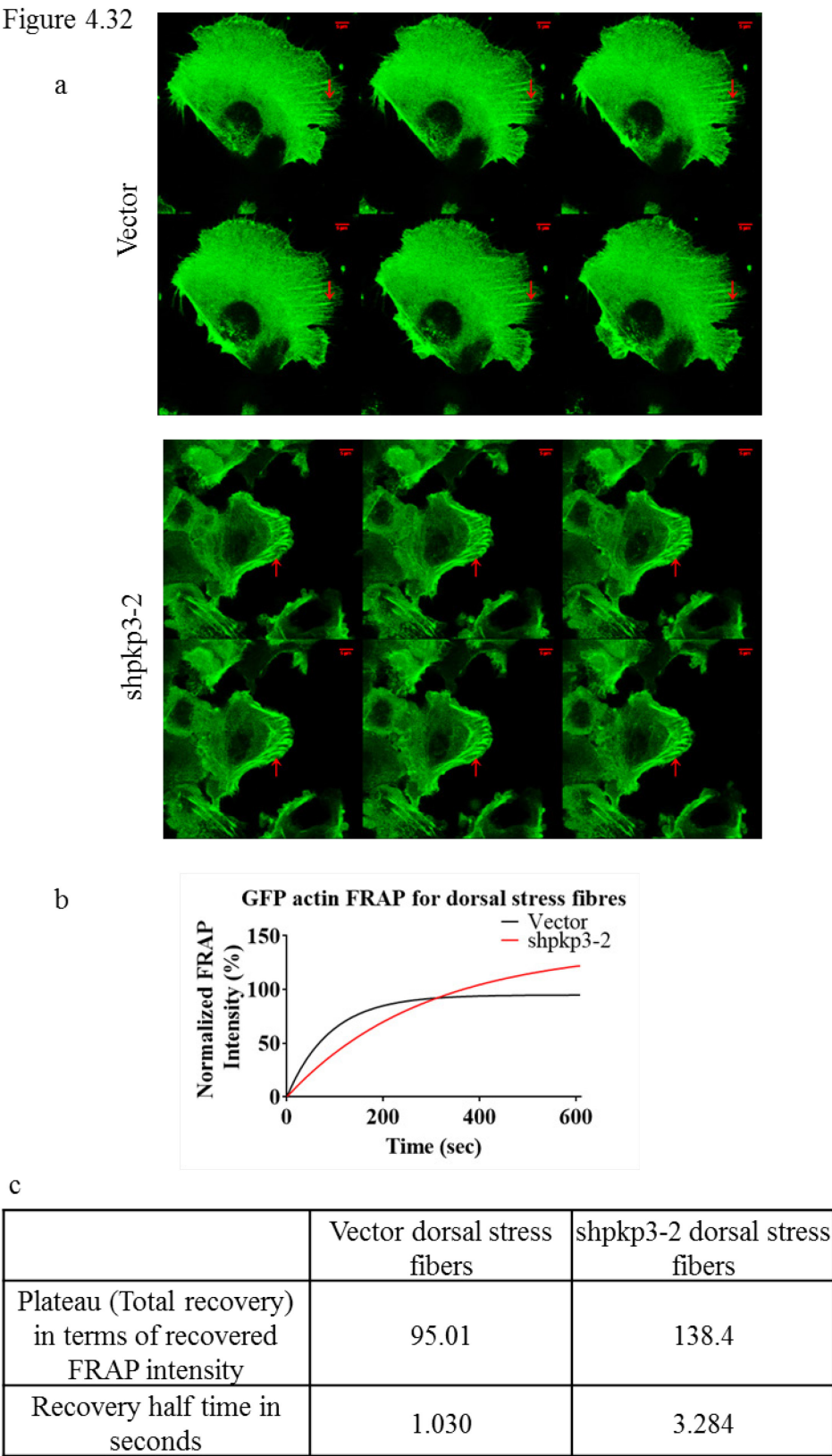


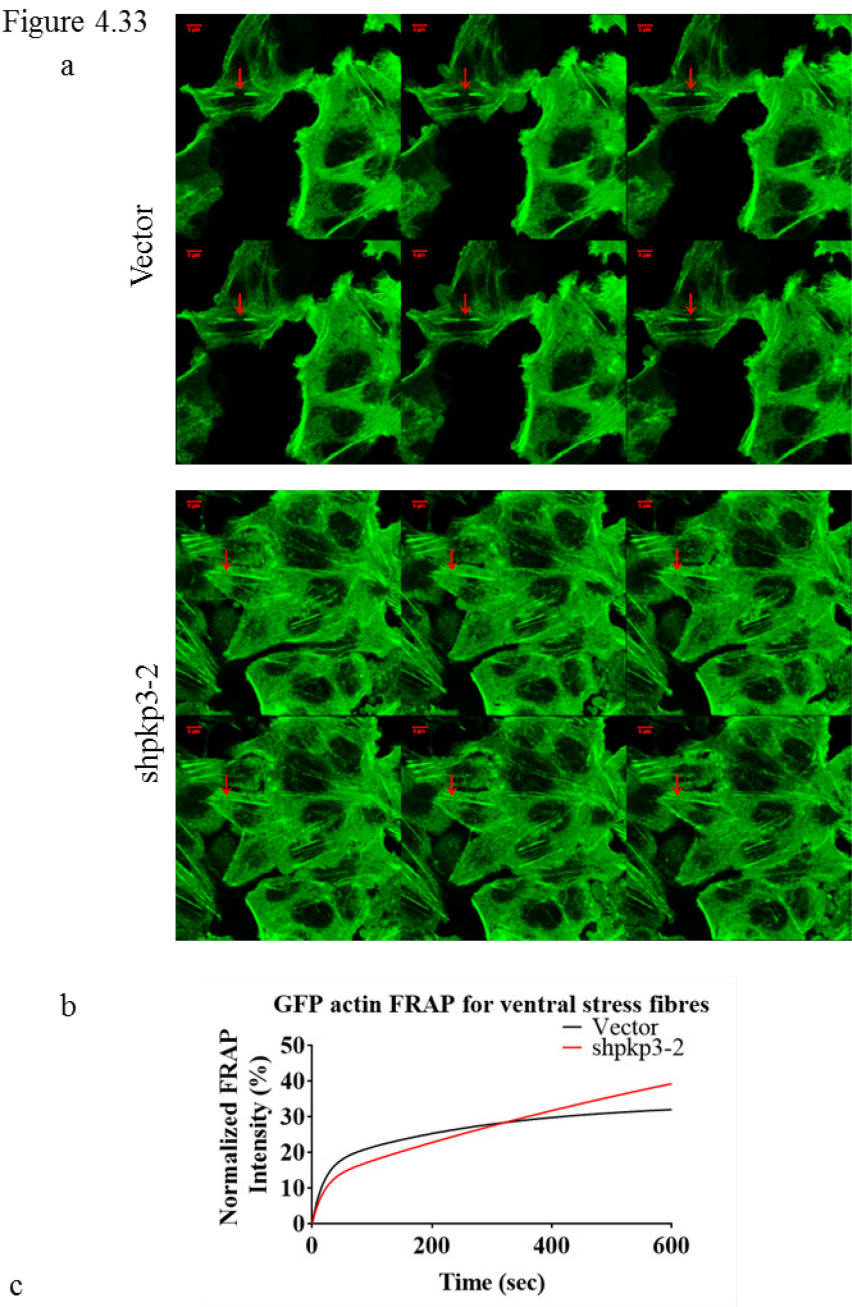
Figure 4.32. PKP3 knockdown slows F-actin turnover in dorsal stress fibres – *PKP3 knockdown and vector control cells stably transfected with EGFP-actin or vector plasmid, were cultured as a monolayer and FRAP was performed using 63x oil immersion lens and 488-Argon laser bleaching on a confocal microscope on dorsal stress fibres of migrating cells along the wound edge. a. Representative time lapse images are shown. b. FRAP curves were plotted using GraphPad Prism software using non-linear regression curve fitting. c. Constants derived from the non-linear regression curve fitting analysis are shown in the table. Scale bars are included in all images.*

Myosin IIA is a motor protein associated with actin filaments in non-muscle cells that has functions in regulating rear edge cell contractility during cell migration. Previous reports suggest that myosin IIA is a tumour suppressor [266] and that myosin IIA knockdown can increase cell motility [267, 268]. PKP3 loss decreases myosin IIA protein but has no effect on myosin IIA mRNA (Figure 4.34 c). Thus PKP3 loss could increase cell migration by reducing myosin IIA protein levels.

4.2.3. PKP3 knockdown does not have an effect on the activity of small Rho GTPases

Rho GTPases like RhoA, Rac1 and cdc42 are the master regulators of actin polymerization (reviewed in [10]). Although PKP3 loss does not change the levels of these Rho GTPases, we hypothesized that PKP3 loss could bring about changes in actin polymerization by making Rho GTPases more active. Active Rho GTPase assays using GST-RBD (Rhotekin's RhoA binding domain) or GST-PAK CRIB (PAK1 kinase's cdc42 and Rac binding domain) to specifically pull down the GTP-

Figure 4.33



	Vector ventral stress fibers	shpkp3-2 ventral stress fibers
Plateau (Total recovery) in terms of recovered FRAP intensity	33.84	88.19
Fast recovery half time in seconds	11.86	14.48
Slow recovery half time in seconds	185.5	953.2

Figure 4.33. PKP3 knockdown slows F-actin turnover in ventral stress fibres – PKP3 knockdown and vector control cells stably transfected with EGFP-actin or vector plasmid, were cultured as a monolayer and FRAP was performed using 63x oil immersion lens and 488-Argon laser bleaching on a confocal microscope on ventral stress fibres of stationary cells in the monolayer. *a.* Representative time lapse images are shown. *b.* FRAP curves were plotted using GraphPad Prism software using non-linear regression curve fitting. *c.* Constants derived from the non-linear regression curve fitting analysis are shown in the table. Scale bars are included in all images.

bound active form of the Rho GTPases showed that PKP3 loss does not change active RhoA, Rac 1/2/3 or cdc42 levels (Figure 4.35). PKP2, a closely related isoform of PKP3, has been shown to affect RhoA activity and contribute to cortical actin remodelling during de novo desmosome formation [84]. Surprisingly, we found both PKP3 loss as well as PKP3 overexpression to lead to increase in active RhoA levels in calcium switch assays 15 minutes after switching from low calcium medium to normal calcium medium (Figure 4.36). Thus although PKP3 loss does not affect the activity of Rho GTPases, PKP3 affects RhoA activity during de novo cell-cell adhesion junction formation.

4.2.4. PKP3 interacts with actin regulating proteins like PAK1, RhoA and filamin A

The active Rho GTPase assays lead to a serendipitous observation that PKP3 interacts with the CRIB domain of PAK1 (Figure 4.37 a,b). Immunoprecipitation experiments followed by Western blots confirmed that PKP3 interacts with PAK1 kinase (Figure 4.37 c). PAK1 kinase is an important regulator of actin dynamics and activated PAK1 can lead to increased F-actin ([269] and reviewed in [270]). It can be hypothesized

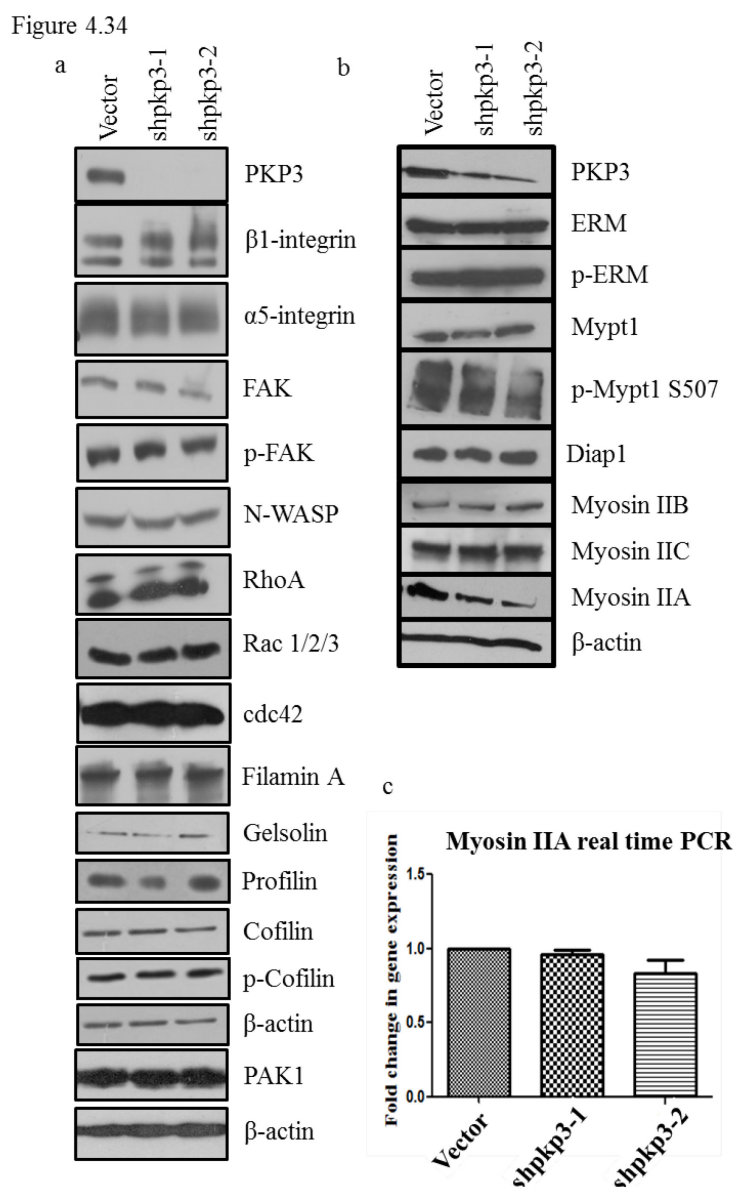


Figure 4.34. PKP3 knockdown reduces Myosin IIA protein levels, but does not affect Myosin IIA mRNA – PKP3 knockdown and vector control cells were cultured as a monolayer and a,b. Protein lysates were separated on an SDS-PAGE gel and immunoblotted as shown with the indicated antibodies using β actin as a loading control. b. Adapted from [7] and c. RNA was purified and real time PCR analysis was performed for Myosin IIA mRNA with GAPDH as a control. The values were normalized to 1 for the vector control cell line and error bars are plotted using GraphPad Prism software. The fold change in gene expression was compared using Student's t-test.

Figure 4.35

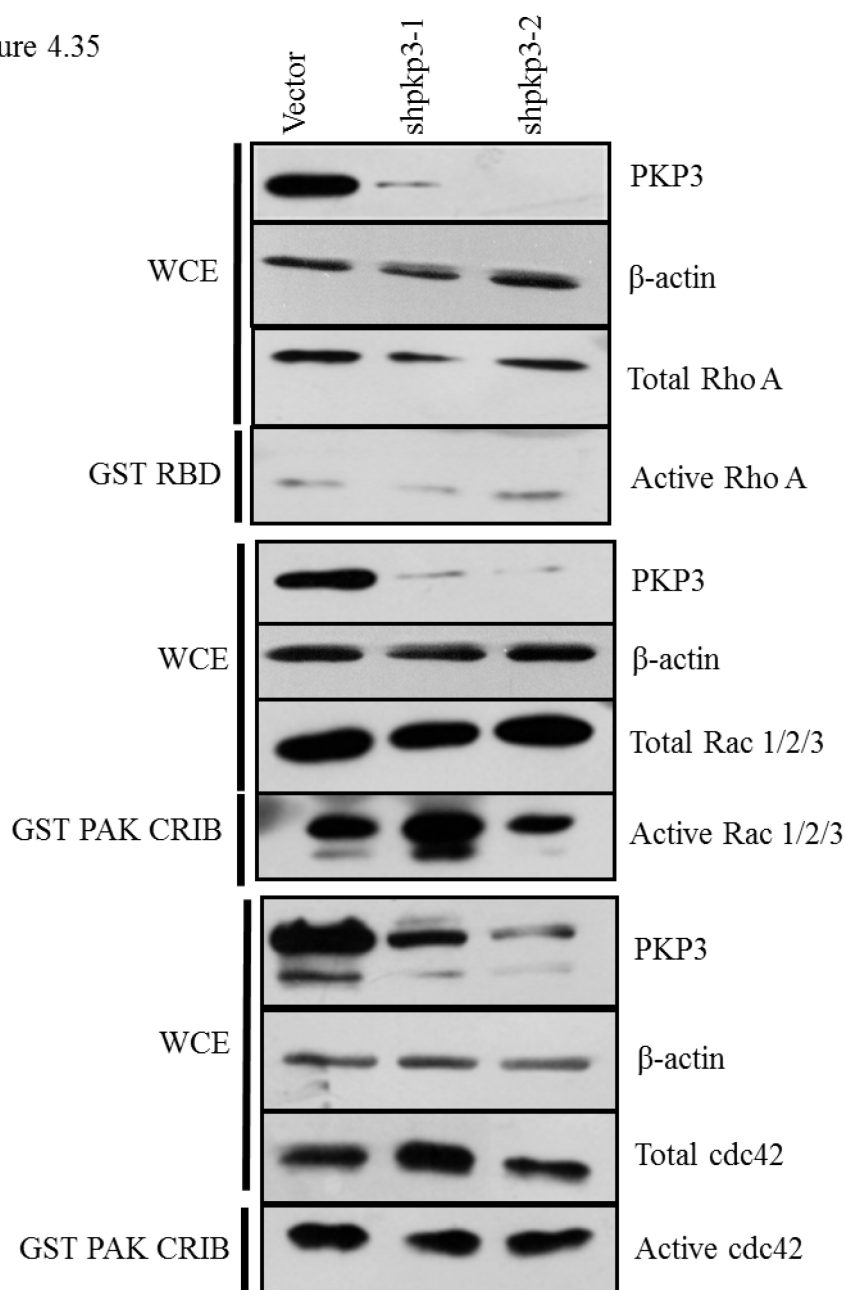


Figure 4.35. PKP3 knockdown does not have an effect on the activity of small Rho GTPases –PKP3 knockdown and vector control cells were cultured as a monolayer. RIPA extracts were incubated with the indicated GST proteins for precipitation of GST bound complexes. The GST bound complexes were resolved on a SDS-PAGE gel and Western blotted with the indicated antibodies.

Figure 4.36

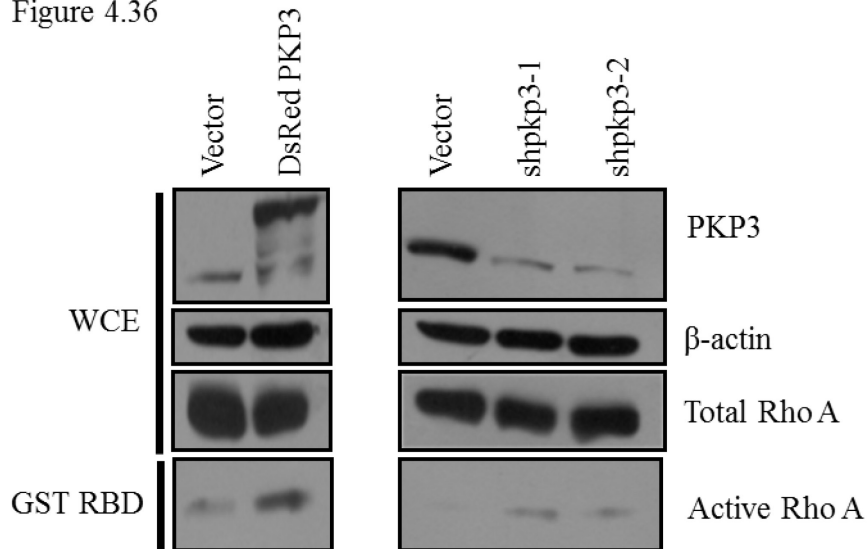


Figure 4.36. PKP3 knockdown does not have an effect on the activity of small Rho GTPases, except in the context of de novo cell-cell adhesion junction formation – *PKP3 knockdown and vector control cells or DsRed PKP3 cells and the vector control cells and were cultured in low calcium medium for 20 hours. Calcium was replenished in the medium and cells harvested after 15 minutes. RIPA extracts were incubated with the indicated GST proteins for precipitation of GST bound complexes. The GST bound complexes were resolved on a SDS-PAGE gel and Western blotted with the indicated antibodies.*

that PKP3 interaction with PAK1 at the CRIB domain of PAK1 could be inhibitory for PAK1 binding with active Rho GTPases and could in turn inhibit PAK1 function. The loss of PKP3 could hence lead to more active PAK1 and more F-actin. Further experiments would be required to test this hypothesis. GST pulldown assays and immunoprecipitation experiments followed by Western blots also showed that the N-terminal of PKP3, particularly the first 100 aa of PKP3, can bind to RhoA and filamin A (Figure 4.38). As mentioned earlier, PKP2 is known to affect RhoA activity in the context of desmosome formation [84]. Also, loss of PG, which is also an armadillo protein, has been shown to promote cell migration through RhoA activity [271]. RhoA signalling

Figure 4.37

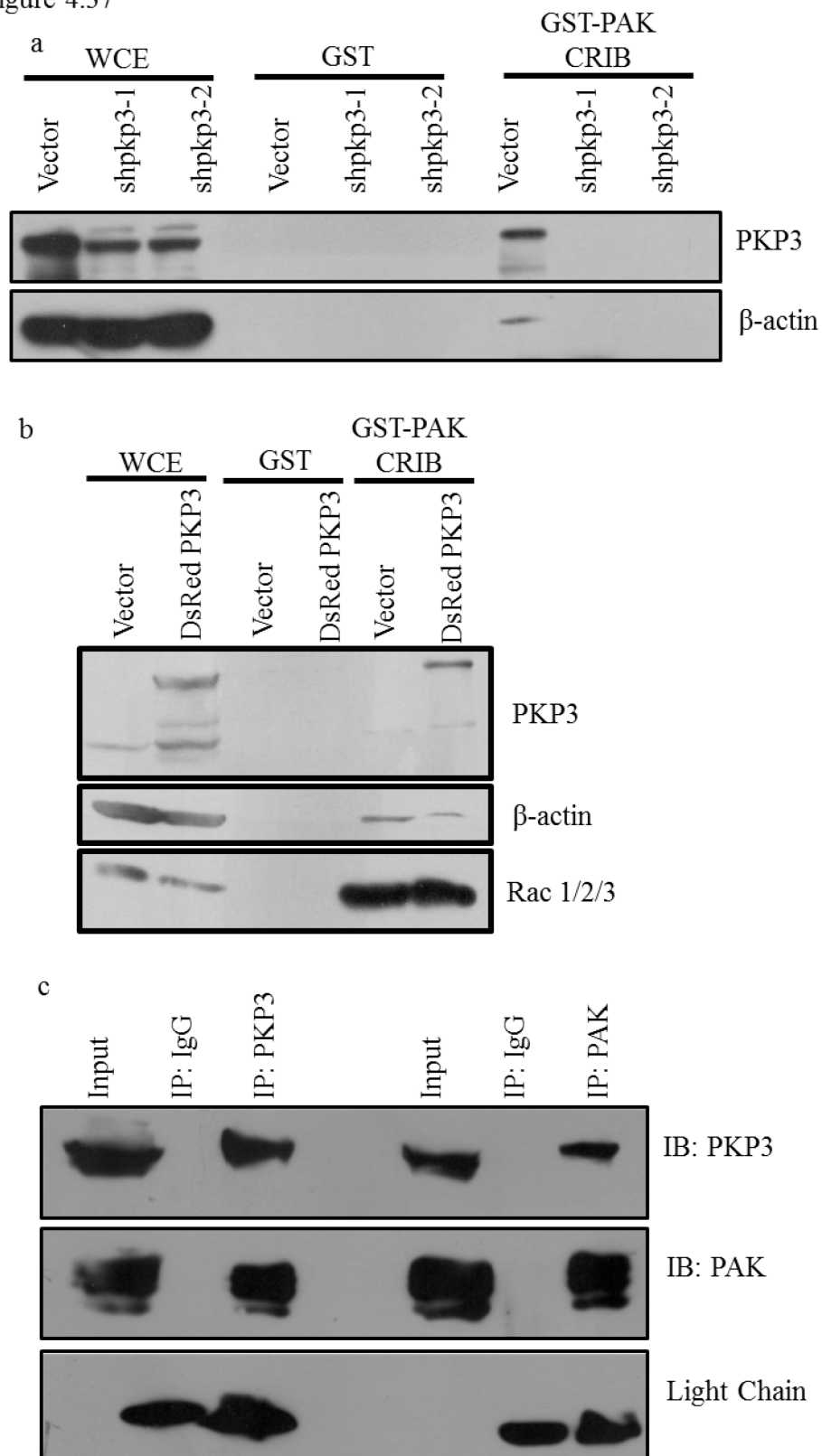


Figure 4.37. PKP3 interacts with the actin regulating protein like PAK1 – a,b.

PKP3 knockdown and vector control cells or DsRed PKP3 cells and the vector control cells were as a monolayer, RIPA extracts were incubated with the indicated GST proteins for precipitation of GST bound complexes. The GST bound complexes were resolved on a SDS-PAGE gel and Western blotted with the indicated antibodies. c. EBC extracts of HCT116 wild type cells were incubated with the indicated antibodies for immunoprecipitation. The immune complexes were resolved on a SDS-PAGE gel and Western blotted with the indicated antibodies.

is also required for differentiation of keratinocytes and expression of DSG-1 [72]. PKP3 affects RhoA activity during de novo cell-cell adhesion junction formation (Figure 4.36). Thus, the interaction between PKP3 and RhoA could be required for cell-cell adhesion. Filamin A is an actin crosslinking protein that has been shown to interact with PAK1 at the CRIB domain of PAK1 and get phosphorylated by PAK1 [272]. It can be postulated that PKP3, PAK1 and filamin A are part of a larger complex that regulates actin dynamics. Further experiments are required to delineate the role of these novel interactions between PKP3 and the actin regulating proteins PAK1, RhoA and filamin A.

Figure 4.38

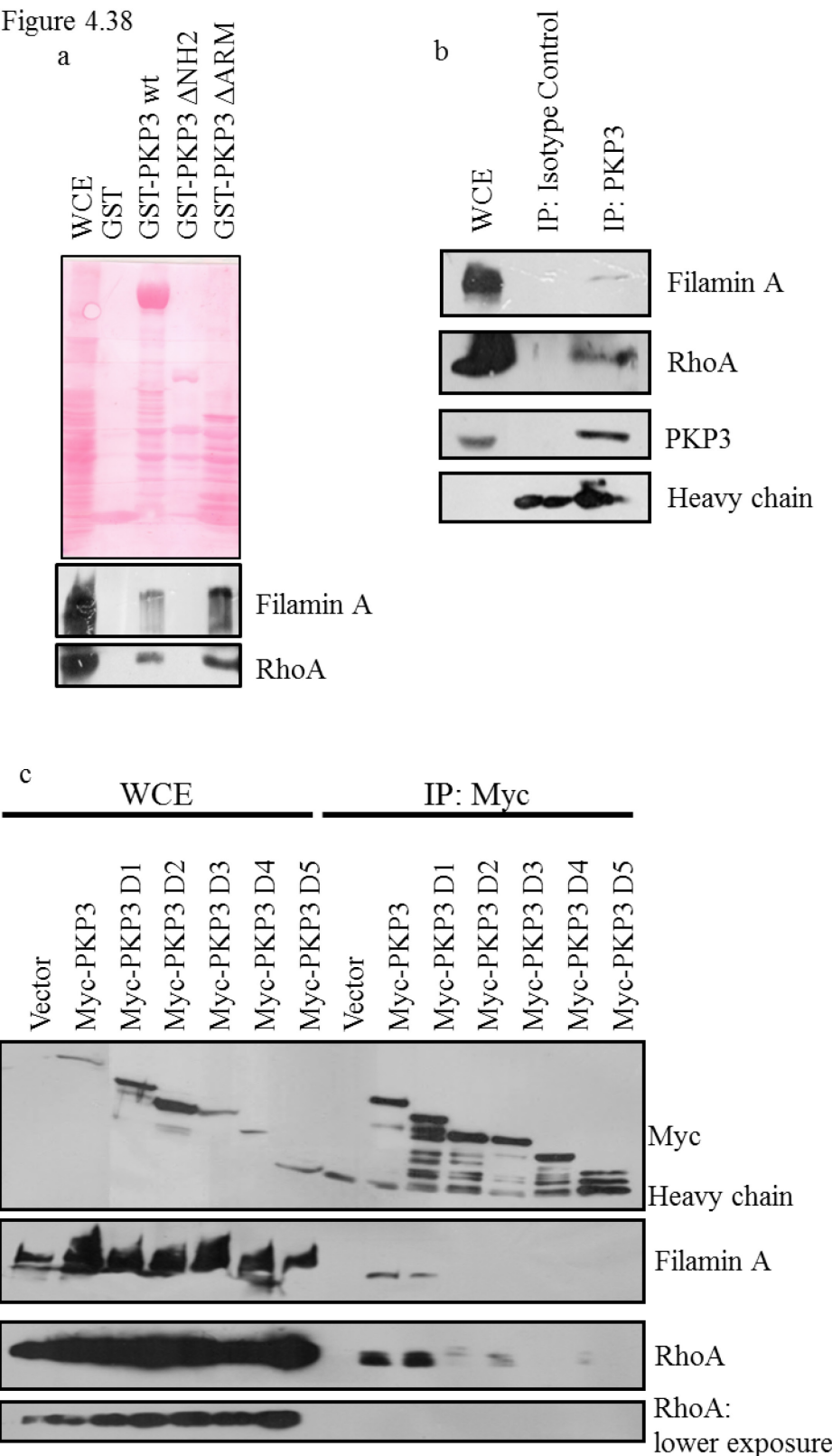


Figure 4.38. PKP3 interacts with actin regulating proteins like RhoA and filamin

A – a. EBC extracts of HCT116 wild type cells were incubated with the indicated GST proteins for precipitation of GST bound complexes. The GST bound complexes were resolved on a SDS-PAGE gel and Western blotted with the indicated antibodies. b. EBC extracts of HCT116 wild type cells were incubated with the indicated antibodies for immunoprecipitation. The immune complexes were resolved on a SDS-PAGE gel and Western blotted with the indicated antibodies. c. EBC extracts of HEK293 cells transfected with the indicated plasmids were incubated with the Myc antibody for immunoprecipitation. The immune complexes were resolved on a SDS-PAGE gel and Western blotted with the indicated antibodies.

4.3. Role of PKP3 in regulating cell adhesion, cell migration and EMT.

4.3.1. PKP3 loss does not lead to EMT in vitro and in vivo

Our lab has previously reported that loss of PKP3 results in increased tumour formation and metastasis in vivo [108]. EMT has been shown to play a crucial role in cancer progression and metastasis (reviewed in [273]). This leads to the hypothesis that PKP3 loss plays a role in induction of EMT. The established regulators of EMT are the transcription factors Snail, Slug, Twist 1 and Zeb 1. Snail, Slug, Twist 1 and Zeb 1 are all known to directly or indirectly repress E-cadherin expression and induce vimentin expression while Slug and Zeb1 are also known to promote dissolution of desmosomes (reviewed in [25]). Snail was the only EMT regulating transcription factor expressed in the HCT116 based PKP3 knockdown cells and it did not show any change on PKP3 loss as determined by quantitative real time PCR assays Figure 4.39 a,b). Our laboratory has

also demonstrated that vimentin is not expressed in the HCT116 based vector control or the PKP3 knockdown cells [274]. We have also observed that PKP3 loss does not change E-cadherin localization to the cell membrane [169]. Thus PKP3 knockdown does not lead to change in any of the tested molecular markers of EMT in vitro. An increase in cell migration accompanied by a decrease in cell-ECM adhesion is an important functional change observed in EMT. PKP3 knockdown leads to an increase in cell migration [108], hence we investigated whether PKP3 loss also leads to a decrease in cell-ECM adhesion. Cell-ECM substrate adhesion assays showed that PKP3 loss does not result in a decrease in cell-ECM substrate adhesion that is characteristic of the EMT phenotype (Figure 4.39 c). Although PKP3 knockdown did not show expression of EMT markers in vitro, the increase in primary tumour growth and lung metastasis observed in immunocompromised mice lead to the question whether these cells undergo EMT when they grow as tumours in immunocompromised mice. Immunohistochemical analysis of the tumour as well as the lung metastasis, in both the vector control as well as the PKP3 knockdown samples of tumours grown in immunocompromised mice show that expression of mesenchymal markers like vimentin and MMP9 is present but it is not enhanced by PKP3 loss (Figure 4.40). Thus PKP3 knockdown does not induce or enhance EMT in vivo.

Figure 4.39

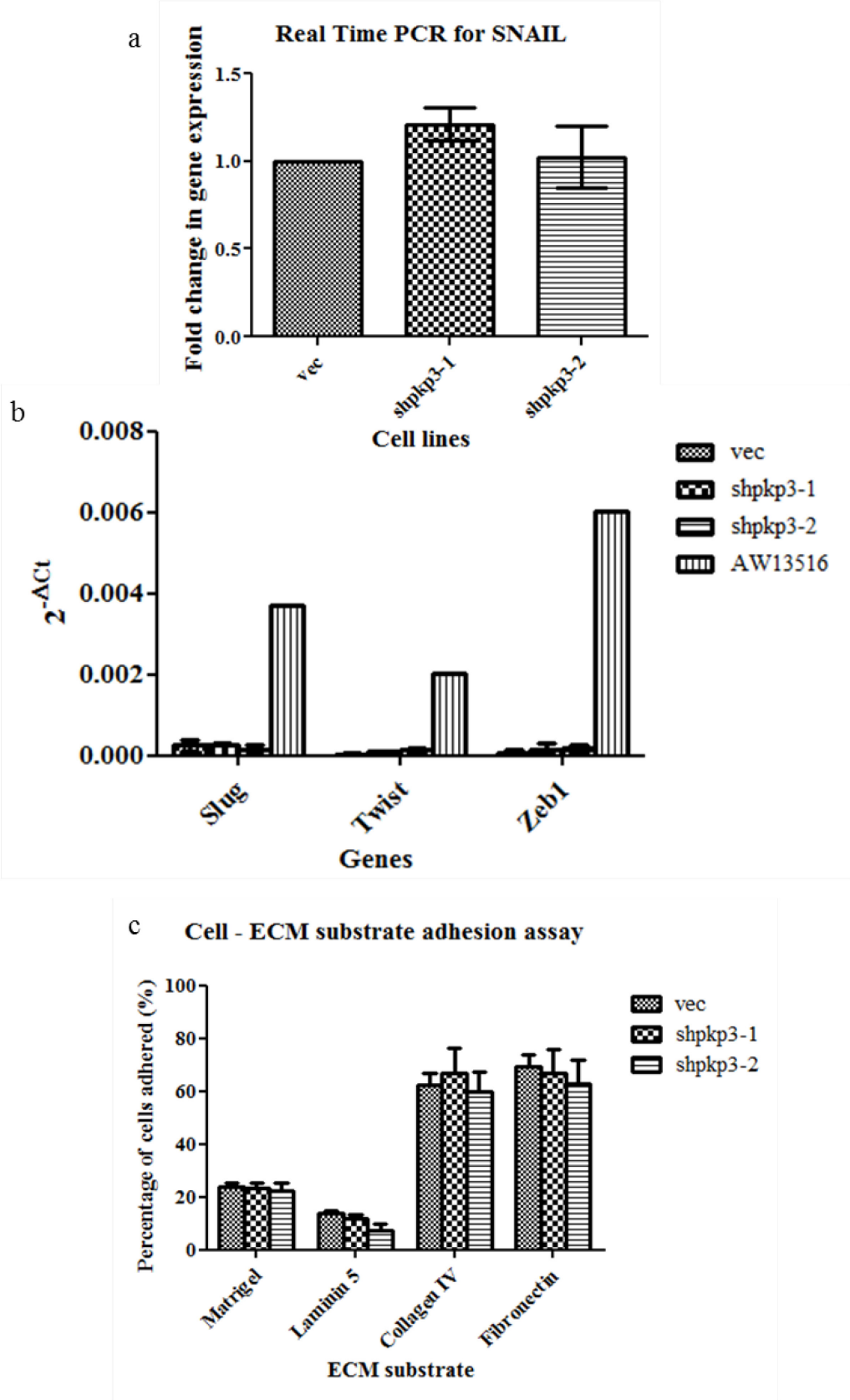


Figure 4.39. Plakophilin 3 knockdown does not lead to EMT in vitro– *a. RNA was isolated from PKP3 knockdown and vector control cells and quantitative real time PCR was performed to detect the levels of Snail using GAPDH as a control. The values were normalized to 1 for the vector control cell line and error bars are plotted using GraphPad Prism software. The fold change in gene expression was compared using Student's t-test. b. RNA was isolated from the indicated cell types and quantitative real time PCR was performed to detect the levels of Slug, Twist and Zeb1 using GAPDH as a control. $2^{-\Delta Ct}$ values are plotted on the Y-axis using GraphPad Prism software. c. Cell – ECM substrate adhesion assays were performed with the indicated ECM substrates and the percentage of adhered cells determined and the mean and standard deviation from three independent experiments was plotted on the Y-axis using GraphPad Prism software. Statistical significance was determined using Student's t-test.*

Figure 4.40

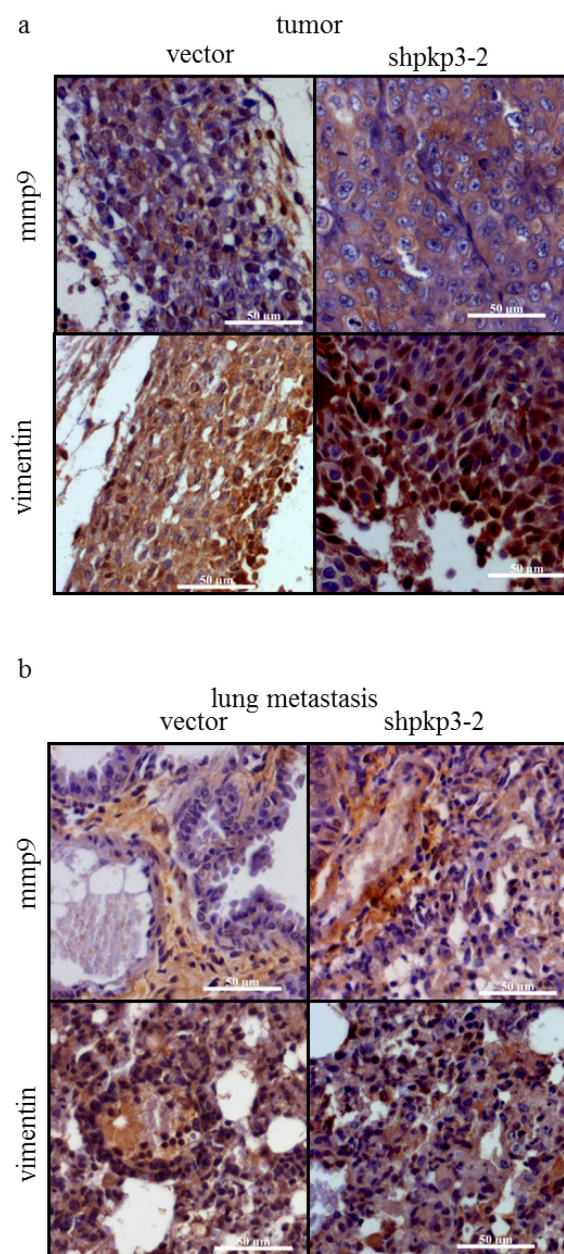


Figure 4.40. Plakophilin 3 knockdown does induce EMT in vivo – PKP3 knockdown and vector control cells were injected subcutaneously in immunocompromised mice and immunohistochemical staining was performed on paraffin embedded sections of the primary tumour and lung metastases with the indicated antibodies. Images were captured on a Zeiss Axiovert upright microscope with a 40x objective. Representative images are shown.

DISCUSSION

5. DISCUSSION

The desmosomal protein PKP3 has previously been established as an essential component of the desmosomes that might also function in the nucleus. However, the mechanisms by which PKP3 regulates desmosome formation, its ability to regulate cell migration and whether PKP3 loss leads to activation of the EMT were not examined earlier. The work presented in this thesis defines a role for PKP3 in regulating desmosomal protein expression thereby impacting desmosome formation and cell-cell adhesion. We also present evidence of PKP3 affecting myosin IIA expression and PKP3 interacting with other actin cytoskeleton regulating proteins like RhoA, filamin A and PAK1 thereby implicating PKP3 in actin cytoskeleton regulation and affecting cell migration. Finally, experiments performed to elucidate the role of PKP3 in regulating EMT show that PKP3 loss does not induce the EMT.

5.1. Role of PKP3, adherens junctions and actin cytoskeleton in initiation of desmosome formation and regulation of desmosome size and assembly.

Desmosome formation has been shown to be dependent on the presence of calcium as well as the presence of adherens junctions ([168, 169] and reviewed in [5, 43, 46, 61]). PKP3 overexpression resulted in increased desmosome size and reduced the dependency of desmosome formation on calcium (Figure 4.2 - Figure 4.12). This could indicate a role for PKP3 to be a mediator of calcium induced signalling that triggers desmosome formation. However, previous reports show that in the absence of calcium, half desmosomes are still assembled but they are incapable of being retained at the membrane and rapidly get internalised and degraded [55]. PKP3 could hence play a role

in stabilizing the half desmosomes at the cell membrane. This hypothesis is also supported by the fact that we observed other desmosomal proteins as well as the PKP3 interacting adherens junction cadherin E-cadherin to be increased at the cell membrane on PKP3 overexpression (Figure 4.8 - Figure 4.12). Further, PKP3 overexpression increased the expression of other desmosomal proteins at the protein level and this was independent of the increase in DSC2 expression at mRNA level (Figure 1.16, Figure 4.18 and Figure 4.27). PKP3 overexpression was sufficient and necessary for these phenotypes and increased de novo cell-cell adhesion as well as retention of existing cell-cell adhesion (Figure 4.5, Figure 4.14, Figure 4.15 and Figure 4.18). Another isoform of PKP3 – PKP1 was also recently reported to exhibit similar phenotypes in keratinocytes [157, 171, 262] suggesting that this might be a common mechanism by which the PKP family regulates desmosome structure and assembly.

The initial reports describing the characterization of PKP3 suggested that it might localize to nuclear foci (foci) and therefore might have functions in the nucleus similar to that of other PKP family members [199]. However, PKP3 nuclear localization has been observed with one polyclonal antibody when imaged by optical microscopy techniques [199]. Recently, a report on studies performed on the *Xenopus* PKP3 showed the association of PKP3 with ETV1 transcription factor that promoted transcription of ETV1 targets and affected neural crest formation during embryonic development [89]. The work presented in this thesis is the first report of PKP3 positively regulating transcription of a desmosomal protein – DSC2. PKP3 has been reported to be a part of RNA stress granules and known to bind to RNA binding proteins like FXR1, G3BP, and PABPC1, and it has been shown to affect mRNA stability of PKP2 and DP [90, 91]. The mRNA stability assays performed on PKP3 overexpressing cells show that such a mechanism is not responsible for the increase in DSC2 mRNA (Figure 4.19). There could

be different reasons for why the increase in transcription was not observed in the dual luciferase reporter assay for the DSC2 promoter (Figure 4.19). Increase in transcription might not always be replicated in a plasmid based assay as it will not reflect regulation by the native chromatin environment at the promoter of DSC2 and we are in the process of performing a nuclear run-on assay to reflect such changes in transcription. It is also possible that the PKP3 responsive elements in the DSC2 gene are upstream or downstream of the previously identified promoter that was tested and hence using a longer fragment of the gene for the dual luciferase reporter assay could show more conclusive results. Likewise, it is also possible that a PKP3 responsive element is within the tested promoter region but it is being masked by activity of an unknown repressor and thus shorter fragments of the promoter that have the PKP3 responsive element but exclude the repressor binding regions could show conclusive results. Hence, although it is apparent that PKP3 increases DSC2 mRNA by increasing its transcription, further experiments are required to make unequivocal conclusions.

The known transcription factors regulating the expression of DSC2 are CDX1 and CDX2 [215]. The C/EBP family transcription family members – α , β and δ have been shown to affect transcription of the DSC1 and DSC3 isoforms [213]. CDX1 and C/EBP α have been shown to form a complex and this interaction positively regulates the transcription of CDX1 target genes [216]. Microarray data from our laboratory shows a decrease in C/EBP α in PKP3 knockdown cells [228]. The results presented in this thesis identify C/EBP α as a novel interactor of PKP3 and show increased nuclear localization of C/EBP α on PKP3 overexpression (Figure 4.21). Similar changes in localization were not observed for C/EBP β or δ isoforms (Figure 4.22). All C/EBP family members have 2-3 translationally regulated isoforms (reviewed in [226]). Particularly, the truncated isoform of C/EBP α was increased in the nucleus on PKP3 overexpression (Figure 4.21).

C/EBP α is active as a homodimer or a heterodimer formed with other C/EBP family members as well as proteins from other families of transcription factors and is capable of both positive and negative regulation of its targets (reviewed in [4]). Interestingly, the truncated isoform of C/EBP α lacks a transactivation domain and acts as a dominant negative for the full-length isoform by forming a dimer with the full length isoform (reviewed in [4]). We can hence hypothesize that the increased levels of truncated C/EBP α in the nucleus observed upon PKP3 overexpression is relieving a repressor effect mediated by the full length C/EBP α and increasing DSC2 transcription. We are currently in the process of testing this hypothesis by checking the effect of over expressing the truncated C/EBP α isoform in HCT116 cells are determining its effect on DSC2 expression. C/EBP binding sites as well as binding sites for C/EBP heterodimers with other transcription factor families are found in the promoters of a larger variety of proteins part of diverse cellular pathways and these findings implicate a role for PKP3 to regulate them. Further studies would be required to determine such novel targets regulated by PKP3 via C/EBP α truncated isoform.

DSC2 was the only desmosomal protein that was increased at mRNA levels on PKP3 overexpression (Figure 4.17). Since DSC2 is a desmosomal cadherin, it we had hypothesized that it could potentially increase the anchoring of other desmosomal proteins to the cell membrane and thus result in an increase of these other desmosomal proteins at the protein level in PKP3 overexpressing cells. However, our results show that although cell-cell adhesion and localization to the cell membrane of other desmosomal proteins was reduced on DSC2 knockdown in PKP3 overexpressing cells, the protein levels of other desmosomal proteins remained unaffected from the PKP3 overexpressing vector control cells (Figure 4.24 - Figure 4.27). These results showed that increase in DSC2 expression was not required for the increase in other desmosomal proteins on

PKP3 overexpression. These results lead to the conclusion that DSC2 is essential for desmosome formation but not for the increase in stability of other desmosomal proteins on PKP3 overexpression. This also gives rise to more questions about the role played by DSC2 mRNA increase on PKP3 overexpression. If DSC2 is knocked down to wild type HCT116 levels rather than below physiological levels, in PKP3 overexpressing cells, will it still decrease desmosome formation and cell-cell adhesion? What phenotypes can be attributed purely to DSC2 mRNA increase independently of PKP3 overexpression? Further studies would be required to elucidate the role played by the increase in DSC2 mRNA in PKP3 overexpression.

PKP3 overexpression increased the protein levels of other desmosomal proteins as well as increased their cell border/ membrane localization (Figure 4.8 - Figure 4.12). Although desmosomal proteins are highly stable and their half-life is beyond the detection limit of standard biochemical assays, the Triton-X detergent solubility of these proteins is a good indicator of their stability ([51-55] and reviewed in [56]) (Figure 4.29 - Figure 4.30). Previous reports have suggested that desmosomal proteins become Triton-X insoluble shortly after they are synthesized but before they are transported to the cell surface [52, 53]. The results presented in this thesis show that PKP3 overexpression increases the Triton-X insoluble fraction of other desmosomal proteins (Figure 4.30). It can be hypothesized that this phenomenon is responsible for increasing the stability of other desmosomal proteins in PKP3 overexpressing cells. This hypothesis is supported by a recent report which shows that desmosomal components are palmitoylated and the palmitoylation of PKPs is essential for their partitioning into the Triton-X insoluble fraction as well as desmosome formation [57]. The same report also suggested that palmitoylation of PKPs is essential for incorporation of PKPs in caveolin-1 containing lipid rafts which have been shown to contain DSG2 [57, 58]. Thus PKP3 overexpression

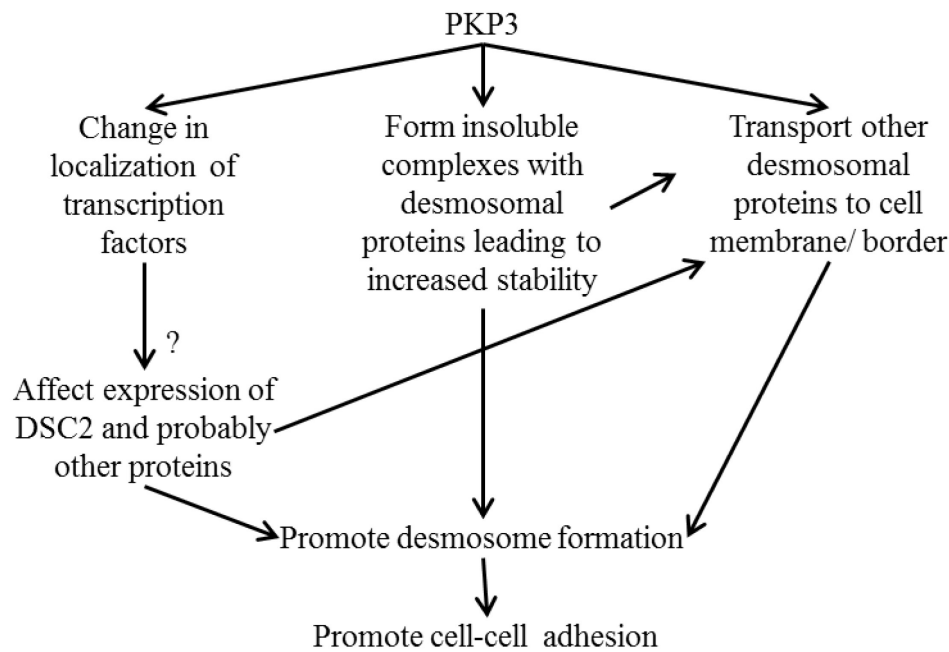


Figure 5.1. Model showing how PKP3 overexpression can lead to increase in cell-cell adhesion.

can stabilize other desmosomal proteins by making them Triton-X insoluble and thus unavailable for the protein degradation machinery of the cell as well as promote their incorporation into membrane associated lipid rafts. A recent report shows that PKP1 overexpression in keratinocytes leads to similar phenotypes of formation of calcium independent desmosomes and Triton-X-X soluble pools of DP and DSG3 decrease while Triton-X-X insoluble pools of DP and DSG3 increase [262].

In conclusion, PKP3 overexpression could promote cell-cell adhesion through multiple downstream effects. PKP3 could bring about changes in transcription by changing the localization of transcription factors like truncated C/EBP α and increase the desmosomal cadherin DSC2 which would increase the available DSC2 in the cell to form more desmosomal contacts with the neighbouring cell as well as anchor other desmosomal proteins at the cell membrane and lead to more desmosome formation (Figure 5.1). The other avenue for PKP3 to promote desmosome formation would be

through formation of insoluble complexes with desmosomal proteins that increases the stability of the desmosomal proteins as well as helps in their cell membrane localization (Figure 5.1). Finally, PKP3 itself is essential for transport of desmosomal proteins to the cell membrane and thus can promote desmosome formation (Figure 5.1). Collectively, these different mechanisms enable PKP3 to greatly enhance cell-cell adhesion.

5.2. Identification of changes in actin filament dynamics and modifications induced by PKP3 loss and their relevance to cell adhesion, migration and metastasis.

The driving force for cell migration is provided by F-actin either by the process of polymerization of F-actin that propels cell membranes forward, or by ATP-driven movement of actomyosin contractile filaments. Context specific spatio-temporally controlled F-actin polymerization is also the end effect of many cell migration promoting pathways that enable the formation of cell protrusions like filopodia and lamellipodia (reviewed in [11, 238]). The data presented in this thesis show that PKP3 knockdown shifts the equilibrium between G-actin and F-actin to F-actin (Figure 4.31). This is accompanied by slower turnover of F-actin in dorsal stress fibres of migrating cells as well as ventral stress fibres of stationary cells in the PKP3 knockdown cells as compared to the vector control cells (Figure 4.32 and Figure 4.33). It could be hypothesized that the shift in equilibrium to F-actin potentiates the PKP3 knockdown cells for cell migration through increased force generation by the increased F-actin. In agreement with our results, a report on the RhoA GTPase effector kinase ROCK shows that ROCK activity increases F-actin formation in HCT116 based xenograft tumours and promotes invasion and angiogenesis [275]. Furthermore, the decrease in F-actin turnover rate could be the underlying cause for the shift in equilibrium from G-actin to F-actin. However, it should

be noted that the plateau of the FRAP recovery curve was higher for PKP3 knockdown cells as compared to the vector control cells and more interestingly beyond 100% in the PKP3 knockdown cells for the dorsal stress fibres of the lamellipodium. FRAP recovery experiments never show even 100% recovery due to a variety of factors. This peculiar nature of the FRAP recovery curve leads to the hypothesis that there might be higher de novo actin filament formation and/ or filament bundling in the PKP3 knockdown cells as compared to the vector control cells which could provide the basis for faster cell migration in the PKP3 knockdown cells.

The actin cytoskeleton reorganization that is required for cell migration is controlled by many different proteins that can affect the actin filament assembly and disassembly cycle (reviewed in [16, 247, 249]). The results presented in this thesis show that the actomyosin filament motor protein myosin IIA is decreased on PKP3 knockdown but myosin IIA mRNA levels are not changed (Figure 4.34). Previous reports suggest that myosin IIA is a tumour suppressor [266] and that myosin IIA knockdown can increase cell motility [267, 268]. Myosin IIA loss has also been reported to increase cell spreading [276]. Myosin IIA has also been shown to contribute to E-cadherin clustering and homophilic E-cadherin adhesion in the adherens junctions [277] and restrict oscillatory motion of E-cadherin [278]. The decrease in myosin IIA could hence further contribute to the decrease in cell-cell adhesion on PKP3 knockdown and which could in turn increase cell migration. Myosin motor proteins are required for forming stronger mature focal adhesion (reviewed in [279]). Myosin IIA has also been shown to retract the lamellipodial extensions during cell spreading negating the effect of myosin IIB that enhances cell spreading [280]. The same report also shows that myosin IIA plays a role in formation of focal contacts at the lamellipodial spreading margins of the cell while myosin IIB plays a role in formation of focal contacts in the central part of the spreading cell [280]. Thus

lack of myosin IIA could lead to weaker immature focal adhesions in the lamellipodia of migrating cells upon PKP3 loss that are more amenable to faster turnover and hence lead to increased cell migration. Further experiments would be required to elucidate the implications of reduced myosin IIA on cell migration upon PKP3 loss. Another interesting avenue to investigate would be to determine the mechanism by which PKP3 loss leads to decrease in myosin IIA protein levels.

In the context of cell migration, Rho GTPases are responsible to initiate a signalling cascade that takes extracellular cues from cell surface receptors to ultimately regulate actin polymerization (reviewed in [10]). The results presented in this thesis show that PKP3 loss does not alter the activity of Rho GTPases as assessed by biochemical assays (Figure 4.35). However, these biochemical assays were performed on confluent monolayers of cells and does not rule out change in Rho GTPase activity spatio-temporally regulated at the leading edge of migrating cells. The results also show a novel interaction between RhoA and the first 100 a.a. of PKP3 (Figure 4.38). Previous reports have shown other members of the PKP family, PKP2 and PKP4 interact with RhoA and function in desmosomal cell-cell adhesion and cytokinesis respectively [84, 281]. The results presented in this thesis show that RhoA activity is increased both on PKP3 loss and PKP3 overexpression in the context of formation of de novo cell-cell adhesion junctions in a calcium switch assay (Figure 4.36). These results further indicate a possible role for PKP3 interaction with RhoA even in the context of cell migration that was probably not detected in the biochemical assays performed. Further experiments based using advanced microscopy techniques could help in drawing conclusions about the role of Rho GTPases in increasing cell migration on PKP3 loss.

Pak1 overexpression or mutational activation is reported in many cancer types and associated with increased tumorigenesis and angiogenesis (reviewed in [282]). Pak1

kinase is a downstream effector of the Rho GTPases Rac1 and cdc42 that plays a role in F-actin turnover as well as focal adhesion turnover ([269] and reviewed in [10, 248]). The CRIB domain of Pak1 is responsible for its interaction with active Rho GTPases and this interaction is required for activating Pak1 function (reviewed in [270, 283]). The results presented in this thesis show a novel interaction between PKP3 and the CRIB domain of Pak1 (Figure 4.37). It is possible that the interaction of PKP3 with Pak1 at the CRIB domain could block the interaction between Pak1 and its upstream activator Rho GTPases inhibiting Pak1 function. Loss of PKP3 could hence lead to an increase in active Pak1 and hence increased F-actin formation and increased focal adhesion turnover that ultimately results in increased cell migration. Further studies would be required to conclusively determine the role played by PKP3 and Pak1 interaction.

Filamin A is a large 280 kDa actin cross linking protein that functions as a dimer and acts as a scaffold for the interaction for over 90 known protein interactors thereby having functions many cell signalling pathways including roles in formation of F-actin meshwork, focal adhesion stability, mechanosensing and cell migration (reviewed in [284-286]). The results presented in this thesis show a novel interaction between filamin A and the first 100 a.a. of PKP3 (Figure 4.38). It is interesting to note that filamin A is also a Pak1 kinase substrate and particularly binds to the CRIB domain of Pak1 [272]. These results collectively indicate a role for filamin A acting as a scaffold that mediates complex formation between PKP3 and Pak1. Similarly, filamin A is also known to bind to RhoA [287] and could hence act as a scaffold for PKP3 and RhoA interaction. However, further studies would be required to draw conclusions on the role of this novel interaction between PKP3 and filamin A.

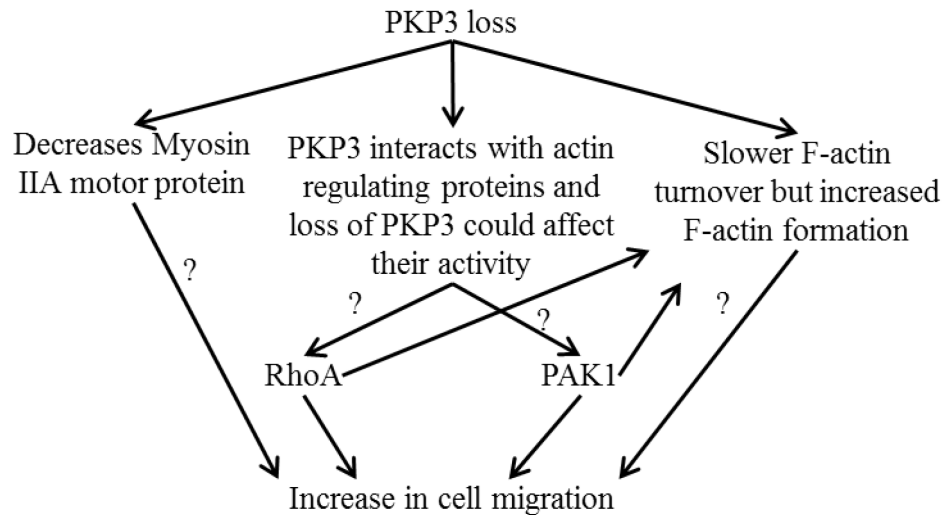


Figure 5.2. Model showing how PKP3 loss could lead to increased cell migration.

In conclusion, PKP3 loss can affect actin reorganization in multiple ways that ultimately results in increased cell migration. PKP3 loss can decrease myosin IIA protein levels and lead to slower actin turnover but increased F-actin formation to promote cell migration (Figure 5.2). PKP3 also interacts with actin reorganization regulating proteins like RhoA and Pak1, possibly through the scaffold filamin A (Figure 5.2). These novel interactions of PKP3 might be the underlying mechanism for the changes in actin turnover and increased F-actin formation (Figure 5.2). Collectively, these different mechanisms might be responsible for the increase in cell migration on PKP3 loss (Figure 5.2).

5.3. Role of PKP3 in regulating cell adhesion, cell migration and EMT.

The established “master” regulators of EMT are the transcription factors Snail, Slug, Twist 1 and Zeb 1. Snail, Slug, Twist 1 and Zeb 1 are all known to directly or indirectly repress E-cadherin expression and induce vimentin expression while Slug and Zeb1 are also known to promote dissolution of desmosomes (reviewed in [255-257]).

Previous reports from the laboratory show that neither E-cadherin expression nor localization is perturbed on PKP3 loss [169]. We have also previously reported that PKP3 loss does not induce vimentin expression [274]. The results presented in this thesis show that Snail is the only EMT promoting transcription factor expressed in the HCT116 based PKP3 knockdown cells and does not show any significant changes in mRNA levels on PKP3 loss (Figure 4.39). PKP3 loss also did not lead to any changes in cell-substrate adhesion (Figure 4.39). Thus there was no in vitro evidence of PKP3 inducing EMT. Likewise, mesenchymal markers like vimentin and MMP9 were expressed in xenograft tumours formed in nude mice as well as their lung metastases but PKP3 loss did not increase expression of these markers (Figure 4.40). Thus, PKP3 loss does not induce EMT in vivo either. Since our previous reports showed PKP3 loss to lead to mesenchymal cells like characteristics like decrease in cell-cell adhesion and an increase in cell migration, anchorage independent growth and tumour formation [108], it stands to reason that PKP3 loss could be one of the many downstream effects of the EMT program and hence might not show all the characteristics of EMT. This hypothesis is supported by previous reports demonstrating that PKP3 expression is repressed by the binding of the EMT transcription factor Zeb 1 and Snail to the E-box sites in the PKP3 promoter [110]. Also, Zeb 1 decreases PKP3 expression at the tumour host interface, thus promoting increased invasiveness and migration of the tumours [258]. Thus PKP3 loss does not induce EMT but is rather one of the effects of EMT.

REFERENCES

6. REFERENCES

1. Bloomfield SA, Volgyi B: **The diverse functional roles and regulation of neuronal gap junctions in the retina.** *Nature reviews Neuroscience* 2009, **10**:495-506.
2. Perez-Moreno M, Jamora C, Fuchs E: **Sticky business: orchestrating cellular signals at adherens junctions.** *Cell* 2003, **112**:535-548.
3. Lamouille S, Xu J, Derynck R: **Molecular mechanisms of epithelial-mesenchymal transition.** *Nature reviews Molecular cell biology* 2014, **15**:178-196.
4. Tsukada J, Yoshida Y, Kominato Y, Auron PE: **The CCAAT/enhancer (C/EBP) family of basic-leucine zipper (bZIP) transcription factors is a multifaceted highly-regulated system for gene regulation.** *Cytokine* 2011, **54**:6-19.
5. Desai BV, Harmon RM, Green KJ: **Desmosomes at a glance.** *J Cell Sci* 2009, **122**:4401-4407.
6. Muhmer M, Ditthardt D, Jakel J, Wischmann V, Moll R, Schmidt A: **An alternative promoter of the human plakophilin-3 gene controls the expression of the new isoform PKP3b.** *Cell and tissue research* 2014, **355**:143-162.
7. Shetty TP: **Role of plakophilin-3 in regulating PAK1.** *MSc. Narsee Monjee Institute of Management Studies University*, 2014.
8. Alberts B: *Molecular biology of the cell.* New York: Garland Science; 2002.
9. Atak A: **To study the effect of PKP3 over-expression on cell-ECM adhesion, cell migration and actin reorganization.** *BTech thesis.* Padmashree Dr. D. Y. Patil University, Biotechnology; 2013.
10. Raftopoulou M, Hall A: **Cell migration: Rho GTPases lead the way.** *Developmental biology* 2004, **265**:23-32.

11. Tojkander S, Gateva G, Lappalainen P: **Actin stress fibers--assembly, dynamics and biological roles.** *Journal of Cell Science* 2012, **125**:1855-1864.
12. Niessen CM: **Tight junctions/adherens junctions: basic structure and function.** *The Journal of investigative dermatology* 2007, **127**:2525-2532.
13. Harmon RM, Green KJ: **Structural and functional diversity of desmosomes.** *Cell Commun Adhes* 2013, **20**:171-187.
14. Furuse M: **Molecular basis of the core structure of tight junctions.** *Cold Spring Harbor perspectives in biology* 2010, **2**:a002907.
15. Dusek RL, Attardi LD: **Desmosomes: new perpetrators in tumour suppression.** *Nature reviews Cancer* 2011, **11**:317-323.
16. Pollard TD, Blanchoin L, Mullins RD: **Actin dynamics.** *Journal of cell science* 2001, **114**:3-4.
17. Goodenough DA, Paul DL: **Gap junctions.** *Cold Spring Harbor perspectives in biology* 2009, **1**:a002576.
18. Berx G, van Roy F: **Involvement of members of the cadherin superfamily in cancer.** *Cold Spring Harbor perspectives in biology* 2009, **1**:a003129.
19. Dembitzer HM, Herz F, Schermer A, Wolley RC, Koss LG: **Desmosome development in an in vitro model.** *The Journal of cell biology* 1980, **85**:695-702.
20. Fey EG, Wan KM, Penman S: **Epithelial cytoskeletal framework and nuclear matrix-intermediate filament scaffold: three-dimensional organization and protein composition.** *The Journal of cell biology* 1984, **98**:1973-1984.
21. Baker J, Garrod D: **Epithelial cells retain junctions during mitosis.** *Journal of Cell Science* 1993, **104 (Pt 2)**:415-425.
22. Gilbert SF: *Developmental biology*. Sunderland, Mass.: Sinauer Assoc.; 1997.

23. Anderson JM, Van Itallie CM: **Physiology and function of the tight junction.** *Cold Spring Harbor perspectives in biology* 2009, **1**:a002584.
24. Balda MS, Matter K: **Tight junctions at a glance.** *Journal of Cell Science* 2008, **121**:3677-3682.
25. Zeisberg M, Neilson EG: **Biomarkers for epithelial-mesenchymal transitions.** *J Clin Invest* 2009, **119**:1429-1437.
26. Meng W, Takeichi M: **Adherens junction: molecular architecture and regulation.** *Cold Spring Harbor perspectives in biology* 2009, **1**:a002899.
27. Cavey M, Lecuit T: **Molecular bases of cell-cell junctions stability and dynamics.** *Cold Spring Harbor perspectives in biology* 2009, **1**:a002998.
28. Michels C, Buchta T, Bloch W, Krieg T, Niessen CM: **Classical cadherins regulate desmosome formation.** *J Invest Dermatol* 2009, **129**:2072-2075.
29. Baum B, Georgiou M: **Dynamics of adherens junctions in epithelial establishment, maintenance, and remodeling.** *The Journal of cell biology* 2011, **192**:907-917.
30. Place RF, Li LC, Pookot D, Noonan EJ, Dahiya R: **MicroRNA-373 induces expression of genes with complementary promoter sequences.** *Proceedings of the National Academy of Sciences of the United States of America* 2008, **105**:1608-1613.
31. Merrill BJ, Gat U, DasGupta R, Fuchs E: **Tcf3 and Lef1 regulate lineage differentiation of multipotent stem cells in skin.** *Genes & development* 2001, **15**:1688-1705.
32. Behrens J, von Kries JP, Kuhl M, Bruhn L, Wedlich D, Grosschedl R, Birchmeier W: **Functional interaction of beta-catenin with the transcription factor LEF-1.** *Nature* 1996, **382**:638-642.

33. Moon RT, Bowerman B, Boutros M, Perrimon N: **The promise and perils of Wnt signaling through beta-catenin.** *Science* 2002, **296**:1644-1646.
34. Nielsen MS, Axelsen LN, Sorgen PL, Verma V, Delmar M, Holstein-Rathlou NH: **Gap junctions.** *Comprehensive Physiology* 2012, **2**:1981-2035.
35. Defamie N, Chepied A, Mesnil M: **Connexins, gap junctions and tissue invasion.** *FEBS letters* 2014, **588**:1331-1338.
36. Getsios S, Huen AC, Green KJ: **Working out the strength and flexibility of desmosomes.** *Nat Rev Mol Cell Biol* 2004, **5**:271-281.
37. Yin T, Green KJ: **Regulation of desmosome assembly and adhesion.** *Seminars in cell & developmental biology* 2004, **15**:665-677.
38. Chidgey M, Dawson C: **Desmosomes: a role in cancer?** *British journal of cancer* 2007, **96**:1783-1787.
39. Dusek RL, Godsel LM, Green KJ: **Discriminating roles of desmosomal cadherins: beyond desmosomal adhesion.** *Journal of dermatological science* 2007, **45**:7-21.
40. Stokes DL: **Desmosomes from a structural perspective.** *Current opinion in cell biology* 2007, **19**:565-571.
41. Garrod D, Chidgey M: **Desmosome structure, composition and function.** *Biochim Biophys Acta* 2008, **1778**:572-587.
42. Delva E, Tucker DK, Kowalczyk AP: **The desmosome.** *Cold Spring Harb Perspect Biol* 2009, **1**:a002543.
43. Garrod D: **Desmosomes in vivo.** *Dermatology research and practice* 2010, **2010**:212439.
44. Peltonen S, Raiko L, Peltonen J: **Desmosomes in developing human epidermis.** *Dermatology research and practice* 2010, **2010**:698761.

45. Thomason HA, Scothern A, McHarg S, Garrod DR: **Desmosomes: adhesive strength and signalling in health and disease.** *The Biochemical journal* 2010, **429**:419-433.
46. Dubash AD, Green KJ: **Desmosomes.** *Current biology : CB* 2011, **21**:R529-531.
47. Skerrow CJ, Matoltsy AG: **Chemical characterization of isolated epidermal desmosomes.** *The Journal of cell biology* 1974, **63**:524-530.
48. Rash JE, Shay JW, Biesele JJ: **Urea extraction of Z bands, intercalated disks, and desmosomes.** *Journal of ultrastructure research* 1968, **24**:181-189.
49. Skerrow CJ, Matoltsy AG: **Isolation of epidermal desmosomes.** *The Journal of cell biology* 1974, **63**:515-523.
50. Penn EJ, Burdett ID, Hobson C, Magee AI, Rees DA: **Structure and assembly of desmosome junctions: biosynthesis and turnover of the major desmosome components of Madin-Darby canine kidney cells in low calcium medium.** *The Journal of cell biology* 1987, **105**:2327-2334.
51. Pasdar M, Nelson WJ: **Kinetics of desmosome assembly in Madin-Darby canine kidney epithelial cells: temporal and spatial regulation of desmoplakin organization and stabilization upon cell-cell contact. I. Biochemical analysis.** *The Journal of cell biology* 1988, **106**:677-685.
52. Penn EJ, Hobson C, Rees DA, Magee AI: **Structure and assembly of desmosome junctions: biosynthesis, processing, and transport of the major protein and glycoprotein components in cultured epithelial cells.** *The Journal of cell biology* 1987, **105**:57-68.
53. Penn EJ, Hobson C, Rees DA, Magee AI: **The assembly of the major desmosome glycoproteins of Madin-Darby canine kidney cells.** *FEBS letters* 1989, **247**:13-16.

54. Burdett ID: **Internalisation of desmosomes and their entry into the endocytic pathway via late endosomes in MDCK cells. Possible mechanisms for the modulation of cell adhesion by desmosomes during development.** *Journal of Cell Science* 1993, **106 (Pt 4)**:1115-1130.
55. McHarg S, Hopkins G, Lim L, Garrod D: **Down-regulation of desmosomes in cultured cells: the roles of PKC, microtubules and lysosomal/proteasomal degradation.** *PloS one* 2014, **9**:e108570.
56. Harmon RM, Green KJ: **Structural and functional diversity of desmosomes.** *Cell communication & adhesion* 2013, **20**:171-187.
57. Roberts BJ, Johnson KE, McGuinn KP, Saowapa J, Svoboda RA, Mahoney MG, Johnson KR, Wahl JK, 3rd: **Palmitoylation of plakophilin is required for desmosome assembly.** *Journal of Cell Science* 2014, **127**:3782-3793.
58. Brennan D, Peltonen S, Dowling A, Medhat W, Green KJ, Wahl JK, 3rd, Del Galdo F, Mahoney MG: **A role for caveolin-1 in desmoglein binding and desmosome dynamics.** *Oncogene* 2012, **31**:1636-1648.
59. Garrod DR, Merritt AJ, Nie Z: **Desmosomal cadherins.** *Current opinion in cell biology* 2002, **14**:537-545.
60. Kimura TE, Merritt AJ, Lock FR, Eckert JJ, Fleming TP, Garrod DR: **Desmosomal adhesiveness is developmentally regulated in the mouse embryo and modulated during trophectoderm migration.** *Developmental biology* 2012, **369**:286-297.
61. Berika M, Garrod D: **Desmosomal adhesion in vivo.** *Cell communication & adhesion* 2014, **21**:65-75.

62. Garrod DR, Berika MY, Bardsley WF, Holmes D, Tabernero L: **Hyper-adhesion in desmosomes: its regulation in wound healing and possible relationship to cadherin crystal structure.** *Journal of Cell Science* 2005, **118**:5743-5754.
63. Wallis S, Lloyd S, Wise I, Ireland G, Fleming TP, Garrod D: **The alpha isoform of protein kinase C is involved in signaling the response of desmosomes to wounding in cultured epithelial cells.** *Molecular biology of the cell* 2000, **11**:1077-1092.
64. Bass-Zubek AE, Hobbs RP, Amargo EV, Garcia NJ, Hsieh SN, Chen X, Wahl JK, 3rd, Denning MF, Green KJ: **Plakophilin 2: a critical scaffold for PKC alpha that regulates intercellular junction assembly.** *The Journal of cell biology* 2008, **181**:605-613.
65. Hobbs RP, Amargo EV, Somasundaram A, Simpson CL, Prakriya M, Denning MF, Green KJ: **The calcium ATPase SERCA2 regulates desmoplakin dynamics and intercellular adhesive strength through modulation of PKCα signaling.** *FASEB journal : official publication of the Federation of American Societies for Experimental Biology* 2011, **25**:990-1001.
66. Thomason HA, Cooper NH, Ansell DM, Chiu M, Merrit AJ, Hardman MJ, Garrod DR: **Direct evidence that PKCalpha positively regulates wound re-epithelialization: correlation with changes in desmosomal adhesiveness.** *The Journal of pathology* 2012, **227**:346-356.
67. Nitoiu D, Etheridge SL, Kelsell DP: **Insights into desmosome biology from inherited human skin disease and cardiocutaneous syndromes.** *Cell communication & adhesion* 2014, **21**:129-140.

68. Amagai M, Matsuyoshi N, Wang ZH, Andl C, Stanley JR: **Toxin in bullous impetigo and staphylococcal scalded-skin syndrome targets desmoglein 1.** *Nature medicine* 2000, **6**:1275-1277.
69. Broussard JA, Getsios S, Green KJ: **Desmosome regulation and signaling in disease.** *Cell and tissue research* 2015.
70. Dusek RL, Getsios S, Chen F, Park JK, Amargo EV, Cryns VL, Green KJ: **The differentiation-dependent desmosomal cadherin desmoglein 1 is a novel caspase-3 target that regulates apoptosis in keratinocytes.** *The Journal of biological chemistry* 2006, **281**:3614-3624.
71. Nava P, Laukoetter MG, Hopkins AM, Laur O, Gerner-Smidt K, Green KJ, Parkos CA, Nusrat A: **Desmoglein-2: a novel regulator of apoptosis in the intestinal epithelium.** *Molecular biology of the cell* 2007, **18**:4565-4578.
72. Dubash AD, Koetsier JL, Amargo EV, Najor NA, Harmon RM, Green KJ: **The GEF Bcr activates RhoA/MAL signaling to promote keratinocyte differentiation via desmoglein-1.** *The Journal of cell biology* 2013, **202**:653-666.
73. Getsios S, Simpson CL, Kojima S, Harmon R, Sheu LJ, Dusek RL, Cornwell M, Green KJ: **Desmoglein 1-dependent suppression of EGFR signaling promotes epidermal differentiation and morphogenesis.** *The Journal of cell biology* 2009, **185**:1243-1258.
74. Brennan D, Hu Y, Joubert S, Choi YW, Whitaker-Menezes D, O'Brien T, Uitto J, Rodeck U, Mahoney MG: **Suprabasal Dsg2 expression in transgenic mouse skin confers a hyperproliferative and apoptosis-resistant phenotype to keratinocytes.** *Journal of Cell Science* 2007, **120**:758-771.
75. Lorch JH, Klessner J, Park JK, Getsios S, Wu YL, Stack MS, Green KJ: **Epidermal growth factor receptor inhibition promotes desmosome assembly and**

- strengthens intercellular adhesion in squamous cell carcinoma cells.** *The Journal of biological chemistry* 2004, **279**:37191-37200.
76. Klessner JL, Desai BV, Amargo EV, Getsios S, Green KJ: **EGFR and ADAMs cooperate to regulate shedding and endocytic trafficking of the desmosomal cadherin desmoglein 2.** *Molecular biology of the cell* 2009, **20**:328-337.
 77. Dusek RL, Godsel LM, Chen F, Strohecker AM, Getsios S, Harmon R, Muller EJ, Caldelari R, Cryns VL, Green KJ: **Plakoglobin deficiency protects keratinocytes from apoptosis.** *The Journal of investigative dermatology* 2007, **127**:792-801.
 78. Li L, Chapman K, Hu X, Wong A, Pasdar M: **Modulation of the oncogenic potential of beta-catenin by the subcellular distribution of plakoglobin.** *Molecular carcinogenesis* 2007, **46**:824-838.
 79. Williamson L, Raess NA, Caldelari R, Zakher A, de Bruin A, Posthaus H, Bolli R, Hunziker T, Suter MM, Muller EJ: **Pemphigus vulgaris identifies plakoglobin as key suppressor of c-Myc in the skin.** *The EMBO journal* 2006, **25**:3298-3309.
 80. Kolligs FT, Kolligs B, Hajra KM, Hu G, Tani M, Cho KR, Fearon ER: **gamma-catenin is regulated by the APC tumor suppressor and its oncogenic activity is distinct from that of beta-catenin.** *Genes & development* 2000, **14**:1319-1331.
 81. Kolly C, Zakher A, Strauss C, Suter MM, Muller EJ: **Keratinocyte transcriptional regulation of the human c-Myc promoter occurs via a novel Lef/Tcf binding element distinct from neoplastic cells.** *FEBS letters* 2007, **581**:1969-1976.
 82. Sobolik-Delmaire T, Reddy R, Pashaj A, Roberts BJ, Wahl JK, 3rd: **Plakophilin-1 localizes to the nucleus and interacts with single-stranded DNA.** *The Journal of investigative dermatology* 2010, **130**:2638-2646.

83. Wolf A, Krause-Gruszczynska M, Birkenmeier O, Ostareck-Lederer A, Huttelmaier S, Hatzfeld M: **Plakophilin 1 stimulates translation by promoting eIF4A1 activity.** *The Journal of cell biology* 2010, **188**:463-471.
84. Godsel LM, Dubash AD, Bass-Zubek AE, Amargo EV, Klessner JL, Hobbs RP, Chen X, Green KJ: **Plakophilin 2 couples actomyosin remodeling to desmosomal plaque assembly via RhoA.** *Molecular biology of the cell* 2010, **21**:2844-2859.
85. Koetsier JL, Amargo EV, Todorovic V, Green KJ, Godsel LM: **Plakophilin 2 affects cell migration by modulating focal adhesion dynamics and integrin protein expression.** *The Journal of investigative dermatology* 2014, **134**:112-122.
86. Mertens C, Kuhn C, Franke WW: **Plakophilins 2a and 2b: constitutive proteins of dual location in the karyoplasm and the desmosomal plaque.** *The Journal of cell biology* 1996, **135**:1009-1025.
87. Muller J, Ritt DA, Copeland TD, Morrison DK: **Functional analysis of C-TAK1 substrate binding and identification of PKP2 as a new C-TAK1 substrate.** *The EMBO journal* 2003, **22**:4431-4442.
88. Mertens C, Hofmann I, Wang Z, Teichmann M, Sepehri Chong S, Schnolzer M, Franke WW: **Nuclear particles containing RNA polymerase III complexes associated with the junctional plaque protein plakophilin 2.** *Proceedings of the National Academy of Sciences of the United States of America* 2001, **98**:7795-7800.
89. Munoz WA, Lee M, Miller RK, Ahmed Z, Ji H, Link TM, Lee GR, Kloc M, Ladbury JE, McCrea PD: **Plakophilin-3 catenin associates with the ETV1/ER81 transcription factor to positively modulate gene activity.** *PloS one* 2014, **9**:e86784.
90. Fischer-Keso R, Breuninger S, Hofmann S, Henn M, Rohrig T, Strobel P, Stoecklin G, Hofmann I: **Plakophilins 1 and 3 bind to FXR1 and thereby influence**

- the mRNA stability of desmosomal proteins.** *Molecular and cellular biology* 2014, **34**:4244-4256.
91. Hofmann I, Casella M, Schnolzer M, Schlechter T, Spring H, Franke WW: **Identification of the junctional plaque protein plakophilin 3 in cytoplasmic particles containing RNA-binding proteins and the recruitment of plakophilins 1 and 3 to stress granules.** *Molecular biology of the cell* 2006, **17**:1388-1398.
 92. Lechler T, Fuchs E: **Desmoplakin: an unexpected regulator of microtubule organization in the epidermis.** *The Journal of cell biology* 2007, **176**:147-154.
 93. Sumigay KD, Chen H, Lechler T: **Lis1 is essential for cortical microtubule organization and desmosome stability in the epidermis.** *The Journal of cell biology* 2011, **194**:631-642.
 94. Chidgey M: **Desmosomes and disease: an update.** *Histology and histopathology* 2002, **17**:1179-1192.
 95. Brown L, Wan H: **Desmoglein 3: a help or a hindrance in cancer progression?** *Cancers* 2015, **7**:266-286.
 96. Stahley SN, Kowalczyk AP: **Desmosomes in acquired disease.** *Cell and tissue research* 2015.
 97. Tselepis C, Chidgey M, North A, Garrod D: **Desmosomal adhesion inhibits invasive behavior.** *Proceedings of the National Academy of Sciences of the United States of America* 1998, **95**:8064-8069.
 98. Savagner P, Yamada KM, Thiery JP: **The zinc-finger protein slug causes desmosome dissociation, an initial and necessary step for growth factor-induced epithelial-mesenchymal transition.** *The Journal of cell biology* 1997, **137**:1403-1419.

99. Savagner P, Kusewitt DF, Carver EA, Magnino F, Choi C, Gridley T, Hudson LG: **Developmental transcription factor slug is required for effective re-epithelialization by adult keratinocytes.** *Journal of cellular physiology* 2005, **202**:858-866.
100. Hiraki A, Shinohara M, Ikebe T, Nakamura S, Kurahara S, Garrod DR: **Immunohistochemical staining of desmosomal components in oral squamous cell carcinomas and its association with tumour behaviour.** *British journal of cancer* 1996, **73**:1491-1497.
101. Collins JE, Taylor I, Garrod DR: **A study of desmosomes in colorectal carcinoma.** *British journal of cancer* 1990, **62**:796-805.
102. Parker HR, Li Z, Sheinin H, Lauzon G, Pasdar M: **Plakoglobin induces desmosome formation and epidermoid phenotype in N-cadherin-expressing squamous carcinoma cells deficient in plakoglobin and E-cadherin.** *Cell motility and the cytoskeleton* 1998, **40**:87-100.
103. Aberle H, Bierkamp C, Torchard D, Serova O, Wagner T, Natt E, Wirsching J, Heidkamper C, Montagna M, Lynch HT, et al.: **The human plakoglobin gene localizes on chromosome 17q21 and is subjected to loss of heterozygosity in breast and ovarian cancers.** *Proceedings of the National Academy of Sciences of the United States of America* 1995, **92**:6384-6388.
104. Shiina H, Breault JE, Basset WW, Enokida H, Urakami S, Li LC, Okino ST, Deguchi M, Kaneuchi M, Terashima M, et al: **Functional Loss of the gamma-catenin gene through epigenetic and genetic pathways in human prostate cancer.** *Cancer research* 2005, **65**:2130-2138.
105. Winn RA, Bremnes RM, Bemis L, Franklin WA, Miller YE, Cool C, Heasley LE: **gamma-Catenin expression is reduced or absent in a subset of human lung**

- cancers and re-expression inhibits transformed cell growth.** *Oncogene* 2002, **21**:7497-7506.
106. Canes D, Chiang GJ, Billmeyer BR, Austin CA, Kosakowski M, Rieger-Christ KM, Libertino JA, Summerhayes IC: **Histone deacetylase inhibitors upregulate plakoglobin expression in bladder carcinoma cells and display antineoplastic activity in vitro and in vivo.** *International journal of cancer Journal international du cancer* 2005, **113**:841-848.
107. Papagerakis S, Shabana AH, Depondt J, Gehanno P, Forest N: **Immunohistochemical localization of plakophilins (PKP1, PKP2, PKP3, and p0071) in primary oropharyngeal tumors: correlation with clinical parameters.** *Human pathology* 2003, **34**:565-572.
108. Kundu ST, Gosavi P, Khapare N, Patel R, Hosing AS, Maru GB, Ingle A, Decaprio JA, Dalal SN: **Plakophilin3 downregulation leads to a decrease in cell adhesion and promotes metastasis.** *International journal of cancer* 2008, **123**:2303-2314.
109. Vandewalle C, Comijn J, De Craene B, Vermassen P, Bruyneel E, Andersen H, Tulchinsky E, Van Roy F, Berx G: **SIP1/ZEB2 induces EMT by repressing genes of different epithelial cell-cell junctions.** *Nucleic acids research* 2005, **33**:6566-6578.
110. Aigner K, Descovich L, Mikula M, Sultan A, Dampier B, Bonne S, van Roy F, Mikulits W, Schreiber M, Brabletz T, et al: **The transcription factor ZEB1 (deltaEF1) represses Plakophilin 3 during human cancer progression.** *FEBS letters* 2007, **581**:1617-1624.
111. Furukawa C, Daigo Y, Ishikawa N, Kato T, Ito T, Tsuchiya E, Sone S, Nakamura Y: **Plakophilin 3 oncogene as prognostic marker and therapeutic target for lung cancer.** *Cancer research* 2005, **65**:7102-7110.

112. Valladares-Ayerbes M, Diaz-Prado S, Reboredo M, Medina V, Lorenzo-Patino MJ, Iglesias-Diaz P, Haz M, Pertega S, Santamarina I, Blanco M, et al: **Evaluation of plakophilin-3 mRNA as a biomarker for detection of circulating tumor cells in gastrointestinal cancer patients.** *Cancer epidemiology, biomarkers & prevention : a publication of the American Association for Cancer Research, cosponsored by the American Society of Preventive Oncology* 2010, **19**:1432-1440.
113. Demirag GG, Sullu Y, Yucel I: **Expression of Plakophilins (PKP1, PKP2, and PKP3) in breast cancers.** *Medical oncology* 2012, **29**:1518-1522.
114. Khan K, Hardy R, Haq A, Ogunbiyi O, Morton D, Chidgey M: **Desmocollin switching in colorectal cancer.** *British journal of cancer* 2006, **95**:1367-1370.
115. Knosel T, Chen Y, Hotovy S, Settmacher U, Altendorf-Hofmann A, Petersen I: **Loss of desmocollin 1-3 and homeobox genes PITX1 and CDX2 are associated with tumor progression and survival in colorectal carcinoma.** *International journal of colorectal disease* 2012, **27**:1391-1399.
116. Fang WK, Liao LD, Li LY, Xie YM, Xu XE, Zhao WJ, Wu JY, Zhu MX, Wu ZY, Du ZP, et al: **Down-regulated desmocollin-2 promotes cell aggressiveness through redistributing adherens junctions and activating beta-catenin signalling in oesophageal squamous cell carcinoma.** *The Journal of pathology* 2013, **231**:257-270.
117. Cui T, Chen Y, Yang L, Knosel T, Zoller K, Huber O, Petersen I: **DSC3 expression is regulated by p53, and methylation of DSC3 DNA is a prognostic marker in human colorectal cancer.** *British journal of cancer* 2011, **104**:1013-1019.
118. Kolegraff K, Nava P, Helms MN, Parkos CA, Nusrat A: **Loss of desmocollin-2 confers a tumorigenic phenotype to colonic epithelial cells through activation of Akt/beta-catenin signaling.** *Molecular biology of the cell* 2011, **22**:1121-1134.

119. Oshiro MM, Kim CJ, Wozniak RJ, Junk DJ, Munoz-Rodriguez JL, Burr JA, Fitzgerald M, Pawar SC, Cress AE, Domann FE, Futscher BW: **Epigenetic silencing of DSC3 is a common event in human breast cancer.** *Breast cancer research : BCR* 2005, **7**:R669-680.
120. Biedermann K, Vogelsang H, Becker I, Plaschke S, Siewert JR, Hofler H, Keller G: **Desmoglein 2 is expressed abnormally rather than mutated in familial and sporadic gastric cancer.** *The Journal of pathology* 2005, **207**:199-206.
121. Kurzen H, Munzing I, Hartschuh W: **Expression of desmosomal proteins in squamous cell carcinomas of the skin.** *Journal of cutaneous pathology* 2003, **30**:621-630.
122. Harada T, Shinohara M, Nakamura S, Shimada M, Oka M: **Immunohistochemical detection of desmosomes in oral squamous cell carcinomas: correlation with differentiation, mode of invasion, and metastatic potential.** *International journal of oral and maxillofacial surgery* 1992, **21**:346-349.
123. Cirillo N, Lanza M, De Rosa A, Cammarota M, La Gatta A, Gombos F, Lanza A: **The most widespread desmosomal cadherin, desmoglein 2, is a novel target of caspase 3-mediated apoptotic machinery.** *Journal of cellular biochemistry* 2008, **103**:598-606.
124. Chen YJ, Chang JT, Lee L, Wang HM, Liao CT, Chiu CC, Chen PJ, Cheng AJ: **DSG3 is overexpressed in head neck cancer and is a potential molecular target for inhibition of oncogenesis.** *Oncogene* 2007, **26**:467-476.
125. Huber O: **Structure and function of desmosomal proteins and their role in development and disease.** *Cellular and molecular life sciences : CMLS* 2003, **60**:1872-1890.

126. Nie Z, Merritt A, Rouhi-Parkouhi M, Tabernero L, Garrod D: **Membrane-impermeable cross-linking provides evidence for homophilic, isoform-specific binding of desmosomal cadherins in epithelial cells.** *The Journal of biological chemistry* 2011, **286**:2143-2154.
127. Syed SE, Trinnaman B, Martin S, Major S, Hutchinson J, Magee AI: **Molecular interactions between desmosomal cadherins.** *The Biochemical journal* 2002, **362**:317-327.
128. Chitaev NA, Troyanovsky SM: **Direct Ca²⁺-dependent heterophilic interaction between desmosomal cadherins, desmoglein and desmocollin, contributes to cell-cell adhesion.** *The Journal of cell biology* 1997, **138**:193-201.
129. Waschke J, Menendez-Castro C, Bruggeman P, Koob R, Amagai M, Gruber HJ, Drenckhahn D, Baumgartner W: **Imaging and force spectroscopy on desmoglein 1 using atomic force microscopy reveal multivalent Ca(2+)-dependent, low-affinity trans-interaction.** *The Journal of membrane biology* 2007, **216**:83-92.
130. Getsios S, Amargo EV, Dusek RL, Ishii K, Sheu L, Godsel LM, Green KJ: **Coordinated expression of desmoglein 1 and desmocollin 1 regulates intercellular adhesion.** *Differentiation; research in biological diversity* 2004, **72**:419-433.
131. North AJ, Bardsley WG, Hyam J, Bornslaeger EA, Cordingley HC, Trinnaman B, Hatzfeld M, Green KJ, Magee AI, Garrod DR: **Molecular map of the desmosomal plaque.** *Journal of Cell Science* 1999, **112 (Pt 23)**:4325-4336.
132. Vielmuth F, Hartlieb E, Kugelmann D, Waschke J, Spindler V: **Atomic force microscopy identifies regions of distinct desmoglein 3 adhesive properties on living keratinocytes.** *Nanomedicine : nanotechnology, biology, and medicine* 2015, **11**:511-520.

133. Eshkind L, Tian Q, Schmidt A, Franke WW, Windoffer R, Leube RE: **Loss of desmoglein 2 suggests essential functions for early embryonic development and proliferation of embryonal stem cells.** *European journal of cell biology* 2002, **81**:592-598.
134. Koch PJ, Mahoney MG, Ishikawa H, Pulkkinen L, Uitto J, Shultz L, Murphy GF, Whitaker-Menezes D, Stanley JR: **Targeted disruption of the pemphigus vulgaris antigen (desmoglein 3) gene in mice causes loss of keratinocyte cell adhesion with a phenotype similar to pemphigus vulgaris.** *The Journal of cell biology* 1997, **137**:1091-1102.
135. Koch PJ, Mahoney MG, Cotsarelis G, Rothenberger K, Lavker RM, Stanley JR: **Desmoglein 3 anchors telogen hair in the follicle.** *Journal of Cell Science* 1998, **111** (Pt 17):2529-2537.
136. Baron S, Hoang A, Vogel H, Attardi LD: **Unimpaired skin carcinogenesis in Desmoglein 3 knockout mice.** *PloS one* 2012, **7**:e50024.
137. Lenox JM, Koch PJ, Mahoney MG, Lieberman M, Stanley JR, Radice GL: **Postnatal lethality of P-cadherin/desmoglein 3 double knockout mice: demonstration of a cooperative effect of these cell adhesion molecules in tissue homeostasis of stratified squamous epithelia.** *The Journal of investigative dermatology* 2000, **114**:948-952.
138. Elias PM, Matsuyoshi N, Wu H, Lin C, Wang ZH, Brown BE, Stanley JR: **Desmoglein isoform distribution affects stratum corneum structure and function.** *The Journal of cell biology* 2001, **153**:243-249.
139. Merritt AJ, Berika MY, Zhai W, Kirk SE, Ji B, Hardman MJ, Garrod DR: **Suprabasal desmoglein 3 expression in the epidermis of transgenic mice results in**

- hyperproliferation and abnormal differentiation.** *Molecular and cellular biology* 2002, **22**:5846-5858.
140. Allen E, Yu QC, Fuchs E: **Mice expressing a mutant desmosomal cadherin exhibit abnormalities in desmosomes, proliferation, and epidermal differentiation.** *The Journal of cell biology* 1996, **133**:1367-1382.
141. Hanakawa Y, Matsuyoshi N, Stanley JR: **Expression of desmoglein 1 compensates for genetic loss of desmoglein 3 in keratinocyte adhesion.** *The Journal of investigative dermatology* 2002, **119**:27-31.
142. Amagai M, Tsunoda K, Suzuki H, Nishifuji K, Koyasu S, Nishikawa T: **Use of autoantigen-knockout mice in developing an active autoimmune disease model for pemphigus.** *The Journal of clinical investigation* 2000, **105**:625-631.
143. Hata T, Nishifuji K, Shimoda K, Sasaki T, Yamada T, Nishikawa T, Koyasu S, Amagai M: **Transgenic rescue of desmoglein 3 null mice with desmoglein 1 to develop a syngeneic mouse model for pemphigus vulgaris.** *Journal of dermatological science* 2011, **63**:33-39.
144. Chidgey M, Brakebusch C, Gustafsson E, Cruchley A, Hail C, Kirk S, Merritt A, North A, Tselepis C, Hewitt J, et al: **Mice lacking desmocollin 1 show epidermal fragility accompanied by barrier defects and abnormal differentiation.** *The Journal of cell biology* 2001, **155**:821-832.
145. Cheng X, Mihindukulasuriya K, Den Z, Kowalczyk AP, Calkins CC, Ishiko A, Shimizu A, Koch PJ: **Assessment of splice variant-specific functions of desmocollin 1 in the skin.** *Molecular and cellular biology* 2004, **24**:154-163.
146. Rimpler U: **Funktionelle Charakterisierung von Desmocollin 2 während der Embryonalentwicklung und im adulten Herzen in der Maus.** Mathematisch-Naturwissenschaftliche Fakultät I, 2014.

147. Den Z, Cheng X, Merched-Sauvage M, Koch PJ: **Desmocollin 3 is required for pre-implantation development of the mouse embryo.** *Journal of Cell Science* 2006, **119**:482-489.
148. Chen J, Den Z, Koch PJ: **Loss of desmocollin 3 in mice leads to epidermal blistering.** *Journal of Cell Science* 2008, **121**:2844-2849.
149. Rafei D, Muller R, Ishii N, Llamazares M, Hashimoto T, Hertl M, Eming R: **IgG autoantibodies against desmocollin 3 in pemphigus sera induce loss of keratinocyte adhesion.** *The American journal of pathology* 2011, **178**:718-723.
150. Henkler F, Strom M, Mathers K, Cordingley H, Sullivan K, King I: **Trangenic misexpression of the differentiation-specific desmocollin isoform 1 in basal keratinocytes.** *The Journal of investigative dermatology* 2001, **116**:144-149.
151. Hardman MJ, Liu K, Avilion AA, Merritt A, Brennan K, Garrod DR, Byrne C: **Desmosomal cadherin misexpression alters beta-catenin stability and epidermal differentiation.** *Molecular and cellular biology* 2005, **25**:969-978.
152. Kowalczyk AP, Bornslaeger EA, Borgwardt JE, Palka HL, Dhaliwal AS, Corcoran CM, Denning MF, Green KJ: **The amino-terminal domain of desmoplakin binds to plakoglobin and clusters desmosomal cadherin-plakoglobin complexes.** *The Journal of cell biology* 1997, **139**:773-784.
153. Bierkamp C, McLaughlin KJ, Schwarz H, Huber O, Kemler R: **Embryonic heart and skin defects in mice lacking plakoglobin.** *Developmental biology* 1996, **180**:780-785.
154. Ruiz P, Brinkmann V, Ledermann B, Behrend M, Grund C, Thalhammer C, Vogel F, Birchmeier C, Gunthert U, Franke WW, Birchmeier W: **Targeted mutation of plakoglobin in mice reveals essential functions of desmosomes in the embryonic heart.** *The Journal of cell biology* 1996, **135**:215-225.

155. Bierkamp C, Schwarz H, Huber O, Kemler R: **Desmosomal localization of beta-catenin in the skin of plakoglobin null-mutant mice.** *Development* 1999, **126**:371-381.
156. Charpentier E, Lavker RM, Acquista E, Cowin P: **Plakoglobin suppresses epithelial proliferation and hair growth in vivo.** *The Journal of cell biology* 2000, **149**:503-520.
157. South AP, Wan H, Stone MG, Dopping-Hepenstal PJ, Purkis PE, Marshall JF, Leigh IM, Eady RA, Hart IR, McGrath JA: **Lack of plakophilin 1 increases keratinocyte migration and reduces desmosome stability.** *Journal of Cell Science* 2003, **116**:3303-3314.
158. Grossmann KS, Grund C, Huelsken J, Behrend M, Erdmann B, Franke WW, Birchmeier W: **Requirement of plakophilin 2 for heart morphogenesis and cardiac junction formation.** *The Journal of cell biology* 2004, **167**:149-160.
159. Cerrone M, Noorman M, Lin X, Chkourko H, Liang FX, van der Nagel R, Hund T, Birchmeier W, Mohler P, van Veen TA, et al: **Sodium current deficit and arrhythmogenesis in a murine model of plakophilin-2 haploinsufficiency.** *Cardiovascular research* 2012, **95**:460-468.
160. Sklyarova T, Bonne S, D'Hooge P, Denecker G, Goossens S, De Rycke R, Borgonie G, Bosl M, van Roy F, van Hengel J: **Plakophilin-3-deficient mice develop hair coat abnormalities and are prone to cutaneous inflammation.** *The Journal of investigative dermatology* 2008, **128**:1375-1385.
161. Gallicano GI, Kouklis P, Bauer C, Yin M, Vasioukhin V, Degenstein L, Fuchs E: **Desmoplakin is required early in development for assembly of desmosomes and cytoskeletal linkage.** *The Journal of cell biology* 1998, **143**:2009-2022.

162. Gallicano GI, Bauer C, Fuchs E: **Rescuing desmoplakin function in extra-embryonic ectoderm reveals the importance of this protein in embryonic heart, neuroepithelium, skin and vasculature.** *Development* 2001, **128**:929-941.
163. Vasioukhin V, Bowers E, Bauer C, Degenstein L, Fuchs E: **Desmoplakin is essential in epidermal sheet formation.** *Nature cell biology* 2001, **3**:1076-1085.
164. Burdett ID: **Aspects of the structure and assembly of desmosomes.** *Micron* 1998, **29**:309-328.
165. Matthey DL, Garrod DR: **Splitting and internalization of the desmosomes of cultured kidney epithelial cells by reduction in calcium concentration.** *Journal of Cell Science* 1986, **85**:113-124.
166. Demlehner MP, Schafer S, Grund C, Franke WW: **Continual assembly of half-desmosomal structures in the absence of cell contacts and their frustrated endocytosis: a coordinated Sisyphus cycle.** *The Journal of cell biology* 1995, **131**:745-760.
167. Aoyama Y, Yamamoto Y, Yamaguchi F, Kitajima Y: **Low to high Ca²⁺ -switch causes phosphorylation and association of desmocollin 3 with plakoglobin and desmoglein 3 in cultured keratinocytes.** *Experimental dermatology* 2009, **18**:404-408.
168. Michels C, Buchta T, Bloch W, Krieg T, Niessen CM: **Classical cadherins regulate desmosome formation.** *The Journal of investigative dermatology* 2009, **129**:2072-2075.
169. Gosavi P, Kundu ST, Khapare N, Sehgal L, Karkhanis MS, Dalal SN: **E-cadherin and plakoglobin recruit plakophilin3 to the cell border to initiate desmosome assembly.** *Cellular and molecular life sciences : CMLS* 2011, **68**:1439-1454.

170. Taniguchi T, Miyazaki M, Miyashita Y, Arima T, Ozawa M: **Identification of regions of alpha-catenin required for desmosome organization in epithelial cells.** *International journal of molecular medicine* 2005, **16**:1003-1008.
171. Wahl JK, 3rd: **A role for plakophilin-1 in the initiation of desmosome assembly.** *Journal of cellular biochemistry* 2005, **96**:390-403.
172. Palka HL, Green KJ: **Roles of plakoglobin end domains in desmosome assembly.** *Journal of Cell Science* 1997, **110 (Pt 19)**:2359-2371.
173. Yin T, Getsios S, Caldelari R, Godsel LM, Kowalczyk AP, Muller EJ, Green KJ: **Mechanisms of plakoglobin-dependent adhesion: desmosome-specific functions in assembly and regulation by epidermal growth factor receptor.** *The Journal of biological chemistry* 2005, **280**:40355-40363.
174. Acehan D, Petzold C, Gumper I, Sabatini DD, Muller EJ, Cowin P, Stokes DL: **Plakoglobin is required for effective intermediate filament anchorage to desmosomes.** *The Journal of investigative dermatology* 2008, **128**:2665-2675.
175. Sehgal L, Mukhopadhyay A, Rajan A, Khapare N, Sawant M, Vishal SS, Bhatt K, Ambatipudi S, Antao N, Alam H, et al: **14-3-3 γ -mediated transport of plakoglobin to the cell border is required for the initiation of desmosome assembly in vitro and in vivo.** *Journal of Cell Science* 2014, **127**:2174-2188.
176. Godsel LM, Hsieh SN, Amargo EV, Bass AE, Pascoe-McGillicuddy LT, Huen AC, Thorne ME, Gaudry CA, Park JK, Myung K, et al: **Desmoplakin assembly dynamics in four dimensions: multiple phases differentially regulated by intermediate filaments and actin.** *The Journal of cell biology* 2005, **171**:1045-1059.
177. Roberts BJ, Pashaj A, Johnson KR, Wahl JK, 3rd: **Desmosome dynamics in migrating epithelial cells requires the actin cytoskeleton.** *Experimental cell research* 2011, **317**:2814-2822.

178. Kowalczyk AP, Hatzfeld M, Bornslaeger EA, Kopp DS, Borgwardt JE, Corcoran CM, Settler A, Green KJ: **The head domain of plakophilin-1 binds to desmoplakin and enhances its recruitment to desmosomes. Implications for cutaneous disease.** *The Journal of biological chemistry* 1999, **274**:18145-18148.
179. Sobolik-Delmaire T, Katafiasz D, Wahl JK, 3rd: **Carboxyl terminus of Plakophilin-1 recruits it to plasma membrane, whereas amino terminus recruits desmoplakin and promotes desmosome assembly.** *The Journal of biological chemistry* 2006, **281**:16962-16970.
180. Todorovic V, Koetsier JL, Godsel LM, Green KJ: **Plakophilin 3 mediates Rap1-dependent desmosome assembly and adherens junction maturation.** *Molecular biology of the cell* 2014, **25**:3749-3764.
181. Nekrasova OE, Amargo EV, Smith WO, Chen J, Kreitzer GE, Green KJ: **Desmosomal cadherins utilize distinct kinesins for assembly into desmosomes.** *The Journal of cell biology* 2011, **195**:1185-1203.
182. Ivanov AI, McCall IC, Babbin B, Samarin SN, Nusrat A, Parkos CA: **Microtubules regulate disassembly of epithelial apical junctions.** *BMC cell biology* 2006, **7**:12.
183. Lowndes M, Rakshit S, Shafraz O, Borghi N, Harmon RM, Green KJ, Sivasankar S, Nelson WJ: **Different roles of cadherins in the assembly and structural integrity of the desmosome complex.** *Journal of Cell Science* 2014, **127**:2339-2350.
184. Troyanovsky SM, Eshkind LG, Troyanovsky RB, Leube RE, Franke WW: **Contributions of cytoplasmic domains of desmosomal cadherins to desmosome assembly and intermediate filament anchorage.** *Cell* 1993, **72**:561-574.
185. Troyanovsky SM, Troyanovsky RB, Eshkind LG, Krutovskikh VA, Leube RE, Franke WW: **Identification of the plakoglobin-binding domain in desmoglein and**

- its role in plaque assembly and intermediate filament anchorage.** *The Journal of cell biology* 1994, **127**:151-160.
186. Andl CD, Stanley JR: **Central role of the plakoglobin-binding domain for desmoglein 3 incorporation into desmosomes.** *The Journal of investigative dermatology* 2001, **117**:1068-1074.
187. Ishii K, Norvell SM, Bannon LJ, Amargo EV, Pascoe LT, Green KJ: **Assembly of desmosomal cadherins into desmosomes is isoform dependent.** *The Journal of investigative dermatology* 2001, **117**:26-35.
188. Fujiwara M, Nagatomo A, Tsuda M, Obata S, Sakuma T, Yamamoto T, Suzuki ST: **Desmocollin-2 alone forms functional desmosomal plaques, with the plaque formation requiring the juxtamembrane region and plakophilins.** *Journal of biochemistry* 2015.
189. Burdett ID, Sullivan KH: **Desmosome assembly in MDCK cells: transport of precursors to the cell surface occurs by two phases of vesicular traffic and involves major changes in centrosome and Golgi location during a Ca(2+) shift.** *Experimental cell research* 2002, **276**:296-309.
190. Andersen NJ, Yeaman C: **Sec3-containing exocyst complex is required for desmosome assembly in mammalian epithelial cells.** *Molecular biology of the cell* 2010, **21**:152-164.
191. Resnik N, Sepcic K, Plemenitas A, Windoffer R, Leube R, Veranic P: **Desmosome assembly and cell-cell adhesion are membrane raft-dependent processes.** *The Journal of biological chemistry* 2011, **286**:1499-1507.
192. Stahley SN, Saito M, Faundez V, Koval M, Mattheyses AL, Kowalczyk AP: **Desmosome assembly and disassembly are membrane raft-dependent.** *PloS one* 2014, **9**:e87809.

193. Kurrle N, Vollner F, Eming R, Hertl M, Banning A, Tikkanen R: **Flotillins directly interact with gamma-catenin and regulate epithelial cell-cell adhesion.** *PloS one* 2013, **8**:e84393.
194. Windoffer R, Borchert-Stuhltrager M, Leube RE: **Desmosomes: interconnected calcium-dependent structures of remarkable stability with significant integral membrane protein turnover.** *Journal of Cell Science* 2002, **115**:1717-1732.
195. Roberts BJ, Reddy R, Wahl JK, 3rd: **Stratifin (14-3-3 sigma) limits plakophilin-3 exchange with the desmosomal plaque.** *PloS one* 2013, **8**:e77012.
196. Hatzfeld M: **Plakophilins: Multifunctional proteins or just regulators of desmosomal adhesion?** *Biochim Biophys Acta* 2007, **1773**:69-77.
197. Bass-Zubek AE, Godsel LM, Delmar M, Green KJ: **Plakophilins: multifunctional scaffolds for adhesion and signaling.** *Current opinion in cell biology* 2009, **21**:708-716.
198. Hatzfeld M, Wolf A, Keil R: **Plakophilins in desmosomal adhesion and signaling.** *Cell communication & adhesion* 2014, **21**:25-42.
199. Bonne S, van Hengel J, Nollet F, Kools P, van Roy F: **Plakophilin-3, a novel armadillo-like protein present in nuclei and desmosomes of epithelial cells.** *Journal of Cell Science* 1999, **112 (Pt 14)**:2265-2276.
200. Schmidt A, Langbein L, Pratzel S, Rode M, Rackwitz HR, Franke WW: **Plakophilin 3--a novel cell-type-specific desmosomal plaque protein.** *Differentiation; research in biological diversity* 1999, **64**:291-306.
201. Bonne S, Gilbert B, Hatzfeld M, Chen X, Green KJ, van Roy F: **Defining desmosomal plakophilin-3 interactions.** *The Journal of cell biology* 2003, **161**:403-416.

202. Munoz WA, Kloc M, Cho K, Lee M, Hofmann I, Sater A, Vleminckx K, McCrea PD: **Plakophilin-3 is required for late embryonic amphibian development, exhibiting roles in ectodermal and neural tissues.** *PloS one* 2012, **7**:e34342.
203. Wahl JK, 3rd: **Mechanisms affecting desmosome dynamics.** University of Nebraska Medical Center, Omaha, NE, United States. Grant No. 1R15AR065074-01A1:National Institute of Health (NIH). *Grantome*, 2014, <http://grantome.com/grant/NIH/R15-AR065074-01A1>.
204. Kundu S: **Regulation of the G2 / M DNA damage checkpoint and neoplastic progression by 14-3-3 sigma and Plakophilin 3.** *Ph.D. Thesis*. Advanced Centre for Treatment Research and Education in Cancer (ACTREC), Cancer Research Institute (CRI), Sorab Dalal Lab; 2009.
205. Raychaudhuri K, Gurjar M, Dalal SN: **Plakophilin3 and Plakoglobin recycling are differentially regulated during the disassembly of desmosomes.** *Journal of Bioscience And Technology* 2015, **6**:634-642.
206. Nassa G, Tarallo R, Ambrosino C, Bamundo A, Ferraro L, Paris O, Ravo M, Guzzi PH, Cannataro M, Baumann M, et al: **A large set of estrogen receptor beta-interacting proteins identified by tandem affinity purification in hormone-responsive human breast cancer cell nuclei.** *Proteomics* 2011, **11**:159-165.
207. Nagano M, Hoshino D, Sakamoto T, Akizawa T, Koshikawa N, Seiki M: **ZF21 is a new regulator of focal adhesion disassembly and a potential member of the spreading initiation center.** *Cell adhesion & migration* 2011, **5**:23-28.
208. Knowlton ML, Selfors LM, Wrobel CN, Gu TL, Ballif BA, Gygi SP, Polakiewicz R, Brugge JS: **Profiling Y561-dependent and -independent substrates of CSF-1R in epithelial cells.** *PloS one* 2010, **5**:e13587.

209. Valladares-Ayerbes M, Diaz-Prado S, Reboredo M, Medina V, Iglesias-Diaz P, Lorenzo-Patino MJ, Campelo RG, Haz M, Santamarina I, Anton-Aparicio LM: **Bioinformatics approach to mRNA markers discovery for detection of circulating tumor cells in patients with gastrointestinal cancer.** *Cancer detection and prevention* 2008, **32**:236-250.
210. Collins JE, Lorimer JE, Garrod DR, Pidsley SC, Buxton RS, Fleming TP: **Regulation of desmocollin transcription in mouse preimplantation embryos.** *Development* 1995, **121**:743-753.
211. Fleming TP, Garrod DR, Elsmore AJ: **Desmosome biogenesis in the mouse preimplantation embryo.** *Development* 1991, **112**:527-539.
212. Marsden MD, Collins JE, Greenwood MD, Adams MJ, Fleming TP, Magee AI, Buxton RS: **Cloning and transcriptional analysis of the promoter of the human type 2 desmocollin gene (DSC2).** *Gene* 1997, **186**:237-247.
213. Smith C, Zhu K, Merritt A, Picton R, Youngs D, Garrod D, Chidgey M: **Regulation of desmocollin gene expression in the epidermis: CCAAT/enhancer-binding proteins modulate early and late events in keratinocyte differentiation.** *The Biochemical journal* 2004, **380**:757-765.
214. Keller MS, Ezaki T, Guo RJ, Lynch JP: **Cdx1 or Cdx2 expression activates E-cadherin-mediated cell-cell adhesion and compaction in human COLO 205 cells.** *American journal of physiology Gastrointestinal and liver physiology* 2004, **287**:G104-114.
215. Funakoshi S, Ezaki T, Kong J, Guo RJ, Lynch JP: **Repression of the desmocollin 2 gene expression in human colon cancer cells is relieved by the homeodomain transcription factors Cdx1 and Cdx2.** *Molecular cancer research : MCR* 2008, **6**:1478-1490.

216. Park MJ, Kim HY, Kim K, Cheong J: **Homeodomain transcription factor CDX1 is required for the transcriptional induction of PPARgamma in intestinal cell differentiation.** *FEBS letters* 2009, **583**:29-35.
217. Tokonzaba E, Chen J, Cheng X, Den Z, Ganeshan R, Muller EJ, Koch PJ: **Plakoglobin as a regulator of desmocollin gene expression.** *The Journal of investigative dermatology* 2013, **133**:2732-2740.
218. Kurinna S, Schafer M, Ostano P, Karouzakis E, Chiorino G, Bloch W, Bachmann A, Gay S, Garrod D, Lefort K, et al: **A novel Nrf2-miR-29-desmocollin-2 axis regulates desmosome function in keratinocytes.** *Nature communications* 2014, **5**:5099.
219. Silberg DG, Swain GP, Suh ER, Traber PG: **Cdx1 and cdx2 expression during intestinal development.** *Gastroenterology* 2000, **119**:961-971.
220. Hryniuk A, Grainger S, Savory JG, Lohnes D: **Cdx function is required for maintenance of intestinal identity in the adult.** *Developmental biology* 2012, **363**:426-437.
221. Grainger S: **The Role of Cdx in Intestinal Development.** *PhD.* University of Ottawa, Médecine cellulaire et moléculaire / Cellular and Molecular Medicine; 2013.
222. Colleypriest BJ, Palmer RM, Ward SG, Tosh D: **Cdx genes, inflammation and the pathogenesis of Barrett's metaplasia.** *Trends in molecular medicine* 2009, **15**:313-322.
223. Olsen J, Espersen ML, Jess P, Kirkeby LT, Troelsen JT: **The clinical perspectives of CDX2 expression in colorectal cancer: a qualitative systematic review.** *Surgical oncology* 2014, **23**:167-176.
224. Houde M, Laprise P, Jean D, Blais M, Asselin C, Rivard N: **Intestinal epithelial cell differentiation involves activation of p38 mitogen-activated protein kinase**

- that regulates the homeobox transcription factor CDX2.** *The Journal of biological chemistry* 2001, **276**:21885-21894.
225. Freund JN, Duluc I, Reimund JM, Gross I, Domon-Dell C: **Extending the functions of the homeotic transcription factor Cdx2 in the digestive system through nontranscriptional activities.** *World journal of gastroenterology : WJG* 2015, **21**:1436-1443.
226. Ramji DP, Foka P: **CCAAT/enhancer-binding proteins: structure, function and regulation.** *The Biochemical journal* 2002, **365**:561-575.
227. Nerlov C: **C/EBPs: recipients of extracellular signals through proteome modulation.** *Current opinion in cell biology* 2008, **20**:180-185.
228. Basu S, Thorat R, Dalal SN: **MMP7 Is Required to Mediate Cell Invasion and Tumor Formation upon Plakophilin3 Loss.** *PloS one* 2015, **10**:e0123979.
229. Ridley AJ: **Life at the leading edge.** *Cell* 2011, **145**:1012-1022.
230. Schwab A, Fabian A, Hanley PJ, Stock C: **Role of ion channels and transporters in cell migration.** *Physiological reviews* 2012, **92**:1865-1913.
231. Huttenlocher A, Horwitz AR: **Integrins in cell migration.** *Cold Spring Harbor perspectives in biology* 2011, **3**:a005074.
232. Pankova K, Rosel D, Novotny M, Brabek J: **The molecular mechanisms of transition between mesenchymal and amoeboid invasiveness in tumor cells.** *Cellular and molecular life sciences : CMLS* 2010, **67**:63-71.
233. Rorth P: **Fellow travellers: emergent properties of collective cell migration.** *EMBO reports* 2012, **13**:984-991.
234. Peglion F, Llense F, Etienne-Manneville S: **Adherens junction treadmilling during collective migration.** *Nature cell biology* 2014, **16**:639-651.

235. Hirata E, Park D, Sahai E: **Retrograde flow of cadherins in collective cell migration.** *Nature cell biology* 2014, **16**:621-623.
236. Heath JP: **Behaviour and structure of the leading lamella in moving fibroblasts. I. Occurrence and centripetal movement of arc-shaped microfilament bundles beneath the dorsal cell surface.** *Journal of Cell Science* 1983, **60**:331-354.
237. Khatau SB, Hale CM, Stewart-Hutchinson PJ, Patel MS, Stewart CL, Searson PC, Hodzic D, Wirtz D: **A perinuclear actin cap regulates nuclear shape.** *Proceedings of the National Academy of Sciences of the United States of America* 2009, **106**:19017-19022.
238. Vallotton P, Small JV: **Shifting views on the leading role of the lamellipodium in cell migration: speckle tracking revisited.** *Journal of Cell Science* 2009, **122**:1955-1958.
239. Hotulainen P, Lappalainen P: **Stress fibers are generated by two distinct actin assembly mechanisms in motile cells.** *The Journal of cell biology* 2006, **173**:383-394.
240. Tojkander S, Gateva G, Schevzov G, Hotulainen P, Naumanen P, Martin C, Gunning PW, Lappalainen P: **A molecular pathway for myosin II recruitment to stress fibers.** *Current biology : CB* 2011, **21**:539-550.
241. Pellegrin S, Mellor H: **Actin stress fibres.** *Journal of Cell Science* 2007, **120**:3491-3499.
242. Chen WT: **Mechanism of retraction of the trailing edge during fibroblast movement.** *The Journal of cell biology* 1981, **90**:187-200.
243. Mitchison TJ, Cramer LP: **Actin-based cell motility and cell locomotion.** *Cell* 1996, **84**:371-379.

244. Luxton GW, Gomes ER, Folker ES, Vintinner E, Gundersen GG: **Linear arrays of nuclear envelope proteins harness retrograde actin flow for nuclear movement.** *Science* 2010, **329**:956-959.
245. Nagayama K, Yahiro Y, Matsumoto T: **Stress fibers stabilize the position of intranuclear DNA through mechanical connection with the nucleus in vascular smooth muscle cells.** *FEBS letters* 2011, **585**:3992-3997.
246. Murphy DA, Courtneidge SA: **The 'ins' and 'outs' of podosomes and invadopodia: characteristics, formation and function.** *Nature reviews Molecular cell biology* 2011, **12**:413-426.
247. Carlsson AE: **Actin dynamics: from nanoscale to microscale.** *Annual review of biophysics* 2010, **39**:91-110.
248. Hanna S, El-Sibai M: **Signaling networks of Rho GTPases in cell motility.** *Cellular signalling* 2013, **25**:1955-1961.
249. Nurnberg A, Kitzing T, Grosse R: **Nucleating actin for invasion.** *Nature reviews Cancer* 2011, **11**:177-187.
250. Dominguez R: **Actin filament nucleation and elongation factors--structure-function relationships.** *Critical reviews in biochemistry and molecular biology* 2009, **44**:351-366.
251. dos Remedios CG, Chhabra D, Kekic M, Dedova IV, Tsubakihara M, Berry DA, Nosworthy NJ: **Actin binding proteins: regulation of cytoskeletal microfilaments.** *Physiological reviews* 2003, **83**:433-473.
252. Baum B, Settlemann J, Quinlan MP: **Transitions between epithelial and mesenchymal states in development and disease.** *Seminars in cell & developmental biology* 2008, **19**:294-308.

253. Kalluri R, Weinberg RA: **The basics of epithelial-mesenchymal transition.** *The Journal of clinical investigation* 2009, **119**:1420-1428.
254. Thiery JP, Sleeman JP: **Complex networks orchestrate epithelial-mesenchymal transitions.** *Nature reviews Molecular cell biology* 2006, **7**:131-142.
255. Lee JM, Dedhar S, Kalluri R, Thompson EW: **The epithelial-mesenchymal transition: new insights in signaling, development, and disease.** *The Journal of cell biology* 2006, **172**:973-981.
256. Zeisberg M, Neilson EG: **Biomarkers for epithelial-mesenchymal transitions.** *The Journal of clinical investigation* 2009, **119**:1429-1437.
257. Moreno-Bueno G, Peinado H, Molina P, Olmeda D, Cubillo E, Santos V, Palacios J, Portillo F, Cano A: **The morphological and molecular features of the epithelial-to-mesenchymal transition.** *Nature protocols* 2009, **4**:1591-1613.
258. Aigner K, Descovich L, Mikula M, Sultan A, Dampier B, Bonne S, van Roy F, Mikulits W, Schreiber M, Brabletz T, et al: **The transcription factor ZEB1 (deltaEF1) represses Plakophilin 3 during human cancer progression.** *FEBS Lett* 2007, **581**:1617-1624.
259. Sehgal L: **Generation of knockdown mice that lack 14-3-3 ϵ and 14-3-3 γ using RNA interference.** *PhD.* Homi Bhabha National Institute, Life Sciences; 2012.
260. Bane S: **Study of C/EBP and CDX2 transcription factors role in regulation of DSC2 transcription.** *MSc thesis.* University of Mumbai, Biotechnology; 2015.
261. Fang WK, Liao LD, Li LY, Xie YM, Xu XE, Zhao WJ, Wu JY, Zhu MX, Wu ZY, Du ZP, et al: **Down-regulated desmocollin-2 promotes cell aggressiveness through redistributing adherens junctions and activating beta-catenin signalling in oesophageal squamous cell carcinoma.** *J Pathol* 2013, **231**:257-270.

262. Tucker DK, Stahley SN, Kowalczyk AP: **Plakophilin-1 protects keratinocytes from pemphigus vulgaris IgG by forming calcium-independent desmosomes.** *The Journal of investigative dermatology* 2014, **134**:1033-1043.
263. Campbell JJ, Knight MM: **An improved confocal FRAP technique for the measurement of long-term actin dynamics in individual stress fibers.** *Microscopy research and technique* 2007, **70**:1034-1040.
264. Campbell JJ, Blain EJ, Chowdhury TT, Knight MM: **Loading alters actin dynamics and up-regulates cofilin gene expression in chondrocytes.** *Biochem Biophys Res Commun* 2007, **361**:329-334.
265. Yilmaz M, Christofori G: **Mechanisms of motility in metastasizing cells.** *Molecular cancer research : MCR* 2010, **8**:629-642.
266. Schramek D, Sendoel A, Segal JP, Beronja S, Heller E, Oristian D, Reva B, Fuchs E: **Direct in vivo RNAi screen unveils myosin IIa as a tumor suppressor of squamous cell carcinomas.** *Science* 2014, **343**:309-313.
267. Jorrich MH, Shih W, Yamada S: **Myosin IIA deficient cells migrate efficiently despite reduced traction forces at cell periphery.** *Biology open* 2013, **2**:368-372.
268. Even-Ram S, Doyle AD, Conti MA, Matsumoto K, Adelstein RS, Yamada KM: **Myosin IIA regulates cell motility and actomyosin-microtubule crosstalk.** *Nature cell biology* 2007, **9**:299-309.
269. Delorme-Walker VD, Peterson JR, Chernoff J, Waterman CM, Danuser G, DerMardirossian C, Bokoch GM: **Pak1 regulates focal adhesion strength, myosin IIA distribution, and actin dynamics to optimize cell migration.** *J Cell Biol* 2011, **193**:1289-1303.
270. Bokoch GM: **Biology of the p21-activated kinases.** *Annu Rev Biochem* 2003, **72**:743-781.

271. Todorovic V, Desai BV, Patterson MJ, Amargo EV, Dubash AD, Yin T, Jones JC, Green KJ: **Plakoglobin regulates cell motility through Rho- and fibronectin-dependent Src signaling.** *Journal of Cell Science* 2010, **123**:3576-3586.
272. Vadlamudi RK, Li F, Adam L, Nguyen D, Ohta Y, Stossel TP, Kumar R: **Filamin is essential in actin cytoskeletal assembly mediated by p21-activated kinase 1.** *Nat Cell Biol* 2002, **4**:681-690.
273. Thiery JP: **Epithelial-mesenchymal transitions in tumour progression.** *Nat Rev Cancer* 2002, **2**:442-454.
274. Khapare N, Kundu ST, Sehgal L, Sawant M, Priya R, Gosavi P, Gupta N, Alam H, Karkhanis M, Naik N, et al: **Plakophilin3 loss leads to an increase in PRL3 levels promoting K8 dephosphorylation, which is required for transformation and metastasis.** *PloS one* 2012, **7**:e38561.
275. Croft DR, Sahai E, Mavria G, Li S, Tsai J, Lee WM, Marshall CJ, Olson MF: **Conditional ROCK activation in vivo induces tumor cell dissemination and angiogenesis.** *Cancer Res* 2004, **64**:8994-9001.
276. Betapudi V, Licate LS, Egelhoff TT: **Distinct roles of nonmuscle myosin II isoforms in the regulation of MDA-MB-231 breast cancer cell spreading and migration.** *Cancer Res* 2006, **66**:4725-4733.
277. Smutny M, Cox HL, Leerberg JM, Kovacs EM, Conti MA, Ferguson C, Hamilton NA, Parton RG, Adelstein RS, Yap AS: **Myosin II isoforms identify distinct functional modules that support integrity of the epithelial zonula adherens.** *Nat Cell Biol* 2010, **12**:696-702.
278. Smutny M, Wu SK, Gomez GA, Mangold S, Yap AS, Hamilton NA: **Multicomponent analysis of junctional movements regulated by myosin II isoforms at the epithelial zonula adherens.** *PLoS One* 2011, **6**:e22458.

279. Gallegos L, Ng MR, Brugge JS: **The myosin-II-responsive focal adhesion proteome: a tour de force?** *Nat Cell Biol* 2011, **13**:344-346.
280. Betapudi V: **Myosin II motor proteins with different functions determine the fate of lamellipodia extension during cell spreading.** *PLoS One* 2010, **5**:e8560.
281. Wolf A, Keil R, Gotzl O, Mun A, Schwarze K, Lederer M, Huttelmaier S, Hatzfeld M: **The armadillo protein p0071 regulates Rho signalling during cytokinesis.** *Nature cell biology* 2006, **8**:1432-1440.
282. Radu M, Semenova G, Kosoff R, Chernoff J: **PAK signalling during the development and progression of cancer.** *Nat Rev Cancer* 2014, **14**:13-25.
283. Arias-Romero LE, Chernoff J: **A tale of two Paks.** *Biol Cell* 2008, **100**:97-108.
284. Kim H, McCulloch CA: **Filamin A mediates interactions between cytoskeletal proteins that control cell adhesion.** *FEBS Lett* 2011, **585**:18-22.
285. Nakamura F, Stossel TP, Hartwig JH: **The filamins: organizers of cell structure and function.** *Cell Adh Migr* 2011, **5**:160-169.
286. Razinia Z, Makela T, Ylanne J, Calderwood DA: **Filamins in mechanosensing and signaling.** *Annu Rev Biophys* 2012, **41**:227-246.
287. Ohta Y, Suzuki N, Nakamura S, Hartwig JH, Stossel TP: **The small GTPase RalA targets filamin to induce filopodia.** *Proc Natl Acad Sci U S A* 1999, **96**:2122-2128.

**REPRINTS OF PUBLISHED
PAPERS FROM THESIS**

Loss of the desmosomal plaque protein plakophilin 3 does not induce the epithelial mesenchymal transition.

Mansa Gurjar, Kumarkrishna Raychaudhuri, Sorab N. Dalal*.

KS215, Advanced Centre for Treatment Research and Education in Cancer (ACTREC),
Tata Memorial Centre, Kharghar Node, Navi Mumbai - 410210, Maharashtra, India.

Email: sdalal@actrec.gov.in

Abstract:

Aims: We investigated whether the increased neoplastic progression promoted by PKP3 loss is accompanied by induction of EMT. **Methods:** Quantitative real time PCR, Cell-ECM adhesion assay and Immunohistochemistry. **Results:** There was no significant difference in the levels of EMT regulating transcription factors and cell-ECM adhesion between vector control and PKP3 knockdown HCT116 derived cells or EMT markers in primary tumour and lung metastasis samples. **Conclusion:** PKP3 knockdown does not lead to induction of EMT both *in vitro* and *in vivo*.

Keywords:

Desmosomes, Epithelial Mesenchymal Transition, Plakophilin 3, Snail, Vimentin.

1. INTRODUCTION:

The Epithelial Mesenchymal Transition (EMT) is a developmental process by which epithelial cells get reprogrammed to a mesenchymal phenotype during gastrulation and neural crest formation. EMT leads to the dissolution of cell-cell adhesion junctions like desmosomes and an increase in cell migration and invasion, which leads to the acquisition of metastatic properties in primary tumour cells. The loss of desmosomal cell-cell adhesion is considered to be a hallmark for EMT (reviewed in [13]). Desmosomes are cell-cell adhesion junctions that are found in all epithelial tissues and cardiac muscle. The primary role of desmosomal junctions is to maintain tissue integrity and structure by providing mechanical strength.

The adhesion is mediated by calcium dependent homophilic and heterophilic interactions between transmembrane desmosomal cadherins, namely desmocollins and desmogleins. On the intracellular side, the desmosomal cadherins interact with armadillo family proteins like plakophilins and plakoglobin, which in turn interact with the plakin family protein desmoplakin. Desmoplakin anchors intermediate filaments of the cell that leads to an appearance of an electron dense region when imaged with an

electron microscope ([4] and reviewed in [57]).

Desmosome composition varies depending on tissue type with different tissues expressing different desmosomal cadherins and different plakophilin family members (reviewed in [57]). However, in contrast to other plakophilin family members, plakophilin 3 (PKP3) is ubiquitously expressed in all epithelial tissues with the exception of hepatocytes [8; 9]. PKP3 has been shown to interact with almost all other desmosomal proteins like desmoglein 1, desmoglein 2, desmoglein 3, desmocollin 3a, desmocollin 3b, plakoglobin, desmoplakin, and keratin 18 [10]. Our laboratory has previously demonstrated that PKP3 is essential for desmosome assembly and loss of PKP3 is accompanied by a decrease in desmosome size and cell-cell adhesion, and an increase in cell migration, anchorage independent growth and, tumour formation and lung metastasis in immunocompromised mice [11; 12]. As metastasis is often accompanied by the induction of EMT, the levels of molecular markers of EMT (reviewed in [13-15]) were studied in the PKP3 knockdown cells in comparison to the vector control, to determine whether the increased metastasis observed on PKP3 loss is due to an increase in EMT.

2. MATERIALS AND METHODS:

2.2. Cell lines

The HCT-116 based PKP3 knockdown clones used in this study were previously described [11]. Cells were cultured in Dulbecco's modified Eagles medium (DMEM) (GIBCO) supplemented with 10% Fetal bovine Serum (GIBCO), 100 U of penicillin (Nicholas Piramal), 100 µg/ml of streptomycin (Nicholas Piramal) and 2 µg/ml of amphotericin B (HiMedia) as well as 5 µg/ml of blasticidin (Invitrogen) for selection.

2.3. Real time PCR

RNA was prepared using RNeasy Plus kit (Qiagen). 2µg of RNA was converted to cDNA using High-Capacity cDNA Reverse Transcription Kit (Applied Biosystems). Quantitative real time PCR was performed using SYBR® Green PCR Master Mix (Applied Biosystems) using GAPDH as a control. Fold change was determined by relative quantitation method by determining $2^{-\Delta\Delta C_t}$ values or quantitation was done by determining the $2^{-\Delta C_t}$ values. The significance was determined using the Student's t-test. The primer sequences used are listed in table 1.

2.4. Cell-extracellular matrix adhesion assay

The extracellular matrix (ECM) substrates – Matrigel (BD Biosciences), laminin 5 (Sigma), collagen IV (Sigma) and fibronectin (BD Biosciences) were coated at the concentration of 10 µg/mL in a 96-well plate and incubated overnight at 4°C. After a wash with PBS, the ECM substrates were incubated with 2% BSA for 2 hours at 37°C. 40,000 cells in 100 µL of DMEM with 0.1% BSA were seeded and incubated at 37°C with 5% CO₂ for 30-60 minutes. Non adherent cells were washed gently twice with PBS and the adherent cells were quantitated using MTT (Sigma).

2.5. Immunohistochemistry

The tissue blocks used for immunohistochemistry have been described earlier [11]. Five micron sections of paraffin-embedded formalin fixed tissues were prepared and immunohistochemistry was performed by standard methods [11]. Antigen retrieval was performed by microwaving the tissue for 10 minutes in 3M sodium citrate buffer. Vimentin antibody was used at 1:50 dilution (Sigma M 0725) and staining was performed using M.O.M. staining kit (Vector Laboratories) according to manufacturer's instructions. MMP9 antibody was used at 1:100 dilution (Abcam ab38898) and staining was performed using ABC staining kit (Vector Laboratories) according to manufacturer's instructions. Images were captured using a 10x objective on a Zeiss Axiovert upright microscope.

3. RESULTS AND DISCUSSION:

3.1. PKP3 knockdown does not increase expression of mesenchymal transcription factors *in vitro*

Our lab had previously reported that PKP3 knockdown led to an increase in cell migration, decreased cell-cell adhesion, increased anchorage independent growth and an increase in tumour formation and lung metastasis in immunocompromised mice in HCT116 cells [11]. These phenotypes are characteristic of the changes observed upon induction of EMT (reviewed in [13]). The established “master” regulators of EMT are the transcription factors Snail, Slug, Twist 1 and Zeb 1. Snail, Slug, Twist 1 and Zeb 1 are all known to directly or indirectly repress E-cadherin expression and induce vimentin expression while Slug and Zeb1 are also known to promote dissolution of desmosomes (reviewed in [13,15]). Real time PCR demonstrated that Snail was the only EMT regulating transcription factor that was expressed in both the HCT116 derived vector

control and PKP3 knockdown cells shpkp3-1 and shpkp3-2 (Figure 1A and 1B). However, no significant difference was observed in the Snail expression between the vector control and the PKP3 knockdown cells (Figure 1A). The EMT regulating transcription factors Slug, Twist 1 and Zeb1 were absent in both the vector control and the PKP3 knockdown cells, AW13516 [16; 17] cells were used as a positive control to validate the primers used (Figure 1B). Thus PKP3 knockdown does not lead to any change in the expression of EMT regulating transcription factors with Snail being the only tested EMT regulating transcription factor that is expressed with no significant difference between the HCT116 derived vector control and the PKP3 knockdown cells.

Repression of E-cadherin expression, an adherens cell-cell junction cadherin or change in E-cadherin localization from cell membrane to cytoplasm and induction of vimentin expression, a type III intermediate filament protein, are classical markers of EMT (reviewed in [1315]). Previous results from our lab have demonstrated that vimentin is not expressed in the vector control or the PKP3 knockdown cells [16]. We have also observed that PKP3 knockdown does not change E-cadherin localization to the membrane [12]. Thus PKP3 knockdown does not lead to change in any of the tested molecular markers of EMT *in vitro*.

3.2. PKP3 knockdown does not change cell-ECM substrate adhesion

Cells interact with their microenvironment through integrin based focal adhesions or hemidesmosomes. The physical interaction of integrin with the proteins in the extracellular matrix (ECM) leads to activation of integrin based signal transduction cascades through activation of integrin associated kinases like Src or FAK (reviewed in [13; 18; 19]). The activation of these signalling cascades is

promoted by an increase in focal adhesion turnover and reduced focal adhesion strength that aides cell migration and decreases cell-ECM adhesion [18; 19]. An increase in cell migration accompanied by a decrease in cell-ECM adhesion is thus an important functional change observed in EMT. As our previous results showed that PKP3 knockdown leads to an increase in cell migration [11], we hence investigated whether PKP3 loss also leads to a decrease in cell-ECM adhesion. Cell-ECM substrate adhesion assays showed that PKP3 knockdown does not change the cell adhesion to any of the substrates tested like Matrigel, fibronectin, laminin 5 and collagen IV (Figure 1C). This shows that Pkp3 knockdown does not show the EMT phenotype of decrease in cell-ECM substrate adhesion.

3.3. PKP3 knockdown does not increase expression of mesenchymal factors *in vivo*

Although PKP3 knockdown did not show expression of EMT markers *in vitro*, the increased primary tumour growth and lung metastasis observed in immunocompromised mice lead to the question whether an EMT is observed in when these cells grow as tumours in immunocompromised mice.

Immunohistochemistry studies with markers of mesenchymal cells such as vimentin and MMP9, a matrix metalloprotease that is known to promote invasion and aide metastasis (reviewed in [1315]), showed the presence of both mesenchymal markers vimentin and MMP9, in the tumour as well as the lung metastasis, in both the vector control as well as the PKP3 knockdown shpkp3-2 samples (Figure 1D and 1E). The presence of these mesenchymal markers shows that EMT does indeed take place *in vivo*, but it is not induced or enhanced by PKP3 knockdown. Thus PKP3 knockdown does not induce or enhance EMT *in vivo*.

Table: 1**List of primers used for real time PCR.**

S. No.	Name of primer	Sequence
1	Slug fwd	AGACCCCCATGCCATTGAAG
2	Slug rev	GGCCAGCCCAGAAAAAGTTG
3	Snail fwd	TAGCGAGTGGTTCTTCTGCG
4	Snail rev	AGGGCTGCTGGAAGGTAAAC
5	Twist 1 fwd	AGCTGAGCAAGATTCAGACCC
6	Twist 1 rev	GCAGCTTGCCATCTTGGAGT
7	Zeb 1 fwd	AGGATGACCTGCCAACAGAC
8	Zeb 1 rev	CTTCAGGCCCCAGGATTCTT

4. CONCLUSION:

Multiple reports in the literature suggest that the induction of EMT is required for tumour progression and metastasis (reviewed in [13]). Our lab had previously shown that PKP3 knockdown promotes neoplastic progression and metastasis [11]. Some of the effects of PKP3 knockdown like an increase in cell migration, decrease in cell-cell adhesion as well as increase in tumour formation and lung metastasis are synonymous with characteristics of EMT [11]. However, in the present study, we show that PKP3 knockdown does not induce or enhance expression of any of the tested mesenchymal markers nor does it change cell-ECM adhesion. We conclude that PKP3 knockdown does not promote neoplastic progression through the process of EMT.

List of abbreviations used:

EMT = epithelial mesenchymal transition
 PKP3 = plakophilin 3
 ECM = extracellular matrix
 FAK = focal adhesion kinase
 Src = sarcoma
 MMP9 = matrix metalloprotease 9
 PCR = polymerase chain reaction

Competing interests:

The authors declare that they have no competing interests.

Acknowledgements:

We would like to thank Mr. Mohd Yasser and Dr. Tanuja Teni for providing AW13516 mRNA samples. We thank the ACTREC histology and microscope facilities. M.G. and K.R. were supported by fellowships from CSIR. This work was supported in part by grants from the Department of Biotechnology (DBT) and ACTREC.

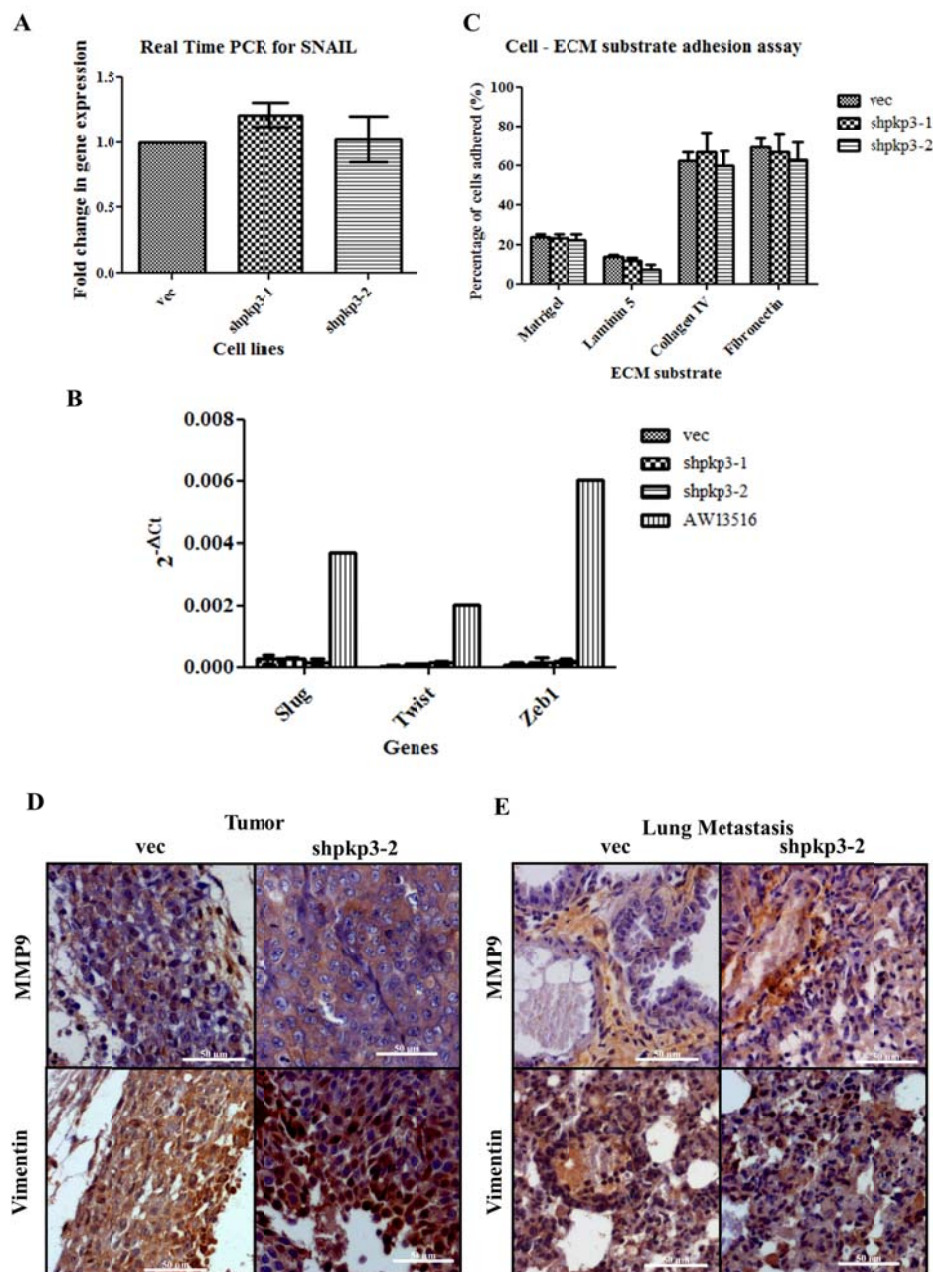
Figure 1

Figure 1. Plakophilin 3 knockdown does not lead to EMT both *in vitro* and *in vivo*. A. RNA was isolated from the HCT116 derived vector control (vec) and PKP3 knockdown clones (shpkp3-1 and shpkp3-2) and quantitative real time PCR was performed to detect the levels of Snail. GAPDH was used as a control. The fold change in expression is plotted on the Y-axis. B. RNA was isolated from the indicated cell types and quantitative real time PCR was performed to detect the levels of Slug, Twist and Zeb1. GAPDH was used as a control. $2^{-\Delta Ct}$ values are plotted on the Y-axis. Note that the HCT116 derived cells do not express these transcription factors in contrast to the AW13516 cells. C. Cell – ECM substrate adhesion assays were performed with the indicated ECM substrates and the percentage of adhered cells determined and the mean and standard deviation from three independent experiments was plotted on the Y-axis. D-E. Cells were injected subcutaneously in immunocompromised mice and immunohistochemical staining was performed on paraffin embedded sections of the primary tumour and lung metastases with the indicated antibodies. Images were captured on a Zeiss Axiovert upright microscope with a 40x objective. Representative images are shown. (A-C. p values were determined using a Student's t-test.)

5. REFERENCES:

- [1]. Baum, B., J. Settleman, and M. P. Quinlan (2008) Transitions between epithelial and mesenchymal states in development and disease. *Semin Cell Dev Biol.* 19: 294-308.
- [2]. Kalluri, R., and R. A. Weinberg (2009) The basics of epithelial-mesenchymal transition. *J Clin Invest.* 119: 1420-1428.
- [3]. Thiery, J. P., and J. P. Sleeman (2006) Complex networks orchestrate epithelial-mesenchymal transitions. *Nat Rev Mol Cell Biol.* 7: 131-142.
- [4]. North, A. J., W. G. Bardsley, J. Hyam, E. A. Bornslaeger, H. C. Cordingley, B. Trinnaman, M. Hatzfeld, K. J. Green, A. I. Magee, and D. R. Garrod (1999) Molecular map of the desmosomal plaque. *J Cell Sci.* 112 (Pt 23): 4325-4336.
- [5]. Harmon, R. M., and K. J. Green (2013) Structural and functional diversity of desmosomes. *Cell Commun Adhes.* 20: 171-187.
- [6]. Garrod, D. (2010) Desmosomes in vivo. *Dermatol Res Pract.* 2010: 212439.
- [7]. Desai, B. V., R. M. Harmon, and K. J. Green (2009) Desmosomes at a glance. *J Cell Sci.* 122: 4401-4407.
- [8]. Bonne, S., J. van Hengel, F. Nollet, P. Kools, and F. van Roy (1999) Plakophilin-3, a novel armadillo-like protein present in nuclei and desmosomes of epithelial cells. *J Cell Sci.* 112 (Pt 14): 2265-2276.
- [9]. Schmidt, A., L. Langbein, S. Pratzel, M. Rode, H. R. Rackwitz, and W. W. Franke (1999) Plakophilin 3--a novel cell-type-specific desmosomal plaque protein. *Differentiation.* 64: 291-306.
- [10]. Bonne, S., B. Gilbert, M. Hatzfeld, X. Chen, K. J. Green, and F. van Roy (2003) Defining desmosomal plakophilin-3 interactions. *J Cell Biol.* 161: 403-416.
- [11]. Kundu, S. T., P. Gosavi, N. Khapare, R. Patel, A. S. Hosang, G. B. Maru, A. Ingle, J. A. Decaprio, and S. N. Dalal (2008) Plakophilin3 downregulation leads to a decrease in cell adhesion and promotes metastasis. *Int J Cancer.* 123: 2303-2314.
- [12]. Gosavi, P., S. T. Kundu, N. Khapare, L. Sehgal, M. S. Karkhanis, and S. N. Dalal (2011) E-cadherin and plakoglobin recruit plakophilin3 to the cell border to initiate desmosome assembly. *Cell Mol Life Sci.* 68: 1439-1454.
- [13]. Lee, J. M., S. Dedhar, R. Kalluri, and E. W. Thompson (2006) The epithelial-mesenchymal transition: new insights in signaling, development, and disease. *J Cell Biol.* 172: 973-981.
- [14]. Zeisberg, M., and E. G. Neilson (2009) Biomarkers for epithelial-mesenchymal transitions. *J Clin Invest.* 119: 1429-1437.
- [15]. Moreno-Bueno, G., H. Peinado, P. Molina, D. Olmeda, E. Cubillo, V. Santos, J. Palacios, F. Portillo, and A. Cano (2009) The morphological and molecular features of the epithelial-to-mesenchymal transition. *Nat Protoc.* 4: 1591-1613.
- [16]. Khapare, N., S. T. Kundu, L. Sehgal, M. Sawant, R. Priya, P. Gosavi, N. Gupta, H. Alam, M. Karkhanis, N. Naik, M. M. Vaidya, and S. N. Dalal (2012) Plakophilin3 loss leads to an increase in PRL3 levels promoting K8 dephosphorylation, which is required for transformation and metastasis. *PLoS One.* 7: e38561.
- [17]. Alam, H., S. T. Kundu, S. N. Dalal, and M. M. Vaidya (2011) Loss of keratins 8 and 18 leads to alterations in alpha6beta4-integrin-mediated signalling and decreased neoplastic progression in an oral-tumour-derived cell line. *J Cell Sci.* 124: 2096-2106.
- [18]. Gardel, M. L., I. C. Schneider, Y. Aratyn-Schaus, and C. M. Waterman (2010) Mechanical integration of actin and adhesion dynamics in cell migration. *Annu Rev Cell Dev Biol.* 26: 315-333.
- [19]. Nagano, M., D. Hoshino, N. Koshikawa, T. Akizawa, and M. Seiki (2012) Turnover of focal adhesions and cancer cell migration. *Int J Cell Biol.* 2012: 310616.

Plakophilin3 and Plakoglobin recycling are differentially regulated during the disassembly of desmosomes.

K. Raychaudhuri, M. Gurjar and S. N. Dalal*.

KS230, Advanced Centre for Treatment, Research and Education in Cancer (ACTREC), Tata Memorial Centre, Sector 22, Kharghar, Navi Mumbai, 410210, India.

*For Correspondence: sdalal@actrec.gov.in

ABSTRACT:

During cell migration, wound healing and tissue remodeling the desmosome goes through cycles of assembly and disassembly. Desmosome assembly requires the localization of two armadillo (ARM) repeat containing proteins, plakophilin3 (PKP3) and plakoglobin (PG), at the cell border. **Aims:** The goal of this study was to determine the regulation of transport of PKP3 and PG during desmosome assembly and disassembly. We particularly investigated the contribution of microtubules (MT) in the transport of these proteins to and from the cell border during desmosome assembly and disassembly. **Methods:** Nocodazole was used to disrupt microtubules in HCT116 cells and anterograde and retrograde transport of desmosomal proteins were investigated by calcium switch and calcium chelation experiments respectively followed by confocal microscopy. **Results:** The results in this paper demonstrate that microtubule dependent anterograde transport is required for the localization of PKP3 and PG to the cell border. However, during desmosome disassembly, retrograde transport of PKP3 but not PG, was dependent on an intact microtubule network. PKP3 is retained at the cell border, unlike other desmosomal proteins, when microtubule organization was disrupted. **Conclusion:** These results suggest that PKP3 transport from the cell border to the cytoplasm occurs via a mechanism that is distinct from other desmosomal proteins and might reflect functions of PKP3 that are independent of its role in desmosome formation and maintenance.

Key words:

Desmosome;
Plakophilin3;
Plakoglobin;
Microtubule;
Anterograde transport;
Retrograde transport.

1. INTRODUCTION

Desmosomes are calcium dependent cell-cell junctions that anchor intermediate filaments (IF) to the cell membrane resulting in the formation of a tissue wide IF network and provide mechanical strength and rigidity to tissues [1,2,3]. Desmosomes are composed of the plasma membrane spanning cadherins (desmogleins [DSGs] and desmocollins [DSCs]), the ARM family proteins (plakoglobin [PG] and plakophilins [PKPs]) and a Plakin family member such as desmoplakin (DP), which connects the desmosome to the IF network [2,4]. Desmosomes are very dynamic structures [5], especially when cells migrate in a specific direction during wound healing [6,7]. The rate of cell migration is determined by the assembly and disassembly of desmosomes. Deregulation of the desmosome assembly-disassembly cycle can lead to abnormal

development, tumor progression or to diseases such as Pemphigus Vulgaris (PV) [8,9,10,11,12,13,14].

During desmosome assembly, the desmosomal proteins are transported from the cytoplasm to the cell border and during desmosome disassembly; the desmosomal proteins are transported from the cell border to the cytoplasm. Multiple reports have demonstrated that both actin filaments and microtubules are required for the transport of desmosomal proteins during desmosome assembly e.g. transport of DP is dependent on an actin filament network, whereas an intact microtubule network is required for the transport of desmosomal cadherins and PG to the cell border. [9,15,16,17,18]. However, the mechanisms underlying the retrograde transport of desmosomal proteins i.e. from the cell border to the cytoplasm remain unclear [11,15,16,17,19].

The regulation of transport of PKP3 and PG to and from the cell border is important as our previous results suggest that depletion of either PG or PKP3 led to defects in desmosome assembly as the other desmosomal proteins fail to localize to the cell border [11,12,20]. PG transport to the desmosome is microtubule dependent and is mediated by 14-3-3 γ and the KIF5B motor protein and is required for desmosome formation [9]. Therefore, we wished to determine whether the transport of PG and PKP3 are regulated by the same mechanisms during desmosome assembly and disassembly. To our surprise we observed that while both proteins required an intact microtubule network for transport to the cell border, only PKP3 required an intact microtubule network for transport from the cell border to the cytoplasm during desmosome disassembly.

2. MATERIALS AND METHODS

2.1 Tissue culture.

The HCT116 (ATCC) cell line was cultured in Dulbecco's modified Eagles medium (DMEM) (GIBCO) supplemented with 10% Fetal bovine Serum (JRH), 100 U of penicillin (Nicholas Piramal), 100 μ g/ml of streptomycin (Nicholas Piramal) and 2 μ g/ml of amphotericin B (HiMedia).

2.2 Immunofluorescence.

HCT116 cells were fixed in absolute methanol for 10 minutes at -20°C to detect α -tubulin, PKP3 and DP or in 4% paraformaldehyde for 20 minutes at room temperature to detect DSC2/3. After fixation, cells were permeabilized with Triton X-100 as described previously [11]. PKP3, DP DSC2/3 and α -tubulin antibodies were used for immunofluorescence analysis as described previously [9,10,11,12]. DAPI was used to stain the nucleus as previously described [9]. Confocal images were obtained by using a

LSM 510 Meta Carl Zeiss confocal system with argon 488-nm laser. All images were obtained by using LSM meta software at a magnification of X630 (X63 objective and X10 eyepiece) with 1X, 2X or 4X optical zoom. The fluorescence intensity of staining at the cell border was measured for the different proteins in a minimum of 30 cells using the Image J software (NIH). Mean and standard deviation were plotted and p values determined using a student's t test.

3. RESULTS

3.1. Anterograde transport of PKP3 and PG is microtubule dependent.

Our previous results suggest that PG transport to the cell border requires an intact microtubule network and that PKP3 and PG are required for desmosome assembly [9,11]. To address whether microtubules (MT) are required for the initiation of desmosome formation and transport of PKP3 to the cell border in HCT116 cells, nocodazole (NOC) was used to disrupt the microtubule network. Incubation of HCT116 cells with 10 μ M NOC for 3 hours completely disrupted the MT network (Fig 1A). To determine the role of MT in anterograde transport of PKP3 during desmosome assembly, a calcium switch experiment was performed in cells treated with NOC (to disrupt MT) or DMSO (vehicle control) as described in Fig 1B. An immunofluorescence analysis showed that cell border localization of both PKP3 and PG was compromised upon disruption of MT post addition of calcium in comparison to DMSO treated cells (Fig 1C & E). Quantitation of the fluorescence intensity at the cell border after 30 minutes of calcium addition showed that recovery of both PKP3 and PG border staining intensity was significantly compromised in NOC treated cells compared to DMSO treated cells (Fig 1D & F). However, no appreciable difference in cell border localization was observed at 0 minute post calcium switch in

cell border intensity of either PKP3 or PG between NOC and DMSO treated cells (Fig 1C-F). Line scans drawn across the cell showed that at 0 minute post calcium switch both PKP3 and PG did not localize at the cell border and remained cytoplasmic and at 30 minutes post calcium switch localized to the cell border in DMSO treated cells but not in NOC treated cells (Fig 2). These results confirmed that the cell border recruitment of PKP3 and PG are dependent on an intact MT network and both these proteins followed a similar pattern of anterograde transport.

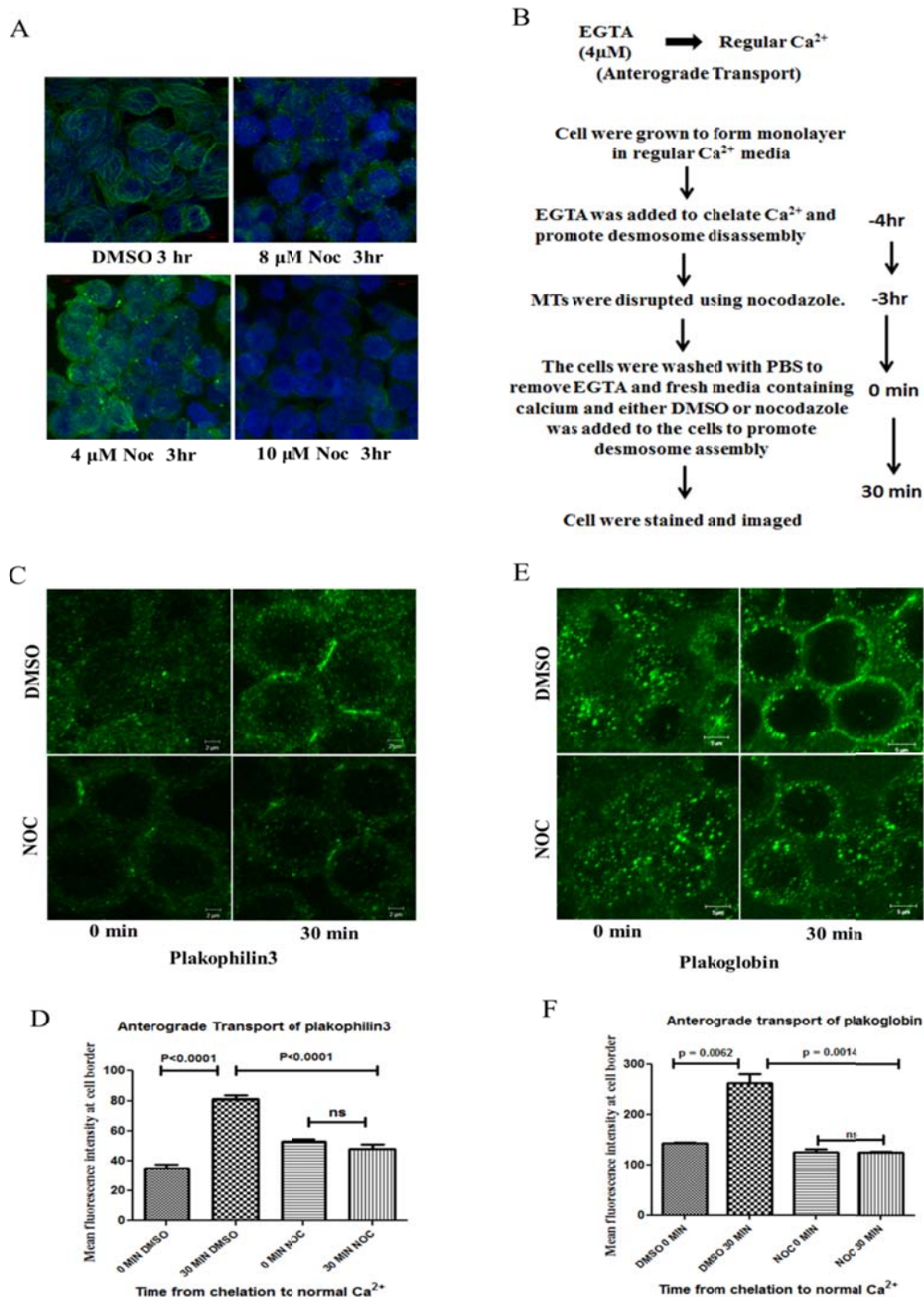
3.2. The retrograde transport of PKP3 and PG are differentially regulated.

Since desmosomes are dynamic and undergo continual assembly and disassembly during cell migration [6], we wished to determine the mechanism of transport of PKP3 and PG from the cell border to the cytoplasm during desmosome disassembly. To investigate the role of MT in the regulation of PKP3 transport during desmosome disassembly, EGTA was added to the medium to chelate calcium as described [21,22], either in the presence or absence of NOC (Fig 3A). Three hours post addition of EGTA, PKP3 was localized at the cell border in NOC treated cells. In contrast, PKP3 levels decreased at the cell border in cells treated with DMSO upon chelation of calcium (Fig 3B). No difference was observed in the localization of PKP3 in NOC and DMSO treated cells prior to addition of EGTA (Fig 3B). Quantitation of fluorescence intensities at the cell border established that these differences were statistically significant (Fig 3C). Consistent with these observations, line scans drawn across the cell showed a peak of fluorescence intensity for PKP3 staining at the cell border on NOC treatment, which was not observed in DMSO treated cells (Fig 4). These results suggest that retrograde transport of PKP3 from the cell border to the cytoplasm is dependent on MT. In contrast, it was

observed that NOC treatment had no effect on retrograde transport of PG upon addition of EGTA. PG localized to the cytoplasm in both NOC and DMSO treated cells 3hr post addition of EGTA (Fig 3D-E). Line scans drawn across the cell showed extensive cytoplasmic accumulation of PG at 3hr post EGTA addition in both NOC and DMSO treated cells (Fig 4). These results suggest that an intact MT network is not required for the retrograde transport of PG and different mechanisms regulate the retrograde transport of PKP3 and PG during desmosome disassembly.

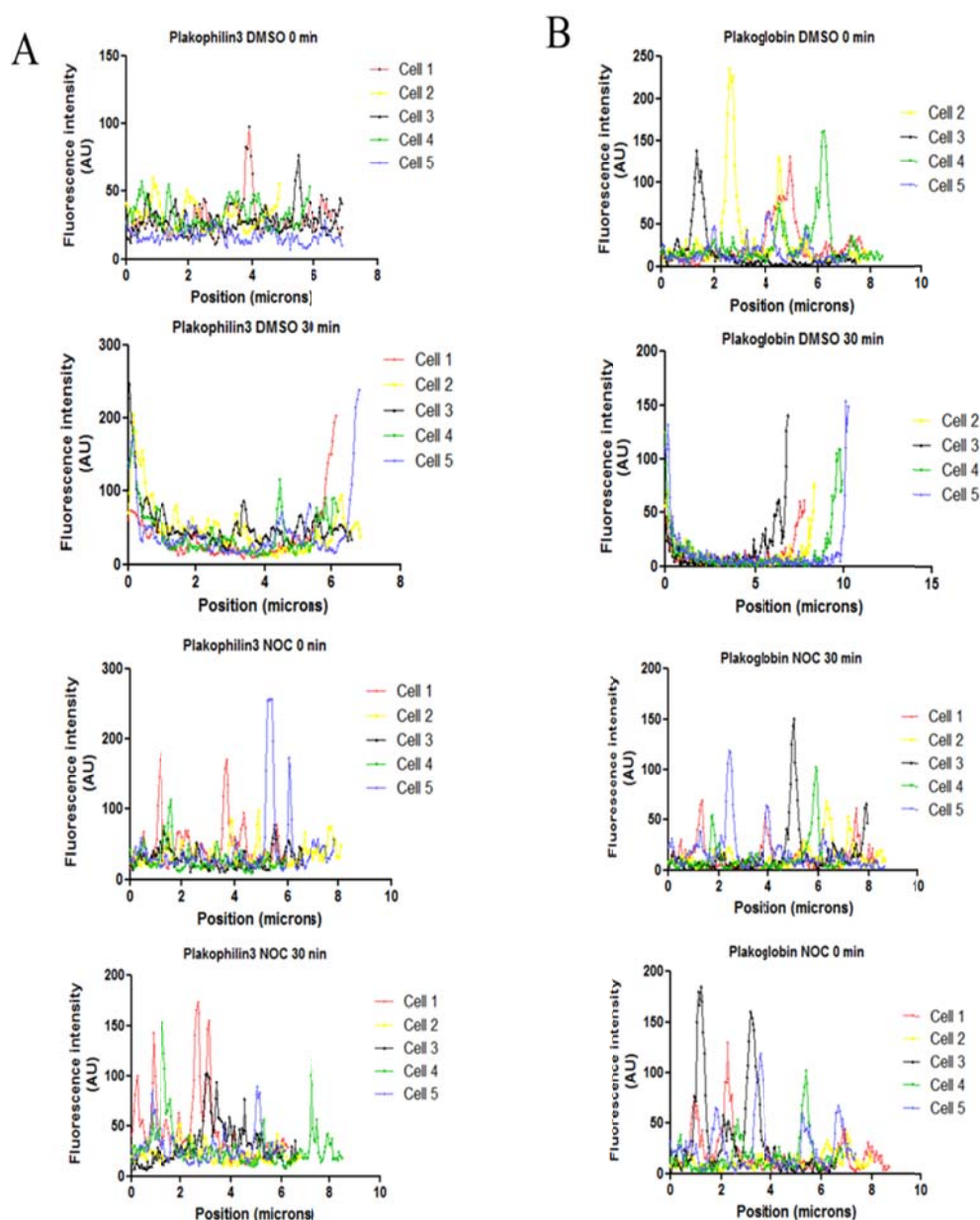
3.3. Inhibition of retrograde transport of PKP3 does not inhibit desmosome disassembly.

We have previously shown that PKP3 is required for transport of desmosomal proteins such as DSC2/3, DSG2, PKP2 and DP to the cell border and is required for initiation of desmosome assembly in HCT116 and HaCaT cells [11]. Similarly, other groups have demonstrated that loss of PKP3 leads to diffused cytoplasmic localization of DP in HaCaT and SCC9 cells [20]. To determine whether retention of PKP3 at the cell border resulted in the retention of other desmosomal proteins at the cell border, the localization of DP and DSC2/3 in cells treated with NOC during desmosome disassembly was determined as described above. Though PKP3 is retained at the cell border 3hr post calcium chelation, both DP and DSC2/3 were not retained at the cell border (Fig 3F&H). At 3hr post chelation, the levels of DP and DSC2/3 were diminished at the cell border in both NOC and DMSO treated cells, a phenotype similar to that observed for PG (Fig 3G&I). These results suggest that PKP3 retention at the cell border upon calcium chelation is not sufficient for the retention of other desmosomal proteins at the cell border.

Figure 1.**Anterograde transport of PKP3 and PG is dependent on an intact microtubule network.**

(A) HCT116 cells were treated with DMSO or the indicated concentration of NOC for 3hrs. Cells were stained with antibodies to α -tubulin to visualize MT and counterstained with DAPI. Magnification is X630 magnification with 2X optical zoom. (B) Scheme of experiment to study anterograde transport of PKP3 and PG. (C-F) HCT116 cells treated with EGTA and NOC or DMSO were fixed and stained with antibodies to PKP3 (C-D) or PG (E-F) followed by confocal microscopy. The intensity of border staining for both PKP3 and PG was measured for in least 30 cells in three independent experiments and the mean and standard deviation were plotted. Magnification is X630 with 4X optical zoom and bars indicate 5 μ m. p values were generated using a student's t test.

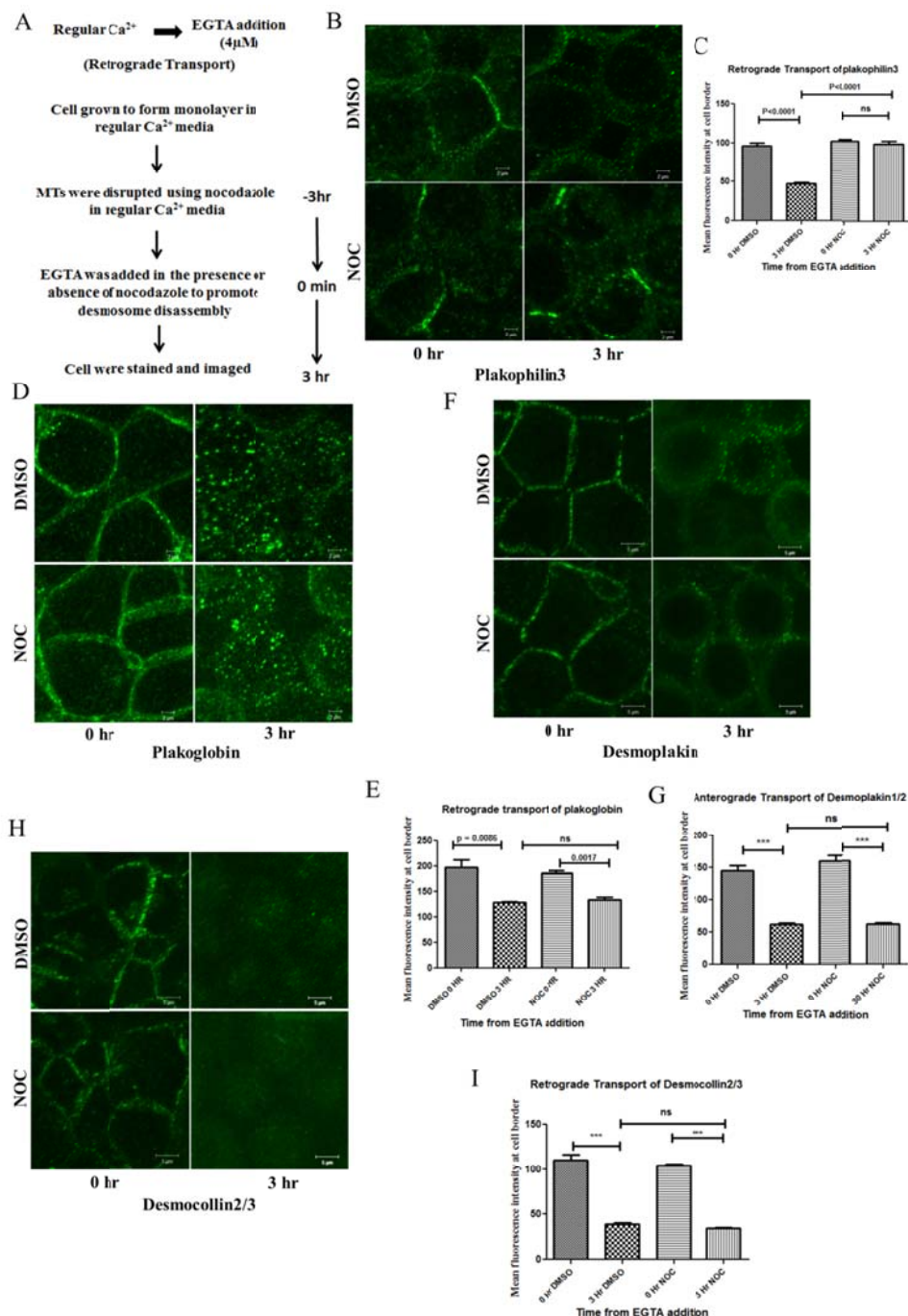
Figure. 2
Effect of nocodazole on anterograde transport of plakophilin3 and plakoglobin.



(A-B) Line scans were drawn across 5 random cells that were immunostained for PKP3

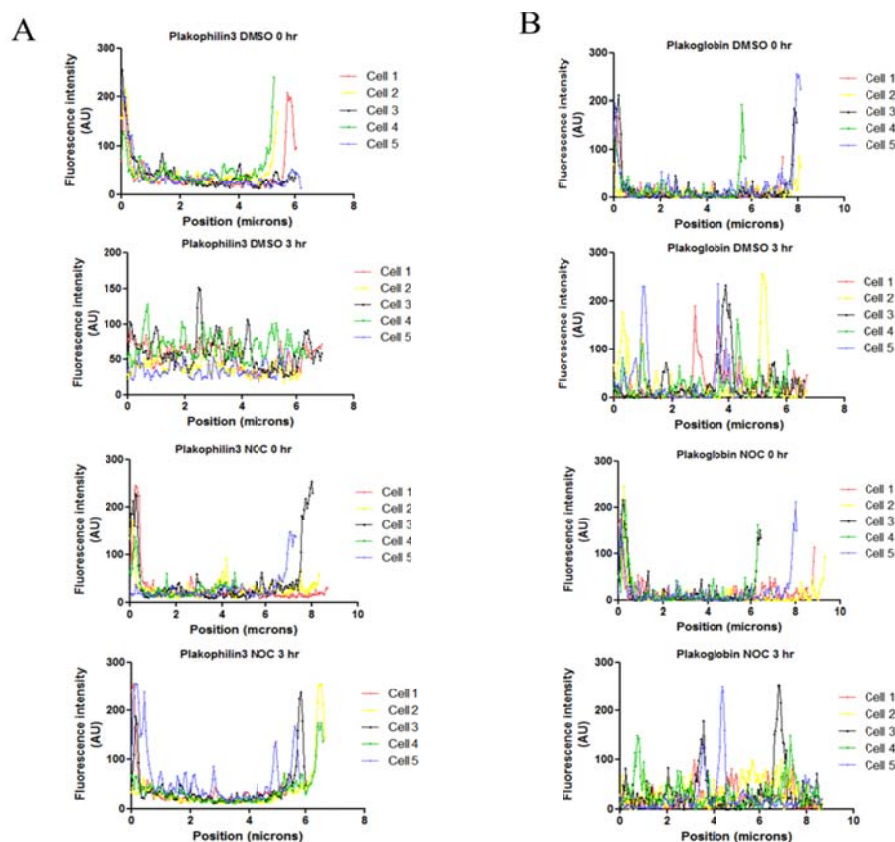
(A) or PG (B) 30 minutes post calcium addition. Fluorescence intensities were measured across the line using Image J and were plotted on the Y-axis. X axis represents position along the line that was drawn across the diameter of the cell.

Figure 3.
Disruption of the microtubule network blocks retrograde transport of PKP3
but does not inhibit desmosome disassembly.



(A) Scheme of experiment to study retrograde transport of desmosomal proteins. (B-I) HCT116 cells were treated with EGTA and NOC or DMSO and stained with antibodies to PKP3 (B-C), PG (D-E) DP (F-G) and DSC2/3 (H-I) followed by confocal microscopy. The intensity of staining at the cell border was measured for at least 30 cells in three independent experiments and mean and standard deviation were plotted. Note that disruption of the MT network results in a defect in the transport of PKP3 from the cell border to the cytoplasm in contrast to the results observed for the other desmosomal proteins. Confocal images were acquired at X630 magnification and 4X optical zoom. Bars indicate 5 μm . p values were generated using a student's t-test.

Figure 4.
Effect of nocodazole on retrograde transport of plakophilin3 and plakoglobin.



(A-B) Line scans were drawn across 5 random cells that were immunostained for PKP3 (A) or PG (B) three hours post addition of EGTA. Fluorescence intensities were measured across the line using Image J and were plotted on the Y-axis. X axis represents position along the line that was drawn across the diameter of the cell.

4. DISCUSSION

The process of desmosome assembly and disassembly is not completely understood, especially the process of desmosome disassembly. As the process of desmosome assembly and disassembly is essential for cell migration during wound healing and other developmental processes, this report focused on the identifying the requirements for the transport PG and PKP3, which are both required for desmosome formation, during desmosome assembly. The results presented in this report demonstrate that the transport of PG and PKP3 from the cell border to the cytoplasm upon desmosome disassembly is differentially regulated, with an intact MT

network being an absolute requirement for the retrograde transport of PKP3. These results suggest that the different ARM proteins are transported to the cytoplasm by different pathways upon desmosome disassembly.

It is also interesting to note that border retention of PKP3 on treatment with NOC at 3hr post calcium chelation was not sufficient to retain DP and DSC2/3 at the cell border. While PKP3 plays a crucial role in recruiting DP, PKP2, DSG2 and DSC2/3 proteins to the cell border [10,11,15,20], the results reported here suggest that PKP3 might not play a similar role during desmosome disassembly. It is possible that loss of PKP3 from the cell border is not required for desmosome

disassembly and that the PKP3 present at the cell border under conditions of calcium chelation might have desmosome independent functions or serve as a marker for the formation of new desmosomes upon the restoration of calcium to the medium. Further, Kowalczyk *et.al.* have shown that PV IgG antibodies against DSG3 that are produced during the autoimmune disease PV cause dissolution of desmosomes, retraction of keratin filaments and internalization of DSG3 in a complex with PG and DP in a membrane raft dependent manner [23,24,25]. It is possible that upon addition of EGTA, PKP3 is localized to a portion of the membrane not associated with membrane rafts; thereby preventing its internalization along with the other desmosomal proteins.

Both PG and PKP3 required an intact MT network to be transported to the cell border and transport of PG to the cell border is dependent on KIF5B and KLC1 [9]. However, unlike PKP3, transport of PG from the cell border to the cytoplasm upon calcium chelation did not require an intact MT network. These results indicate that some other yet unidentified transport process is responsible for retrograde transport of PG and other desmosomal proteins such as DP and DSC2/3 that is independent of an intact MT network. Other reports suggest that both MT and actin filaments are required for the transport of DSC2 to the cell border [15,17]. Therefore, an actin based mechanism might regulate the retrograde transport of PG, DP and DSC2/3 in HCT116 cells.

5. CONCLUSION

In conclusion, our studies have determined that an intact MT network is required for the retrograde transport of PKP3 during desmosome disassembly and suggest that PKP3 and PG might have different roles to play during desmosome disassembly. However, additional studies are required to

address the significance of the MT network in regulating desmosome disassembly and in regulation of PKP3 transport.

Conflict of Interest

The authors have no conflict of interest.

Acknowledgements

We thank Dr. Rita Mulherkar for critically reading the manuscript. KK and MG were supported by a fellowship from Council of Scientific and Industrial Research, Ministry of Human Resource and Development. This work was supported by grants from the Department of Biotechnology, Government of India and ACTREC.

6. REFERENCES

- [1]. B.V. Desai, R.M. Harmon, K.J. Green, Desmosomes at a glance, *Journal of cell science* 122 (2009) 4401-4407.
- [2]. E. Delva, D.K. Tucker, A.P. Kowalczyk, The desmosome, *Cold Spring Harbor perspectives in biology* 1 (2009) a002543.
- [3]. K.J. Green, C.L. Simpson, Desmosomes: new perspectives on a classic, *The Journal of investigative dermatology* 127 (2007) 2499-2515.
- [4]. B. Holthofer, R. Windoffer, S. Troyanovsky, R.E. Leube, Structure and function of desmosomes, *International review of cytology* 264 (2007) 65-163.
- [5]. R. Windoffer, M. Borchert-Stuhltrager, R.E. Leube, Desmosomes: interconnected calcium-dependent structures of remarkable stability with significant integral membrane protein turnover, *Journal of cell science* 115 (2002) 1717-1732.
- [6]. K.J. Green, S. Getsios, S. Troyanovsky, L.M. Godsel, Intercellular junction assembly, dynamics, and homeostasis, *Cold Spring Harbor perspectives in biology* 2 (2010) a000125.
- [7]. O. Ilina, P. Friedl, Mechanisms of collective cell migration at a glance, *Journal of cell science* 122 (2009) 3203-3208.
- [8]. Y. Kitajima, New insights into desmosome regulation and pemphigus blistering as a desmosome-remodeling disease, *The Kaohsiung journal of medical sciences* 29 (2013) 1-13.
- [9]. L. Sehgal, A. Mukhopadhyay, A. Rajan, N. Khapare, M. Sawant, S.S. Vishal, K. Bhatt, S. Ambatipudi, N. Antao, H. Alam, M. Gurjar, S. Basu, R. Mathur, L. Borde, A.S. Hosing, M.M.

- Vaidya, R. Thorat, F. Samaniego, U. Kolthur-Seetharam, S.N. Dalal, 14-3-3gamma-Mediated transport of plakoglobin to the cell border is required for the initiation of desmosome assembly in vitro and in vivo, *Journal of cell science* 127 (2014) 2174-2188.
- [10]. N. Khapare, S.T. Kundu, L. Sehgal, M. Sawant, R. Priya, P. Gosavi, N. Gupta, H. Alam, M. Karkhanis, N. Naik, M.M. Vaidya, S.N. Dalal, Plakophilin3 loss leads to an increase in PRL3 levels promoting K8 dephosphorylation, which is required for transformation and metastasis, *PloS one* 7 (2012) e38561.
- [11]. P. Gosavi, S.T. Kundu, N. Khapare, L. Sehgal, M.S. Karkhanis, S.N. Dalal, E-cadherin and plakoglobin recruit plakophilin3 to the cell border to initiate desmosome assembly, *Cellular and molecular life sciences : CMLS* 68 (2011) 1439-1454.
- [12]. S.T. Kundu, P. Gosavi, N. Khapare, R. Patel, A.S. Hosing, G.B. Maru, A. Ingle, J.A. Decaprio, S.N. Dalal, Plakophilin3 downregulation leads to a decrease in cell adhesion and promotes metastasis, *International journal of cancer. Journal international du cancer* 123 (2008) 2303-2314.
- [13]. J.P. Dou, B. Jiao, J.J. Sheng, Z.B. Yu, [Dynamic assembly of intercalated disc during postnatal development in the rat myocardium], *Sheng li xue bao : [Acta physiologica Sinica]* 66 (2014) 569-574.
- [14]. A. Vreeker, L. van Stuijvenberg, T.J. Hund, P.J. Mohler, P.G. Nikkels, T.A. van Veen, Assembly of the cardiac intercalated disk during pre- and postnatal development of the human heart, *PloS one* 9 (2014) e94722.
- [15]. B.J. Roberts, A. Pashaj, K.R. Johnson, J.K. Wahl, 3rd, Desmosome dynamics in migrating epithelial cells requires the actin cytoskeleton, *Experimental cell research* 317 (2011) 2814-2822.
- [16]. L.M. Godsel, S.N. Hsieh, E.V. Amargo, A.E. Bass, L.T. Pascoe-McGillicuddy, A.C. Huen, M.E. Thorne, C.A. Gaudry, J.K. Park, K. Myung, R.D. Goldman, T.L. Chew, K.J. Green, Desmoplakin assembly dynamics in four dimensions: multiple phases differentially regulated by intermediate filaments and actin, *The Journal of cell biology* 171 (2005) 1045-1059.
- [17]. O.E. Nekrasova, E.V. Amargo, W.O. Smith, J. Chen, G.E. Kreitzer, K.J. Green, Desmosomal cadherins utilize distinct kinesins for assembly into desmosomes, *The Journal of cell biology* 195 (2011) 1185-1203.
- [18]. S. McHarg, G. Hopkins, L. Lim, D. Garrod, Down-regulation of desmosomes in cultured cells: the roles of PKC, microtubules and lysosomal/proteasomal degradation, *PloS one* 9 (2014) e108570.
- [19]. I.D. Burdett, K.H. Sullivan, Desmosome assembly in MDCK cells: transport of precursors to the cell surface occurs by two phases of vesicular traffic and involves major changes in centrosome and Golgi location during a Ca(2+) shift, *Experimental cell research* 276 (2002) 296-309.
- [20]. V. Todorovic, J.L. Koetsier, L.M. Godsel, K.J. Green, Plakophilin 3 mediates Rap1-dependent desmosome assembly and adherens junction maturation, *Molecular biology of the cell* 25 (2014) 3749-3764.
- [21]. C. Ramachandran, S.P. Srinivas, Formation and disassembly of adherens and tight junctions in the corneal endothelium: regulation by actomyosin contraction, *Investigative ophthalmology & visual science* 51 (2010) 2139-2148.
- [22]. B. Rothen-Rutishauser, F.K. Riesen, A. Braun, M. Gunthert, H. Wunderli-Allenspach, Dynamics of tight and adherens junctions under EGTA treatment, *The Journal of membrane biology* 188 (2002) 151-162.
- [23]. J.M. Jennings, D.K. Tucker, M.D. Kottke, M. Saito, E. Delva, Y. Hanakawa, M. Amagai, A.P. Kowalczyk, Desmosome disassembly in response to pemphigus vulgaris IgG occurs in distinct phases and can be reversed by expression of exogenous Dsg3, *The Journal of investigative dermatology* 131 (2011) 706-718.
- [24]. S.N. Stahley, M. Saito, V. Faundez, M. Koval, A.L. Mattheyses, A.P. Kowalczyk, Desmosome assembly and disassembly are membrane raft-dependent, *PloS one* 9 (2014) e87809.
- [25]. C.C. Calkins, S.V. Setzer, J.M. Jennings, S. Summers, K. Tsunoda, M. Amagai, A.P. Kowalczyk, Desmoglein endocytosis and desmosome disassembly are coordinated responses to pemphigus autoantibodies, *The Journal of biological chemistry* 281 (2006) 7623-7634.

RESEARCH ARTICLE

14-3-3 γ -mediated transport of plakoglobin to the cell border is required for the initiation of desmosome assembly *in vitro* and *in vivo*

Lalit Sehgal^{1,2}, Amitabha Mukhopadhyay¹, Anandi Rajan^{1,*}, Nileema Khapare^{1,*}, Mugdha Sawant^{1,*}, Sonali S. Vishal¹, Khyati Bhatt¹, Srikant Ambatipudi¹, Noelle Antao¹, Hunain Alam¹, Mansa Gurjar¹, Srikanta Basu¹, Rohit Mathur², Lalit Borde³, Amol S. Hosing¹, Milind M. Vaidya¹, Rahul Thorat¹, Felipe Samaniego², Ullas Kolthur-Seetharam³ and Sorab N. Dalal^{1,†}

ABSTRACT

The regulation of cell–cell adhesion is important for the processes of tissue formation and morphogenesis. Here, we report that loss of 14-3-3 γ leads to a decrease in cell–cell adhesion and a defect in the transport of plakoglobin and other desmosomal proteins to the cell border in HCT116 cells and cells of the mouse testis. 14-3-3 γ binds to plakoglobin in a PKC μ -dependent fashion, resulting in microtubule-dependent transport of plakoglobin to cell borders. Transport of plakoglobin to the border is dependent on the KIF5B–KLC1 complex. Knockdown of KIF5B in HCT116 cells, or in the mouse testis, results in a phenotype similar to that observed upon 14-3-3 γ knockdown. Our results suggest that loss of 14-3-3 γ leads to decreased desmosome formation and a decrease in cell–cell adhesion *in vitro*, and in the mouse testis *in vivo*, leading to defects in testis organization and spermatogenesis.

KEY WORDS: 14-3-3 γ , Desmosome, Plakoglobin, KIF5B, Spermatogenesis

INTRODUCTION

Desmosomes are adherens-like junctions that anchor intermediate filaments, leading to the generation of a tissue-wide intermediate filament network. Three different protein families contribute to desmosome structure and function – the desmosomal cadherins desmocollins (DSCs) and desmogleins (DSGs), the armadillo (ARM) proteins and the plakins (Green and Gaudry, 2000). Desmosome composition varies with respect to tissue type and differentiation status, as the cadherins and the associated ARM family members show tissue- and cell-type-specific expression (Bass-Zubek et al., 2009; Dusek et al., 2007), leading to changes in the organization and function of desmosomes in different tissues.

The ARM proteins participate in the regulation of desmosome assembly and cell–cell adhesion (Marcozzi et al., 1998; Palka and Green, 1997). Plakoglobin (encoded by *JUP*) localizes to both

desmosomes and adherens junctions and is required for the initiation of desmosome formation by adherens junctions (Acehan et al., 2008; Knudsen and Wheelock, 1992; Lewis et al., 1997). Decreases in DSG3, the density of the plaque and the levels of plakophilin 1 (PKP1) at the cell border have been observed in plakoglobin-null keratinocytes (Acehan et al., 2008; Caldelari et al., 2001), suggesting that plakoglobin is required for desmosome formation and function in cultured keratinocytes. Plakoglobin-knockout mice die during embryogenesis owing to defects in desmosome formation in cardiac tissue (Ruiz et al., 1996). Some discrepancies exist in the literature regarding the effects of plakoglobin loss on desmosome formation in the epidermis. Ruiz and colleagues have reported that the epidermis of embryos at 11.5 days post coitum are normal upon loss of plakoglobin (Ruiz et al., 1996), whereas others have reported that defects in epidermal organization and desmosome function are observed in mice lacking plakoglobin at 17.5 days post coitum (Bierkamp et al., 1996). Plakoglobin has been reported to form a complex with both P-cadherin and E-cadherin, and the total levels of the classical cadherins dictate desmosome formation and organization (Lewis et al., 1997; Michels et al., 2009; Tinkle et al., 2008). These results suggest that plakoglobin and other ARM proteins might serve as a link between adherens junction formation and desmosome formation. Consistent with this hypothesis, plakoglobin and E-cadherin are independently required for the recruitment of plakophilin 3 (PKP3) to the cell border in order to initiate desmosome formation in HCT116 cells (Gosavi et al., 2011), whereas plakoglobin and the plakophilin family members collaborate with the desmoplakin N-terminus to regulate the clustering of the desmosomal cadherins at the cell surface (Chen et al., 2002). These data are indicative of plakoglobin being required for the initiation of desmosome formation and maintenance. However, the mechanisms by which the ARM proteins are transported to the cell border to initiate the process of desmosome formation remain unclear.

Spermatogenesis occurs in seminiferous tubules in the testis and is intrinsically dependent upon cell–cell adhesion between spermatocytes and Sertoli cells, and the formation of the blood–testis barrier between two Sertoli cells (Russell et al., 1990). These adhesive interactions are crucial for the progression of spermatogenesis. The blood–testis barrier comprises tight junctions, basal ectoplasmic specializations, gap junctions and desmosome-like junctions (Cheng and Mruk, 2002; Lie et al., 2011). Disruption of cell–cell adhesion perturbs the normal progression of spermatogenesis (Wong et al., 2004). Importantly,

¹KS215, ACTREC, Tata Memorial Centre Kharghar Node, Navi Mumbai 410210, India. ²Department of Lymphoma/Myeloma, The University of Texas MD Anderson Cancer Center, 1515 Holcombe Boulevard, Houston, TX 77030, USA. ³Department of Biological Sciences, Tata Institute of Fundamental Research, Homi Bhabha Road, Mumbai 400005, India.

*These authors contributed equally to this work

†Author for correspondence (sdalal@actrec.gov.in)

decreasing the expression of PKP2, DSG2 and DSC2 affects cell–cell adhesion, indicating that the development of spermatozoa is regulated by the formation of desmosome-like junctions in the testis (Li et al., 2009; Lie et al., 2010).

The 14-3-3 protein family is a family of small acidic proteins (Yaffe, 2002) that bind to proteins that contain a phosphorylated serine residue in a consensus motif (Muslin et al., 1996; Yaffe et al., 1997). Loss of 14-3-3 ϵ and 14-3-3 γ leads to the overriding of checkpoint function and premature entry into mitosis (Hosing et al., 2008; Telles et al., 2009). Therefore, we wanted to determine whether loss of 14-3-3 γ in the mouse led to defects in checkpoint function. When we attempted to generate 14-3-3 γ -knockdown mice by using a novel transgenic protocol that had been developed in our laboratory (Sehgal et al., 2011), we observed that loss of 14-3-3 γ led to sterility in male mice due to a decrease in cell–cell adhesion and a defect in the transport of plakoglobin and other desmosomal proteins to the cell border in the seminiferous tubules of mice. Similar results were obtained in the human HCT116 colorectal cancer cell line. Furthermore, our results demonstrate that 14-3-3 γ might load plakoglobin onto the KIF5B–KLC1 complex in order to transport plakoglobin to the cell border to initiate desmosome formation, both in HCT116 cells in culture and in the mouse testis, thus demonstrating that 14-3-3 γ is required for desmosome formation.

RESULTS

Loss of 14-3-3 γ leads to sterility in male mice

To determine whether loss of 14-3-3 γ leads to a loss of checkpoint regulation *in vivo*, we attempted to generate knockdown mice for 14-3-3 γ by using a sperm-mediated gene transfer protocol that was developed in our laboratory (Sehgal et al., 2011). However, when mice that had been injected with viruses expressing the shRNA construct against 14-3-3 γ were mated with female mice, no pups were obtained. The levels of 14-3-3 γ were substantially decreased in the testis of mice that had been injected with viruses expressing the shRNA construct against 14-3-3 γ (sh14-3-3 γ) in comparison with the mice that had been injected with the vector control (Vec, Fig. 1A). Loss of 14-3-3 γ led to an almost complete absence of mature spermatozoa in the epididymis in comparison with the control mice (Fig. 1B,C). In addition, the organization of the seminiferous tubule was severely disrupted upon 14-3-3 γ knockdown, as evidenced by individual sections of the seminiferous tubule being dissociated from one another in comparison with those of control mice (Fig. 1B). Furthermore, primary germ cells and Sertoli cells were detached from the basal lamina. This did not lead to a large increase in transferase dUTP nick end labeling (TUNEL)-positive cells (supplementary material Fig. S1A). Finally, histological examination revealed an abrogation of cell–cell adhesion between Sertoli cells, and between Sertoli cells and germ cells, in the testis, upon knockdown of 14-3-3 γ (Fig. 1D), which was confirmed by electron microscopy (Fig. 1E). Thus, these results suggest that loss of 14-3-3 γ leads to a decrease in cell–cell adhesion *in vivo*.

14-3-3 γ loss leads to defects in cell adhesion and desmosome assembly

To identify the mechanisms that lead to a decrease in cell–cell adhesion, we used a HCT116 cell line model in which 14-3-3 γ had been knocked down (sh14-3-3 γ) (described previously by Hosing et al., 2008). 14-3-3 γ mRNA and protein levels were lower in the sh14-3-3 γ cells in comparison with the control cells

(Fig. 2A,B). The protein levels of 14-3-3 ϵ and 14-3-3 σ , or the mRNA levels of 14-3-3 ϵ , 14-3-3 β , 14-3-3 τ and 14-3-3 ζ (Fig. 2A,B) were not altered in the sh14-3-3 γ cells in comparison with vector control cells (Fig. 2A). In comparison with the control cells, the sh14-3-3 γ cells showed a decrease in cell–cell adhesion in hanging-drop assays (Fig. 2C,D), and cell adhesion to fibronectin and collagen IV was also diminished in these cells (supplementary material Fig. S1B), which is consistent with the detachment of cells in the testis from the basal lamina.

To determine whether the defect in cell–cell adhesion was induced specifically by the loss of 14-3-3 γ , cells that had been subjected to 14-3-3 ϵ knockdown were generated (sh14-3-3 ϵ). Western blot analysis demonstrated that, although 14-3-3 ϵ protein levels were decreased in sh14-3-3 ϵ cells, the levels of 14-3-3 γ were unaltered. No substantial difference was observed in cell–cell adhesion in the sh14-3-3 ϵ -knockdown cells in comparison with the control cells (Fig. 2F,G). These results suggest that the differences in cell–cell adhesion that are observed upon knockdown of 14-3-3 γ are specific to the 14-3-3 γ isoform.

To determine the causes of the decrease in cell–cell adhesion, the levels of adhesion proteins in the control and sh14-3-3 γ cells were determined by western blot analysis or reverse transcription PCR (RT-PCR) (Fig. 3A–C). The levels of these proteins or mRNAs were not decreased upon 14-3-3 γ knockdown. However, in the case of DSG2, and DSC2 and DSC3, increased protein levels were observed in the 14-3-3 γ knockdown cells (Fig. 3B), although no substantial increase was observed in mRNA levels (Fig. 3C). PKP2 mRNA levels were not altered substantially in the sh14-3-3 γ cells in comparison with the control cells (Fig. 3C), and our previous reports have suggested that HCT116 cells do not express PKP1 (Kundu et al., 2008). Notably, the levels of the desmosomal proteins plakoglobin, PKP3, desmoplakin, DSC2 and DSC3, DSG2 and PKP2 were significantly lower at the cell borders in sh14-3-3 γ cells than in control cells (Fig. 3E,F), even though the total levels of these proteins were unaltered in the sh14-3-3 γ cells. Intensity profiles for the staining are shown in supplementary material Fig. S2. Importantly, no change in the detergent solubility of the desmosomal proteins was observed in the 14-3-3 γ -knockdown cells when compared with the control cells (supplementary material Fig. S4D).

By contrast, the levels of adherens junction components [E-cadherin (also known as CDH1), P-cadherin (also known as CDH3), β -catenin, p120-catenin (also known as CTNND1) and α -E-catenin], tight junction components (ZO-1) and polarity proteins (Par-3, also known as PARD3) were not reduced at the cell border in sh14-3-3 γ cells (supplementary material Fig. S1D,E). Loss of 14-3-3 ϵ did not result in a decrease in the levels of plakoglobin at the cell border (Fig. 3D). HCT116 cells that lacked both copies of 14-3-3 σ (Chan et al., 1999) showed a decrease in plakoglobin levels (supplementary material Fig. S4A) and a decrease in cell–cell adhesion (supplementary material Fig. S4B). However, there was no defect in localization of plakoglobin to the border in these cells (supplementary material Fig. S4C), suggesting that 14-3-3 σ is required to maintain plakoglobin protein levels, but not plakoglobin localization to the border.

Expression of a green fluorescent protein (GFP)-tagged shRNA-resistant 14-3-3 γ cDNA (GFP-14-3-3 γ R) resulted in the recruitment of plakoglobin to the cell border in sh14-3-3 γ cells in contrast with cells transfected with GFP alone (Fig. 4A). To determine whether the desmosomal proteins formed a complex with 14-3-3 γ , protein extracts from HCT116 cells

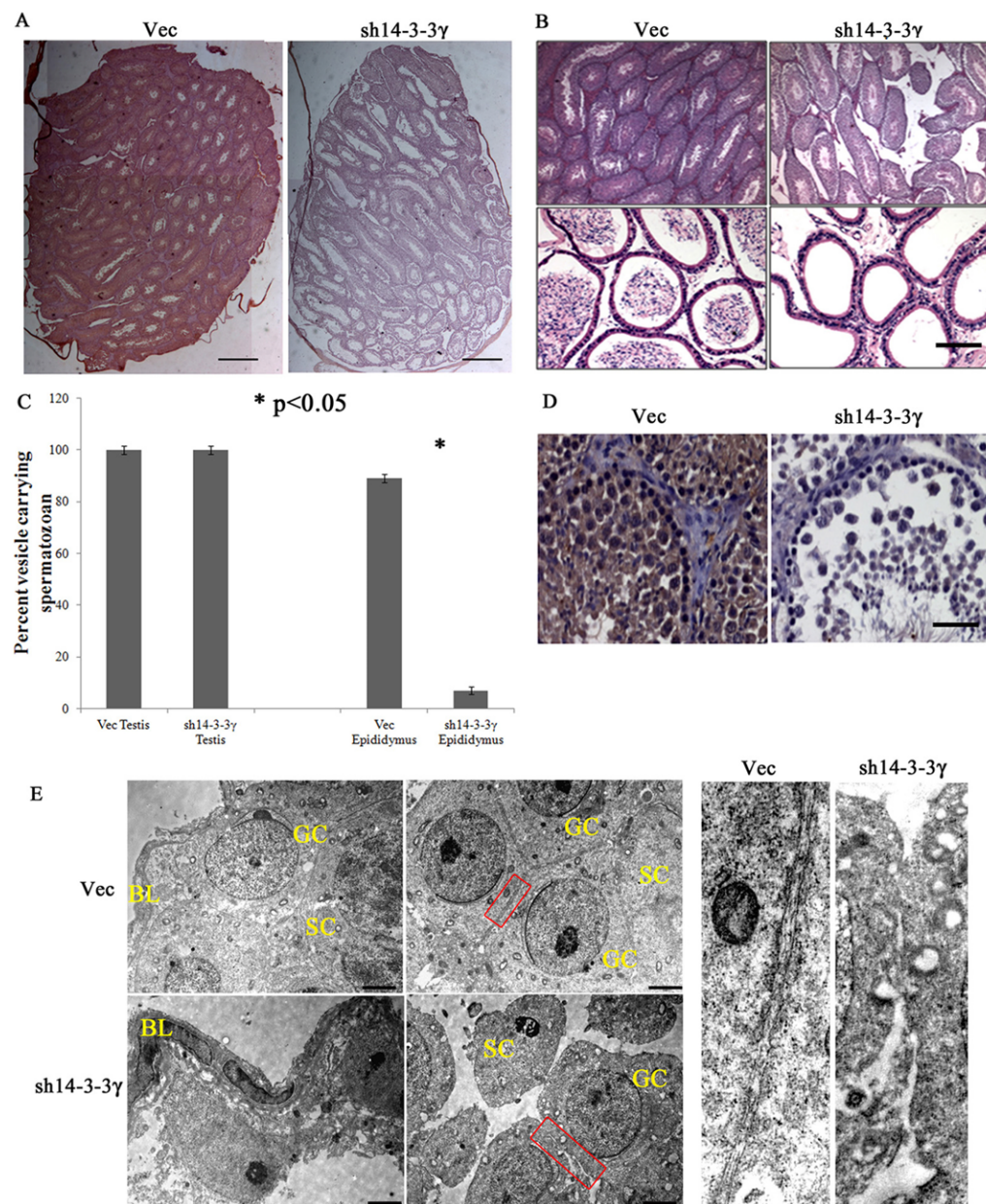


Fig. 1. Loss of 14-3-3 γ leads to disruption of cell-cell adhesion.

(A–D) Tissue sections from mouse testis that had been injected with either the 14-3-3 γ -knockdown construct (sh14-3-3 γ) or the vector control (Vec) were stained with antibodies against 14-3-3 γ and visualized by using light microscopy (A shows the entire testis, D shows a single seminiferous tubule), or were stained with hematoxylin and eosin (B) to visualize either the seminiferous tubules (top panels) or the epididymis (bottom panels). The percentage of vesicles that contained spermatozoa in the epididymis is shown and the error bars represent the mean \pm s.d. for three different animals (C). (E) Electron micrographs of testis that had been injected with either the 14-3-3 γ knockdown virus or the vector control. Sertoli cells (SC), and germ cells (GC) are indicated. The panels on the far right are higher magnification images of the boxed areas indicated. Scale bars: 5 μ m (A,B,D); 2 μ m (E).

were incubated with either glutathione S-transferase (GST) alone or GST–14-3-3 γ . 14-3-3 γ formed a complex with plakoglobin, PKP3 and desmoplakin but not with DSG2 or adherens junction proteins, such as E-cadherin (Fig. 4B). Our previous results have suggested that plakoglobin is present at the cell border in low-calcium medium, and that plakoglobin is required for the recruitment of other desmosomal proteins to the cell border in HCT116 cells and for the initiation of desmosome formation upon the addition of calcium (Gosavi et al., 2011). Therefore, to determine whether 14-3-3 γ is required for the initiation of desmosome formation, calcium-switch assays were performed. Plakoglobin was present at the cell border in low-calcium medium and the levels at the border increased upon the addition of calcium in the vector control cells. DSC2 and DSC3 were not detectable at the border in the control cells in low-calcium medium. However, DSC2 and DSC3 localized to the border 60 minutes after the addition of calcium in the control cells. By contrast, in the sh14-3-3 γ cells, plakoglobin, DSC2 and DSC3

were not present at the border in low-calcium medium and accumulated at significantly lower levels at the border upon the addition of calcium in comparison with the control cells (Fig. 4C). E-cadherin levels at the border were unaffected in the sh14-3-3 γ cells in comparison with the control cells (Fig. 4C). These results suggest that 14-3-3 γ specifically is required for the localization of plakoglobin to cell borders and is required for the initiation of desmosome formation.

We observed that, although the levels of DSC2 and DSC3 at the cell borders were lower in 14-3-3 γ -knockdown cells than in the control cells, a substantial fraction of DSC2 and DSC3, nevertheless still localized to the borders in the knockdown cells. These results suggested that, to some extent, localization of DSC2 and DSC3 to the border might be independent of the presence of 14-3-3 γ and plakoglobin at the cell border. We have previously shown that, in this cell system, plakoglobin is required to recruit PKP3 and desmoplakin to the cell border (Gosavi et al., 2011). To determine whether plakoglobin is required for the recruitment of

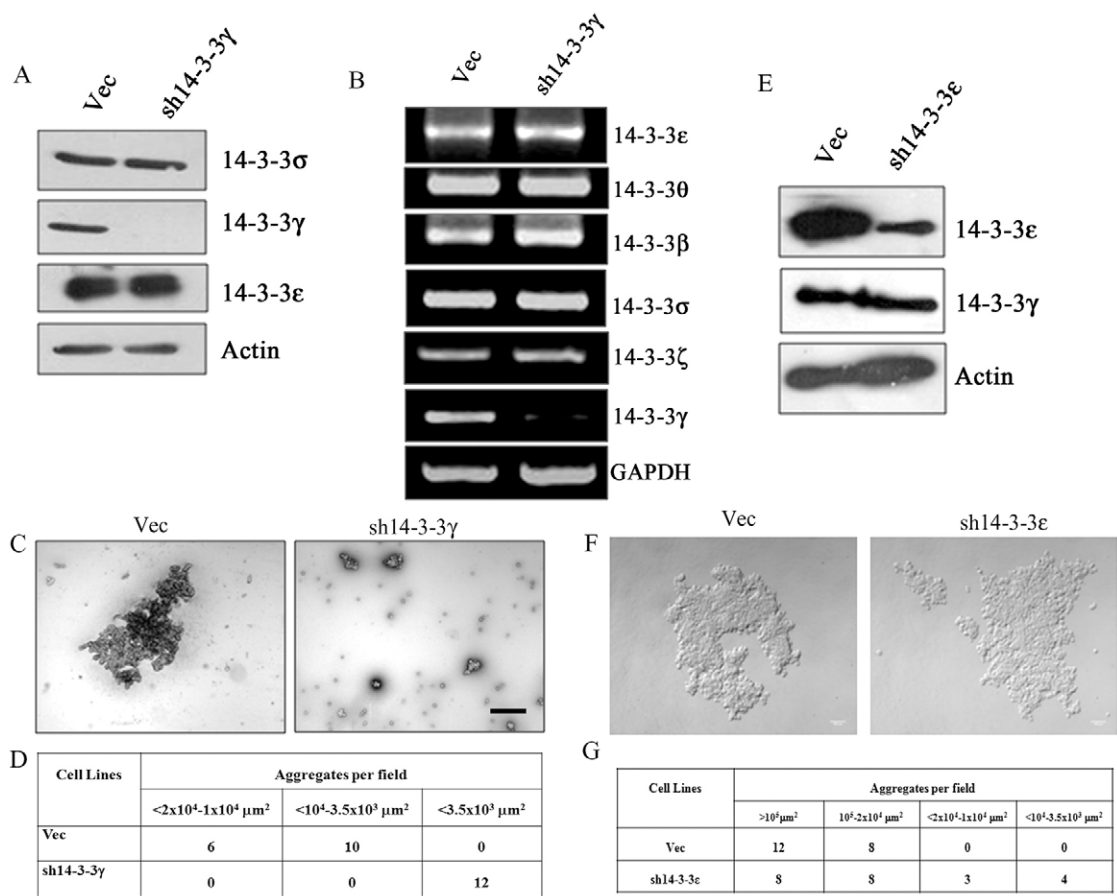


Fig. 2. Loss of 14-3-3 γ leads to a decrease in cell–cell adhesion. (A) Protein extracts from the vector control (Vec) and 14-3-3 γ -knockdown (sh14-3-3 γ) cells were resolved on SDS-PAGE gels followed by western blotting with the indicated antibodies. Actin served as a loading control. (B) mRNA was prepared from the control and sh14-3-3 γ cells and RT-PCR reactions were performed with oligonucleotide pairs specific for the indicated genes. GAPDH served as a reaction control. (C,D) Hanging-drop assays were performed on the control and sh14-3-3 γ cells. The images (C) of the clumps and the quantification (D) of cluster number and size are shown. (E) Protein extracts from the control and sh14-3-3 ϵ cells were resolved on SDS-PAGE gels followed by western blotting with the indicated antibodies. Actin served as a loading control. (F,G) Hanging-drop assays were performed on the control and sh14-3-3 γ cells. The images (F) of the clumps and the quantification (G) of cluster number and size are shown. Scale bar: 200 μ m.

desmosomal cadherins to the border, the localization of these cadherins was studied in HCT116-derived plakoglobin-knockdown cells, which have been described previously (Gosavi et al., 2011). The levels of DSC2 and DSC3, and DSG2, were not reduced at the border in the plakoglobin-knockdown cells (supplementary material Fig. S1C), suggesting that 14-3-3 γ , in addition to being required for plakoglobin localization to the border, might have other functions in desmosome formation. These data are consistent with the observation that 14-3-3 γ forms a complex with PKP3 and desmoplakin (Fig. 4B).

Complex formation between plakoglobin and 14-3-3 γ requires PKC μ

Analysis of the plakoglobin amino acid sequence led to the identification of a potential 14-3-3 binding site at serine residue 236 (S236) (supplementary material Fig. S3A) (Obenauer et al., 2003). To determine whether S236 is required for an interaction between plakoglobin and 14-3-3 γ and to mediate the targeting of plakoglobin to the surface, residue S236 was replaced with alanine (S236A), and the ability of this mutant to bind to 14-3-3 γ and to localize to the border was investigated. GST–14-3-3 γ formed a complex with wild-type plakoglobin but not with that of the S236A mutant (Fig. 5A). In contrast with wild-type plakoglobin, which

localized to the cell border, we observed reduced levels of the S236A protein at the border and an increased pan-cellular localization (Fig. 5B). Although some of the S236A mutant protein still localized to the border, the localization to the border was attenuated in comparison with that of the wild-type protein, suggesting that binding of plakoglobin to 14-3-3 γ is required for the efficient localization of plakoglobin to the border.

The S236 residue is a potential site for phosphorylation by PKC μ (supplementary material Fig. S3A), suggesting that phosphorylation of plakoglobin by PKC μ is required for plakoglobin localization to the border. HCT116 cells were treated with the vehicle control dimethyl sulfoxide (DMSO), a pan PKC inhibitor that doesn't inhibit PKC μ (bisindolylmaleimide I, BisI) or an inhibitor that is specific for PKC μ and PKC α (Go6976). A GST pull-down assay was then performed using 14-3-3 γ . Importantly, GST–14-3-3 γ was unable to pull down plakoglobin from protein extracts that had been prepared from cells treated with Go6976, in contrast to cells that had been treated with DMSO (Fig. 5C), suggesting that the activity of either PKC α or PKC μ is required for complex formation with 14-3-3 γ and localization of plakoglobin to the cell border. However, 14-3-3 γ formed a complex with desmoplakin and PKP3 in extracts that had been derived from cells treated with the inhibitor (Fig. 5C),

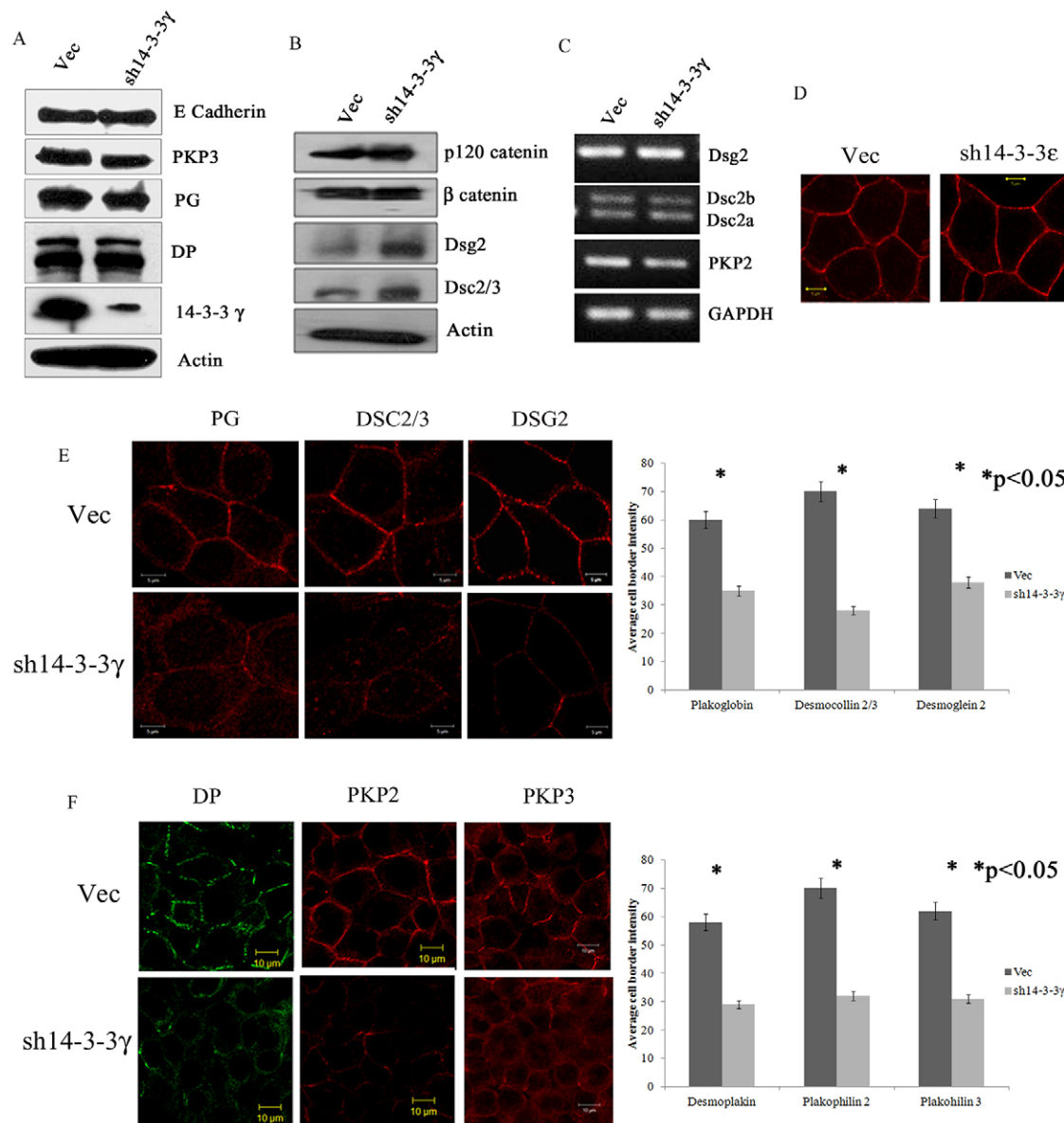


Fig. 3. Localization of plakoglobin is altered in sh14-3-3γ cells. (A,B) Protein extracts from the vector control (Vec) and 14-3-3γ-knockdown (sh14-3-3γ) cells were resolved on SDS-PAGE gels followed by western blotting with the indicated antibodies. Western blotting for actin served as a loading control. (C) mRNA was prepared from the control and sh14-3-3γ cells, and RT-PCR reactions were performed with oligonucleotide pairs specific for the indicated genes. The oligonucleotides used for DSC2 amplified both splice isoforms, DSC2a and DSC2b, as indicated. GAPDH served as a reaction control. (D) Plakoglobin (PG) levels at the cell borders were determined in the vector control and 14-3-3ε knockdown cells. Note that plakoglobin levels did not change at the cell border upon knockdown of 14-3-3ε (sh14-3-3ε). (E,F) Control and sh14-3-3γ cells were stained with the indicated antibodies, and the staining was observed by using confocal microscopy. Representative images are shown. The border intensity was measured for at least 20 cells in three different experiments. The mean±s.d. is shown for three independent experiments. Scale bars: 5 μm (D,E); 10 μm (F). DP, desmoplakin.

suggesting that the activity of PKCμ or PKCα is not required for the association of desmoplakin or PKP3 with 14-3-3γ. In agreement with these results, immunofluorescence analysis using antibodies against plakoglobin demonstrated that the treatment of cells with Go6976 decreased the localization of plakoglobin at the cell border in comparison with that of cells that had been treated with either DMSO or BisI (Fig. 5D).

Because the motif scan software identified S236 as a potential site for phosphorylation by PKCμ, we inhibited the expression of PKCμ using vector-driven RNA interference (RNAi) in HCT116 cells using a previously described sequence that inhibits PKCμ expression but not PKCα expression (Park et al.,

2009). HCT116 cells were transfected with either the vector plasmid or a plasmid that expressed shRNA sequences that target PKCμ (shPKCμ). Forty-eight hours post transfection, the cells were transferred to medium containing puromycin in order to enrich for transfected cells. Western blot analysis demonstrated that PKCμ levels were reduced, as expected; however, plakoglobin and desmoplakin protein levels were reduced in cells that had been transfected with the shRNA against PKCμ, suggesting that PKCμ might also regulate the stability of these proteins (Fig. 5E). No change in the levels of PKP3 was observed, and western blots for actin were performed as loading controls. The levels of plakoglobin, desmoplakin and

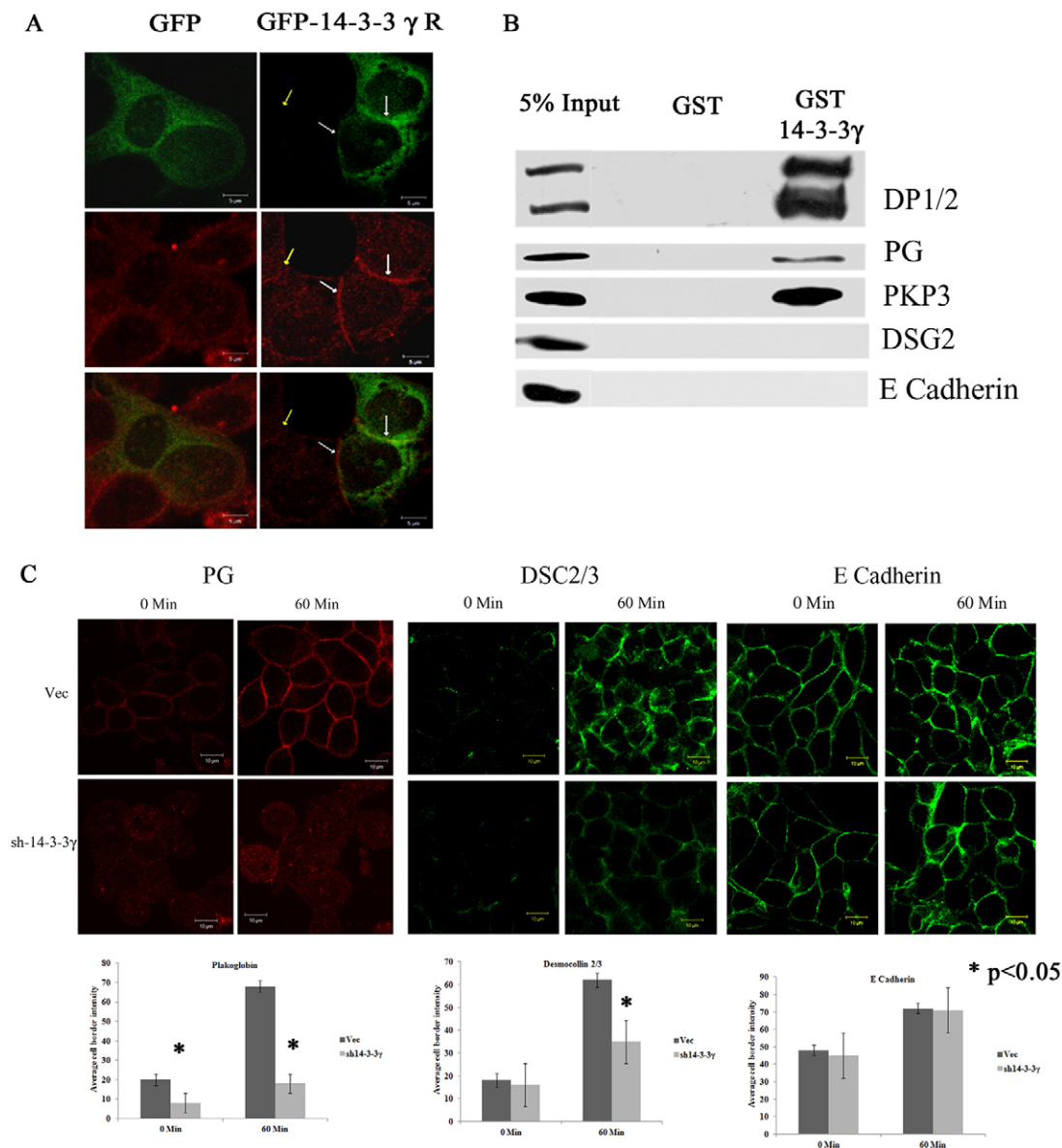


Fig. 4. 14-3-3 γ is required to initiate desmosome formation. (A) 14-3-3 γ -knockdown (sh14-3-3 γ) cells were transfected with either GFP alone or a GFP-14-3-3 γ construct that was resistant to RNAi (GFP-14-3-3 γ R). The cells were stained with antibodies to plakoglobin (PG, red) and analyzed by using confocal microscopy. (B) Protein extracts of HCT116 cells were incubated with either GST or GST-14-3-3 γ . The reactions were resolved on SDS-PAGE gels, and followed by western blotting with the indicated antibodies. (C) Vector control (Vec) and sh14-3-3 γ cells were incubated in low-calcium medium for 24 hours (0 min). After calcium addition for 60 minutes, the cells were fixed and then stained with the indicated antibodies and analyzed by using confocal microscopy. Note that the levels of the desmosomal proteins do not increase at the border in sh14-3-3 γ cells in comparison with control cells. No change in E-cadherin staining was observed. The border intensity was measured for at least 20 cells in three different experiments. The mean and standard deviation for three independent experiments is shown. Scale bars: 5 μ m (A); 10 μ m (C).

PKP3 at the cell borders were decreased in cells that had been transfected with the PKC μ shRNA in comparison with cells that had been transfected with the vector control, and the remaining protein in these cells was not localized to the border (Fig. 5F). These results suggest that, in addition to the decreased protein levels, there is a decrease in the localization of the desmosomal components to the cell borders in the absence of PKC μ . This is in contrast with the results obtained for cells that lacked 14-3-3 σ , in which a decrease in the levels of plakoglobin was observed but there was no defect in plakoglobin localization to the border (supplementary material Fig. S4C). To determine whether PKC μ phosphorylated plakoglobin directly, the first 300 amino

acids of plakoglobin, which comprise the putative 14-3-3-binding site, were purified from bacteria as a GST fusion protein and used as a substrate in an *in vitro* kinase assay using purified PKC μ . A peptide derived from CREB (catalog number C50-58, Signal Chem) was used as a positive control in these assays. As shown in Fig. 5G, the GST-PG1-300 fusion protein was phosphorylated *in vitro* by PKC μ , and the level of phosphorylation increased markedly with an increase in substrate concentration, in contrast with the results observed with GST alone. These results suggest that PKC μ regulates localization of plakoglobin to the cell border, and plakoglobin expression or stability.

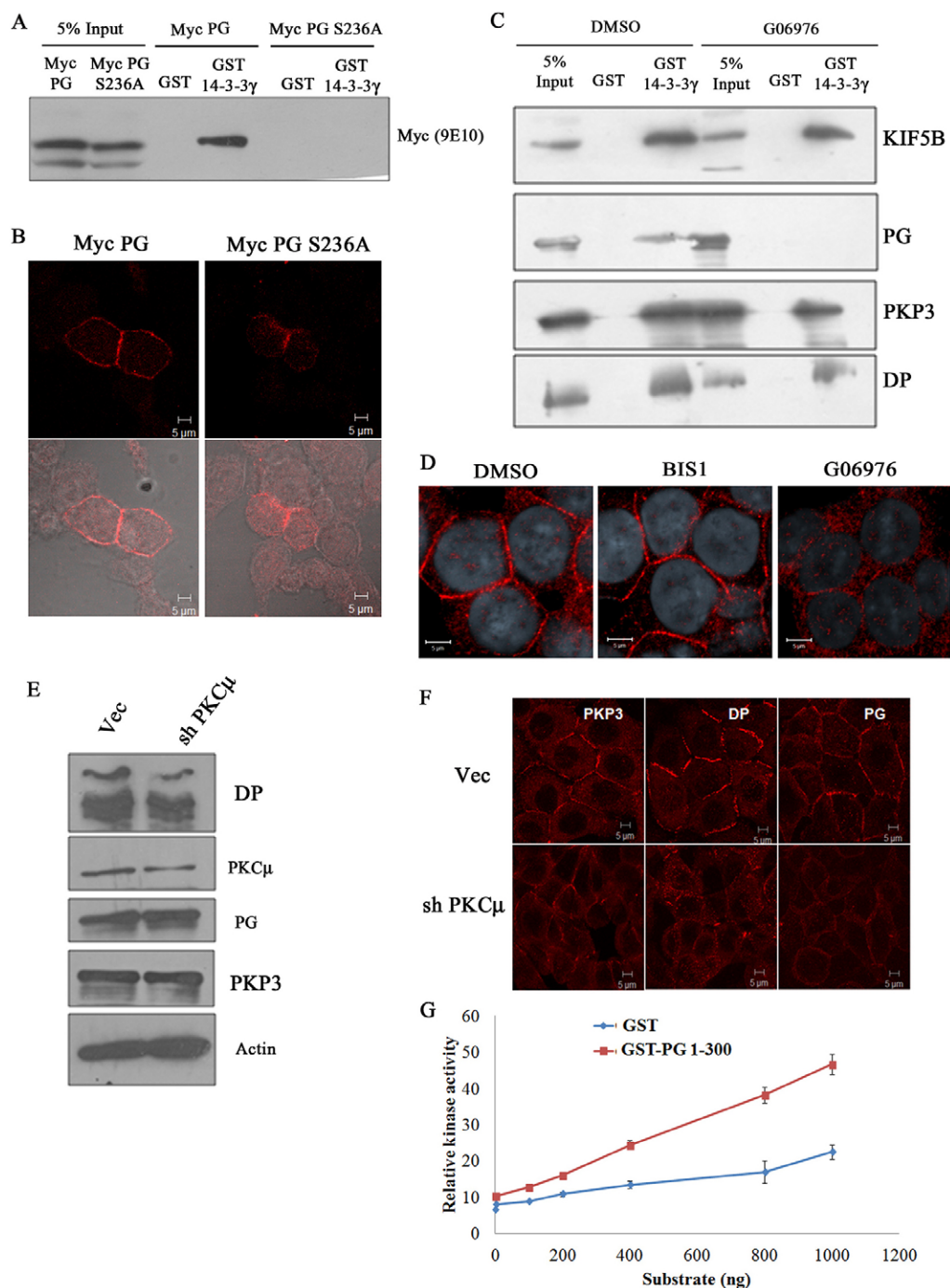


Fig. 5. The association of 14-3-3 γ with plakoglobin requires PKC μ activity. (A,B) HCT116 cells were transfected with either MYC-epitope-tagged wild-type plakoglobin (PG) or the S236A mutant of plakoglobin. 48 hours post transfection, protein extracts were incubated with GST or GST–14-3-3 γ followed by western blotting with antibodies against MYC (A), or the cells were stained with antibodies against the MYC-epitope (B). Differential interference contrast images for the fields are shown in the lower panels. (C,D) HCT116 cells were treated with either the vehicle control (DMSO), the pan-PKC inhibitor (Bis1), or the PKC α - and PKC μ -specific inhibitor (Go6976). Protein extracts from these cells were incubated with either GST or GST–14-3-3 γ , the reactions were resolved on SDS-PAGE gels, and western blots were performed with the indicated antibodies (C). The cells were also stained with antibodies against plakoglobin (D). (E,F) Protein extracts from vector control (Vec) or PKC μ -knockdown cells (shPKC μ) were resolved on SDS-PAGE gels, and western blots were performed with the indicated antibodies. Note that there is a decrease in plakoglobin and desmoplakin (DP) levels upon PKC μ knockdown, but no difference in PKP3 levels is observed. (F) Control cells and shPKC μ cells were fixed and then stained with the indicated antibodies. (G) The PG1-300 construct, comprising the first 300 amino acids of plakoglobin, was produced in bacteria as a GST fusion protein, and kinase assays were performed using recombinant PKC μ . GST alone was used as a negative control in this assay. Different concentrations of the substrate are shown on the x-axis and enzyme activity is recorded on the y-axis. The mean \pm s.d. is shown. Note that an increase in kinase activity is observed upon an increase in the concentration of PG1-300 but not with an increase in the concentration of GST alone. Scale bars: 10 μ m (B); 5 μ m (D,F).

KIF5B binds to 14-3-3γ and is required for desmosome assembly

A proteomic screen conducted in our laboratory identified the kinesin 1 family member KIF5B (Cross and Carter, 2000) as a potential ligand for 14-3-3γ (data not shown). As kinesin motor proteins are required for the transport of proteins to the cell border (Cross and Carter, 2000) and have been shown to be required for the transport of the desmosomal cadherins to the cell border (Nekrasova et al., 2011), we hypothesized that plakoglobin was transported to the border by KIF5B. To determine whether

14-3-3γ forms a complex with KIF5B, HCT116 cells were transfected with either the vector control (pcDNA3) or hemagglutinin (HA)-tagged 14-3-3γ, and immunoprecipitation reactions were performed using antibodies to the HA epitope. 14-3-3γ formed a complex with KIF5B, suggesting that 14-3-3γ might load plakoglobin onto KIF5B and lead to the transport of plakoglobin to the cell border (Fig. 6A). To test this hypothesis, KIF5B expression was stably downregulated using vector-driven RNAi. Five clones (K1–K5) were isolated that showed a decrease in KIF5B protein expression in comparison with the vector

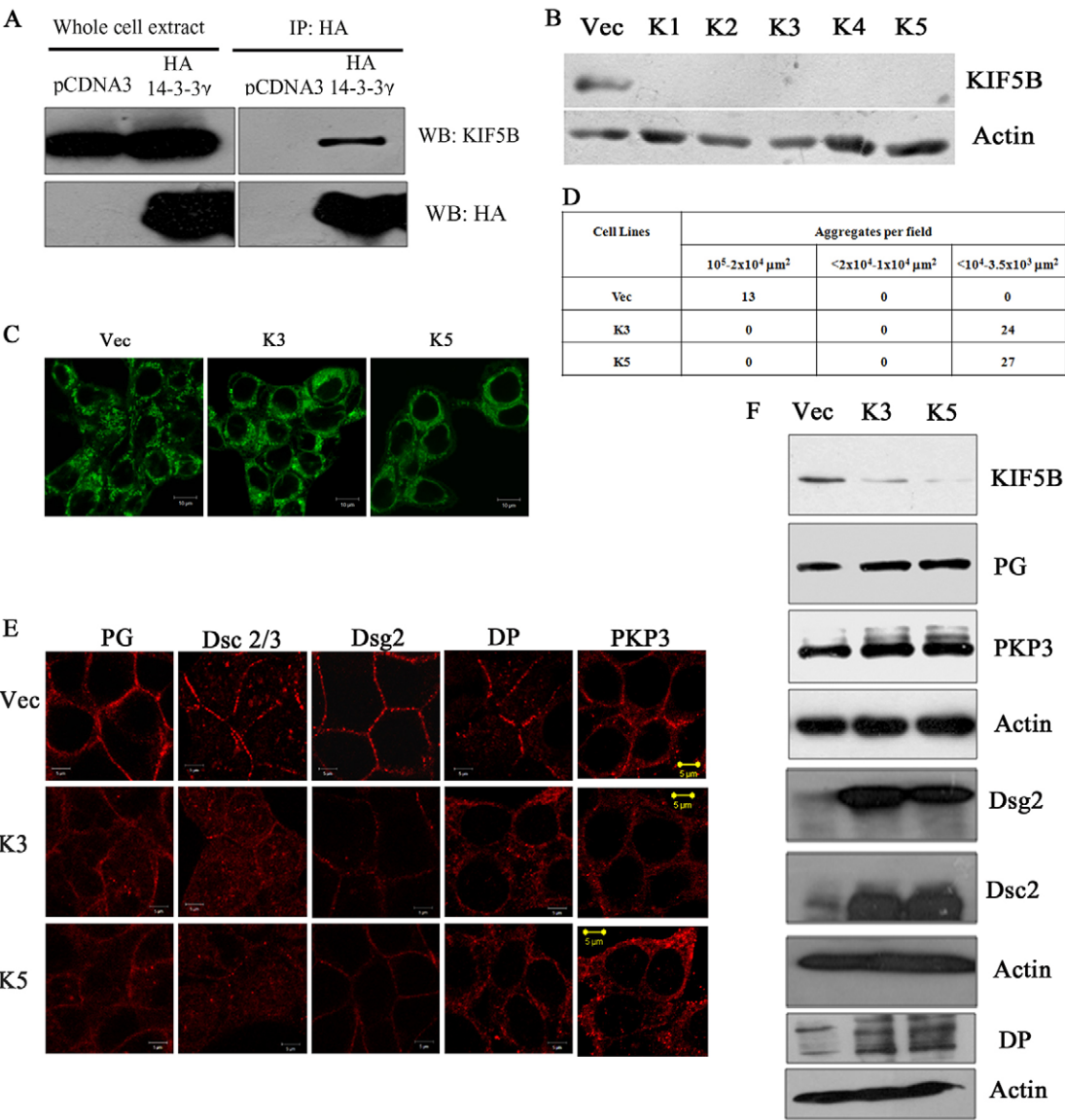


Fig. 6. KIF5B is required for the transport of plakoglobin to the cell border. (A) HCT116 cells were transfected with the vector control (pcDNA3) or HA-14-3-3γ and immunoprecipitations (IP) were performed with antibodies against the HA epitope. The reactions were resolved on SDS-PAGE gels, and then western blots (WB) were performed with the indicated antibodies. (B) HCT116 cells were transfected with constructs expressing an shRNA targeting KIF5B. Individual cell clones were expanded, and protein extracts from these clones were resolved on SDS-PAGE gels followed by western blotting with antibodies to KIF5B. A western blot for actin was performed as a loading control. Note that the knockdown clones (K1–K5) have a lower level of KIF5B than the vector control (Vec). A western blot for actin served as a loading control. (C) Vector control or the KIF5B-knockdown clones K3 and K5 were incubated with Mitotracker Green FM. (D) Hanging-drop assays were performed to determine cell–cell adhesion. K3 and K5 formed fewer and smaller clumps in comparison with the control cells. (E) Control, K3 and K5 cells were stained with antibodies against plakoglobin (PG), DSC2 and DSC3, DSG2, desmoplakin (DP) and PKP3 and the intensity of the surface staining was quantified by using confocal microscopy. The total magnification was ×630 with ×2 optical zoom. Bars correspond to 5 μM. (F) Protein extracts prepared from the control, K3 and K5 cells were resolved on SDS-PAGE gels and then analyzed by western blotting with the indicated antibodies. Scale bars: 10 μm (C); 5 μM (E).

control cells (Fig. 6B). Loss of KIF5B led to a perinuclear accumulation of mitochondria, as reported previously (Tanaka et al., 1998) (Fig. 6C). Furthermore, hanging-drop assays demonstrated that loss of KIF5B led to a decrease in cell–cell adhesion in comparison with the control cells (Fig. 6D; supplementary material Fig. S3B).

To determine whether the decrease in cell–cell adhesion that was observed upon KIF5B knockdown was accompanied by a decrease in the localization of the desmosomal proteins to the cell borders, the control cells and the KIF5B knockdown clones K3 and K5 were stained with antibodies against components of desmosomes or adherens junctions. Similar to that observed in the sh14-3-3 γ cells, the levels of plakoglobin, PKP3, desmoplakin, DSC2 and DSC3, and DSG2 substantially decreased at the border in K3 and K5 KIF5B-knockdown cells – a phenotype similar to that of the control cells (Fig. 6E,F). Intensity profiles for the staining are shown in supplementary material Fig. S2. By contrast, knockdown of KIF5B did not lead to a decrease in the levels of E-cadherin, p120 catenin, α -E-catenin and β -catenin at the cell border (supplementary material Fig. S3C,F,G). The decrease in the levels of desmosomal proteins at the border was not due to a decrease in protein expression levels, as indicated by western blot analysis. In contrast with the results that were observed for plakoglobin, PKP3 and desmoplakin, a large increase in the levels of DSC2 and DSC3, and DSG2 were observed in the kinesin-knockdown cells (Fig. 6F), although this was not observed at the mRNA level (supplementary material Fig. S3E). In cells that had been fixed with methanol, we observed low levels of DSC2 and DSC3, and DSG2, in the cytoplasm (Fig. 6E); however, fixation with paraformaldehyde revealed high levels of DSC2 and DSC3, and DSG2, in the cytoplasm (supplementary material Fig. S4E), suggesting that these proteins accumulate in the cytoplasm upon loss of KIF5B. PKP2 mRNA levels were not altered upon knockdown of kinesin (supplementary material Fig. S3E).

Because kinesin motor proteins transport their cargo on microtubules, we investigated whether disruption of the microtubule network would lead to a decrease in the concentration of plakoglobin at the cell border. Treatment with nocodazole, but not the vehicle control, did indeed lead to a decrease in the levels of plakoglobin at the border (supplementary material Fig. S3D). To then determine whether complex formation between KIF5B and plakoglobin is dependent upon PKC μ , protein extracts from Go6976- or DMSO-treated HCT116 cells were incubated with GST–14-3-3 γ . GST–14-3-3 γ formed a complex with KIF5B under both conditions but did not interact with plakoglobin in protein extracts from cells that had been treated with Go6976 (Fig. 5C), indicating a requirement for active PKC μ for the association between plakoglobin and 14-3-3 γ but not for the association between KIF5B and 14-3-3 γ .

To further confirm the role of KIF5B in transporting plakoglobin to the border, we determined whether a dominant-negative KIF5B construct could inhibit transport of plakoglobin to the cell border. The dominant-negative kinesin heavy chain constructs used here have a point mutation in the ATPase domain (see Materials and Methods), which results in an inability of the proteins to move along the microtubules but preserves the ability of kinesins to bind to cargo (Cross and Carter, 2000). Yellow fluorescent protein (YFP)-tagged versions of wild-type and dominant-negative (mutation T92N) KIF5B, or the GFP-tagged wild-type and dominant-negative (mutation T107N) kinesin 2 family member KIF3A (Cross and Carter, 2000) constructs were

transfected into HCT116 cells. After transfection, the cells were stained with antibodies against plakoglobin and visualized by using confocal microscopy. Cells that expressed wild-type YFP–KIF5B showed border staining for plakoglobin. By contrast, plakoglobin was not localized at the cell border in cells that expressed dominant-negative YFP–KIF5B (Fig. 7A). Cells that had been transfected with either of the KIF3A constructs showed border staining for plakoglobin. Cells that had been transfected with either of the dominant-negative constructs had round edges and showed a morphology that was different from that of cells that had been transfected with either of the wild-type constructs, presumably because overexpression of the dominant-negative constructs affects other cellular processes, such as microtubule organization (Silver and Harrison, 2011). However, despite the change in morphology, only the cells that had been transfected with the dominant-negative KIF5B construct, and not those transfected with the dominant-negative KIF3A construct, showed a disruption of plakoglobin localization (Fig. 7A). These results suggest that KIF5B specifically is required for transport of plakoglobin to the border.

Kinesin motor proteins are heterodimers that consist of two heavy chains and two light chains (Cross and Carter, 2000). KIF5B associates with two different kinesin light chains (KLCs) – KLC1 and KLC2 (Verhey and Hammond, 2009). To determine which of these is required for plakoglobin transport to the cell border, bacterially produced GST-tagged KLC1 and KLC2 were incubated with protein extracts that had been prepared from HCT116 cells, and the reactions were resolved on SDS-PAGE gels followed by western blotting with antibodies against plakoglobin, KIF5B and 14-3-3 γ . Both KLC1 and KLC2 formed a complex with KIF5B; however, only KLC1 could form a complex with both plakoglobin and 14-3-3 γ (Fig. 7B). KLCs contain a coiled-coiled domain, which is required for complex formation with the kinesin heavy chain, and a cargo-binding domain [which comprises tetratricopeptide repeats (TPRs)] (Verhey and Hammond, 2009) (Fig. 7C). To determine whether the coiled-coiled domain of KLC1 could form a complex with plakoglobin, protein extracts from HCT116 cells were incubated with either GST–KLC1 or the GST-tagged coiled-coiled domain of KLC1. GST–KLC1 could form a complex with KIF5B, plakoglobin and 14-3-3 γ , whereas the coiled-coiled domain bound to KIF5B but not to plakoglobin and 14-3-3 γ (Fig. 7D). Therefore, the coiled-coiled domain of KLC1 might be acting as a dominant-negative mutant because it should bind to the heavy chain but fail to form a complex with plakoglobin and 14-3-3 γ . To test this hypothesis, HCT116 cells were transfected with either GFP–KLC1 or the GFP-tagged KLC1 coiled-coiled domain only and stained with antibodies against plakoglobin. Overexpression of the KLC1 coiled-coiled domain disrupted the transport of plakoglobin to the cell border, whereas cells that expressed the wild-type protein did not show any alteration in plakoglobin localization (Fig. 7E). These results suggest that the KIF5B–KLC1 complex is required for the transport of plakoglobin to the cell border.

Loss of KIF5B leads to sterility in male mice

The results described above suggest that 14-3-3 γ and KIF5B are required for desmosome formation in epithelial cells. To determine whether loss of KIF5B leads to a decrease in cell–cell adhesion in the seminiferous epithelium, KIF5B expression was inhibited in the testis, as described previously (Sehgal et al., 2011). Loss of KIF5B in the testis led to a phenotype similar to that observed for

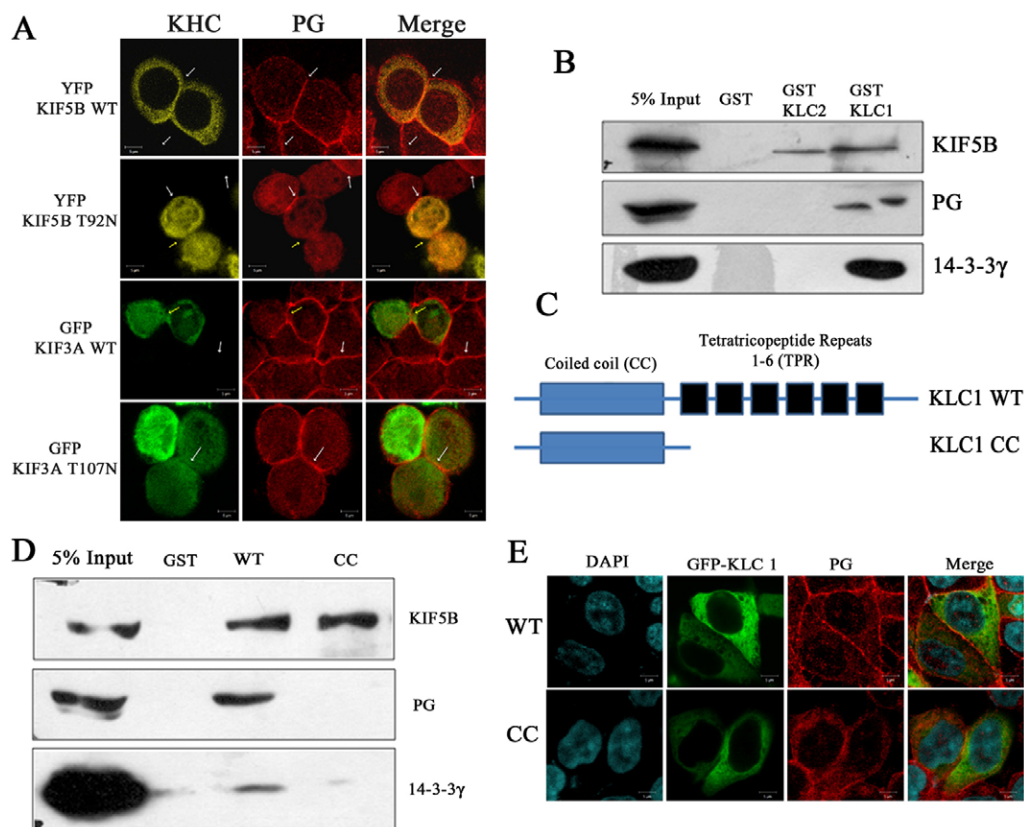


Fig. 7. Dominant-negative mutants of KIF5B and KLC1 inhibit plakoglobin transport to the border. (A) HCT116 cells were transfected with kinesin heavy chain constructs (KHC) – YFP-tagged wild-type (WT) or dominant-negative (T92N) KIF5B, or GFP-tagged wild-type or dominant-negative (T107N) KIF3A. Post transfection, the cells were fixed and stained with antibodies against plakoglobin (PG). (B) Protein extracts from HCT116 cells were incubated with GST alone or GST–KLC1 or GST–KLC2. The reactions were resolved on SDS-PAGE gels followed by western blotting with the indicated antibodies. (C) The KLC1 mutant KLC1-CC comprises only the coiled-coiled domain and not the tetraco-peptide repeat domain (TPR). (D) Protein extracts from HCT116 cells were incubated with GST alone, wild-type GST–KLC1 and GST–KLC1-CC. The reactions were resolved on SDS-PAGE gels followed by western blotting with the indicated antibodies. (E) GFP–KLC1 or GFP–KLC1-CC were transfected into HCT116 cells. Forty-eight hours post transfection, the cells were fixed and then stained with antibodies against plakoglobin. The nuclei were stained with DAPI. Total magnification is $\times 630$ with $\times 2$ optical zoom. Scale bars: 5 μ m.

the loss of 14-3-3 γ (Fig. 8A–C), suggesting that both KIF5B and 14-3-3 γ are independently required to regulate cell–cell adhesion in the testis. Importantly, an immunohistochemical analysis demonstrated that loss of either KIF5B or 14-3-3 γ did not lead to a decrease in the levels of the other protein (Fig. 8B). Loss of 14-3-3 ϵ did not lead to a decrease in cell–cell adhesion and spermatogenesis, suggesting that the effects observed upon knockdown of 14-3-3 γ are specific to 14-3-3 γ (Fig. 8A,B), a result that is consistent with those observed in HCT116 cells (Fig. 2). In addition, loss of either 14-3-3 γ or KIF5B led to a detachment of the cells from the basal lamina. To determine whether the detachment of the primary germ cells and the Sertoli cells from the basal lamina led to an increase in cell death, the testis sections were stained using a TUNEL staining kit. As shown in supplementary material Fig. S1A, treatment of the positive-control sections with DNase resulted in a strong positive signal in the TUNEL assay. Testis sections from mice that had been injected with the 14-3-3 γ -knockdown construct showed low levels of TUNEL positivity in comparison with testis sections from the control or KIF5B-knockdown mice. Given that the testis morphology of the KIF5B-knockdown mice and the 14-3-3 γ -knockdown mice was very similar, it is likely that the loss of cell–matrix adhesion does not lead to cell death, which is consistent

with our results in the cell line model. These results suggest that cell–cell adhesion in the testis requires both 14-3-3 γ and KIF5B and that loss of either protein leads to defects in cell–cell adhesion.

To determine whether desmosome organization was altered in the 14-3-3 γ - and KIF5B-knockdown testis, testis sections were stained with antibodies against plakoglobin, PKP3, DSC2 and DSC3, N-cadherin and E-cadherin. Plakoglobin, PKP3 and DSC2 and DSC3 localized to the border in testis that had been injected with the control virus; however, the levels of these proteins at the cell border were greatly diminished in the 14-3-3 γ - and KIF5B-knockdown testis (Fig. 8D). By contrast, there was no change in E-cadherin localization in the 14-3-3 γ - and KIF5B-knockdown testis in comparison with testis sections that had been injected with the vector control, a phenotype similar to that observed in HCT116 cells in culture. In contrast with the results obtained for E-cadherin, it was observed that N-cadherin localized to the border in the vector control and 14-3-3 γ -knockdown testis but not in the KIF5B-knockdown testis (Fig. 8D). These results are consistent with our observations that the KIF5B-knockdown testis showed a more severe adhesion phenotype than the 14-3-3 γ -knockdown testis and that KIF5B might be required for the transport of other cell–cell adhesion molecules to the border, in addition to desmosomal proteins. Overall, our results suggest that

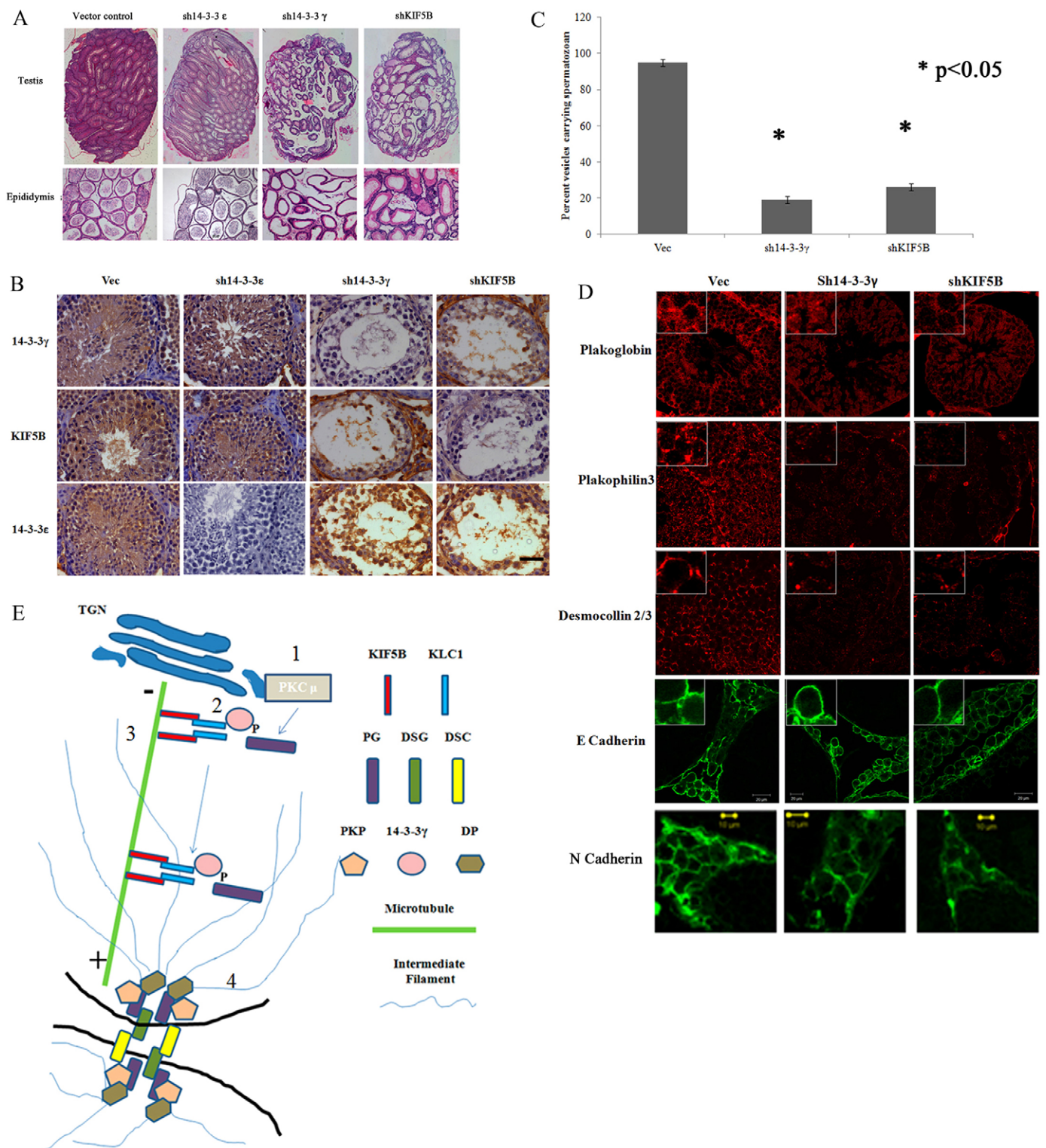


Fig. 8. See next page for legend.

14-3-3 γ and KIF5B are required for the formation of desmosomes *in vivo*.

DISCUSSION

Our results suggest that 14-3-3 γ and the KIF5B–KLC1 complex are required for the transport of plakoglobin to cell borders in

human cell lines and in the mouse testis, and disruption of this interaction with 14-3-3 γ leads to a defect in the localization of plakoglobin. In addition, loss of 14-3-3 γ leads to a disruption of cell–matrix adhesion, which might affect cell–cell adhesion *in vitro* and *in vivo*. The association of plakoglobin with 14-3-3 γ , and the transport of plakoglobin to the border is dependent on

Fig. 8. Loss of KIF5B and 14-3-3 γ in the testis leads to a disruption of desmosome formation and sterility. (A–D) Lentiviruses encoding the vector control or shRNAs targeting 14-3-3 ϵ , 14-3-3 γ or KIF5B were injected into the testes of Swiss mice (sh14-3-3 ϵ , sh14-3-3 γ and shKIF5B, respectively). 35 days post-injection the mice were killed, sections of the epididymis and testes were stained with hematoxylin and eosin and examined by using microscopy (A). Immunohistochemical analysis using antibodies against the different proteins that were knocked down demonstrated that the expression of 14-3-3 ϵ , 14-3-3 γ and KIF5B is inhibited in the testis that had been injected with the appropriate lentivirus (B). The percentage of epididymal vesicles that showed the presence of mature spermatozoa in three different animals was determined and the means \pm s.d. are shown. (C) Testis sections were stained with antibodies against plakoglobin (PG), plakophilin 3 (PKP3), desmocollins (DSC)2 and DSC3, N-cadherin and E-cadherin. (D) The total magnification was $\times 630$ with $\times 2$ optical zoom. The inset images show a higher magnification of the cells to demonstrate border localization. (E) Desmosome assembly based on the experimental findings presented here. (1) PKC μ phosphorylates plakoglobin, thereby, allowing association with 14-3-3 γ and resulting in the loading of plakoglobin onto the KIF5B–KLC1 complex. (2) The motor protein complex containing plakoglobin moves along microtubules (3) resulting in desmosome assembly at the border (4). TGN, trans-Golgi network. Scale bars: 20 μ m (B); 10 μ m (C).

PKC μ activity; thus, loss of either 14-3-3 γ or KIF5B inhibits plakoglobin transport, resulting in a decrease in desmosome formation and cell–cell adhesion in HCT116 cells and the testis, leading to male sterility. The decrease in the levels of N-cadherin at cell borders in KIF5B-knockdown testis resulted in a more drastic phenotype in these animals than in those that had been subjected to knockdown of 14-3-3 γ , suggesting that N-cadherin is required for cell–cell adhesion in the testis as previously reported (Andersson et al., 1994; Lee et al., 2003).

Previous results have shown that loss of plakoglobin leads to the depletion of desmosomal proteins from the cell border and to defects in desmosome formation (Acehan et al., 2008; Gosavi et al., 2011; Knudsen and Wheelock, 1992; Lewis et al., 1997). Although the presence of a classical cadherin seems to be required for plakoglobin recruitment to the cell border (Michels et al., 2009; Tinkle et al., 2008), the mechanisms by which plakoglobin is transported have not been identified. The results presented here suggest that phosphorylation of plakoglobin by PKC μ at residue S236 leads to the generation of a binding site for 14-3-3 γ , and that 14-3-3 γ is required for the transport of plakoglobin to the cell border in order to initiate desmosome formation, presumably in a complex with a classical cadherin (Michels et al., 2009; Tinkle et al., 2008). 14-3-3 γ might be required to load plakoglobin onto the KIF5B–KLC1 complex, which precedes the transport of plakoglobin on microtubules (Fig. 8E). This is consistent with previous observations that showed that PKC μ localizes to the Golgi complex (Hausser et al., 2002; Prestle et al., 1996) and is required for the fission of vesicles carrying cargo to the cell border (Liljedahl et al., 2001). A 14-3-3 γ dimer is required for carrier formation at the Golgi complex along with PKC μ (Valente et al., 2012), suggesting that the loss of 14-3-3 γ could disrupt desmosome formation owing to defects in plakoglobin transport.

The treatment of cells with an inhibitor that inactivates both PKC α and PKC μ led to a decrease in the localization of plakoglobin at cell borders and abolished complex formation between plakoglobin and 14-3-3 γ . However, treatment with the inhibitor does not inhibit the interaction between 14-3-3 γ and other desmosomal proteins or KIF5B. These results suggest that phosphorylation of plakoglobin by PKC μ is required for complex formation between plakoglobin and 14-3-3 γ and the loading of

plakoglobin onto KIF5B, which is essential for the transport of plakoglobin. Alternatively, it is possible that plakoglobin, desmoplakin and PKP3 are transported independently to the border and that the absence of plakoglobin at the border prevents the formation of a functional desmosome. Furthermore, it was observed that loss of plakoglobin did not affect the localization of DSC2 and DSC3, and DSG2 to cell borders, unlike the loss of 14-3-3 γ or KIF5B. This might be because 14-3-3 γ is required for the localization of PKP3, desmoplakin and plakoglobin; therefore, the defects in the localization of the desmosomal cadherins that is observed upon 14-3-3 γ loss are not observed upon plakoglobin loss. Plakoglobin is probably required to stabilize and maintain the organization of the desmosome, which is why loss of plakoglobin leads to a decrease in cell–cell adhesion in these cells as previously reported (Gosavi et al., 2011). PKC μ was also shown to directly phosphorylate a peptide comprising the first 300 amino acids in plakoglobin, which contains the S236 residue, consistent with the notion that S236 serves as site for phosphorylation by PKC μ . This does not exclude the possibility that PKC μ phosphorylates other residues in plakoglobin and might provide an explanation for the observation that plakoglobin protein levels decreased when PKC μ expression was inhibited. It is possible that PKC μ regulates other aspects of plakoglobin function that are not limited to the transport of plakoglobin to the cell border, such as the retention of plakoglobin at the border or the stability of the plakoglobin protein.

In the absence of KIF5B, or upon expression of a dominant-negative KIF5B construct, plakoglobin does not localize to the cell border, leading to a decrease in the recruitment of other components of the desmosome, as previously reported (Gosavi et al., 2011; Lewis et al., 1997). Previous experiments have suggested that inhibiting KIF5B expression does not affect the localization of plakoglobin to the border in SCC9 cells (Nekrasova et al., 2011). Our results, however, suggest that loss of KIF5B in HCT116 cells and the testis results in an inhibition of plakoglobin transport to the border. Consistent with the results reported by Nekrasova and colleagues (Nekrasova et al., 2011), we did not observe any defects in plakoglobin localization upon expression of a dominant-negative KIF3A mutant. The discrepancy in these two reports might be due to the use of different cell types; other kinesin-family members could regulate plakoglobin transport in SCC9 cells in the absence of KIF5B. Similarly, Pasdar and colleagues have reported that a microtubule network is not essential for desmosome formation (Pasdar et al., 1991); however, the results from this report and others suggest that the transport of desmosomal components to the border is dependent on an intact microtubule network (Gloushankova et al., 2003; Nekrasova et al., 2011). This is consistent with reports that suggest that desmosome organization, function and composition vary in different cell types (reviewed in Cross and Carter, 2000; Garrod and Chidgey, 2007; Getsios et al., 2004; Green and Gaudry, 2000; Hatzfeld, 2007) and with the observations that loss of the different desmosomal components in the mouse leads to a vast variety of phenotypes (Chidgey et al., 2001; Gallicano et al., 1998; Grossmann et al., 2004; Koch et al., 1997; Lechler and Fuchs, 2007; Ruiz et al., 1996; Sklyarova et al., 2008; Vasioukhin et al., 2001).

Although 14-3-3 γ seems to be required for the transport of plakoglobin, it might also be required for the transport of PKP3 and desmoplakin to the cell border in a manner that is independent of plakoglobin transport. This is consistent with our observation that inhibition of both PKC α and PKC μ did not

lead to the disruption of the interaction between 14-3-3 γ and desmoplakin or PKP3. The transport of DSG2 to the border is dependent on KIF5B, whereas the transport of DSC2 requires KIF3A and PKP2 (Nekrasova et al., 2011). Our results suggest that plakoglobin transport to the border is dependent on KIF5B, but not KIF3A, suggesting that the transport of desmosomal cadherins and plaque proteins to the border occurs through independent microtubule-dependent pathways. Alternatively, because 14-3-3 proteins bind to their ligands as dimers, with each member of the dimer forming a complex with a phosphopeptide (Brunet et al., 2002; Yaffe et al., 1997), it is possible that 14-3-3 γ bridges interactions between the different desmosomal plaque proteins, thereby allowing the formation of an intact desmosome, as previously postulated by Bonn   and colleagues (Bonn   et al., 2003). The only argument against this hypothesis is that, according to our study, 14-3-3 γ does not localize to the desmosome (Fig. 4A). In fact, the lack of any colocalization between 14-3-3 γ and plakoglobin suggests that any function that 14-3-3 γ performs, with respect to plakoglobin localization, is transient in nature; therefore, we favor the hypothesis that 14-3-3 γ is required for loading plakoglobin onto the KIF5B–KLC1 complex.

In contrast with the results reported here, previous work has suggested that 14-3-3 γ -knockout mice are viable, and no adhesion or sterility defects have been reported in these mice (Steinacker et al., 2005). Plakoglobin-knockout mice die during embryogenesis owing to cardiac defects arising as a result of decreased desmosome formation, and, as these mice die before the testis is formed, no information is available on the effects of loss of plakoglobin in the testis (Ruiz et al., 1996). Taken together, these previously published reports suggest that the functions of plakoglobin that are required for desmosome formation are not altered in the 14-3-3 γ ^{−/−} mice. Our results indicate that 14-3-3 γ regulates desmosome formation in multiple cell types, as loss of 14-3-3 γ in HCT116 cells, which are derived from the colon, and in the seminiferous epithelium leads to a decrease in cell–cell adhesion and in desmosome formation. Our results are also consistent with the previously reported role of 14-3-3 γ in the transport of proteins from the Golgi complex to the cell border (Valente et al., 2012). One reason for the differences in these results and those reported by Steinacker and colleagues (Steinacker et al., 2005) could be that another 14-3-3 family member binds to plakoglobin and stimulates desmosome formation in the 14-3-3 γ ^{−/−} mice, and that this compensation is not observed upon shRNA-mediated knockdown in the testis. Another possibility is that these are strain-specific variations that are due to differences in the genetic background of the mice used in the two studies. The generation of an inducible knockdown of 14-3-3 γ , in either the Swiss mice used in this study or in other mouse strains, could help determine whether loss of 14-3-3 γ leads to defects in desmosome formation and cell–cell adhesion in other tissues and not just in the testis.

The results described above point to the following model. 14-3-3 γ binds to plakoglobin that has been phosphorylated at residue S236 by PKC μ and loads plakoglobin onto the KIF5B–KLC1 complex for transport to the cell border (Fig. 8E). Loss of either 14-3-3 γ or KIF5B, or the dominant-negative versions of KIF5B and KLC1, inhibit the transport of plakoglobin to the border. Because 14-3-3 γ forms a complex with PKP3 and desmoplakin, loss of 14-3-3 γ might also lead to defects in transport of these proteins to the border. As loss of plakoglobin does not substantially affect the localization of the cadherins to the

border, it is possible that loss of plakoglobin leads to a defect in cadherin retention or the formation of an intact desmosome at the border in the absence of 14-3-3 γ . Furthermore, loss of KIF5B in the testis led to sterility and a decrease in desmosome formation. This is consistent with previously reported results that showed that disruption of cell–cell adhesion (Cheng and Mruk, 2002) and desmosome-like junction formation in the testis leads to an increase in sterility (Li et al., 2009; Lie et al., 2010).

To conclude, 14-3-3 γ and the KIF5B–KLC1 complex are required for regulating the transport of plakoglobin to the cell border. A decrease in 14-3-3 γ levels leads to a decrease in desmosome formation and the recruitment of other desmosomal proteins to the border. 14-3-3 γ might be required to maintain cell–cell adhesion in multiple tissues; however, this can only be confirmed by additional experiments *in vivo*.

MATERIALS AND METHODS

Animals

Swiss mice Crl:CFW(SW) were bred and maintained in the laboratory animal facility of the Advanced Centre for Treatment Research and Education in Cancer (ACTREC). Protocols for the experiments were approved by the Institutional Animal Ethics Committee of ACTREC. The animal study proposal number is 11/2008 dated August 19, 2008. The testis injections were performed as previously described (Sehgal et al., 2011).

Plasmids

Details of the oligonucleotides used in this study are available in supplementary material Table S1. The GST–14-3-3 γ , HA-epitope-tagged 14-3-3 γ and shRNA-resistant GFP–14-3-3 γ constructs have been previously described (Hosing et al., 2008). Site-directed mutagenesis (Stratagene) was used to generate the MYC–PG-S236A construct. The full-length KLC1 and KLC2 cDNA (Rahman et al., 1998), KLC-1 deletion (GST–KLC1 WT, GST–KLC1-CC and GST–KLC1-TPR) (Aoyama et al., 2009), GFP–KIF3A (Haraguchi et al., 2006), wild-type YFP–KIF5B (Gu et al., 2006), dominant-negative kinesin (GFP–KIF3A-T107N and YFP–KIF5B-T92N) (Wiesner et al., 2010), wild-type GFP–KLC1 and the GFP-tagged KLC1 coiled-coiled domain (Araki et al., 2007) constructs have been described previously. To generate the shRNA constructs against KIF5B and PKC μ , oligonucleotide pairs (supplementary material Table S1) were ligated into the pLKO.1 Puro or pLKO.1 EGFP-f Puro vectors as described previously (Sehgal et al., 2011). GST–PG1-300 was generated by amplifying the first 300 amino acids of plakoglobin (supplementary material Table S1) and cloning the fragment into the pGEX4T1 vector (Amersham).

Cell lines and transfections

The HCT116 (American Type Culture Collection) and the HCT116-derived stable cell lines were cultured as described previously (Hosing et al., 2008). To generate the KIF5B-knockdown clones in the HCT116 cell line, the cells were transfected with 1 μ g of the shRNA constructs that targeted human KIF5B. Sixty hours post transfection, the cells were transferred to medium that contained 0.5 μ g/ml of puromycin (Sigma) to generate single-cell clones. The clones K3 and K5 were used for the indicated experiments. The HCT116-derived plakoglobin-knockdown clones have been described previously (Gosavi et al., 2011).

Antibodies and western blotting

The antibodies against PKP3, both DSC2 and DSC3, DSG2, plakoglobin, desmoplakin, K8 (keratin 8), actin, E-cadherin, β -catenin and α -E-catenin were used in western blots as previously described (Gosavi et al., 2011; Khapare et al., 2012; Kundu et al., 2008). Tissue culture supernatants of the antibodies against HA (12CA5), 14-3-3 γ (CG31) and 14-3-3 σ (CS112) were used at a dilution of 1:50. The antibodies against 14-3-3 ϵ (T-16, Santa Cruz, dilution of 1:2000), p120 catenin (mouse monoclonal from BD Transductions, catalog number 610134, dilution of 1:1000) and

PKC μ (rabbit monoclonal obtained from Abcam, catalog number 3146-1, dilution of 1:500) were used for western blot analysis. The secondary antibodies against mouse and rabbit IgGs were conjugated to horseradish peroxidase and used at a dilution of 1:1000 (Invitrogen) and 1:5000 (Pierce), respectively.

Immunofluorescence and calcium-switch assays

The cells were cultured on chromic-acid-treated, poly-L-lysine-coated glass coverslips at a confluence of 70–80%. Before fixation, the cells were carefully washed twice with 1 \times PBS. HCT116-derived clones were fixed in absolute methanol for 10 minutes at -20°C to detect α -tubulin, KIF5B, PKP2, Par3, ZO1, P-cadherin, desmoplakin, plakoglobin, DSC2 and DSC3, DSG2, E-cadherin and PKP3. In some experiments, cells were fixed in 4% paraformaldehyde and permeabilized with Triton X-100 as described previously (Gosavi et al., 2011). The antibodies against PKP3, both DSC2 and DSC3, DSG2, plakoglobin, desmoplakin, K8, actin, E-cadherin, β -catenin, ZO-1 and α -E-catenin were used in immunofluorescence analysis as described previously (Gosavi et al., 2011; Khapare et al., 2012; Kundu et al., 2008). Antibodies against PKP2 (BD Clontech, dilution 1:25), KIF5B (Abcam, dilution 1:100), α -tubulin (Abcam, dilution 1:150), Par3 (Millipore, dilution 1:50), ZO-1 (Abcam, dilution 1:100), P-cadherin (BD Transduction Laboratories, dilution 1:100), HA (12CA5, supernatant), p120 catenin (BD Transductions, dilution 1:100), N-cadherin (Life Technologies, catalog number 33-3900, dilution 1:50), α -E-catenin (Santa Cruz Biotechnology, dilution 1:25) and E-cadherin (clone 36/E-cadherin, mouse monoclonal, BD Transduction Laboratories, dilution 1:100) were incubated with the cells for 1 hour at room temperature at the indicated dilutions as described previously (Gosavi et al., 2011). To stain mitochondria, Mitotracker Green FM (Invitrogen) was used at a concentration of 100 nM to stain live cells. Confocal images were obtained by using a LSM 510 Meta Carl Zeiss confocal system with argon 488-nm and HeNe 543-nm lasers. All images were obtained by using an Axio Observer Z.1 microscope (numerical aperture 1.4) at a magnification of $\times 630$ ($\times 63$ objective and $\times 10$ eyepiece) with a $\times 2$ or $\times 4$ optical zoom. The surface intensity of staining was measured for the different proteins in a minimum of 24 cells using the Axiovision software, and the mean and standard deviation were plotted.

Hanging-drop assays

Hanging-drop assays were used to measure cell adhesion as described previously (Kundu et al., 2008).

GST-pulldown and immunoprecipitation assays

These assays were performed as described previously (Dalal et al., 1999).

GST-plakoglobin production and kinase assays

GST alone or GST-PG1-300 was purified from bacteria as described previously (Dalal et al., 2004). The purified proteins were used in kinase assays with recombinant PKC μ and a peptide that had been derived from CREB as a positive control (Signal Chem). Kinase activity was determined by using the ADP glow assay kit (Promega) according to the manufacturer's instructions.

Histology and immunohistochemistry

Mouse testes were fixed in 10% formaldehyde overnight and processed for histology as described previously (Kundu et al., 2008). TUNEL assays were performed as per the manufacturer's instructions (Promega).

Electron microscopy

Wild-type and 14-3-3 γ -knockdown testes were fixed with 3% glutaraldehyde and post-fixed with 1% osmium tetroxide (Tedpella). Grids were contrasted with alcoholic uranyl acetate for 1 minute and lead citrate for 30 seconds. The grids were observed under a Carl Zeiss LIBRA120 EFTEM transmission electron microscope at an accelerating voltage of 120 kV and at $\times 325,000$ magnification. Images were captured using a Slow Scan CCD camera (TRS, Germany).

Statistical Analysis

All *P*-values were generated using a Student's *t*-test.

Acknowledgements

We thank Young-hoon Lee (Korea Advanced Institute of Science and Technology, Daejeon, Korea), Stefan Linder (Institute of Medical Microbiology, Hamburg, Germany), Tetsu Akiyama (University of Tokyo, Tokyo, Japan), Chen Gu (Ohio State University, Columbus, OH) and Lawrence Goldstein (University of California San Diego, San Diego, CA) for supplying us with constructs that were used during the course of this study. We would also like to thank the ACTREC imaging facility for help with confocal microscopy, the ACTREC animal facility, and Sharda Sawant for helping with the preparation of the grids for electron microscopy.

Competing interests

The authors declare no competing interests.

Author contributions

L.S., M.M.V., F.S., U.K. and S.N.D. designed experiments and wrote the manuscript. L.S. performed the majority of the experiments with contributions from A.R., N.K., M.S., K.B., S.A. and N.A. A.M. determined that 14-3-3 γ forms a complex with KIF5B, S.S.V. performed the PKC μ -knockdown experiments and solubility assays, L.B. performed electron microscopy, R.M. performed the PKC μ kinase assays, M.G. and S.B. performed the RT-PCR assays and helped with confocal microscopy, H.A. performed the cell–matrix adhesion assays, R.T. performed the testis injections and A.S.H. generated the 14-3-3 ϵ -knockdown clones.

Funding

This work was supported by grants from the Department of Biotechnology, India [grant numbers BT/PR6521/Med/14/828/2005 and BT/PR12578/MED/31/75/2009]; and the Advanced Centre for Treatment Research and Education in Cancer (to L.S. and S.N.D.). A fellowship from the University Grants Commission supported A.M.

Supplementary material

Supplementary material available online at <http://jcs.biologists.org/lookup/suppl/doi:10.1242/jcs.125807/-DC1>

References

- Acehan, D., Petzold, C., Gumper, I., Sabatini, D. D., Müller, E. J., Cowin, P. and Stokes, D. L. (2008). Plakoglobin is required for effective intermediate filament anchorage to desmosomes. *J. Invest. Dermatol.* **128**, 2665–2675.
- Andersson, A. M., Edvardsen, K. and Skakkebaek, N. E. (1994). Expression and localization of N- and E-cadherin in the human testis and epididymis. *Int. J. Androl.* **17**, 174–180.
- Aoyama, T., Hata, S., Nakao, T., Tanigawa, Y., Oka, C. and Kawaichi, M. (2009). Cayman ataxia protein caytaxin is transported by kinesin along neurites through binding to kinesin light chains. *J. Cell Sci.* **122**, 4177–4185.
- Araki, Y., Kawano, T., Taru, H., Saito, Y., Wada, S., Miyamoto, K., Kobayashi, H., Ishikawa, H. O., Ohsugi, Y., Yamamoto, T. et al. (2007). The novel cargo Alcadein induces vesicle association of kinesin-1 motor components and activates axonal transport. *EMBO J.* **26**, 1475–1486.
- Bass-Zubek, A. E., Godsel, L. M., Delmar, M. and Green, K. J. (2009). Plakophilins: multifunctional scaffolds for adhesion and signaling. *Curr. Opin. Cell Biol.* **21**, 708–716.
- Bierkamp, C., McLaughlin, K. J., Schwarz, H., Huber, O. and Kemler, R. (1996). Embryonic heart and skin defects in mice lacking plakoglobin. *Dev. Biol.* **180**, 780–785.
- Bonné, S., Gilbert, B., Hatzfeld, M., Chen, X., Green, K. J. and van Roy, F. (2003). Defining desmosomal plakophilin-3 interactions. *J. Cell Biol.* **161**, 403–416.
- Brunet, A., Kanai, F., Stehn, J., Xu, J., Sarbassova, D., Frangioni, J. V., Dalal, S. N., DeCaprio, J. A., Greenberg, M. E. and Yaffe, M. B. (2002). 14-3-3 transits to the nucleus and participates in dynamic nucleocytoplasmic transport. *J. Cell Biol.* **156**, 817–828.
- Caldelari, R., de Bruin, A., Baumann, D., Suter, M. M., Bierkamp, C., Balmer, V. and Müller, E. (2001). A central role for the armadillo protein plakoglobin in the autoimmune disease pemphigus vulgaris. *J. Cell Biol.* **153**, 823–834.
- Chan, T. A., Hermeking, H., Lengauer, C., Kinzler, K. W. and Vogelstein, B. (1999). 14-3-3 σ is required to prevent mitotic catastrophe after DNA damage. *Nature* **401**, 616–620.
- Chen, X., Bonne, S., Hatzfeld, M., van Roy, F. and Green, K. J. (2002). Protein binding and functional characterization of plakophilin 2. Evidence for its diverse roles in desmosomes and β -catenin signaling. *J. Biol. Chem.* **277**, 10512–10522.
- Cheng, C. Y. and Mruk, D. D. (2002). Cell junction dynamics in the testis: Sertoli-germ cell interactions and male contraceptive development. *Physiol. Rev.* **82**, 825–874.

- Chidgey, M., Brakebusch, C., Gustafsson, E., Cruchley, A., Hail, C., Kirk, S., Merritt, A., North, A., Tselepis, C., Hewitt, J. et al. (2001). Mice lacking desmocollin 1 show epidermal fragility accompanied by barrier defects and abnormal differentiation. *J. Cell Biol.* **155**, 821–832.
- Cross, R. A. and Carter, N. J. (2000). Molecular motors. *Curr. Biol.* **10**, R177–R179.
- Dalal, S. N., Schweitzer, C. M., Gan, J. and DeCaprio, J. A. (1999). Cytoplasmic localization of human cdc25C during interphase requires an intact 14-3-3 binding site. *Mol. Cell. Biol.* **19**, 4465–4479.
- Dalal, S. N., Yaffe, M. B. and DeCaprio, J. A. (2004). 14-3-3 family members act coordinately to regulate mitotic progression. *Cell Cycle* **3**, 670–675.
- Dusek, R. L., Godsel, L. M. and Green, K. J. (2007). Discriminating roles of desmosomal cadherins: beyond desmosomal adhesion. *J. Dermatol. Sci.* **45**, 7–21.
- Gallicano, G. I., Kouklis, P., Bauer, C., Yin, M., Vasioukhin, V., Degenstein, L. and Fuchs, E. (1998). Desmoplakin is required early in development for assembly of desmosomes and cytoskeletal linkage. *J. Cell Biol.* **143**, 2009–2022.
- Garrod, D. and Chidgey, M. (2007). Desmosome structure, composition and function. *Biochim. Biophys. Acta* **1778**, 572–587.
- Getsios, S., Huen, A. C. and Green, K. J. (2004). Working out the strength and flexibility of desmosomes. *Nat. Rev. Mol. Cell Biol.* **5**, 271–281.
- Gloushankova, N. A., Wakatsuki, T., Troyanovsky, R. B., Elson, E. and Troyanovsky, S. M. (2003). Continual assembly of desmosomes within stable intercellular contacts of epithelial A-431 cells. *Cell Tissue Res.* **314**, 399–410.
- Gosavi, P., Kundu, S. T., Khapare, N., Sehgal, L., Karkhanis, M. S. and Dalal, S. N. (2011). E-cadherin and plakoglobin recruit plakophilin3 to the cell border to initiate desmosome assembly. *Cell. Mol. Life Sci.* **68**, 1439–1454.
- Green, K. J. and Gaudry, C. A. (2000). Are desmosomes more than tethers for intermediate filaments? *Nat. Rev. Mol. Cell Biol.* **1**, 208–216.
- Grossmann, K. S., Grund, C., Huelsenken, J., Behrend, M., Erdmann, B., Franke, W. W. and Birchmeier, W. (2004). Requirement of plakophilin 2 for heart morphogenesis and cardiac junction formation. *J. Cell Biol.* **167**, 149–160.
- Gu, C., Zhou, W., Puthenveedu, M. A., Xu, M., Jan, Y. N. and Jan, L. Y. (2006). The microtubule plus-end tracking protein EB1 is required for Kv1 voltage-gated K⁺ channel axonal targeting. *Neuron* **52**, 803–816.
- Haraguchi, K., Hayashi, T., Jimbo, T., Yamamoto, T. and Akiyama, T. (2006). Role of the kinesin-2 family protein, KIF3, during mitosis. *J. Biol. Chem.* **281**, 4094–4099.
- Hatzfeld, M. (2007). Plakophilins: Multifunctional proteins or just regulators of desmosomal adhesion? *Biochim. Biophys. Acta* **1773**, 69–77.
- Hausser, A., Link, G., Bamberg, L., Burzlaff, A., Lutz, S., Pfizenmaier, K. and Johannes, F. J. (2002). Structural requirements for localization and activation of protein kinase C μ (PKC μ) at the Golgi compartment. *J. Cell Biol.* **156**, 65–74.
- Hosing, A. S., Kundu, S. T. and Dalal, S. N. (2008). 14-3-3 Gamma is required to enforce both the incomplete S phase and G2 DNA damage checkpoints. *Cell Cycle* **7**, 3171–3179.
- Khapare, N., Kundu, S. T., Sehgal, L., Sawant, M., Priya, R., Gosavi, P., Gupta, N., Alam, H., Karkhanis, M., Naik, N. et al. (2012). Plakophilin3 loss leads to an increase in PRL3 levels promoting K8 dephosphorylation, which is required for transformation and metastasis. *PLoS ONE* **7**, e38561.
- Knudsen, K. A. and Wheelock, M. J. (1992). Plakoglobin, or an 83-kD homologue distinct from beta-catenin, interacts with E-cadherin and N-cadherin. *J. Cell Biol.* **118**, 671–679.
- Koch, P. J., Mahoney, M. G., Ishikawa, H., Pulkkinen, L., Uitto, J., Shultz, L., Murphy, G. F., Whitaker-Menezes, D. and Stanley, J. R. (1997). Targeted disruption of the pemphigus vulgaris antigen (desmoglein 3) gene in mice causes loss of keratinocyte cell adhesion with a phenotype similar to pemphigus vulgaris. *J. Cell Biol.* **137**, 1091–1102.
- Kundu, S. T., Gosavi, P., Khapare, N., Patel, R., Hosing, A. S., Maru, G. B., Ingle, A., Decaprio, J. A. and Dalal, S. N. (2008). Plakophilin3 downregulation leads to a decrease in cell adhesion and promotes metastasis. *Int. J. Cancer* **123**, 2303–2314.
- Lechler, T. and Fuchs, E. (2007). Desmoplakin: an unexpected regulator of microtubule organization in the epidermis. *J. Cell Biol.* **176**, 147–154.
- Lee, N. P., Mruk, D., Lee, W. M. and Cheng, C. Y. (2003). Is the cadherin/catenin complex a functional unit of cell-cell actin-based adherens junctions in the rat testis? *Biol. Reprod.* **68**, 489–508.
- Lewis, J. E., Wahl, J. K., 3rd, Sass, K. M., Jensen, P. J., Johnson, K. R. and Wheelock, M. J. (1997). Cross-talk between adherens junctions and desmosomes depends on plakoglobin. *J. Cell Biol.* **136**, 919–934.
- Li, M. W., Mruk, D. D., Lee, W. M. and Cheng, C. Y. (2009). Connexin 43 and plakophilin-2 as a protein complex that regulates blood-testis barrier dynamics. *Proc. Natl. Acad. Sci. USA* **106**, 10213–10218.
- Lie, P. P., Cheng, C. Y. and Mruk, D. D. (2010). Crosstalk between desmoglein-2/desmocollin-2/Src kinase and coxsackie and adenovirus receptor/ZO-1 protein complexes, regulates blood-testis barrier dynamics. *Int. J. Biochem. Cell Biol.* **42**, 975–986.
- Lie, P. P., Cheng, C. Y. and Mruk, D. D. (2011). The biology of the desmosome-like junction a versatile anchoring junction and signal transducer in the seminiferous epithelium. *Int. Rev. Cell Mol. Biol.* **286**, 223–269.
- Liljedahl, M., Maeda, Y., Colanzi, A., Ayala, I., Van Lint, J. and Malhotra, V. (2001). Protein kinase D regulates the fission of cell surface destined transport carriers from the trans-Golgi network. *Cell* **104**, 409–420.
- Marcozzi, C., Burdett, I. D., Buxton, R. S. and Magee, A. I. (1998). Coexpression of both types of desmosomal cadherin and plakoglobin confers strong intercellular adhesion. *J. Cell Sci.* **111**, 495–509.
- Michels, C., Buchta, T., Bloch, W., Krieg, T. and Niessen, C. M. (2009). Classical cadherins regulate desmosome formation. *J. Invest. Dermatol.* **129**, 2072–2075.
- Muslin, A. J., Tanner, J. W., Allen, P. M. and Shaw, A. S. (1996). Interaction of 14-3-3 with signaling proteins is mediated by the recognition of phosphoserine. *Cell* **84**, 889–897.
- Nekrasova, O. E., Amargo, E. V., Smith, W. O., Chen, J., Kreitzer, G. E. and Green, K. J. (2011). Desmosomal cadherins utilize distinct kinesins for assembly into desmosomes. *J. Cell Biol.* **195**, 1185–1203.
- Obenaus, J. C., Cantley, L. C. and Yaffe, M. B. (2003). Scansite 2.0: Proteome-wide prediction of cell signaling interactions using short sequence motifs. *Nucleic Acids Res.* **31**, 3635–3641.
- Palka, H. L. and Green, K. J. (1997). Roles of plakoglobin end domains in desmosome assembly. *J. Cell Sci.* **110**, 2359–2371.
- Park, J. E., Kim, Y. I. and Yi, A. K. (2009). Protein kinase D1 is essential for MyD88-dependent TLR signaling pathway. *J. Immunol.* **182**, 6316–6327.
- Pasdar, M., Krzeminski, K. A. and Nelson, W. J. (1991). Regulation of desmosome assembly in MDCK epithelial cells: coordination of membrane core and cytoplasmic plaque domain assembly at the plasma membrane. *J. Cell Biol.* **113**, 645–655.
- Prestle, J., Pfizenmaier, K., Brenner, J. and Johannes, F. J. (1996). Protein kinase C μ is located at the Golgi compartment. *J. Cell Biol.* **134**, 1401–1410.
- Rahman, A., Friedman, D. S. and Goldstein, L. S. (1998). Two kinesin light chain genes in mice. Identification and characterization of the encoded proteins. *J. Biol. Chem.* **273**, 15395–15403.
- Ruiz, P., Brinkmann, V., Ledermann, B., Behrend, M., Grund, C., Thalhammer, C., Vogel, F., Birchmeier, C., Günthert, U., Franke, W. W. et al. (1996). Targeted mutation of plakoglobin in mice reveals essential functions of desmosomes in the embryonic heart. *J. Cell Biol.* **135**, 215–225.
- Russell, L. D., Ettlin, R., Sinha Hikim, A. P. and Clegg, E. D. (1990). *Histological and Histopathological Evaluation of the Testis*. Clearwater, FL: Cache River.
- Sehgal, L., Thorat, R., Khapare, N., Mukhopadhyaya, A., Sawant, M. and Dalal, S. N. (2011). Lentiviral mediated transgenesis by in vivo manipulation of spermatogonial stem cells. *PLoS ONE* **6**, e21975.
- Silver, K. E. and Harrison, R. E. (2011). Kinesin 5B is necessary for delivery of membrane and receptors during Fc γ R-mediated phagocytosis. *J. Immunol.* **186**, 816–825.
- Skiyara, T., Bonné, S., D'Hooge, P., Denecker, G., Goossens, S., De Rycke, R., Borgonie, G., Bösl, M., van Roy, F. and van Hengel, J. (2008). Plakophilin-3-deficient mice develop hair coat abnormalities and are prone to cutaneous inflammation. *J. Invest. Dermatol.* **128**, 1375–1385.
- Steinacker, P., Schwarz, P., Reim, K., Brechlin, P., Jahn, O., Kratzin, H., Aitken, A., Wiltfang, J., Aguzzi, A., Bahn, E. et al. (2005). Unchanged survival rates of 14-3-3gamma knockout mice after inoculation with pathological prion protein. *Mol. Cell. Biol.* **25**, 1339–1346.
- Tanaka, Y., Kanai, Y., Okada, Y., Nonaka, S., Takeda, S., Harada, A. and Hirokawa, N. (1998). Targeted disruption of mouse conventional kinesin heavy chain, kif5B, results in abnormal perinuclear clustering of mitochondria. *Cell* **93**, 1147–1158.
- Telles, E., Hosing, A. S., Kundu, S. T., Venkatraman, P. and Dalal, S. N. (2009). A novel pocket in 14-3-3 ϵ is required to mediate specific complex formation with cdc25C and to inhibit cell cycle progression upon activation of checkpoint pathways. *Exp. Cell Res.* **315**, 1448–1457.
- Tinkle, C. L., Pasolli, H. A., Stokes, N. and Fuchs, E. (2008). New insights into cadherin function in epidermal sheet formation and maintenance of tissue integrity. *Proc. Natl. Acad. Sci. USA* **105**, 15405–15410.
- Valente, C., Turacchio, G., Marigliò, S., Pagliuso, A., Gaibisso, R., Di Tullio, G., Santoro, M., Formiggini, F., Spanò, S., Piccini, D. et al. (2012). A 14-3-3 γ dimer-based scaffold bridges CtBP1-S/BARS to PI(4)KIII β to regulate post-Golgi carrier formation. *Nat. Cell Biol.* **14**, 343–354.
- Vasioukhin, V., Bowers, E., Bauer, C., Degenstein, L. and Fuchs, E. (2001). Desmoplakin is essential in epidermal sheet formation. *Nat. Cell Biol.* **3**, 1076–1085.
- Verhey, K. J. and Hammond, J. W. (2009). Traffic control: regulation of kinesin motors. *Nat. Rev. Mol. Cell Biol.* **10**, 765–777.
- Wiesner, C., Faix, J., Himmel, M., Bentzien, F. and Linder, S. (2010). KIF5B and KIF3A/KIF3B kinesins drive MT1-MMP surface exposure, CD44 shedding, and extracellular matrix degradation in primary macrophages. *Blood* **116**, 1559–1569.
- Wong, C. H., Mruk, D. D., Lui, W. Y. and Cheng, C. Y. (2004). Regulation of blood-testis barrier dynamics: an in vivo study. *J. Cell Sci.* **117**, 783–798.
- Yaffe, M. B. (2002). How do 14-3-3 proteins work? – Gatekeeper phosphorylation and the molecular anvil hypothesis. *FEBS Lett.* **513**, 53–57.
- Yaffe, M. B., Rittinger, K., Volinia, S., Caron, P. R., Aitken, A., Leffers, H., Gambini, S. J., Smerdon, S. J. and Cantley, L. C. (1997). The structural basis for 14-3-3:phosphopeptide binding specificity. *Cell* **91**, 961–971.

Supplementary Figure 1. 14-3-3 γ loss leads to decreased cell-cell adhesion and no changes in other junctional components.

A. Vector control (Vec), 14-3-3 γ knockdown (sh 14-3-3 γ) and KIF5B knockdown (sh KIF5B) testis sections were assayed for cell death by performing terminal deoxynucleotidyl transferase dUTP nick end labeling (TUNEL) assays. Note that although some TUNEL-positive cells were observed in the sh14-3-3 γ testis, no staining was observed in the Vec or the shKIF5B sections. **B.** The Vec or sh 14-3-3 γ cells were incubated with extra cellular matrix (ECM) substrates and a cell-ECM adhesion assay was performed. The mean and standard deviation were plotted on the y-axis. Note that adhesion was decreased on all substrates. The p value was calculated using a students t-test and was <0.05 suggesting that cell ECM adhesion was significantly reduced in sh14-3-3 γ cells as compared to the vector control. **C.** Vec and plakoglobin (PG) knockdown cells (sh PG) were stained with antibodies to DSC2/3 and DSG2 followed by confocal microscopy. The border staining of these proteins was not altered in the shPG cells as compared with the Vec cells. **D.** Vec and sh14-3-3 γ cells were stained with antibodies to E-cadherin, P-cadherin, β -catenin, ZO-1 α -E-catenin, p120 catenin and Par-3 followed by confocal microscopy. The border staining of these proteins was not altered in the sh14-3-3 γ cells as compared to the vector control. **E.** The border intensity was measured for at least 20 cells in three different experiments. The mean and standard deviation are plotted. Total magnification is 630X with 2X optical zoom. *P*-values obtained using Student's t test. A p value of <0.05 was considered significant.

Supplementary Figure 2. Intensity profiles for desmosome proteins in the 14-3-3 γ and KIF5B knockdown cells. The vector control (Vec), 14-3-3 γ knockdown cells (sh

14-3-3 γ) and KIF5B knockdown cells (K3 and K5) were stained with the indicated antibodies and the intensity profiles were determined. Note that the desmosomal proteins show higher intensity at the cell border in the 14-3-3 γ and KIF5B knockdown cells than do the Vec cells. No change was observed in the intensity of adherens junction proteins at the cell border.

Supplementary Figure 3. Plakoglobin (PG) border localization is dependent on 14-3-

3 γ and KIF5B. **A.** Identification of a 14-3-3 binding site and potential PKC μ site in PG using motif scan. **B.** Hanging drop assays were performed to determine cell-cell adhesion. The K3 and K5 KIF5B KD cells formed fewer and smaller clumps as compared to the Vec cells. **C.** Vec, K3 and K5 cells were stained with antibodies to PG and β -catenin. Note that although PG is not localized to the border in K3 and K5, β -catenin localization to the border is not altered in K3 and K5 cells suggesting that KIF5B is required for transport of PG to the cell border. **D.** HCT116 cells were cultured in low calcium medium and then incubated in the presence or absence of Nocodazole (NOC). The cells were stained with antibodies to PG and visualized by confocal microscopy. Staining was quantified and mean and standard deviation for border staining were calculated in three independent experiments and plotted as shown. The p value was calculated using a students t-test and was <0.05 suggesting that PG border staining was significantly reduced upon treatment with nocodazole. Total magnification is 630X with 2X optical zoom. **E.** mRNA was prepared from the Vec and KIF5B knockdown cells (K3 and K5) and converted to cDNA; PCR reactions were performed with oligonucleotide pairs specific for the indicated genes. Glyceraldehyde 3-phosphate dehydrogenase (GAPDH) served as a loading control. **F.** Vec, K3 and K5 cells were stained with the

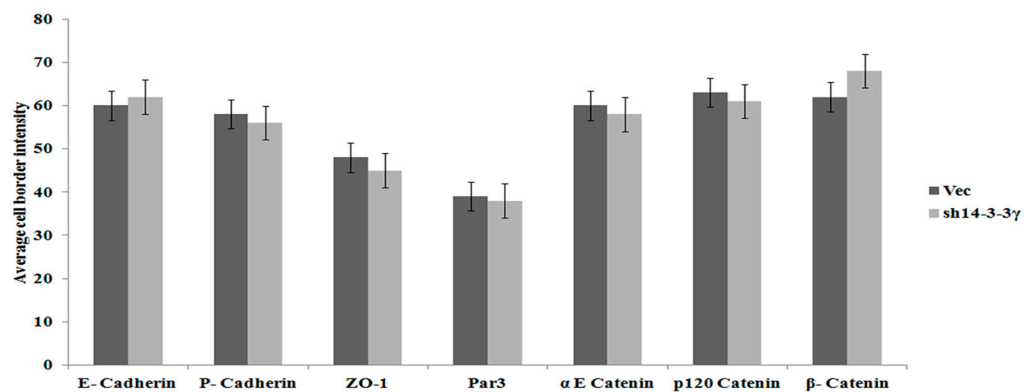
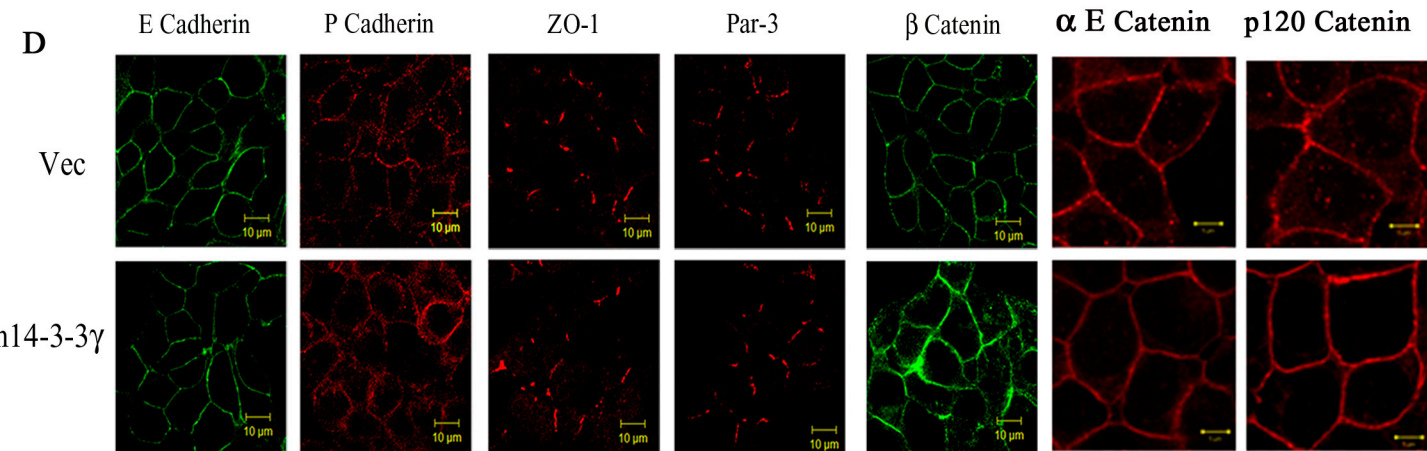
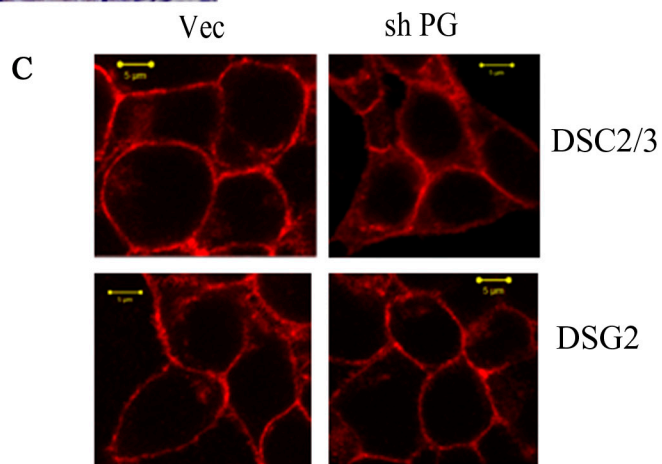
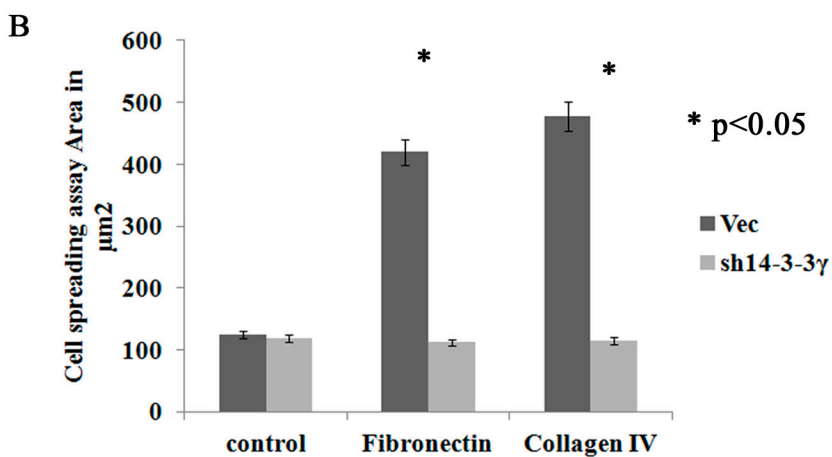
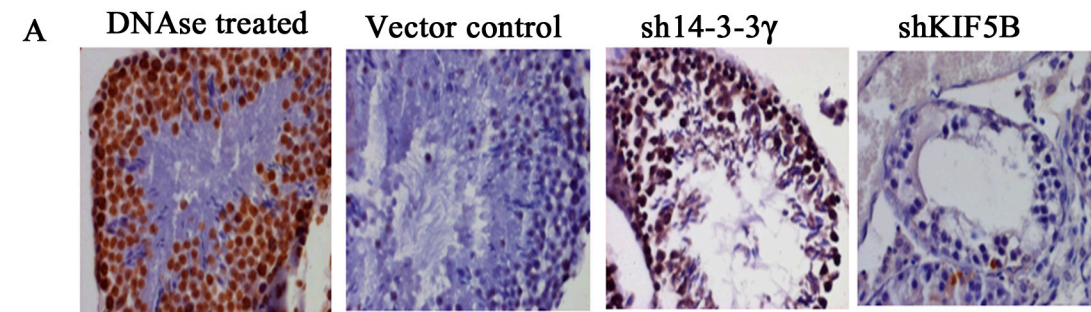
indicated antibodies followed by confocal microscopy. Note that the localization of the adherens junction proteins is not altered upon KIF5B knockdown. **G.** Protein extracts were prepared from Vec, K3 and K5 cells and were resolved on SDS-PAGE gels followed by Western blotting with the indicated antibodies. A Western blot for actin was performed as a loading control. Note that the levels of these proteins are not altered upon KIF5B knockdown.

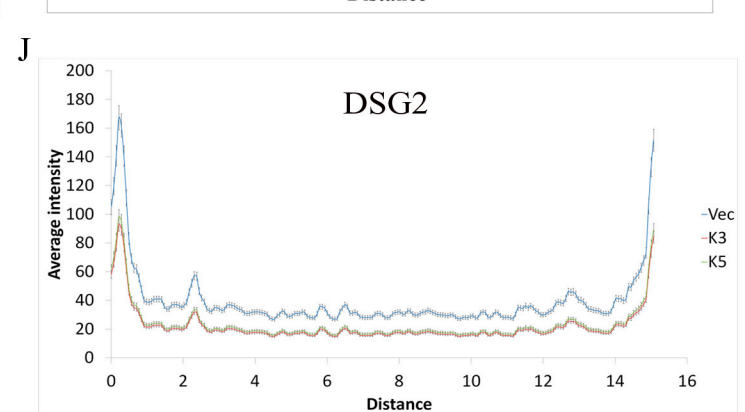
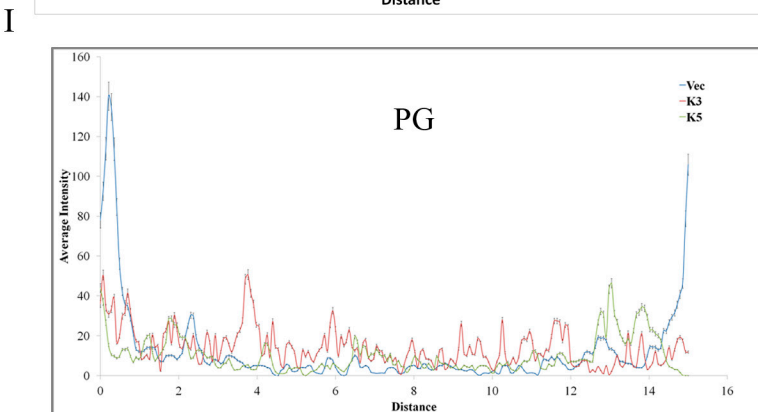
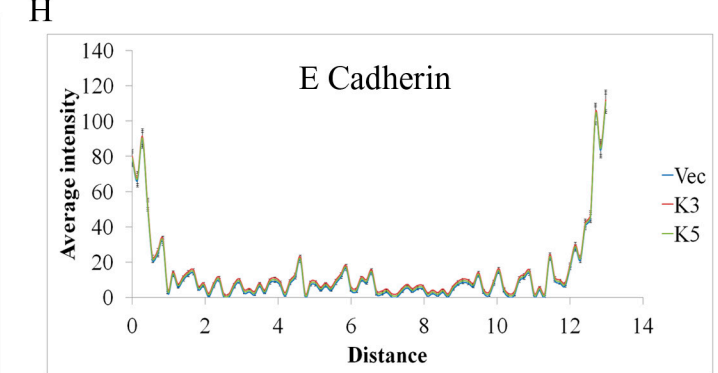
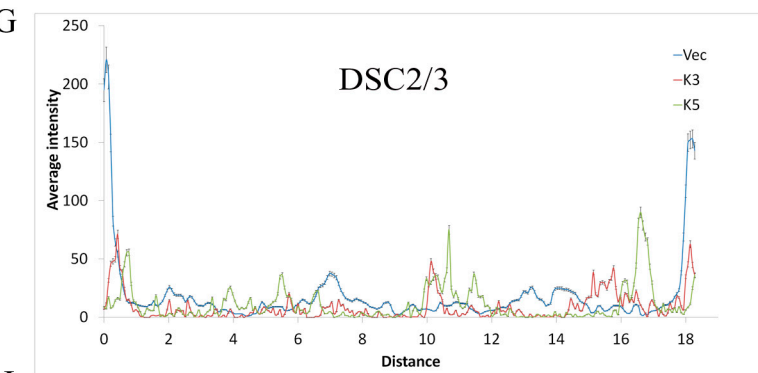
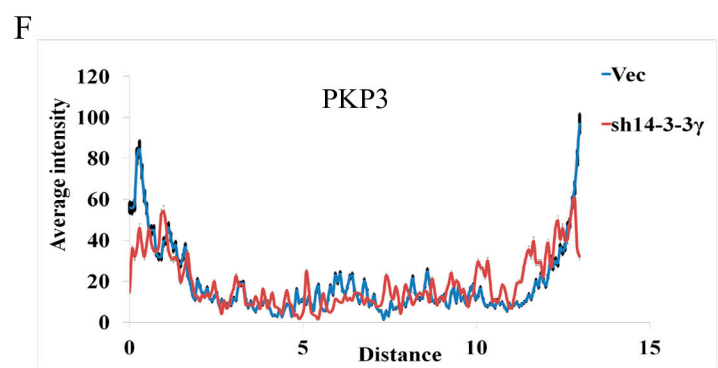
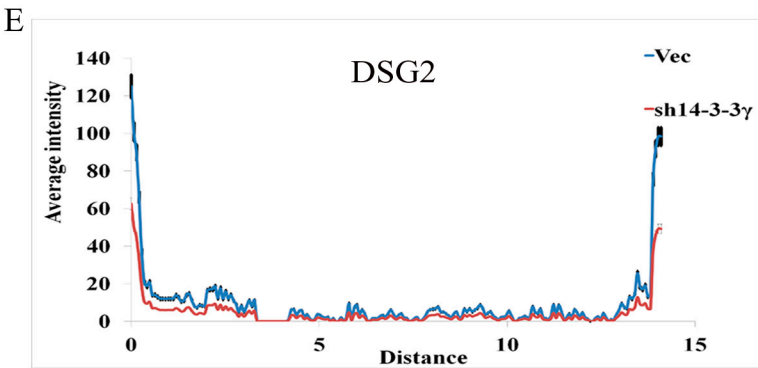
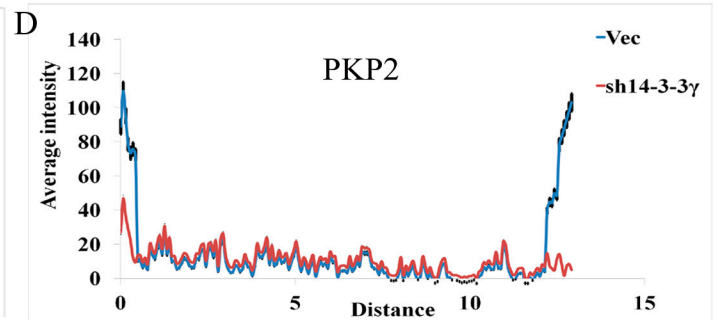
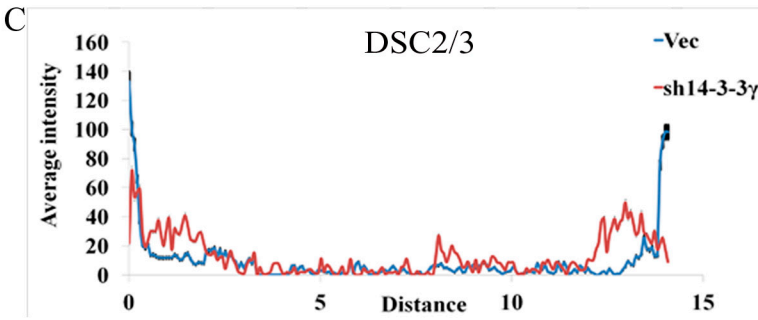
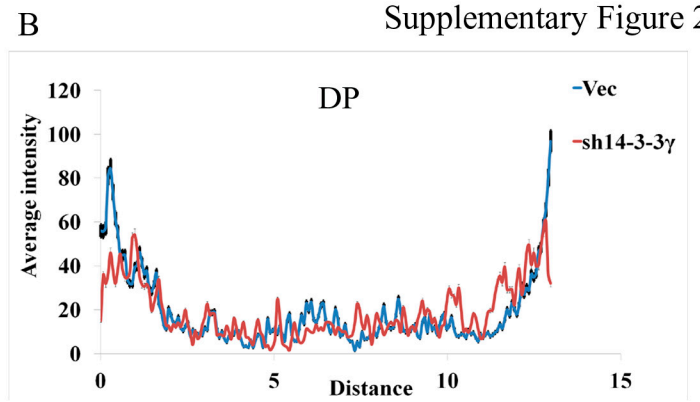
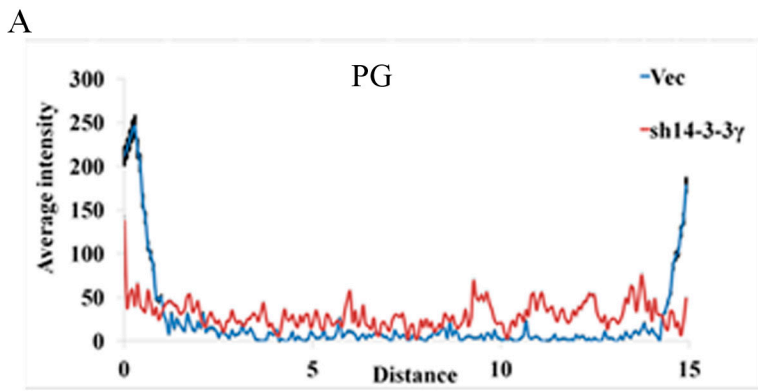
Supplementary Figure 4. Localization of desmosomal proteins in cells lacking 14-3-3 σ or upon KIF5B or 14-3-3 γ knockdown. **A.** Protein lysates were prepared from HCT116 cells either with both copies (14-3-3 σ +/+) or without both copies (14-3-3 σ -/-) of the 14-3-3 σ gene. The lysates were resolved on SDS-PAGE gels and Western blot analysis performed with the indicated antibodies. Note the decrease in PG levels observed in the 14-3-3 σ -/- cells. Actin was used as a loading control. **B.** Hanging drop assays were performed to measure cell-cell adhesion. **C.** The 14-3-3 σ +/+ and 14-3-3 σ -/- cells were stained with antibodies to PG followed by confocal microscopy. Bars correspond to 5 μ M. **D.** NP40 soluble (S) and insoluble (I) extracts prepared from Vec or sh 14-3-3 γ cells were resolved on SDS-PAGE gels and Western blots performed with the indicated antibodies. Please note that the increase in cytoplasmic localization of the desmosomal cadherins is not associated with an increase in solubility. Western blots for keratin and actin were performed as controls. **E.** Cells were fixed with paraformaldehyde and stained with the indicated antibodies. Please note that DSG2 and DSC2/3 localize to the cytoplasm in cells lacking 14-3-3 γ or KIF5B as compared with the negative control. Bars correspond to 5 μ m.

Name	Targeting sequence
14-3-3 γ ShRNA a	CCGGACTATTACCGTTACCTGGCAGTTCTCGCCAGGTA ACGGTAATAGTCCTTTTTTG
14-3-3 γ ShRNA b	AATTCAAAAAAGGACTATTACCGTTACCTGGCGAGAAC TGCCAGGTAACGGTAATAGT
KIF5B shRNA a	CCGGAACCTTCATGATCCAGAAGGCTCGAGCCTTCTGGA TCATGAAGTTTTTTTG
KIF5B shRNA a	AATTCAAAAAAACTTCATGATCCAGAAGGCTCGAGCCT TCTGGATCATGAAGTT
14-3-3 γ Fwd (Mus musculus)	GGGATCCATGGTGGACCGCGAGCAAC
14-3-3 γ Rev (Mus musculus)	GCTCGAGTTAGTTGTTGCCTTCACCG
PG S236A F	GTCCGCATGCTCGCCTCCCCTGTGGAG
PG S236A R	CTCCACAGGGGAGGCGAGCATGCGGAC
PG F	GGATCCATGGAGGTGATGAACC
PG R	CTCGAGCTAGGCCAGCATGTGGTC
PKC μ shRNA a	CCGGCCATTGATCTTATCAATAACTCGAGTTATTGATA AGATCAATGGTTTTTG
PKC μ shRNA b	AATTCAAAAACCATTGATCTTATCAATAACTCGAGTTA TTGATAAGATCAATGG
GAPDH RT 5'	TGCACCACCAACTGCTTAGC
GAPDH RT 3'	GGCATGGACTGTGGTCATGAG
Desmoglein 2 RT 5'	TACGCCCTGCTGCTTCTCC
Desmoglein 2 RT 3'	TCTCCCTCCCGAAGAGCCACG
Desmocollin 2 RT 5'	GTTTTACTCAGCCCCGTCTTG
Desmocollin 2 RT 3'	GCCCATCTTCTTCTTGTCGT
PKP2 RT 5'	AGGTTTGCTGTGGAATTTGTC
PKP2 RT 3'	CGCCAGCAGAACTCATGTTT
PG 5' 1-300	aaGGATCCATGGAGGTGATGAACCTGATGGAG
PG 3' 1-300	aaCTCGAGCTGGTTGCCGTAGGCCAG

Supplementary Table 1. List of oligonucleotides used for cloning and Reverse

Transcriptase PCR reactions.

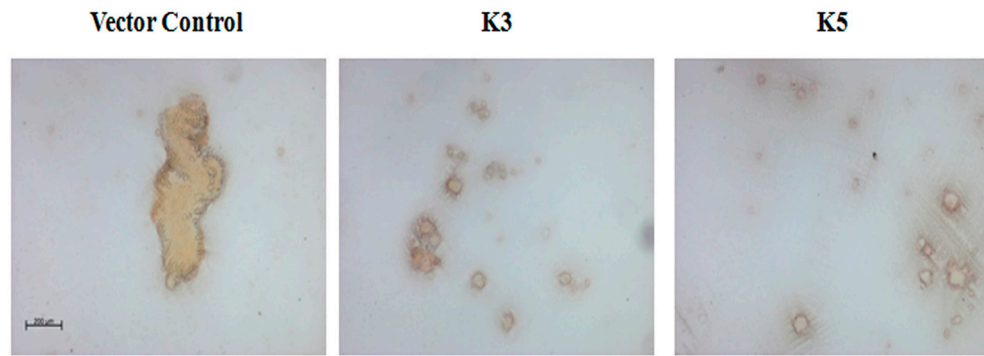




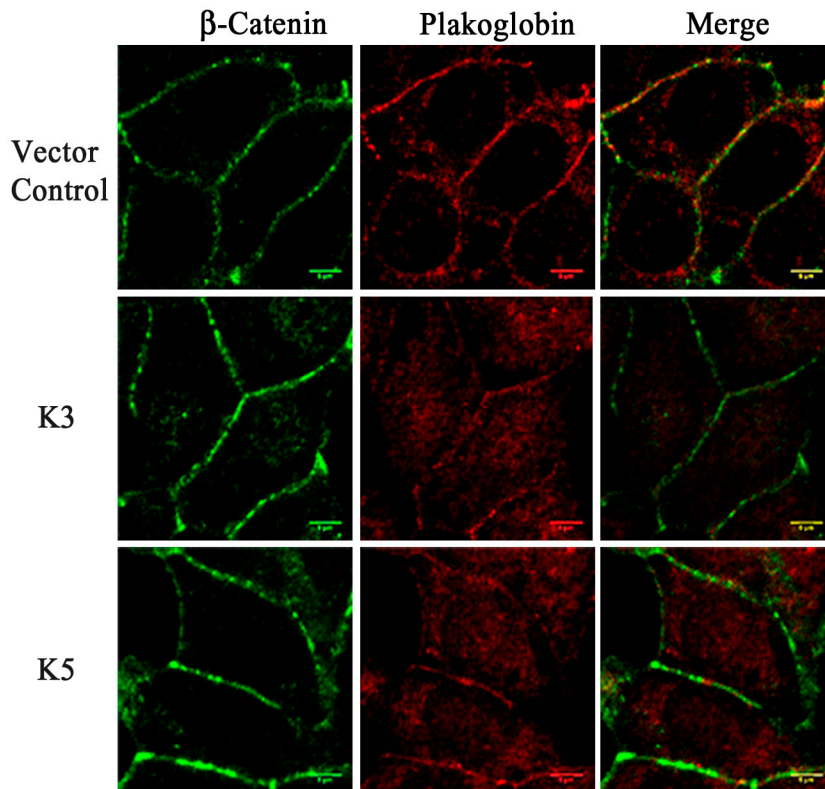
A

Phosphoserine/threonine binding group (pST_bind)					
14-3-3 Mode 1			Gene Card YWHAZ		
Site	Score	Percentile	Sequence	SA	
S236	0.4336	0.606 %	PALVRMLSSPVESVL	0.385	
Basophilic serine/threonine kinase group (Baso ST_kin)					
PKC mu			Gene Card PRKCM		
Site	Score	Percentile	Sequence	SA	
S236	0.4873	0.924 %	PALVRMLSSPVESVL	0.385	

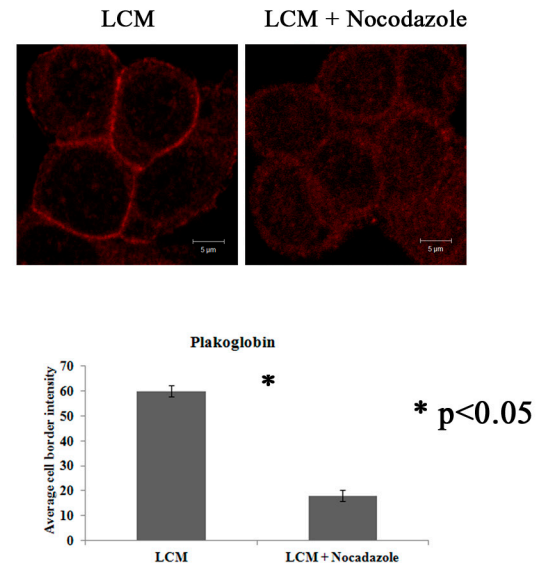
B



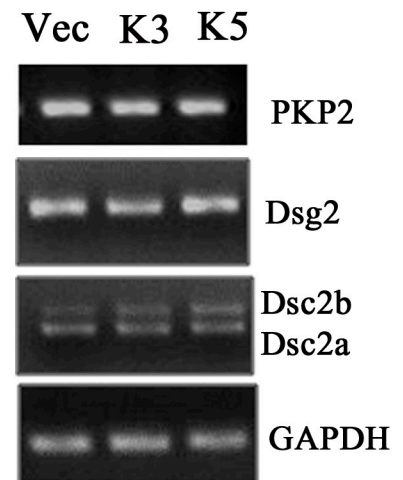
C



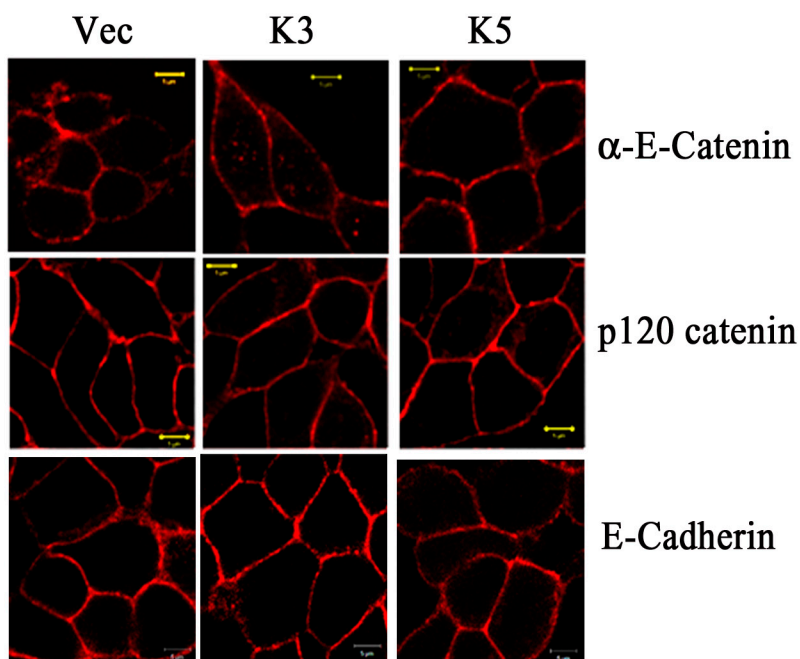
D



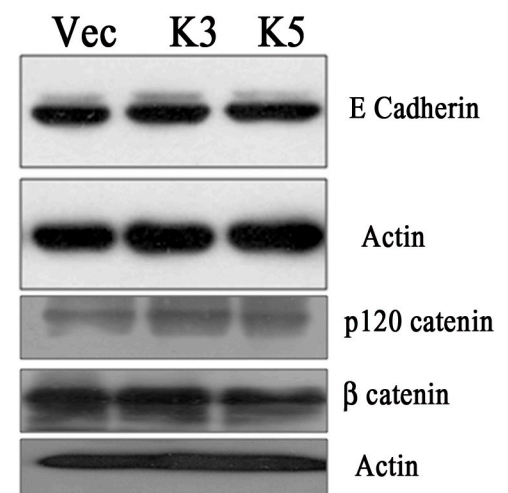
E



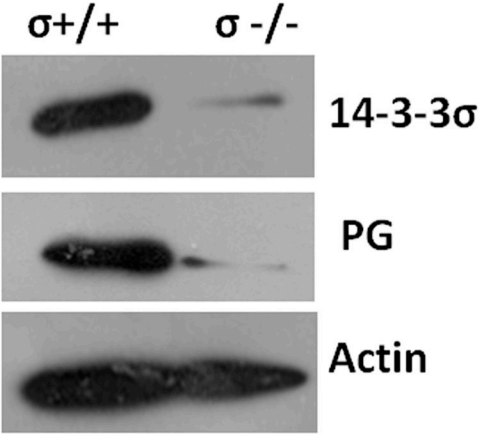
F



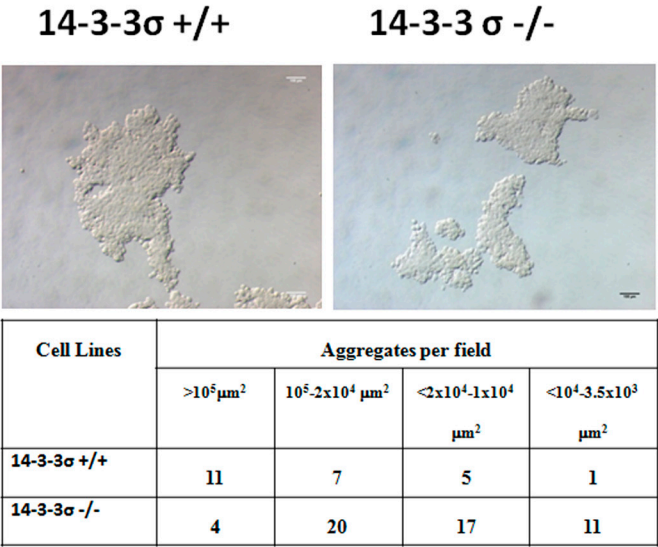
G



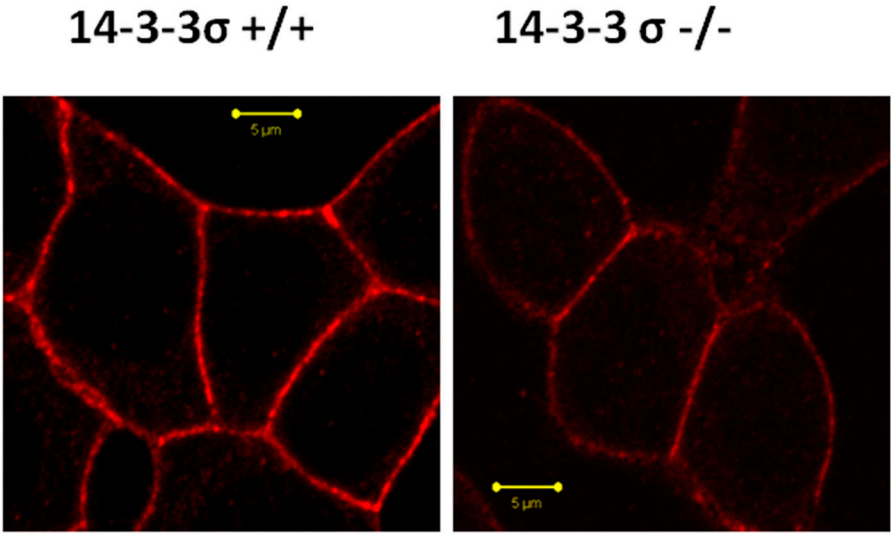
A



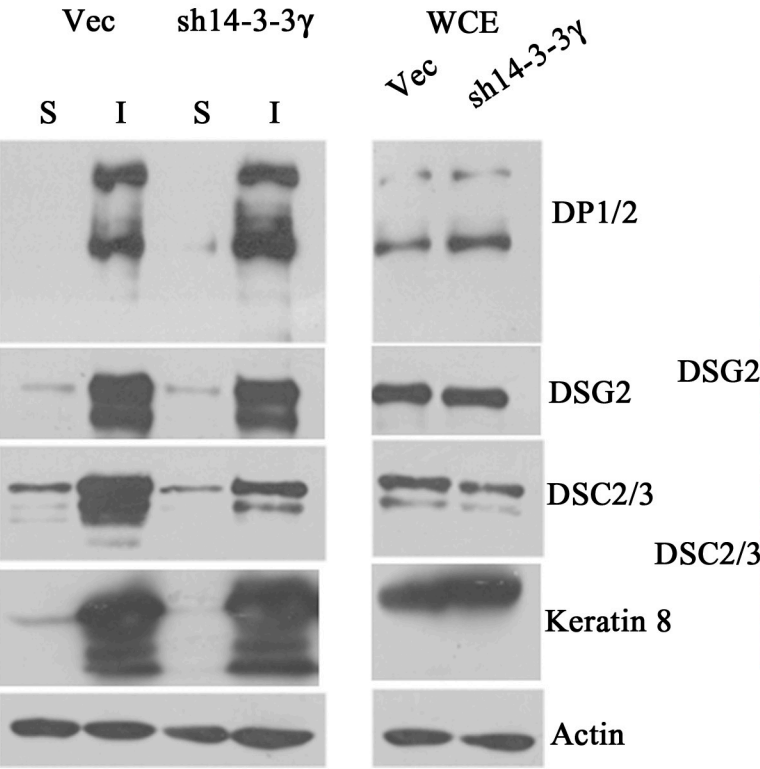
B



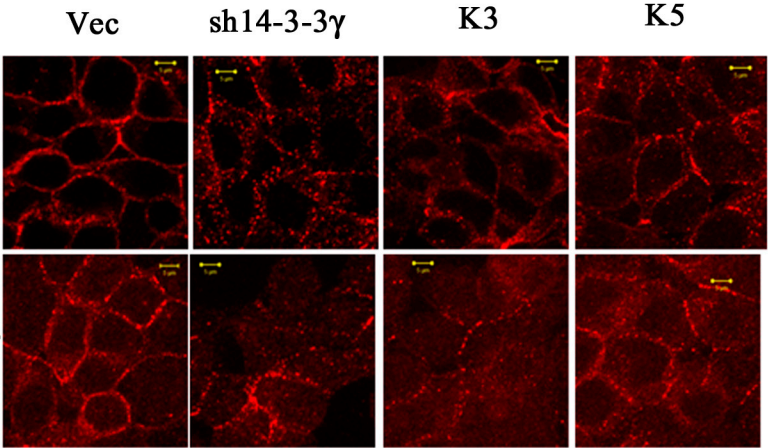
C



D



E



Filamin A stimulates cdc25C function and promotes entry into mitosis

Elphine Telles, Mansa Gurjar, Ketaki Ganti,[†] Dipika Gupta[†] and Sorab N. Dalal*

KS215 Advanced Centre for Treatment Research and Education in Cancer; Tata Memorial Centre Kharghar Node; Navi, Mumbai, India

[†]These authors contributed equally to this work

Key words: cell cycle, filamin A, cdc25C, mitosis, cyclin B1-cdk1

The activity of the dual specificity phosphatase cdc25C is required for mitotic progression though the mechanisms by which cdc25C is activated prior to mitosis in human cells remain unclear. The data presented herein show that the actin binding protein Filamin A forms a complex with cdc25C in vivo and binds preferentially to the mitotic form of cdc25C. Co-expression of Filamin A with cdc25C results in an increase in PCC induced by cdc25C, while knocking down Filamin A expression reduces the levels of PCC induced by cdc25C overexpression. Further, only a Filamin A fragment that forms a complex with both cdc25C and cyclin B1 and retains the dimerization domain can stimulate the ability of cdc25C to induce PCC. These results suggest that Filamin A provides a platform for the assembly of the cyclin B1-cdk1-cdc25C complex resulting in cdk1 activation and mitotic progression.

Introduction

Entry into mitosis is catalyzed by the cyclinB1-cdk1 complex.¹ During interphase, cdk1 is inactivated by phosphorylation at two residues, a threonine at position 14 (T14) and a tyrosine at position 15 (Y15).²⁻⁴ Dephosphorylation of these residues by the dual specificity phosphatase, cdc25C, results in the rapid activation of the cyclinB1-cdk1 complex,⁵ which in turn phosphorylates cdc25C in the N terminus stimulating cdc25C phosphatase activity forming an auto-amplification loop.⁶ During interphase and under conditions of DNA damage or incomplete replication, cdc25C is phosphorylated on a serine residue at position 216 (S216) by CHK1/CHK2 and C-TAK1.⁷⁻⁹ Phosphorylation of S216 generates a binding site for the 14-3-3 family of proteins on cdc25C.¹⁰⁻¹² Association of 14-3-3 proteins with cdc25C masks a NLS in cdc25C preventing its nuclear translocation thus leading to cytoplasmic sequestration of cdc25C.^{10,13,14} Loss of binding to 14-3-3 proteins result in premature activation of cdc25C suggesting that 14-3-3 proteins negatively regulate cdc25C function.^{10,12,13,15-17} During mitosis, cdc25C is not phosphorylated on S216 but is hyperphosphorylated on multiple residues in its N terminus leading to a higher migrating electrophoretic form in SDS gels and a stimulation of phosphatase activity.¹² Dissociation of 14-3-3 proteins from cdc25C accompanied by the dephosphorylation of S216 residue by protein phosphatase 1 (PP1) precedes activation of cdc25C and onset of mitosis in *Xenopus*.¹⁸⁻²⁰ However, the precise molecular mechanisms underlying the dissociation of 14-3-3 proteins from cdc25C and the concomitant hyperphosphorylation of cdc25C remain unclear.

The Filamins are a family of high molecular weight actin binding proteins that organize the actin cytoskeleton by their ability to crosslink F actin leading to the formation of a gel.²¹ Three homologues of Filamin, Filamin A, Filamin B and Filamin C, are found in higher eukaryotes and are encoded by three distinct genes.^{22,23} Filamin A is a homodimer consisting of an actin binding domain at the N terminus followed by an extended rod domain consisting of 24 immunoglobulin fold like repeats. The last repeat, 24, contains residues required for dimerization resulting in the formation of a Y shaped structure by Filamin A. There are two hinge regions positioned between repeats 15–16 and 23–24 that impart flexibility to the Filamin family of proteins.²²⁻²⁴ Repeats 16–24 in Filamin A contain a NLS that enables Filamin A to localize to the nucleus.²⁵ In addition to actin, Filamin A has been observed to bind to over 45 diverse cellular proteins and regulate their function linking Filamin A to cellular signaling pathways (reviewed in ref. 24).

Filamin A has been reported to have a role in regulating the DNA damage checkpoint by virtue of its association with BRCA2,²⁶ and a role in mitotic progression.²⁷ Cukier et al. demonstrated that Filamin A forms a complex with and is phosphorylated by cyclinB1-cdk1 during mitosis.²⁸ However the functional significance of this interaction was not demonstrated in vivo. The experiments reported in this paper identified Filamin A as a binding partner for cdc25C. It was observed that Filamin A preferentially associates with the mitotic form of cdc25C and enhances cdc25C activity in a PCC assay. Further, a knock-down of Filamin A inhibits the ability of cdc25C to induce PCC. These results suggest that Filamin A is required for the ability of

*Correspondence to: Sorab N. Dalal; Email: sdalal@actrec.gov.in
Submitted: 11/29/10; Revised: 01/10/11; Accepted: 01/26/11
DOI: 10.4161/cc.10.5.14954

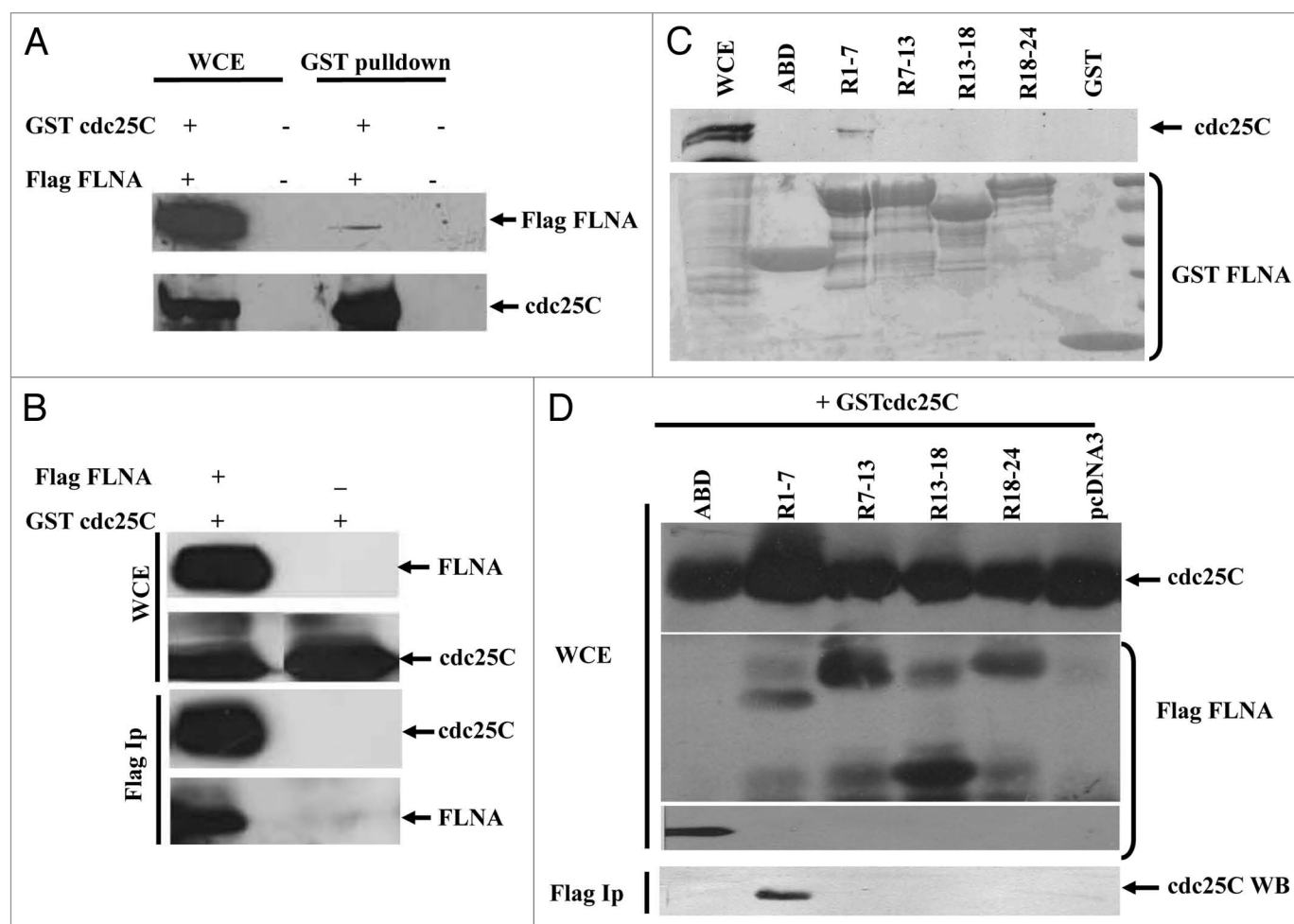


Figure 1. Filamin A forms a complex with cdc25C. (A) Flag tagged Filamin A and GST cdc25C or the vector controls were transfected into HEK293 cells as indicated. 48 hours post transfection, protein extracts were incubated with glutathione sepharose beads and the reactions resolved on SDS-PAGE gels followed by western blots with antibodies to the flag epitope and cdc25C as indicated. (B) GST cdc25C was transfected into cells with either vector control or flag tagged Filamin A followed by immunoprecipitations with antibodies to the Flag epitope. The reactions were resolved on SDS-PAGE gels followed by western blotting with antibodies to cdc25C and the Flag epitope as indicated. (C) The indicated GST-Filamin A fusions or GST alone were incubated with protein extracts from HEK293 cells followed by western blotting with antibodies to cdc25C (top part). The bottom part shows a ponceau stain of the blot showing that all the GST proteins are present at equivalent levels. (D) The indicated Flag-tagged Filamin A mutant constructs were co-transfected with GST-cdc25C into HEK293 cells and immunoprecipitations performed with antibodies to the Flag epitope followed by western blotting with antibodies to Flag or cdc25C as indicated. WCE = Whole cell extract.

cdc25C to promote mitosis, perhaps by serving as a scaffold for assembling the cdc25C-cyclinB1-cdk1 complex.

Results

To identify novel proteins that modulate cdc25C function, a differential yeast two-hybrid screen was performed,²⁹ resulting in the identification of Filamin A²⁴ as an interactor for both cdc25C and 14-3-3 ϵ , while HTTYH3,³⁰ was found to interact solely with 14-3-3 ϵ (Sup. Table 2). Since Filamin A bound to both 14-3-3 ϵ and cdc25C, it was hypothesized that it could be a regulator of cdc25C function. To determine if Filamin A forms a complex with cdc25C in vivo, HEK 293 cells were transfected with Flag Filamin A and GST cdc25C and the complex purified on glutathione sepharose beads. As shown in Figure 1A, Flag Filamin

A was able to form a complex with GST-cdc25C. No signal for Filamin A was detected in cells transfected with cdc25C and empty vector confirming that the interaction between the two proteins was specific (Fig. 1A). To confirm the specificity of the interaction, immunoprecipitations were performed with antibodies to the flag epitope tag followed by western blotting with antibodies to cdc25C and the flag epitope. As shown in Figure 1B, cdc25C co-precipitated with Filamin A. These results suggest that Filamin A forms a complex with cdc25C in vivo. Though the yeast two-hybrid data suggested that Filamin A could form a complex with 14-3-3 ϵ , no such interaction was detected in mammalian cells (data not shown).

To identify the region in Filamin A that is required for complex formation with cdc25C, several deletion mutants of Filamin A [ABD: (Filamin A actin binding domain) R1-7 (Filamin A

Figure 2 (See opposite page). Filamin A stimulates cdc25C function and shows increased association with mitotic cdc25C. (A and B) U-2OS cells were transfected with the indicated constructs followed by immunostaining with antibodies to cdc25C and the Flag epitope. The number of cells showing PCC (premature chromatin condensation), were determined microscopically. (C) HCT116 cells were transfected with Flag tagged Filamin A and the different Filamin A shRNA constructs (FLN1, FLN2, FLN3 and FLN4) or the vector control (vector). 60 hours post transfection, protein extracts were resolved on SDS PAGE gels followed by western blotting with antibodies to the Flag epitope. (D) Protein extracts from U-2OS derived vector control (U1 and U6) or the Filamin A knockdown clones generated with FLN1 (F12 and F13), FLN2 (F23, F24 and F26) and FLN4 (F42 and F47), were resolved on SDS-PAGE gels followed by western blots with antibodies to Filamin A. A western blot with antibodies to β -actin serves as a loading control. (E) The U-2OS derived vector control (U1) or the Filamin A knockdown clones were synchronized in G₁ with mimosine. At various time points post removal of mimosine, cells were fixed and stained with propidium iodide and cell cycle profiles determined by FACS analysis. Representative images of the cell cycle profiles from one experiment are shown. (F) The U-2OS derived vector control (U1) or the Filamin A knockdown clones (F23 and F42) were transfected with GST cdc25C. 48 hours post transfection, the cells were stained with antibodies to cdc25C and the percentage of PCC determined. The p values were calculated using a student's t-test. (G) HEK293 cells were transfected with Flag tagged FilaminA and GSTcdc25C as indicated. In some cases, cells were treated with nocodazole as described. Immunoprecipitations performed with antibodies to the Flag epitope followed by western blotting with antibodies to Flag or cdc25C as indicated. WCE = Whole cell extract. The left part shows a lower exposure for the WCE while the right part shows a higher exposure corresponding to the blot for the IP.

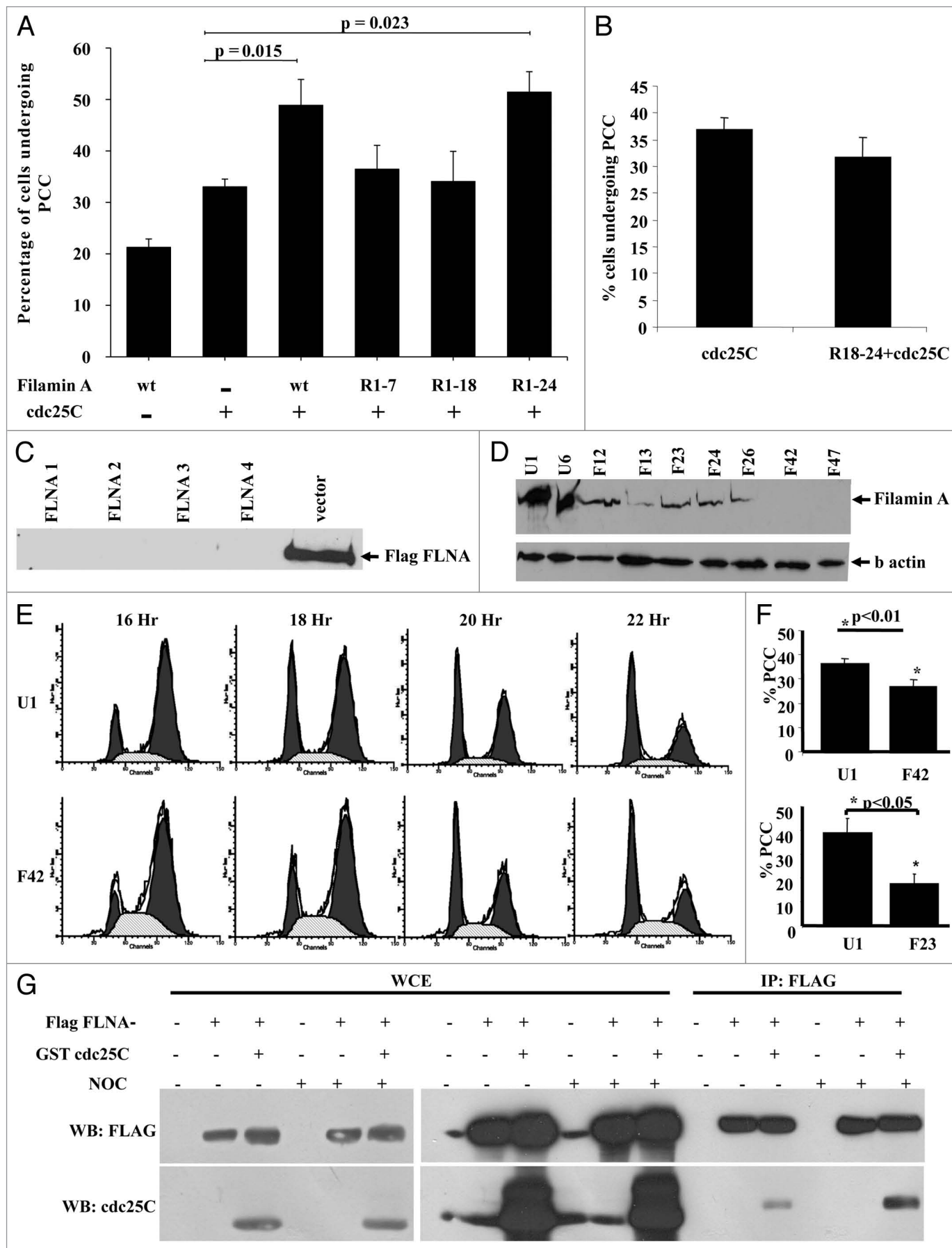
repeats 1–7) R7-13 (Filamin A repeats 7–13)]. R13-18 (Filamin A repeats 13–18 and the first hinge region) R18-24 (Filamin A repeats 18–24 including the second hinge region) were expressed in bacteria as GST fusions and purified on glutathione sepharose beads. The fusion proteins were incubated with protein extracts from HCT116 cells and the reactions resolved on SDS PAGE gels and western blots performed with antibodies to cdc25C. As shown in **Figure 1C**, only the R1-7 deletion containing the first seven repeats formed a complex with cdc25C. None of the other deletion mutants formed a complex with cdc25C, even though all the GST-proteins were present at equivalent levels. To determine if the R1-7 region was required for complex formation with cdc25C in vivo, expression constructs expressing Flag epitope tagged versions of these mutant proteins were transfected into HEK293 cells with GST-cdc25C followed by immunoprecipitations with antibodies to the flag epitope. Only the R1-7 fragment of Filamin A formed a complex with cdc25C in vivo, while the other mutants were unable to form a complex with cdc25C in vivo (**Fig. 1D**). These results suggest that the first seven Filamin A repeats contain a binding site for cdc25C.

To determine whether Filamin A was able to regulate cdc25C function, a PCC assay was carried out as described previously in reference 17. Filamin A when co expressed along with cdc25C led to a 1.5 fold increase in percentage of cells undergoing PCC than in cells expressing cdc25C alone. Filamin A alone was capable of inducing PCC at low levels (**Fig. 2A**). This suggests that Filamin A may cooperate with cdc25C to promote entry of cells into mitosis. The ability of different Filamin A mutant proteins to modulate cdc25C function was determined in a PCC assay. As shown in **Figure 2A**, the R1-7 fragment, which is sufficient for complex formation with cdc25C, did not stimulate the ability of cdc25C to induce PCC. To identify other regions in Filamin A that were required for its ability to stimulate cdc25C activity in vivo, two deletion mutants R1-18 (Filamin A repeats 11–18 and the first hinge region) and R1-24 (Filamin A repeats 1–24 and both hinge regions) were generated. R1-18 contains the cyclin B1 binding site in Filamin A as previously reported in reference 28, and R1-24 contains both the cyclin B1 binding site and the Filamin A dimerization domain (**Fig. 2A**). A region of Filamin A that contains only the dimerization domain R18-24, did not affect the ability of cdc25C to induce PCC in this assay (**Fig. 2B**). These results suggest that in addition to complex

formation with cdc25C, regions in Filamin A required for complex formation with cyclin B1 and Filamin A dimerization are required to activate cdc25C function. The dimerization motif might be necessary to stimulate the mitotic hyperphosphorylation of cdc25C that is required for mitotic progression.

To confirm that Filamin A was required to induce the activation of cdc25C prior to mitosis, Filamin A expression was inhibited using vector driven short hairpin (sh) RNA interference. Four different shRNA constructs (Filamin A1, Filamin A2, Filamin A3 and Filamin A4) were tested for their ability to inhibit Filamin A expression. As shown in **Figure 2C**, all the shRNA constructs were able to inhibit the expression of a Flag tagged Filamin A construct as compared to cells transfected with the vector alone. These shRNA constructs were used to derive stable knockdown clones for Filamin A in U-2OS cells. As shown in **Figure 2D**, several clones (F12, F13, F23, F24, F26, F42, F47) were identified that had reduced levels of Filamin A by western blot analysis as compared to the vector controls (U1 and U6). These clones were generated with three different shRNA constructs. western blots for actin served as a loading control. It has been previously reported that cells that do not express Filamin A show a delayed entry into mitosis upon DNA damage.²⁷ To determine whether the Filamin A knockdown clones generated in this report show a similar phenotype in the absence of DNA damage, the vector stable and Filamin A knockdown clones were synchronized with mimosine, harvested at the indicated time points and analyzed by Flow cytometry. As shown in **Figure 2E and Supplemental Table 3**, the Filamin A knockdown clone F42 shows a delayed entry into G₂ as compared to the vector stable clone. These results suggest that our Filamin A knockdown clones, show a phenotype similar to that reported previously for Filamin A loss.

To determine whether Filamin A regulates cdc25C activity, cdc25C was overexpressed in Filamin A knockdown clones and its ability to induce PCC determined. As shown in **Figure 2F**, the levels of PCC induced by cdc25C were significantly reduced in two different Filamin A clones as compared to the vector control. The Filamin A knockdown clones were generated with two different shRNA constructs (F23 and F42 were generated with FLN2 and FLN4 respectively), suggesting that the phenotypes observed are not due to off target effects of the shRNA constructs. These results show that in the absence of Filamin A,



cdc25C is unable to induce mitosis, presumably by being unable to activate the cyclin B1-cdk1 complex.

Since cdc25C is differentially modified over the cell cycle being phosphorylated on S216 during interphase and hyperphosphorylated on other residues in mitotic cells,⁸ we wished to determine whether Filamin A bound with greater affinity to the interphase or mitotic form of cdc25C. Hence, cells transfected with GST-cdc25C and Flag-Filamin A were treated with nocodazole or left untreated in order to obtain an enriched pool of mitotic cells and immunoprecipitation reactions were performed with antibodies to the flag epitope (Fig. 2G). Increased binding of Filamin A to cdc25C was observed in the presence of nocodazole, suggesting that Filamin A and cdc25C complex formation is enhanced in mitotic cells.

Discussion

The results reported herein suggest that the actin bundling protein, Filamin A, binds to the mitotic phosphatase, cdc25C and stimulates cdc25C activity, leading to mitotic progression. Consistent with this hypothesis, only a Filamin A molecule that can form a complex with both cdc25C and cyclin B1 and dimerize is capable of activating cdc25C function as measured in a PCC assay. Similarly, loss of Filamin A leads to a decrease in the ability of cdc25C to induce PCC. Thus, Filamin A might serve as a scaffold for the assembly of the cyclinB1-cdk1-cdc25C complex, facilitating the dephosphorylation of cdk1 by cdc25C.

Our results suggest that the region in Filamin A required for complex formation with cdc25C is distinct from the region that is required for binding to cyclin B1 as reported by Cukier et al. Our results also suggest that in addition to complex formation with cdc25C, regions in Filamin A required for cyclin B1 binding²⁸ and dimerization²² are also required to activate cdc25C function and mitotic progression (Fig. 2). It has been previously reported that cyclin B1-cdk1 can hyperphosphorylate cdc25C, which leads to a stimulation in its phosphatase activity.⁶ It is possible that the dimerization of Filamin A permits complex formation between an active cyclinB1-cdk1 complex on one monomer in the dimer and an inactive cdc25C molecule on the other monomer resulting in activation of the mitotic cascade.

The results reported in this manuscript suggest that Filamin A could serve as a platform for the interaction between cdc25C and the cyclin B1-cdk1 complex leading to cdk1 dephosphorylation and mitotic progression. This is also consistent with reports that cdk1 remains phosphorylated on Y15 in Filamin A knockout clones for up to 32 hours post irradiation, as compared to the vector control cells, which lose phosphorylation on Y15 16 hours post irradiation,²⁷ indicating that in the absence of Filamin A, the ability of cdc25C to activate the cyclin B1-cdk1 complex is compromised. In addition, data reported in this paper suggest that the ability of cdc25C to activate mitosis is inhibited in cells with a knockdown of Filamin A and that in the absence of Filamin A, progression through G₂ is retarded.

In conclusion, Filamin A is required to activate cdc25C to promote mitotic progression presumably by bringing it into close proximity with the cyclin B1 cdk1 complex.

Materials and Methods

Plasmids and constructs. To generate Flag tagged Filamin A, the N terminus of Filamin A was amplified using the primers listed in Supplemental Table 1. This 1,214 bp fragment and a 6,790 bp fragment generated by digesting the Filamin A cDNA with NotI and BglII were cloned sequentially into pBluescript and then excised from pBluescript with EcoRV and NotI and cloned downstream of the flag epitope tag in pcDNA3. Filamin A truncation mutants were generated using the primers as listed in Supplemental Table 1 and were cloned downstream of the Flag epitope tag in pcDNA3 vector as EcoRV NotI fragments and downstream of the GST tag in pGEX4T1 (Pharmacia). To generate plasmid based short hairpin RNA(shRNA) constructs, the oligonucleotide pairs listed in Supplemental Table 1 were cloned into AgeI-XhoI digested pTU6II(a) plasmid downstream of the U6 promoter.^{31,32}

The 14-3-3 ϵ and cdc25C cDNA's were amplified using the primers listed in Supplemental Table 1 and cloned into the EcoRI and SalI sites in pPC97 plasmid downstream of the GAL4 DBD and the EcoRI and XhoI sites in pHyblex plasmid downstream of the LexA DBD respectively.²⁹ Primers used for the 3' ends of 14-3-3 ϵ and cdc25C have been described previously in reference 13 and 15. The GST-cdc25C fusion construct has been described previously in reference 17.

Differential yeast two hybrid screen. *Saccharomyces cerevisiae* HW18 was used as host strain for the yeast two hybrid assay. The differential yeast two hybrid screen was performed as described to identify interactors for cdc25C and 14-3-3 ϵ .²⁹

Cell lines and transfections. HEK 293, HCT116 and U-2OS cell lines were cultured as described previously in reference 17 and 33. Transfections were performed using calcium phosphate precipitation as described in reference 34.

For in vivo GST pulldown, HEK293 cells in 100 mm dishes were co-transfected with 17.5 μ g of Flag Filamin A plasmid and 5 μ g of GST-cdc25C construct. For enrichment of mitotic cells, nocodazole (sigma) at a concentration of 150 ng/ml was added immediately after the precipitate was removed from cells for 24 hours. For PCC assays in cells co-expressing GST cdc25C and Flag Filamin A, U-2OS cells grown on coverslips in a 60 mm dish were co-transfected with 3 μ g of GST cdc25C plasmid and 4 μ g of Flag Filamin A plasmid. To determine the efficiency of shRNA constructs, U-2OS cells were co-transfected with 2 μ g of shRNA constructs and 2 μ g of flag tagged Filamin A in U-2OS cells followed by western blots with antibody to the Flag epitope. To generate stable Filamin A knockdown clones, U-2OS cells were transfected with pTU6II (a) based plasmid constructs and then shifted to medium containing 5 μ g/ml blasticidin (Invitrogen) to generate stable clones. The clone F23 and F42 were generated using the construct pTU6/F2 and pTU6/F4 respectively. The control clone, U1 was generated using the empty pTU6II(a) plasmid.

Antibodies. For western blotting. Ascitic fluid of the anti-cdc25C antibody (TC14),¹³ was used at a dilution of 1:4,000. The anti-actin antibody (AC74, Sigma) was used at a dilution of 1:5,000. The flag antibody was used at a dilution of 1:2,000. The

anti-Filamin A antibody (M2, Sigma) was used at a dilution of 1:2,000 for western blot analysis. The secondary goat anti-mouse HRP (Pierce) was used at a dilution of 1:5,000 for western blot analysis.

For immunofluorescence. The anti-cdc25C antibody (C-20, Santa Cruz) was used at a dilution of 1:500. The Flag antibody (M2, Sigma) was used at a dilution of 1:500. The secondary goat anti-mouse Alexa 568 (Molecular Probes) and goat anti-rabbit Alexa 488 (Molecular Probes) were used at a dilution of 1:200.

GST pull down assays, immunoprecipitations and western blotting. Filamin A deletion mutants were purified as GST fusion proteins from *E. coli* on glutathione sepharose beads (Pharmacia) and incubated with EBC lysates of HCT116 cells overnight at 4°C. The reactions were washed 3x with NET-N and resolved on SDS PAGE gels followed by western blots with antibodies to cdc25C. The levels of the individual GST proteins were determined by staining the membrane with Ponceau S (Sigma). To determine whether Filamin A formed a complex with cdc25C in vivo, Flag Filamin A and GST cdc25C were transfected into HEK293 cells as described above. 44 hours after transfection, transfected cells were lysed in EBC buffer and immunoprecipitations performed using antibodies to the Flag epitope. Alternatively, the complexes were purified on glutathione sepharose beads as previously described in reference 17. The reactions were resolved on a 6%–10% step gel and followed by western blotting with antibodies to the Flag or HA epitope or to cdc25C. To determine the levels of endogenous Filamin A in stable clones, 50 µg of protein extracts made in Laemmli's buffer were resolved

on SDS-PAGE gels and western blots performed with antibodies against Filamin A and β-actin.

PCC assays. PCC assays in cells co-transfected with plasmids expressing GST-cdc25C were performed as described previously in reference 13, 15 and 17. Co-transfected cells were identified microscopically as cells staining positive with both, the cdc25C antibody (C-20) and the anti-flag antibody (M2). Only exogenously expressed cdc25C was detected at the antibody dilution used in these assays. The images were captured with a 63x objective on an Upright Axio Imager Z1 microscope (Carl Zeiss, Germany).

Cell cycle analysis. Filamin A knockdown cells and vector stable cells were treated with 400 µM mimosine for 20 hours as described in reference 13 and 16. At the indicated time points after release from mimosine cells were collected by trypsinization, resuspended in PBS and fixed by addition of 90% methanol at -20°C for 10 minutes. After fixation cells were stained with propidium iodide (Sigma) solution for 10 minutes at 37°C and cell cycle profiles determined using MODFIT software.

Acknowledgements

E.T. was supported by a fellowship from the Council for Scientific and Industrial Research. This work was supported in part by grants from the Department of Biotechnology (DBT) and ACTREC.

Note

Supplemental materials can be found at: www.landesbioscience.com/journals/cc/article/14954

References

1. Nurse P. Ordering S phase and M phase in the cell cycle. *Cell* 1994; 79:547-50.
2. Den Haese GJ, Walworth N, Carr AM, Gould KL. The wee1 protein kinase regulates T14 phosphorylation of fission yeast cdc2. *Mol Biol Cell* 1995; 6:371-85.
3. Lee MS, Enoch T, Piwnica-Worms H. mik1⁺ encodes a tyrosine kinase that phosphorylates p34^{cdc2} on tyrosine 15. *J Biol Chem* 1994; 269:30530-7.
4. Mueller PA, Coleman TR, Kumagai A, Dunphy WG. Myt1: a membrane-associated inhibitory kinase that phosphorylates cdc2 on both Threonine-14 and Tyrosine-15. *Science* 1995; 270:86-90.
5. Gautier J, Solomon MJ, Booher RN, Bazan JF, Kirschner MW. cdc25 is a specific tyrosine phosphatase that directly activates p34^{cdc2}. *Cell* 1991; 67:197-211.
6. Hoffmann I, Clarke PR, Marcote MJ, Karsenti E, Draetta G. Phosphorylation and activation of human cdc25C by cdc2-cyclin B and its involvement in the self amplification of MPF at mitosis. *EMBO J* 1993; 12:53-63.
7. Chaturvedi P, Eng WK, Zhu Y, Mattern MR, Mishra R, Hurler MR, et al. Mammalian chk2 is a downstream effector of the ATM-dependent DNA damage checkpoint pathway. *Oncogene* 1999; 18:4047-54.
8. Ogg S, Gabrielli B, Piwnica-Worms H. Purification of a serine kinase that associates with and phosphorylates human cdc25C on serine 216. *J Biol Chem* 1994; 269:30461-9.
9. Sanchez Y, Wong C, Thoma RS, Richman R, Wu Z, Piwnica-Worms H, et al. Conservation of the Chk1 checkpoint pathway in mammals: linkage of DNA damage to cdk regulation through cdc25. *Science* 1997; 277:1497-501.
10. Kumagai A, Yakowec PS, Dunphy WG. 14-3-3 proteins act as negative regulators of the mitotic inducer cdc25 in *Xenopus* egg extracts. *Mol Biol Cell* 1998; 9:345-54.
11. Peng CY, Graves PR, Ogg S, Thoma RS, Byrnes MJ, Wu Z, et al. C-TAK1 protein kinase phosphorylates human cdc25C on serine 216 and promotes 14-3-3 protein binding. *Cell Growth Differ* 1998; 9:197-208.
12. Peng CY, Graves PR, Thoma RS, Wu Z, Shaw AS, Piwnica-Worms H. Mitotic and G₂ checkpoint control: regulation of 14-3-3 protein binding by phosphorylation of cdc25C on serine-216. *Science* 1997; 277:1501-5.
13. Dalal SN, Schweitzer CM, Gan J, DeCaprio JA. Cytoplasmic localization of human cdc25C during interphase requires an intact 14-3-3 binding site. *Mol Cell Biol* 1999; 19:4465-79.
14. Graves PR, Lovly CM, Uy GL, Piwnica-Worms H. Localization of human Cdc25C is regulated both by nuclear export and 14-3-3 protein binding. *Oncogene* 2001; 20:1839-51.
15. Dalal SN, Yaffe MB, DeCaprio JA. 14-3-3 family members act coordinately to regulate mitotic progression. *Cell Cycle* 2004; 3:672-7.
16. Hosing AS, Kundu ST, Dalal SN. 14-3-3gamma is required to enforce both the incomplete S phase and G(2) DNA damage checkpoints. *Cell Cycle* 2008; 7:3171-9.
17. Telles E, Hosing AS, Kundu ST, Venkatraman P, Dalal SN. A novel pocket in 14-3-3ε is required to mediate specific complex formation with cdc25C and to inhibit cell cycle progression upon activation of checkpoint pathways. *Exp Cell Res* 2009; 315:1448-57.
18. Kumagai A, Dunphy WG. Binding of 14-3-3 proteins and nuclear export control the intracellular localization of the mitotic inducer cdc25. *Genes and Dev* 1999; 13:1067-72.
19. Margolis SS, Perry JA, Forester CM, Nutt LK, Guo Y, Jardim MJ, et al. Role for the PP2A/B56delta phosphatase in regulating 14-3-3 release from Cdc25 to control mitosis. *Cell* 2006; 127:759-73.
20. Margolis SS, Walsh S, Weiser DC, Yoshida M, Shenolikar S, Kornbluth S. PP1 control of M phase entry exerted through 14-3-3-regulated Cdc25 dephosphorylation. *EMBO J* 2003; 22:5734-45.
21. Wang K. Filamin, a new high-molecular-weight protein found in smooth muscle and nonmuscle cells. Purification and properties of chicken gizzard filamin. *Biochemistry* 1977; 16:1857-65.
22. Stossel TP, Condeelis JS, Cooley L, Hartwig JH, Noegel A, Schleicher M, et al. Filamins as integrators of cell mechanics and signalling. *Nat Rev Mol Cell Biol* 2001; 2:138-45.
23. van der Flier A, Sonnenberg A. Structural and functional aspects of filamins. *Biochim Biophys Acta* 2001; 1538:99-117.
24. Robertson SP. Filamin A: Phenotypic diversity. *Curr Opin Genet Dev* 2005; 15:301-7.
25. Loy CJ, Sim KS, Yong EL. Filamin-A fragment localizes to the nucleus to regulate androgen receptor and coactivator functions. *Proc Natl Acad Sci USA* 2003; 100:4562-7.
26. Yuan Y, Shen Z. Interaction with BRCA2 suggests a role for filamin-1 (hsFLN1) in DNA damage response. *J Biol Chem* 2001; 276:48318-24.
27. Meng X, Yuan Y, Maestas A, Shen Z. Recovery from DNA damage-induced G₂ arrest requires actin-binding protein filamin-A/actin-binding protein 280. *J Biol Chem* 2004; 279:6098-105.
28. Cukier IH, Li Y, Lee JM. Cyclin B1/Cdk1 binds and phosphorylates Filamin A and regulates its ability to cross-link actin. *FEBS Lett* 2007; 581:1661-72.

-
29. Gossel MJ, Wang H, Gadea B, Yeung W, Hinds PW. A yeast-two hybrid system for discerning differential interactions using multiple baits. *Nature Biotechnology* 1999; 17:1232-3.
 30. Suzuki M. The Drosophila tweety family: molecular candidates for large-conductance Ca^{2+} -activated Cl^{-} channels. *Exp Physiol* 2006; 91:141-7.
 31. Kundu ST, Gosavi P, Khapare N, Patel R, Hosing AS, Maru GB, et al. Plakophilin3 downregulation leads to a decrease in cell adhesion and promotes metastasis. *Int J Cancer* 2008; 123:2303-14.
 32. Skaar JR, Arai T, DeCaprio JA. Dimerization of CUL7 and PARC is not required for all CUL7 functions and mouse development. *Mol Cell Biol* 2005; 25:5579-89.
 33. Dalal S, Gao Q, Androphy EJ, Band V. Mutational analysis of Human papillomavirus type 16 E6 demonstrates that p53 degradation is necessary for immortalization of mammary epithelial cells. *J Virol* 1996; 70:683-8.
 34. Spector DL, Goldman RD, Leinwand LA. *Cells: A laboratory Manual*. Cold Spring Harbor: Cold Spring Harbor Laboratory 1998.

©2011 Landes Bioscience.
Do not distribute.